Circadian organization and mechanisms of entrainment in populations of *Drosophila melanogaster* selected for divergent timing of eclosion

Thesis

submitted towards the partial fulfilment for the degree of

Doctor of Philosophy

by

Abhilash Lakshman

Chronobiology and Behavioural Neurogenetics Laboratories

Jawaharlal Nehru Centre for Advanced Scientific Research

Jakkur, Bangalore – 560064, India

January 2020

Dedicated to the memories of Profs. Vijay Kumar Sharma and Serge Daan

Giants on whose shoulders I stand

Table of Contents

Declaration

The work presented in this thesis entitled "**Circadian organization and mechanisms of entrainment in populations of *Drosophila melanogaster* selected for divergent timing of eclosion**" is the result of investigations carried out by me first in the Evolutionary and Organismal Biology Unit of Jawaharlal Nehru Centre for Advanced Scientific Research (JNCASR), Bangalore, India, under the supervision of late Prof. Vijay Kumar Sharma. The studies carried out since October 2016 and composing of the current thesis were done under the supervision of Prof. Sheeba Vasu of the Neuroscience Unit of the Centre. I hereby declare that the work reported here has not been submitted elsewhere for any other degree in this or any other university, except few results of three experiments which were part of my MS thesis (JNCASR) – (i) eclosion rhythm under LD 12:12 at 25 °C (used in Chapter 3 of this thesis) and activity/rest rhythms under (ii) LD 12:12 and (iii) LD 18:06 at 25 °C (used in Chapters 5 and 6 of this thesis). While data from these runs have been used here, they are in no way exactly reproduced from my MS thesis and for the most part, I have used different methods of analyses, owing to the additional data that has been collected.

In keeping with the general practice of reporting scientific observations, due acknowledgement has been made wherever the work described has been based on the findings of other researchers. Any omission which may have occurred is likely due to oversight or an error in judgement and is highly regretted.

Place: Bangalore

January 2020

Abhilash Lakshman

Behavioural Neurogenetics Laboratory

JAWAHARLAL NEHRU CENTRE FOR ADVANCED SCIENTIFIC RESEARCH

P.O. BOX. 6436, JAKKUR, BANGALORE - 560 064, INDIA

January 2020

Certificate

This is to certify that the work described in the thesis entitled "**Circadian organization and mechanisms of entrainment in populations of *Drosophila melanogaster* selected for divergent timing of eclosion***"* is the result of investigations carried out by Mr. Abhilash Lakshman first in the Evolutionary and Organismal Biology Unit of the Jawaharlal Nehru Centre for Advanced Scientific Research, Bangalore, India, under the supervision of late Prof Vijay Kumar Sharma. The studies carried out since October 2016 and composing of the current thesis were supervised by me at the Neuroscience Unit. I certify that the results presented in this thesis have not previously formed the basis for the award of any other diploma, degree or fellowship, except few results of three experiments which were part of his MS thesis (JNCASR) – (i) eclosion rhythm under LD 12:12 at 25 °C (used in Chapter 3 of this thesis) and activity/rest rhythms under (ii) LD 12:12 and (iii) LD 18:06 at 25 °C (used in Chapters 5 and 6 of this thesis). While data from these runs have been used here, they are in no way exactly reproduced from his MS thesis and for the most part, he has used different methods of analyses, owing to the additional data that has been collected.

Sheeba Vasu, PhD

Thesis Supervisor

E-mail: sheeba@jncasr.ac.in; ph – 22082987(off) 22082580 (lab)

Acknowledgments

First and foremost, I would like to thank my MS and PhD advisors, late Prof. Vijay Kumar Sharma (VKS) and Prof. Sheeba Vasu. VKS has been an incredible source of inspiration and support on various issues ranging from personal to professional ones. There are many lessons I have learnt from him that I am sure will be useful for my academic career and life, in general. I want to also extend my heartfelt gratitude to Prof. Sheeba Vasu. She has been extraordinarily helpful and supportive throughout my tenure here at JNCASR. Her kindness, compassion, strength and resilience are exemplary, and I hope to imbibe at least some of it in my life.

I am indebted to late Prof. Serge Daan, Profs. William J. Schwartz, Till Roenneberg, Kenneth P. Wright Jr., Charlotte Helfrich-Förster and Michael Gorman for several very helpful discussions regarding my work. These discussions have allowed me to (i) venture into areas that I otherwise may not have, and (ii) gain deeper insights into the circadian organization in *Drosophila*. I want to also thank Drs. Aya Satoh and Maria Ooshtuizen for freely sharing their data which I used to test the *R* application that I built. I am also thankful to the bioimaging facility at JNCASR for allowing me to use their confocal microscope for one of my experiments, and JNCASR, Science and Engineering Research Board, Department of Science and Technology and the Department of Biotechnology, Government of India for generous funding that enabled me to carry out my research. Parts of my work reported in this thesis have either been published or is under review, and I would like to thank all the anonymous reviewers and the editors of the journals involved for their time and very useful comments. Additionally, I sincerely extend my gratitude to my thesis examiners for their time and effort in reviewing my work.

Laboratory and department environments are crucial for a healthy scientific discourse and in this regard, I have been lucky to have some very interesting colleagues around me. Koustubh Vaze and late Snigdhadip Dey have been instrumental in nurturing my interest in organismal biology as a young researcher in the department, and for the training in rigorous research practices.

I also am grateful to the JNCASR ‘clock-club’ that includes all members of the Chronobiology and Behavioural Neurogenetics Laboratories. The older members, Koustubh, Shahnaz, Nisha,

Pankaj, Nikhil, Vishwanath, Priya, Pavitra, Antara, and Sheetal have been very helpful and have provided critical positive feedback during lab meetings. Other members of the lab, Manishi, Arijit, Chitrang, Rutvij, Pritha, Ratna, Aishwarya, Anuj, Viveka and Pragya have been very interesting and engaging, and this has also been very helpful in terms of the way in which my thought process regarding various issues has evolved. Other than their supportive roles as lab mates, Koustubh, Nikhil, Arijit, Aishwarya, Chitrang and Pragya have been great friends. Aishwarya has also been a wonderful collaborator on one of my projects, and I am thankful for her help with those experiments. Nikhil has been a great colleague and the many discussions with him while he was in the lab, ranging from science to philosophy, have been very interesting.

I must additionally thank the many people who over the years have created and maintained the *Drosophila* populations that I worked with during my summer projects, MS project and my PhD thesis (the populations have been around for nearly 18 years now): Shailesh, Koustubh, Nikhil, Ratna, Swathi, Arijit, Pragya and Shephali. A note to the current and future 'gate-keepers': these populations are a *gold mine*, please look after them carefully, with utmost rigour.

Further, I must acknowledge all the short-term students in the lab – Yeshwant, Rukmini, Tejaswini, Vijayaditya, Gayatri, Sushma, Aparna, Srishti Priya, Arshad, Gokul and Sowmya. Engaging with them and teaching and mentoring them has been an incredibly enriching experience, and I urge anyone reading this section to engage with younger students as much as possible. I must also add all the POBE and Integrated PhD students whom I have taught and mentored, over the years to this list.

Our labs utilise a lot of resources in terms of vials, cages and petri dishes, and autoclaving, washing and maintaining them is a humungous task in itself. For doing this seamlessly, I thank Rajanna and Muniraju from the bottom of my heart. They have become such an integral part of our lab that it is nearly impossible to run the lab without them. More recently, Samuel has joined the work force and has also been of great help with stock maintenance.

I would like to take this opportunity to also acknowledge members of JNCASR outside my department who have been wonderful companions and with whom several discussions on issues outside my specific area of research have helped broaden my perspective. Especially, I am grateful to Prof. Maneesha Inamdar and members of her lab – Abhishek, Ronak, Deeti, Diana, Saloni,

Divyesh, Arindam, Kajal, Roja and Alice. These friendships were essential for sustaining a life in the hostel for several years.

Over the course of these years although I have lost many friendships, I have managed to maintain some old ones and have also made new ones who have become family outside of home, and a constant source of inspiration. Although many of them did not necessarily contribute to the work in this thesis, they deserve my fervent acknowledgments. I thank Koustubh, Narendra, Sumantra, Divyesh, Payel, Arindam, Abhishek and especially Saloni for being part of my post-BSc journey. Saloni has been an incredible collaborator and friend, and I am much more than just thankful to her.

Last but not least, I want to extend sincere thanks to my family. My mother, uncle and aunt, and my grandparents have been unbelievably supportive throughout my life, and especially over the last several years when I decided to get into Grad School. I am really at a loss for words to describe how grateful I am to them. My brother has been an amazing friend and partner in crime and has made my life supremely livelier. Although not an academic, he does not shy away from talking to me about my work and our discussions on politics and philosophy are always fun (maybe not for others around us!), and these are only a few things I am thankful to him for (it will not be possible to list everything out).

Abbreviations and Glossary

Accuracy of entrainment: Inverse of day-to-day variability in phases of entrainment.

After-effects: Change in free-running period (FRP) as a consequence of the entraining regime.

Amplitude expansion: Increase in amplitude of rhythm under entrainment relative to amplitude under constant darkness.

Amplitude response curve (ARC): A plot of change in amplitude of the rhythm/oscillation caused due to a perturbation (using a zeitgeber) at different times of the rhythm under constant conditions.

CC: Abbreviation for cryophase/cryophase (constant darkness at low temperature).

Circadian (rhythm and clock): An endogenous biological rhythm with a natural (or free-running) period (τ) close to, but not necessarily the same as that of the earth's rotation (i.e., 24-h; Latin, *circa*-'about', *dies*-'day'). Any set of mechanisms within the organism that drives such rhythms are called circadian clocks.

Circadian Integrated Response Characteristic (CIRC): A response characteristic of the circadian clock that reflects how the system integrates provided zeitgeber profiles to achieve entrainment.

Cryophase: The cool phase of a temperature cycle.

CT: Circadian Time (a scale of time wherein CT00 is the onset of subjective day).

c_{zg}: Calibration factor, a parameter of the CIRC model of entrainment. It is reflective of how sensitive the circadian system is, for a given strength of the zeitgeber.

DD: Constant darkness.

DN: Dorsal Neurons; a class of neurons in the adult *Drosophila* brain. These are subdivided into DN1s, DN2s and DN3s.

DRC: Dose Response Curve; a plot of phase-shifts incurred by a circadian system in response to different doses of stimuli (either intensity or duration) at different phases of the circadian system

Entrainment: The coupling of a circadian rhythm to a zeitgeber such that both have the same period ($\tau = T$) resulting in a stable and reproducible ψ_{ENT}. Entrainment can only occur within a range of T values and this range is referred to as the 'range of entrainment.'

ExT: External Time; a scale of time wherein ExT00 is the mid-point of the night phase.

Fitness (Darwinian): A measure of an individual's contribution to the gene pool of the next generation.

Frequency demultiplication: The phenomenon wherein a circadian rhythm entrains to zeitgebers with periodicity that are sub-multiples of 24-h with an exactly 24-h period.

FRP: Free-Running Period; also represented as τ. τ_M and τ_E represent the free-running periods of the morning and evening oscillators, respectively (see Chapter 1). In chapter 6, τ_E is used to refer to free-running period of the clock under entrainment (see text for clarification).

Gate-width: Traditionally defined as the 'allowed' zone for adult emergence to occur within a day. It is calculated as the difference between phases of onset and offset of the emergence rhythm.

InT: Internal Time; a scale of time wherein InT00 is the mid-point of the subjective night phase.

LD: Light/Dark.

l-LNv: large Ventral Lateral Neurons.

LNd: Lateral Dorsal Neurons.

PDF: Pigment Dispersing Factor.

PG: Prothoracic Gland.

Phase response curve (PRC): A plot of the shift in an instantaneous state (phase) of the circadian rhythm/oscillation caused due to a perturbation (using a zeitgeber) at different times of the rhythm under constant conditions.

Phase-control: The phenomenon wherein rhythms free-run under constant conditions post entrainment from the phase determined by the last entraining cycle.

Phase-relationship/Phase of entrainment (ψ_{ENT}): Difference in time (either in hours or degrees or any other unit of time) between any instantaneous state (phase) of the circadian rhythm/oscillation and that of a reference phase of the environmental oscillation.

Photophase: Duration of the day when light is present.

Power of a rhythm: The amplitude of a periodogram that measures robustness of τ.

PR: Percent/Percentage Rhythm; proportion of overall variance in the rhythm explained by the fitted model (used in this thesis in the context of fitting a multiple component COSINOR).

PTTH: Prothoracicotropic Hormone.

RHEP: Relative Height of Evening Peak.

SCN: Suprachiasmatic Nucleus.

Scotophase: Duration of the day when light is absent.

Skeleton photoperiod: An entraining regime wherein two pulses, one mimicking dawn and the other mimicking dusk are provided to act as a 'skeleton' to a full photophase.

s-LNv: small Ventral Lateral Neurons.

sNPF: short Neuropeptide F.

Subjective day: Under constant conditions, part of the day when light should have been present, but is not, according to previous entraining regime.

Subjective night: Under constant conditions, part of the day when light should not have been present, and is not, according to previous entraining regime.

TC: Thermophase/Cryophase.

Temperature compensation: Property of circadian rhythms (clocks) wherein period under constant conditions at different ambient temperatures remains constant (by some compensatory mechanisms).

Thermophase: The warm phase of a temperature cycle.

TT: Abbreviation for thermophase:thermophase (constant darkness at high temperature).

Velocity response curve (VRC): Theoretically, a plot of the change in angular velocity of the circadian rhythm/oscillation caused due to a perturbation (using a zeitgeber) at different times of the rhythm under constant conditions.

Zeitgeber (German, *zeit*-'time', *geber*-'giver'): Any forcing oscillation (with period '*T*') in the environment that can entrain a biological oscillation, for instance, light/dark or temperature cycles. Zeitgeber cycles with *T* different from 24-h are referred to as *T*-cycles.

ZT: Zeitgeber Time; ZT00 refers to the time at which lights turn ON. For other zeitgebers, it is time at which the zeitgeber value starts to increase from its lowest value.

Synopsis

In this thesis, I report results from studies carried out to understand the inter-relationship between timing of behaviour, circadian organisation and mechanisms of entrainment. In order to do so, I use laboratory selection as a tool to generate and maintain replicate strains of *Drosophila melanogaster* that exhibit divergent timing of eclosion. One set of lines are selected for predominant eclosion during dawn (*early* stocks/chronotypes) and the other for predominant eclosion during dusk (*late* stocks/chronotypes). Using these *early* and *late* chronotypes, along with their ancestral, unselected *control* lines, I examine, mostly behaviourally, the correlated evolution of circadian organisation and entrainment properties of their circadian clocks using light and temperature cues.

In the first chapter, I describe the background of my study. I first talk about the discovery of 24-hour (h) rhythms and the logical jump from the observation of rhythms to a biological 'clock', regulating and driving them. I then discuss the origin and evolution of circadian clocks. Here, I discuss that a key function of clocks is to schedule behaviour, physiology and metabolism to specific times of the day. Therefore, I describe how appropriate scheduling is indeed a consequence of entrainment. I briefly discuss the different mechanisms of entrainment. Subsequently, I describe the two different models of organisation of the circadian network, i.e., hierarchical entrainment (as in the *master-slave* or *A-B* organisation; originally described to explain timing of eclosion rhythms) and mutual entrainment (as in the *morning* (*M*) – *evening* (*E*) oscillator scheme; originally described to explain timing of activity/rest rhythms). I discuss how these models may interact with mechanisms of entrainment and regulate timing of behaviour, thus

defining the problem I have addressed in my thesis. Further, I develop a case for laboratory selection as an appropriate tool to answer the questions posed.

In the second chapter, I describe the selection regime and population maintenance protocol that our laboratory has used to generate and maintain *early*, *control* and *late* stocks for ~18 years (currently, over 320 generations of selection). Here, I report the direct responses to selection, correlated changes in clock properties of *early* and *late* chronotypes, and briefly review past studies that have been carried out to understand the underlying differences in the circadian clock architecture and entrainment mechanisms driving *early* and *late* eclosion. In the last part of this chapter, I briefly summarise my findings and results reported in this thesis. All subsequent chapters describe results from experiments that I carried out as part of my PhD work.

In the third chapter of my thesis, I report results from experiments that attempted to understand if and how hierarchical organisation of the circadian network regulating adult eclosion rhythm has changed in *early* and *late* stocks. I monitored the adult eclosion rhythm (i) under light/dark (LD) cycles with different constant ambient temperatures, and (ii) LD cycles with temperature cycles but with different amplitudes and different mean temperatures. My results from these experiments revealed that while the *early* chronotypes are invariant to temperature cues, phase of the *late* chronotypes is highly labile and appears to track temperature cycles even in the presence of LD cycles, thereby implying a stronger temperature sensitive clock in these stocks.

While regulation of the eclosion rhythm is typically explained within the framework of a hierarchical organisational scheme, activity/rest is thought to be regulated by a more mutual entrainment scheme wherein both the *M*- and *E*-oscillators are coupled to each other and regulate timing. In the fourth chapter, I attempted to understand differences in the *M*- and *E*-oscillator

organisation in *early* and *late* chronotypes using short LD cycles of 12-h periodicities. I argue that the *late* chronotypes reveal behavioural features attributable to a strong *E*-oscillator in the network.

Owing to (i) the stronger *B*-oscillator in the eclosion rhythm and *E*-oscillator in the activity/rest rhythm of *late* stocks, and (ii) the overlap, to a certain extent, between cells that regulate evening activity and that are sensitive to temperature in *Drosophila melanogaster*, next I asked if entrainment of activity/rest rhythms to temperature cues differ between *early* and *late* chronotypes. Results of these studies are reported in the fifth chapter of my thesis. I find that the activity/rest rhythm of *late* stocks is indeed more sensitive to temperature. Further, under temperature cycles, it is the evening component of the activity bout that shows among-stock difference. Interestingly, most results from these experiments pointed towards the fact that the *early* and *late* stocks may have evolved divergent temperature pulse phase response curves, thereby indicating that entrainment to temperature cues in these stocks is perhaps attributable, more strongly, to the non-parametric model of entrainment.

In the sixth chapter, I describe results of experiments done to systematically test predictions from the non-parametric model of entrainment to light. Further, I used a recent parametric model of entrainment that allows one to make quantitative predictions regarding phases of entrainment (Circadian Integrated Response Characteristic or CIRC). My results indicate that most predictions of the non-parametric model do not hold true in case of our populations and parametric effects of light explain photic entrainment of the *late* stocks.

In my seventh chapter, I summarise results from all previous data chapters. I also discuss a hypothesis regarding the association between timing of behaviour, circadian clock organisation

and relative contributions of parametric and non-parametric effects of time-cues. Further, I discuss future experiments, that may help gain data to test this hypothesis.

My eighth chapter has two sections, both of which are tangential to the main thesis reported here. In the first section I discuss results of a collaborative study with two other members of our laboratory, Dr. Nikhil K.L. (past member) and Mr. Arijit Ghosh (present member), that attempts to understand the genomic signatures associated with *early* and *late* chronotypes. In the second section, I describe an open-source application that I built on the *R* platform for facilitating various analyses and visualisations of biological time-series data. Motivation for this part of my work was derived from the realisation that most software that are convenient to use are paid software and the ones that are free are cumbersome to use. I hope this tool will make analyses of rhythmic data easier and would be beneficial to the biological rhythms research community.

List of publications

1. **Lakshman Abhilash**, Arshad Kalliyil and Vasu Sheeba (2020) Activity/rest rhythms of *Drosophila* populations selected for divergent eclosion timing under temperature cues. *Journal of Experimental Biology* 223(11). bioRxiv: 10.1101/831347.
2. **Lakshman Abhilash**, Aishwarya Ramakrishnan, Srishti Priya and Vasu Sheeba (2020) Waveform plasticity under entrainment to 12-hour *T*-cycles in *Drosophila melanogaster*: behaviour, neuronal network and evolution. *Journal of Biological Rhythms* 35(2): 145–157.
3. **Lakshman Abhilash** and Vijay Kumar Sharma (2020) Mechanisms of photic entrainment of activity/rest rhythms in populations of *Drosophila* selected for divergent timing of eclosion. *Chronobiology International* 37(4): 469–484.
4. **Lakshman Abhilash**, Arijit Ghosh, Vasu Sheeba (2019) Selection for timing of eclosion results in co-evolution of temperature responsiveness in *Drosophila melanogaster*. *Journal of Biological Rhythms* 34(6): 596–609.
5. **Lakshman Abhilash** and Vasu Sheeba (2019) RhythmicAlly: Your R and Shiny based open-source ally for the analysis of biological rhythms. *Journal of Biological Rhythms* 34(5): 551–561.
6. **Lakshman Abhilash** and Vijay Kumar Sharma (2017) Time measurement in living systems: Human understanding and health implications. In *Space, Time and the Limits of Human Understanding* (Eds. Wuppuluri S and Ghirardi G): pp. 337–352. *Springer, Cham*.

7. **Lakshman Abhilash** and Vijay Kumar Sharma (2016) On the relevance of using laboratory selection to study the adaptive value of circadian clocks. *Physiological Entomology* 41(4): 293–306.

Chapter 1. Introduction

Parts of this chapter have been published in the two following review articles:

Abhilash L and Sharma VK (2016) On the relevance of using laboratory selection to study the adaptive value of circadian clocks. Physiological Entomology, 41(4): 293–306.

Abhilash L and Sharma VK (2017) Time Measurement in Living Systems: Human Understanding and Health Implications. In Space, Time and the Limits of Human Understanding (Eds. Wuppuluri S and Ghirardi G): pp. 337–352. Springer, Cham.

1.1. Rhythms of life

The concept of 'time' has been of profound interest and a topic of debate, with deep roots in religion and philosophy, from ancient times to the present day. Some philosophers have even dismissed time as being a mental construct and 'unreal' (Kant, 1781; McTaggart, 1908). While a debate on the 'nature of time' is worthy of a thesis in itself, here I will restrict my discussion to 'time *in* nature'; in other words, time in the biological world.

It is not news that humans sleep at certain times of the day and eat at certain times. It is also known that we work more efficiently at only specific times of the day and less efficiently at other times (Skene and Arendt, 2006). Is such a time-dependent phenomenon restricted only to us humans or is it common to other organisms? More importantly, are such rhythms a mere consequence of the ever-alternating day and night caused due to the earth's rotation?

Aristotle, as early as ~4th century BC, observed that several other animals also sleep at night just like us humans (cited from Daan, 2010). Similar observations regarding daily rhythms were also made by Androsthenes around the same time (cited from Nikhil and Sharma, 2017). While such descriptions of temporal processes on a daily/24-hour (h) scale were among the first of its kind in biology, it took more than 2000 years for the first experimental evidence for (i) the presence of such rhythms in other organisms, and (ii) the endogenous nature of such rhythms; and these experiments, thus paved the way for the study of yet another extraordinary feature of living systems – a biological clock!

A French astronomer, Jean-Jacques d'Ortous de Mairan, in the 18th century observed that the leaves of *Mimosa pudica* (*touch-me-not* plant) droop down every night, as opposed to their upright position during the day. De Mairan wondered if this was a mere consequence of the

presence/absence of sunlight, and to understand the source of the rhythm, transferred the plant to a dark place, outside the influence of sunlight. He found that rhythms in leaf movements persisted even when the plant was not exposed to cycles of light, thereby establishing one of the fundamental properties of such rhythms: persistence in the absence of any external time-cue (reviewed in Daan, 2010). However, it took almost two centuries, and a wide range of additional experiments for the biology community to accept that such rhythms were indeed endogenous. Some of these experiments included observation of conidiation rhythms in *Neurospora* in space (Sulzman et al., 1984), outside the influence of earthly geophysical cycles and wheel running activity in rodents in the South Pole, to avoid potential electromagnetic influences that may drive rhythms (Hamner et al., 1962). These experiments were motivated by the strong opposition to the idea of endogenous rhythms in plants by leading plant physiologists of the time, such as Julius Sachs and Willhelm Pfeffer (see Daan, 2010). While these experiments proved useful to establish the ubiquity of rhythms, much of this effort could have been avoided if some results from the early 19th century were interpreted better. A swiss botanist, Augustin Pyramus de Candolle, performed similar experiments as those of de Mairan by transferring *Mimosa* plants to constant light (LL). De Candolle found that the persistent rhythms of leaf movement had a 'free-running' periodicity (FRP) of ~22-h. This implied that whatever is driving such rhythms must be endogenous and cannot be a consequence of physical factors that may be cycling in the environment as a consequence of the earth's rotation (reviewed in Daan, 2010).

1.2. Circadian timing systems as biological clocks: A timekeeper within?

Such endogenous rhythms, and therefore temporal order, within the organism can be maintained only if time-keeping is efficient, and this raised two major questions that concerned researchers regarding the nature of time-keeping in organisms: (i) Do organisms have the ability to measure the passage of time? and (ii) Can circadian timing systems serve as biological clocks?

Gustav Kramer, a well-known German zoologist and ornithologist, while studying bird navigation stumbled upon some remarkable evidence which suggested that organisms may have the ability to measure time. It was well known at the time that birds migrate north during spring and this they do using the sun as a compass. Kramer argued that it was possible for birds to navigate uniformly in the same direction using the continuously moving sun as a reference only if they had a timekeeping mechanism in place; in other words, *eine biologische uhr* (German for 'a biological clock'; Kramer, 1952). Additionally, experiments by Karl von Frisch, an Austrian ethologist and Nobel laureate demonstrated that organisms could keep time and that circadian timing systems may play a key role in doing so. Von Frisch and his student Ingeborg Beling marked individual bees and trained them to feed on sugar solution from an artificial feeder at the same time every day (once every 24-h) and on the test day did not provide the sugar solution, and noted that most individuals arrived at the feeder within the training time, thereby suggesting time-keeping ability in honeybees. Such training was not successful when the bees were trained to feed once every 19- or 48-h, implying that a 24-h (or circadian Latin for *about-a-day*) timing system was in use for time-measurement (see Moore-Ede et al., 1982).

However, rate of biochemical reactions (that may govern circadian rhythms) vary with changes in temperature akin to early mechanical watches, which had metal balance springs that would expand or contract depending on the ambient temperature, thereby providing incorrect estimates of time. Colin Pittendrigh (one of the pioneers of the study of circadian rhythms) asked if natural selection has solved this problem of accurate time-keeping even under different ambient temperatures in organisms, and since this aspect would be more relevant to poikilotherms (individuals whose body temperature changes with changes in environmental temperatures) and not so much to mammals such as ourselves, he used the fruit-fly (*Drosophila*) model to address this question. Pittendrigh demonstrated that the period of circadian rhythms in *Drosophila* (and therefore its ability to measure time) under constant conditions was indeed maintained stably at constant high or constant low ambient temperatures, a phenomenon referred to as temperature compensation (Moore-Ede et al., 1982; Pittendrigh, 1954).

Several such experiments revealed, for the first time, that the biochemical systems that generate persistent, endogenous and innate circadian rhythms could measure passage of time robustly across temperature fluctuations, thereby suggesting that the functional significance of such systems is to appropriately schedule behavioral, physiological and metabolic activities in-sync with cycling abiotic and biotic factors of the environment. This synchronization of endogenous rhythms to the environmental cycles by daily resetting of the underlying 'biological/circadian clocks' in response to time-cues is known as entrainment and is considered to be one of the clock's most crucial functions.

1.3. Why do we have biological clocks? – Origins and evolution

Although justifying the origins and evolution of biological clocks is a herculean task in itself, here I briefly touch upon tentative answers to the following three questions and redirect the interested reader to Nikhil and Sharma (2017) and Vaze and Sharma (2013) for a detailed discussion of the same.

1.3.1. When did biological clocks originate?

The period of the Earth's rotation has undergone changes, and it is estimated that when cyanobacteria (the earliest organism whose biological clocks are well-studied) originated ~3.5 billion years ago, the length of one day was ~8-h. Our current understanding of biological clocks in cyanobacteria suggests a transcription-translation feedback loop-based mechanism comprising the *KaiABC* gene cluster with a periodicity of ~22-h. However, the *KaiA*, *KaiB* and *KaiC* genes do not appear to have evolved at the same time i.e., during the origin of cyanobacteria (see Figure 1.1). Comparative studies and gene homology analyses across several species suggest that *KaiC* was the first to appear (perhaps providing a negative feedback loop generating rhythms with ~4-h periodicity, by itself), followed quickly by *KaiB* (that may have lengthened periodicity of the clock as day-length on Earth became longer), and *KaiA* is thought to be the most recent addition to the loop (that may have given rise to cyanobacteria's present day periodicity) and is found only in *Synechococcus* spp. (one genus of cyanobacteria). Therefore, our best guess as to when biological clocks originated is at ~3.5 billion years ago (Figure 1.1; see Nikhil and Sharma, 2017 for a detailed discussion on this issue); however, this is only a conjecture.

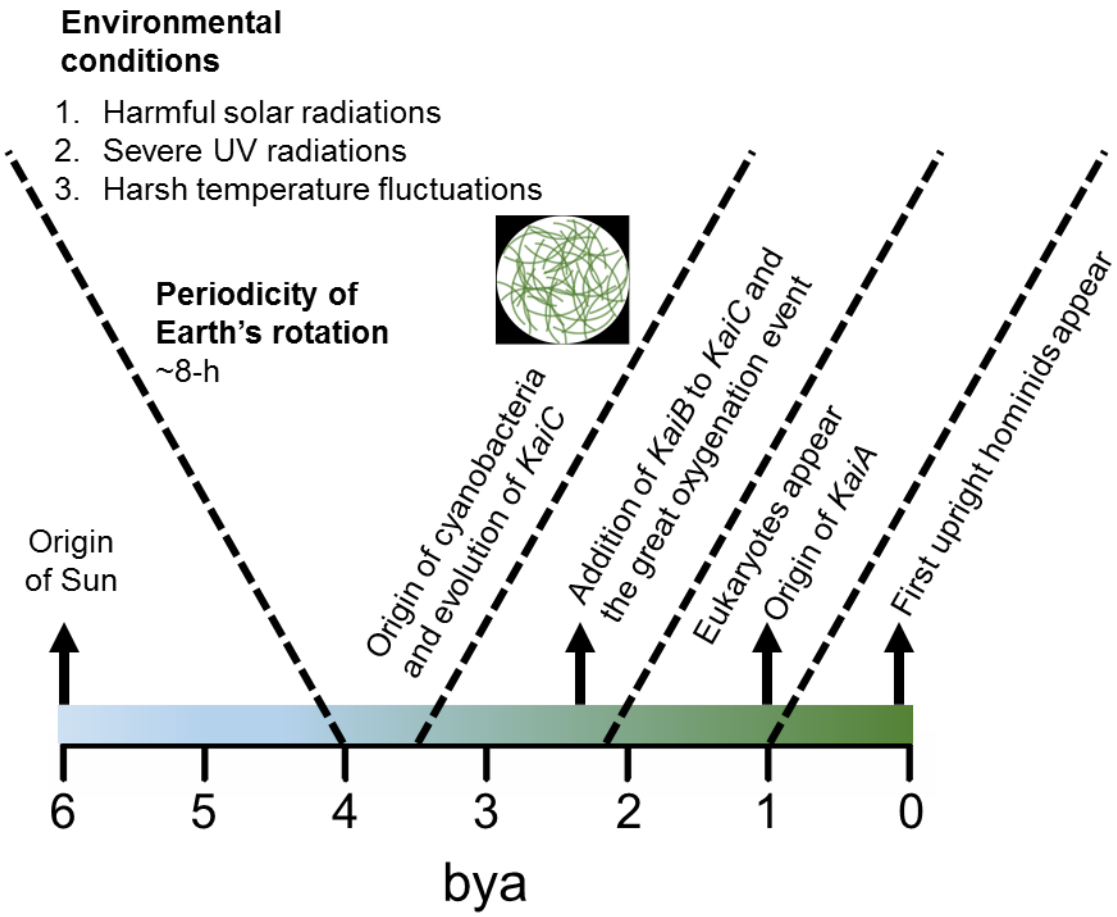

Figure 1.1: A timeline for the origin of biological clocks with respect to important events in the history of Earth. The *x*-axis label, 'bya', refers to billion years ago. See text for details on *Kai* genes.

1.3.2. Why did biological clocks first originate?

Charles Darwin is thought to have provided the first recorded explanation for why organisms may need biological clocks, and what may have driven the evolution of the same in the first place. Around the late 19th century, he systematically recorded movements in plants and made detailed observations of several plants that open and close their leaves at certain times of the day (Darwin and Darwin, 1881). This led him to believe that some features in the environment may be deleterious to the plant's survival, for example, exposure to prolonged duration of light. He argued that to avoid such damage, plants 'choose' to open and close their leaves at relevant times of the

day. Subsequently, two major theories have been proposed to understand the first origins of biological clocks, both of which are discussed at length elsewhere (Nikhil and Sharma, 2017). Organisms such as cyanobacteria, whose biological clocks are extensively studied, originated much before the great oxygenation event that occurred ~2.5 billion years ago (Figure 1.1; reviewed in Nikhil and Sharma, 2017). It is conceivable that organisms that lived on Earth much before this event would have been exposed to extreme temperatures and solar radiations (see Figure 1.1), and these may have been potent factors driving the origin of biological clocks; the idea being that clocks would help time behavior and physiology appropriately to avoid harsh conditions to the best possible extent. In this regard, we have the 'escape from light' hypothesis, where it is hypothesised that factors such as exposure to UV-radiations (an effect of which is increased errors in DNA replication and photochemical RNA and protein reactions) may have led to the origin of biological clocks that may help organisms avoid such harmful effects of environmental factors (Nikhil and Sharma, 2017; Pittendrigh, 1965).

On the other hand, we have the 'endosymbiotic coordination' theory. It is believed that the origin of eukaryotic life-forms (see Figure 1.1) lay in multiple prokaryotes coming together as endosymbionts that formed something of a precursor for the present-day cellular organelles. It was thought that along with cellular compartmentalization of such proto-organelles, temporal coordination of interacting sub-cellular processes is essential to avoid intracellular chaos (Kippert, 1987; Levandowsky, 1981; Nikhil and Sharma, 2017). However, neither of these hypotheses have very convincing data to support them, and hence remain open questions to date.

1.3.3. Why do we need biological clocks in the present day?

Natural factors that may have driven the origin of biological clocks may not be so obvious to us today. Then, why do we still have biological clocks? Do we really need them? What functional

role may it have, to be still retained by natural selection? Two major hypotheses have been raised to understand the same.

1.3.3.1. Intrinsic advantage hypothesis

Although the central rhythm generator for most animals is in the brain, rhythms in peripheral tissues such as adrenal gland, liver, heart and intestines have also been discovered over the years (see Dunlap et al., 2004; Moore-Ede et al., 1982). This implied that for the organism to function optimally, it is crucial for all these internal rhythms (and the clocks that drive them) to be synchronised such that temporal harmony within the organism can be maintained. This hypothesis of how biological clocks may be adaptive is referred to as the intrinsic advantage hypothesis.

Cockroaches were elegantly used to demonstrate that the suboesophageal ganglia (the clock regulating activity-rest rhythm) when out-of-sync with other constituent clocks of the body led to the development of tumours (Harker, 1956). This was later attributed to desynchrony among various biochemical oscillations (reviewed in Vaze and Sharma, 2013). Additionally, in case of intracellular metabolism, components of different biochemical pathways may be incompatible with each other, as is the case with nitrogen fixation and photosynthesis in cyanobacteria, and it is thought that biological clocks may serve to create separate temporal niches to avoid such biochemical clashes (Ditty et al., 2003; Mitsui et al., 1986; Nikhil and Sharma, 2017). Modern lifestyles which include rapid travel across multiple time-zones, or shift-work schedules have revealed that different biological rhythms (such as those in body temperature and psychomotor performance) take different durations to re-adjust to the new time-zone, thereby creating disharmony among constituent physiological processes in humans, leading to much discomfort, a condition known as jetlag (discussed in the next section; Moore-Ede et al., 1982), and this therefore suggests that synchrony among constituent biological clocks is essential for well-being.

Unequivocal evidence for such a hypothesis comes from studies performed in the laboratory that monitors trajectories of biological clock evolution in real-time (Abhilash and Sharma, 2016). If the intrinsic advantage hypothesis were not true, one may hypothesise that biological clocks in populations living under constant (non-cyclic) environments would gradually regress, under the assumption that maintaining circadian clocks is costly to the organism. Several studies using *Drosophila* populations that were reared under constant illumination and darkness for many hundred generations tested this hypothesis (Imafuku and Haramura, 2011; Sheeba et al., 1999, 2002; Sheeba et al., 2001; Shindey et al., 2016). These studies reported the persistence of robust circadian rhythms in their respective *Drosophila* populations despite being reared under non-cyclic environments for several hundreds of generations, suggesting that their biological clocks had not regressed over time. Moreover, it was also observed that populations maintained under constant darkness (DD) indeed evolved increased robustness of rhythms (Shindey et al., 2016).

Such data from multiple experiments compel us to believe that an evolutionary advantage of possessing circadian clocks in the present day would be that they could synchronise and temporally partition internal and incompatible processes.

1.3.3.2. Extrinsic advantage hypothesis

Variation is the essence of natural systems. Daily variations in physical parameters of the earth due to its rotation include cycles in light intensity and spectral composition, temperature, humidity and barometric pressure among several others. Such concerted cycling of several parameters gives rise to a complex network of 'favourable' and 'unfavourable' times of the day for individuals. It is thought that biological clocks exist to help organisms time their various behaviours to such ecologically favourable times of the day so that it is in-sync with its environment, thereby enhancing survival and reproduction.

Evidence for this hypothesis comes from several lines of investigations. Early studies indicated that in cyanobacteria appropriate timing of events with respect to laboratory light/dark (LD) cycles provided competitive advantage over other strains with inappropriate timing (Ouyang et al., 1998). Additionally, some interesting experiments were carried out in the wild to test the extrinsic advantage hypothesis. Antelope ground squirrels are generally diurnal, but it was observed that when their biological clocks are removed, they become more active in the night, and mortality due to predation in these animals was 30% more than the ones with intact clocks (DeCoursey et al., 1997). Similar experiments were performed with free-living chipmunks and the results were strikingly similar (DeCoursey et al., 2000). Furthermore, several studies have shown that aberrant or misaligned biological clocks lead to severe reduction in survival and Darwinian fitness (measure of an individual's contribution to the gene pool of the next generation) in *Drosophila* (reviewed in Nikhil and Sharma, 2017). Additionally, several studies have also reported the adaptive evolution of timing of behaviour in real-time (reviewed in Abhilash and Sharma, 2016), thereby suggesting that appropriate timing of behaviour may be important for survival and reproduction, and biological clocks help organisms 'choose' favourable times to perform functionally relevant tasks.

Studies described in this section have led to our understanding of why biological clocks may have originated, when they may have originated, and what functions they serve today. Although, the present-day adaptive functions of biological clocks are well-studied and agreed upon, the why and when of origins of biological clocks are still open questions awaiting rigorous experimentation and unequivocal data.

1.4. How do circadian clocks schedule behaviours to specific times of the day?

Given the importance of circadian clocks in timing behaviours to specific times of the day, it is crucial to understand how circadian clocks bring about such scheduling. Decades of research and empirical observations have understood this complex phenomenon at two biological levels, each of which shall be discussed here.

1.4.1. Regulation of timing at an organismal level

Our understanding of how timing is regulated at the organismal level stems from treatment of the circadian clock as a single entity and the effect of zeitgeber (German for *time-giver*) impulses on the behaviour of the organism. It is now well established that phase-relationship of behaviour with the zeitgeber is a consequence of entrainment (Daan, 2000; Daan and Aschoff, 2001; Johnson et al., 2003; Pittendrigh, 1981; Roenneberg et al., 2003; Roenneberg, Dragovic et al., 2005; Roenneberg, Hut et al., 2010). Entrainment is the phenomenon by which external time-cues such as light and temperature synchronise circadian rhythms such that their near 24-h periods are now exactly 24-h and therefore behaviours are repeated every day at the same local time. How this phase-relationship is a consequence of entrainment can be understood once we delve into the mechanisms of entrainment.

1.4.1.1. Phasic entrainment (non-parametric model)

Two major models for how entrainment of circadian rhythms happen have been proposed so far, and the more widely accepted model among those is referred to as the non-parametric model (Daan, 2000; Pittendrigh and Daan, 1976a). This idea stemmed from the early discovery that circadian rhythms phase-shift in response to brief light pulses in a time-of-day dependent manner

in *Gonyaulax* (Hastings and Sweeney, 1958), *Drosophila* (Pittendrigh and Bruce, 1959), rodents (reviewed in Daan, 2000) and flying squirrels (DeCoursey, 1960a, 1960b). It was observed that light pulse during the subjective day phase did not shift the rhythm phase, while pulses during early subjective night induced a delay shift whereas during late subjective night induced an advance shift. A plot of extent of phase-shift in response to zeitgeber pulse as a function of the internal time of the organism is referred to as a Phase Response Curve (PRC). Pittendrigh and colleagues made use of PRCs to synthesise a model of entrainment that would describe how organisms synchronise their behaviour to external environments (Pittendrigh and Daan, 1976a). Pittendrigh and Daan proposed that the difference between the free-running period (FRP; τ) and the period of the zeitgeber (T) is reset everyday by phase-shifts. Therefore, in the presence of an LD cycle, it is argued that the organism's PRC will become aligned to the LD cycle such that the net shift in phase ($\Delta\psi$) will be equivalent to the difference between τ and T; or in other words the model can be formalized as $\tau - T = \Delta\psi$. The non-parametric model is also called the phasic model owing to the effect of light occurring via instantaneous changes in the phase of the clock. The model, therefore, assumes that light only during the transitions of an LD cycle are important, and that τ and the PRC are fixed entities. As a consequence of this model, a generally accepted prediction is that organisms with circadian clocks that have longer free-running periods will phase-lead more or phase-lag less relative to the zeitgeber as compared with organisms that have shorter free-running period. Indeed, under the assumptions of a fixed FRP and PRC, the model has received remarkable support from experimental data in being able to predict phases of entrainment in *Neurospora* (Roenneberg, Dragovic et al., 2005), *Drosophila* (Hamblen-Coyle et al., 1992; Srivastava et al., 2019), rodents (Pittendrigh and Daan, 1976a) and humans (Duffy and Czeisler, 2002; Wright et al., 2005).

1.4.1.2. Tonic entrainment (parametric model)

An alternative model for entrainment proposes that entrainment of circadian rhythms occur not via phase-shifts but via continuous changes in the angular velocity of the clock in response to the zeitgeber (Daan, 2000; Daan and Aschoff, 2001; Pittendrigh, 1974; Swade, 1969). Although realistic, this model did not gain as much popularity as the phasic entrainment model perhaps owing to the lack of a quantitative way of making and testing predictions using this model. The parametric model suggested the presence of a so-called Velocity Response Curve (VRC) that describes the change in velocity of phase progression of the clock in response to stimuli as a function of time-of-day (Daan and Pittendrigh, 1976; Swade, 1969). The limitation of the model was that, at any given point, estimating the angular velocity of the clock is not possible. However, this model proved important and plausible because experimental evidence showed that light intensity altered the values of τ (Aschoff, 1960; Daan and Aschoff, 2001; Daan and Pittendrigh, 1976), therefore, violating one major assumption of the non-parametric model. Such after-effects (change in τ caused due to prior entrainment to various light regimes) were taken as evidence to suggest the presence of a parametric effect of prolonged durations of light on the circadian clock such that τ (a parameter of the clock) could change in a time-of-day dependent manner. Owing to the nature of this model, and because light is expected to integrate responses over long durations, it is possible that organisms with different free-running periods show the same phase of entrainment just because the shape of their VRCs are different. This is an important issue that distinguishes the parametric and non-parametric models, in terms of the predictions they yield regarding the association between τ and phase-relationship with the zeitgeber.

1.4.2. Regulation of timing at an organisational level

While the above discussed models have been incredibly important in helping us understand how behaviours are timed to specific parts of the day, they describe how entrainment mechanisms operate at a systemic level to regulate timing. Several studies in the past have demonstrated the multi-oscillator nature of circadian organization and the synergistic effects of multiple zeitgebers on phasing (Bell-Pedersen et al., 2005; Ito and Tomioka, 2016; Yoshii et al., 2009). A multi-oscillator organizational scheme, will therefore, pose complexity in terms of how entrainment mechanisms regulate timing. However, fundamental empirical studies and theory have helped make incredible strides in understanding entrainment at an organizational level.

1.4.2.1. Hierarchical entrainment within the organism

Some experiments in mid-late 1930s by Kalmus and Erwin Buenning suggested that the period of circadian rhythms was dependent on temperature (Kalmus, 1940; Pittendrigh, 1954). Pittendrigh, on the other hand, was of the opinion that for a timekeeper to be of functional relevance, its period must be temperature insensitive or compensated (see earlier section). To tackle this problem, Pittendrigh and colleagues used the *Drosophila* eclosion rhythm. The eclosion rhythm was monitored under LD cycles and immediately upon transfer of these cultures to DD with a drop in temperature, eclosion in the following cycle appeared to be delayed, implying a lengthening of period in response to the temperature drop (Pittendrigh, 1954). Similar results were reported by Kalmus and Buenning. However, Pittendrigh found that this was a temporary effect and the rhythm in DD reverted to its original periodicity fairly quickly in subsequent cycles, a fact ignored by Kalmus. Furthermore, while performing and analyzing results from phase-shift experiments using the *Drosophila* eclosion rhythm, Pittendrigh and colleagues observed a few peculiar results; (i) the steady state phase attained by the rhythm is in response to a zeitgeber pulse seen by the

organism several cycles earlier, (ii) the presence of transients before steady state phase-shift is achieved, and (iii) the number of transients taken, was dependent on the time-of-day when pulse was administered (Pittendrigh et al., 1958; Pittendrigh and Bruce, 1959).

All these results, Pittendrigh and Bruce argued, were incompatible with the idea of a single oscillator. It was argued that these results can be explained within the framework of a hierarchical organization of oscillators within the organism (Pittendrigh, 1974; Pittendrigh and Bruce, 1959). The authors proposed that there is a light sensitive, temperature insensitive pacemaker or master clock (the *A*-oscillator). This drives a second peripheral or slave clock (the *B*-oscillator). The reason transients are observed is because the master clock, after immediately resetting to the phase dictated by the light cycle, entrains the slave clock which takes several cycles to attain the phase dictated by the master clock. Additionally, Pittendrigh proposed that the slave clock's period is temperature sensitive and entrainable by temperature cycles (Pittendrigh, 1974; Pittendrigh and Bruce, 1959).

In line with such a formulation of temporal organization within the organism, many studies have indeed found peripheral clocks in a wide range of tissues outside the site of the pacemaker, which is thought to be the central oscillator, in mammals, birds, mollusks (*Aplysia*) and insects (such as *Drosophila*). Moreover, it has also been found that there is significant heterogeneity in the properties of the slave oscillator (Bell-Pedersen et al., 2005; Ito and Tomioka, 2016). Here I will particularly discuss the hierarchical organization underlying the eclosion rhythm in *Drosophila melanogaster*. While behavioural experiments in Pittendrigh's laboratory helped establish, without doubt, that the *Drosophila* eclosion rhythm is regulated by a system of two hierarchically arranged oscillators, it took more than 40 years to find anatomical substrates for these oscillators. In the early 2000s, by using genetic manipulations, Amita Sehgal's laboratory showed that

molecular clocks in the prothoracic gland (PG) is necessary for rhythmic eclosion, thereby providing anatomical evidence for a peripheral/slave clock for this rhythm (Myers et al., 2003). Moreover, the authors also showed that for appropriate gating of rhythms and functioning of the PG clock, the clock in the small ventral lateral neurons (s-LNvs; the pacemaker in *D. melanogaster*) is necessary. More recently, another study dissected out the circuit regulating the rhythm in greater detail. The authors found that the s-LNvs communicate temporal information to the PTTH (prothoracicotropic hormone) neurons via the inhibitory action of short neuropeptide-F (sNPF). This information is further relayed to the PG clock and this regulates levels of ecdysone, thereby committing to eclosion in the next available gate (Selcho et al., 2017). Additionally, the authors show that knockdown of the PTTH neuropeptide renders eclosion arrhythmic under constant conditions, therefore implying a role for PTTH in circadian rhythmicity. Interestingly, when entrained to temperature cycles, eclosion was rhythmic in these fly lines, implying that the PG clock is directly entrainable to temperature cycles. Furthermore, the authors showed that slowing or speeding the clock in the s-LNvs directly affected the period of eclosion rhythms under constant conditions, as opposed to when the clock speed was altered only in the PG clock. These results conclusively establish that the s-LNvs – PG clock axis function in a hierarchically organized temporal program that regulates eclosion rhythms in *Drosophila*.

Owing to the properties of the individual oscillators in a hierarchical or master-slave organization, it is intuitive that different environmental time-cues (zeitgeber), namely light and temperature may have different entraining effects on the organism's behaviour. These effects are likely to be contingent upon (i) sensitivity of the *A*-oscillator to light, (ii) sensitivity of the *B*-oscillator to temperature, (iii) the coupling strength between the two oscillators, and (iv) the sensitivity of the coupling agent to either zeitgeber. Sensitivity of each of these oscillators to light and temperature,

respectively, is of course determined by the phase/velocity responses of the system to these zeitgebers, thereby indicating a close link between the hierarchical structure of circadian organization and the mechanisms of entrainment.

1.4.2.2. Mutual entrainment within the organism

While many results from a wide range of organisms indicate towards hierarchical structure of temporal organization, another prominent structure of temporal organization within organisms is that of mutual entrainment between multiple oscillators (Pittendrigh, 1974). This idea stems from few entirely different behavioural observations from those discussed above; (i) many organisms under laboratory conditions and in the wild show bimodal activity patterns, with a predominant bout of activity around dawn and another around dusk, and (ii) under LL conditions, it was observed that hamsters gradually become arrhythmic, and after a few weeks show two bouts of activity that stably run with a phase-difference of 180°, until at a point when they merge with each other to display a consolidated single bout of activity. Importantly, these two bouts of activity free-run with different periodicities and they are both different from the periodicity of the consolidated bout, and this 'splitting' phenomenon is dependent on ambient light intensity (Pittendrigh, 1974; Pittendrigh and Daan, 1976b). Such splitting and 're-fusion' of activity was thought possible only as a consequence of at least two mutually coupled and entrained oscillators.

This phenomenon prompted the formulation of a dual oscillator model, that accounted for bimodality in activity and seasonal adaptation of activity in many organisms (Pittendrigh, 1974; Pittendrigh and Daan, 1976b). It was proposed that one oscillator is locked to dawn and regulates the morning component of the total activity bout, hereafter referred to as the *M*-oscillator. The second is locked to dusk and drives the evening component of the activity bout, hereafter referred to as the *E*-oscillator. It was proposed that the period of the *M*-oscillator (τ_M) shortened and that

of the *E*-oscillator (τ_E) lengthened with increasing light intensity. Under mutual coupling, the two oscillators interact such that the system's free-running periodicity (τ) is different from either τ_M or τ_E. Further, the relative influence of each of the oscillator on the other is dependent on the phase-relationship between the two oscillators (ψ_{EM}; Helfrich-Förster, 2009; Pittendrigh and Daan, 1976b).

About 30 years later, almost parallelly, several groups identified anatomical substrates corresponding to the *M*- and *E*-oscillators in rodents and *Drosophila*. Among the first to show anatomically distinct locations responsible for the two oscillators was a study from William Schwartz's laboratory wherein the authors showed that electrical activity peaked at different times in the rostral and caudal Suprachiasmatic Nucleus (SCN; site of the pacemaker for activity rhythm in mammals) in the Syrian hamster (Jagota et al., 2000). Similar results were observed in the Siberian hamster which were suggestive of the fact that perhaps this anatomical organization is present only in photoperiodic mammals (Hazlerigg et al., 2005). Subsequently, a study using non-photoperiodic mice showed similar patterns of electrical activity along the rostrocaudal plane of the SCN, implying the pervasiveness of such an organizational scheme (Naito et al., 2008). *D. melanogaster* activity/rest rhythms under LD cycles are sharply bimodal, with one peak coinciding with dawn and the other coinciding with dusk. Using two different approaches, two groups simultaneously showed that molecular oscillations in the s-LNvs (described in the previous section) are necessary and sufficient for the morning bout of activity (Grima et al., 2004; Stoleru et al., 2004). Further, the lateral dorsal neurons (LNds) and the 5th s-LNv were necessary and sufficient for the evening bout of activity. Since then, the s-LNvs are referred to as the *M*-cells and the LNds and the 5th s-LNv as the *E*-cells. Furthermore, the authors showed that the *M*-cells are sufficient for persistence of rhythms under DD.

It is important to note here that, Pittendrigh and Daan also suggested that under mutual coupling, the system's phase-responses to light could be such that the *E*-oscillator only exhibits phase-delays whereas the *M*-oscillator exhibits only phase-advances, thereby providing a system wherein the two oscillators together determine the PRC of the system. This presumption found evidence in experiments using *Drosophila*. It was found that the organism showed only phase-advances when the *M*-cells (s-LNvs) were activated, and only phase-delays when the *E*-cells along with the large LNvs (l-LNvs) were activated (Eck et al., 2016). These results, akin to the previous section, highlight the intimate link between mutual entrainment of circadian oscillators and the mechanisms of entrainment.

1.5. A mix of hierarchical and mutual entrainment in the adult *Drosophila* brain? – Defining the problem

While at first glance the hierarchical and mutual structures of circadian organization appear to be very different, there is a mix of both in the adult *Drosophila* brain. Many experiments in the past have revealed that the *M*-cells (s-LNvs) are necessary and sufficient for persistent rhythms of activity/rest and adult eclosion in flies, thereby establishing that the *M*-cells are pacemakers (Grima et al., 2004; reviewed in Helfrich-Förster, 2017; Stoleru et al., 2004). In other words, the *M*-cells can be envisaged as being at the top of a hierarchical organization. Further, PDF from the s-LNvs is thought to act as a synchronizer for the rest of the circuit and Pdf^{01} mutants show no rhythmicity under constant conditions and almost no morning activity under LD cycles (Renn et al., 1999). While the *M*-cells appear to be required for persistence of rhythms, recent experiments have shown that other parts of the neuronal circuit are responsible for the determination of power of rhythm and its period under constant conditions (Bulthuis et al., 2019). Further, two recent

studies performed cell specific knockout of molecular clocks using a CRISPR based method and found that the s-LNvs alone are not necessarily required for persistent rhythms in DD (Delventhal et al., 2019; Matthias Schlichting et al., 2019), thereby indicating that s-LNvs may also be part of a mutual entrainment paradigm rather than just at the top of a hierarchical organizational paradigm.

A key difference between the properties of oscillators that have a hierarchical versus mutual organization (besides unidirectional versus bi-directional coupling) is the temperature sensitivity of the slave/driven oscillator (Pittendrigh, 1974). The *Drosophila* brain circuit reveals some interesting similarities in the two schemes of organization in this respect. Studies have hinted that some cells in the dorsal brain (DN1s) are important for the evening component of the activity bout under LD cycles (Murad et al., 2007; Stoleru et al., 2004, 2007), while other studies suggest their importance for temperature entrainment of the circuit and therefore behaviour (Gentile et al., 2013; Yadlapalli et al., 2018; Zhang et al., 2010), thereby hinting at some degree of overlap between the aforementioned *B*-oscillator in hierarchical organisation and *E*-oscillator in the mutual organisation.

A review of such experiments reveals a mix of *M*- and *E*-cell properties that are not exactly within the purview of either the purely hierarchical structure or purely mutual structure of temporal organization. Moreover, while it is amply clear that circadian organization and mechanisms of entrainment are closely dependent on each other and regulate timing of behaviour (see previous sections), the nature of this relationship is not clear and has not been systematically examined. Through the work reported in this thesis, I attempt to understand this inter-dependence and hope that this work will be the foundation for other studies targeted towards understanding this complex relationship. To carry out this study, I have employed a laboratory selection based experimental approach, the rationale of which is discussed below.

1.6. Laboratory selection as a tool

Laboratory selection is an experimental strategy in which a set of replicate populations is derived from control (or ancestral) populations and is subjected to novel ecological conditions. Both these sets of populations are observed over multiple generations at regular intervals, and the control set of replicated populations represents the ancestral state because it is maintained in conditions similar to that of the experimental set except the novel ecology from the beginning of the experiment (Futuyma and Bennett, 2009; Garland and Rose, 2009). It is conceivable that the novel ecology may involve changes in any of the several parameters that describe the ancestral populations' abiotic, biotic or demographic features thereby enabling the novel ecology to provide selective forces that may facilitate the evolution of experimental populations in the laboratory.

The advantages of this method of collecting evidence to study the adaptive evolution of quantitative traits and their inter-relationships are manifold. Primarily, laboratory selection gives the experimenter a hold on replication and control of the experimental setup. Independent population level replicates (unit of replication in evolutionary studies must be populations and not individuals) along with their control/ancestral populations allows one to (i) estimate the contribution of random genetic drift to the evolved trait, and (ii) unravel multiple trajectories that may ultimately lead to the same phenotypic outcome. Use of laboratory selection allows one to make causal arguments in favor of the evolved trait being an adaptation to the imposed novel ecology. Moreover, in case of laboratory selection one need not make assumptions of ancestral relationships as the exact ancestors and the duration of divergence between the control and experimental populations are known. In addition, the functional state of the trait of interest in ancestral populations is also known, and conclusions about the adaptive values of traits are statistically reinforced due to the fact that independent replicate populations are assessed before

making any conclusions. Additionally, population genetic studies have demonstrated that evolutionary trajectories of the traits under selection largely depend on standing additive genetic variance for the trait, mating system, population size and sub-structure, and age-structure of populations among others (Hartl and Clark, 1997). Laboratory selection experiments are able to control for most of these factors as the experimental design requires populations used in the study to be maintained in large outbreeding conditions (keeps the variation high and avoids inbreeding related effects), in well-defined age-structures. Furthermore, laboratory selection in addition to facilitating hypothesis testing encompassing simultaneous reproducibility by replication at the population level and use of control populations, also allows the quantitative estimation of trajectories for the evolution of a trait, and the prospect of detailed genetic analyses (Garland and Rose, 2009). Such advantages of this method drive us to believe that, in comparison to other methods, laboratory selection may be an ideal and potent strategy to study (i) adaptive values of circadian clocks, (ii) the evolution of quantitative traits, and (iii) the inter-relationships between multiple quantitative traits.

As with every experimental approach, the laboratory selection approach also suffers from limitations (Futuyma and Bennett, 2009). Due to the rigor involved, and the emphasis on replication and control, such experiments are best suited for laboratory conditions albeit some successful experiments have also been undertaken in the wild in circadian biology (Daan et al., 2011; Horn et al., 2019). Moreover, to study evolution in real-time in the laboratory, two features are essential (i) large population sizes and (ii) short generation time, and this often limits the choice of model organisms for these studies. Another limitation of laboratory selection approach is the lack of ecological realism. Most of these studies vary only one ecological factor and observe the evolution of a trait based on which hypotheses regarding their adaptive values are proposed. In

the wild, a multitude of factors are likely to affect traits and their evolution, and therefore adaptive values of traits may be different from what we infer after manipulating ecology along only one dimension.

Nevertheless, if one were to weigh the advantages and limitations of all other methods of studying adaptive significance and traits underlying divergent circadian programs, it becomes clear that laboratory selection is among the few ideal strategies currently available (Abhilash and Sharma, 2016). In view of this, and owing to the fact that circadian organization, mechanisms of entrainment and timing of behaviour are quantitative in nature, we employ a laboratory selection-based approach to study the inter-dependence of these three. Using the *Drosophila melanogaster* eclosion rhythm as a model, we created and maintain a long-term laboratory selection experiment wherein strains with divergent timings of eclosion evolve in the laboratory (described in the next chapter). Using these strains, I examine behaviour of the eclosion rhythm and the activity/rest rhythm under a wide range of light and temperature regimes to ask if (i) circadian organization has evolved in these strains, and (ii) different mechanisms of entrainment account for entrained behaviour under light and temperature regimes. I addressed these questions in the hope to understand in more detail the interaction of circadian organization and mechanisms of entrainment to regulate timing of behaviour.

Chapter 2. Evolution of eclosion rhythm waveforms and circadian clock properties in populations of *Drosophila melanogaster* selected for divergent timing of behaviour

Parts of this chapter have been published in the following review article:

Abhilash L and Sharma VK (2016) On the relevance of using laboratory selection to study the adaptive value of circadian clocks. Physiological Entomology, 41(4): 293–306.

2.1. Background

As discussed in the previous chapter, selection in the wild is expected to occur on ψ_{ENT} and therefore studying clock properties that co-evolve with the evolution of timing of behaviour is critical to understand the functional significance of temporal programs in organisms. Prior attempts have been made to study the evolution of timing, all of which have been reviewed here.

In one study, the first of its kind, Pittendrigh (1967) used artificial selection on *D. pseudoobscura* populations to select for earliest eclosing and the very last eclosing flies each day, under LD cycles thereby giving rise to two eclosion chronotypes: *early* populations which eclose earlier in the day (advanced ψ_{ENT}) and *late* populations which eclose later in the day (delayed ψ_{ENT}). After 50 generations of selection, ψ_{ENT} of eclosion rhythm in *early* and *late* populations diverged by 4-h. These populations also diverged in the τ of their eclosion rhythm, where *early* populations had a longer τ relative to *late* populations. However, these populations did not show divergence in their PRCs, which according to one of the models of entrainment should have diverged to promote phase-divergence in behaviour (Pittendrigh, 1967). Subsequent laboratory selection experiments in the moth, *Pectinophora gosypiella* also showed similar results (Pittendrigh and Minis, 1971). However, another study on *D. auraria* showed results which were quite different from that reported for *D. pseudoobscura*, as *early* populations had shorter τ than *late* populations (Pittendrigh and Takamura, 1987). Although all these studies demonstrated that circadian clocks could evolve, there is no information available about population level replication and the maintenance regime. Another confounding factor in these experiments was that of development time. The authors of the above-cited studies have selected for fastest and slowest eclosing flies and this does not necessarily indicate evolution of circadian clocks regulating timing of eclosion but could reflect that the divergence in ψ_{ENT} of eclosion rhythm may be driven by the underlying differences in development time.

Another study reported effects of selection for morning and evening eclosion in two *Drosophila* populations *vis-à-vis*, *Oregon-R* and a wild-caught population, *W2* (Clayton and Paietta, 1972). In this study, unlike

the studies by Pittendrigh and colleagues, the authors selected flies eclosing in a fixed window of time in the morning and evening hours for over 4-5 successive days every generation thus ensuring minimal indirect selection for faster or slower development. Although circadian properties were not measured in these flies, it was reported that after 16 generations of selection, percentage of flies that eclose in the morning and evening selection windows were significantly higher as compared to control flies, suggesting that populations respond to selection on timing of eclosion. However, the authors acknowledged the limitation of using an inbred line (*Oregon-R*) in their study.

Keeping in mind the aforementioned limitations of previous studies, inconsistent results across studies and the lack of detailed analyses of evolution of clock properties in *early* and *late* populations, our laboratory generated and continues to maintain populations of *Drosophila melanogaster* that show divergent timing of the adult eclosion rhythm. These populations have been used for over 320 generations of selection to examine various clock properties underlying divergent timing, results of which are briefly discussed here.

2.2. Generation and maintenance protocol of *early* and *late* strains

Four replicates of *early* ($early_i$=1..4), *control* ($control_j$=1..4) and *late* ($late_k$=1..4) populations were derived from four common ancestral, large and outbred populations approximately 18 years ago. The *early* and *late* populations have been subjected to selection for timing of adult emergence phases since then and are maintained as independent populations for more than 320 generations now. The $early_i$, $control_j$ and $late_k$ populations that share the same subscript ($i = j = k$; referred to as 'blocks') share common ancestry and the populations with different subscripts indicate independent genetic substructure. All the 12 populations, four each of *early*, *control* and *late*, are maintained on banana-jaggery (B-J) medium under conditions of LD 12:12 (with ~70lux light intensity during the photophase) at 25±0.5 °C and ~65-70% RH on a 21-day discrete, non-overlapping generation cycle. Only the flies emerging between ZT21 to ZT01 (Zeitgeber Time 00, or ZT00 is the time of lights-ON in any LD cycle) on days 9^{th} to 13^{th} post egg collection are collected to form the breeding population for the next generation of the *early* populations. Similarly, only

the flies emerging during ZT09 to ZT13 on the same days as that of *early* populations are collected to form the breeding population for the next generation for *late* populations. On the other hand, flies emerging throughout the day are collected to form the next generation of *control* populations. On the 18th day after egg collection, flies are provided with a petri-plate full of B-J medium covered with live yeast paste as protein supplement, for three days. On day 21, cut plates of B-J medium are provided to all the fly populations for ~6-h to lay eggs. These eggs are collected and dispensed into vials in a batch of ~300 eggs/vial to initiate the next generation; we collect 24, 16 and 48 such vials each for the *early*, *control* and *late* populations, respectively, owing to inherent differences in the emergence in their respective windows and as a way of ensuring that there are sufficient flies in the cages for initiating the next generation.

Before performing any of the assays reported in this thesis, fly populations were subjected to one generation of common rearing (standardization) to minimize maternal and non-genetic inheritance effects on the trait being measured (Bonduriansky and Day, 2009). The offspring of the standardized populations are, henceforth, referred to as standardized flies.

2.3. Direct responses to selection

We analysed direct responses to selection using data collected from eclosion rhythm assays performed under LD 12:12 cycles (25 °C) at different times through the course of selection. We estimated percentage of flies eclosing in the morning window as the sum of all flies eclosing after ZT20 and up to ZT02, and in the evening window as the sum of all flies eclosing after ZT08 and up to ZT14. These windows (different from the selection windows as described above) are chosen because eclosion rhythms have been assayed in the laboratory in 2-h intervals at even time-points. Percentage eclosion in each window is estimated for each vial and these are averaged to provide estimates of block means. These block means are used in two mixed model three-way randomised block design ANOVAs to ask if there has been any response to selection across generations, one for each window. In these ANOVAs, genotype/selection regime (*early*, *control* and *late*) and generation number are treated as fixed factors and blocks is treated as a random factor.

Firstly, for the morning window we found a statistically significant effect of genotype × generation number interaction on percentage emergence ($F_{32,96}$ = 16.04, $p << 0.05$; Table 2.1). Tukey's HSD (Honestly Significant Difference) post-hoc test revealed that the *early* stocks started exhibiting increased percentage eclosion from the *control* stocks since as early as 55th generation of selection (Figure 2.1, top). On the other hand, the *late* stocks showed reduced percentage of flies eclosing in this window compared to *control* populations as early as the 30th generation of selection (Figure 2.1, top). Subsequently, the *early* populations continued to exhibit an increase in percentage eclosion till the 100th generation, beyond which the percentage does not change significantly (Figure 2.1, top). The *late* stocks showed continued reduction in percentage eclosion in the morning window till about generation 70, beyond which percentage remained stable (Figure 2.1, top). In the most recent experiment, I found that the *late* stocks showed further statistically significant reduction in percentage eclosion in the morning window compared to all previous generations (Figure 2.1, top). Owing to the fact that all three stocks show a reduction in percentage eclosion in the morning window, I think that this could be a run/experiment specific feature at that generation (Figure 2.1, top). However, the significant reduction in the *late* stocks and the lack of significance in case of the *early* stocks is indicative of this reduction being a possible outcome of stock specific changes to selection, at least in part. Assays in subsequent generations are required to gain clarity on this issue. In the evening window also, there was a significant effect of genotype × generation number interaction on percentage emergence ($F_{32,96}$ = 25.62, $p << 0.05$; Table 2.2). Similar post-hoc analyses as above indicated that while the *control* populations continued to show fairly low eclosion in the window, the *early* chronotypes had reduced their percentage eclosion to almost 0, 100 generations onwards (Figure 2.1, bottom). The *late* chronotypes showed steadily increasing percentage eclosion in the evening window with the most recent generation (310) showing a nearly 100% increase (Figure 2.1, bottom).

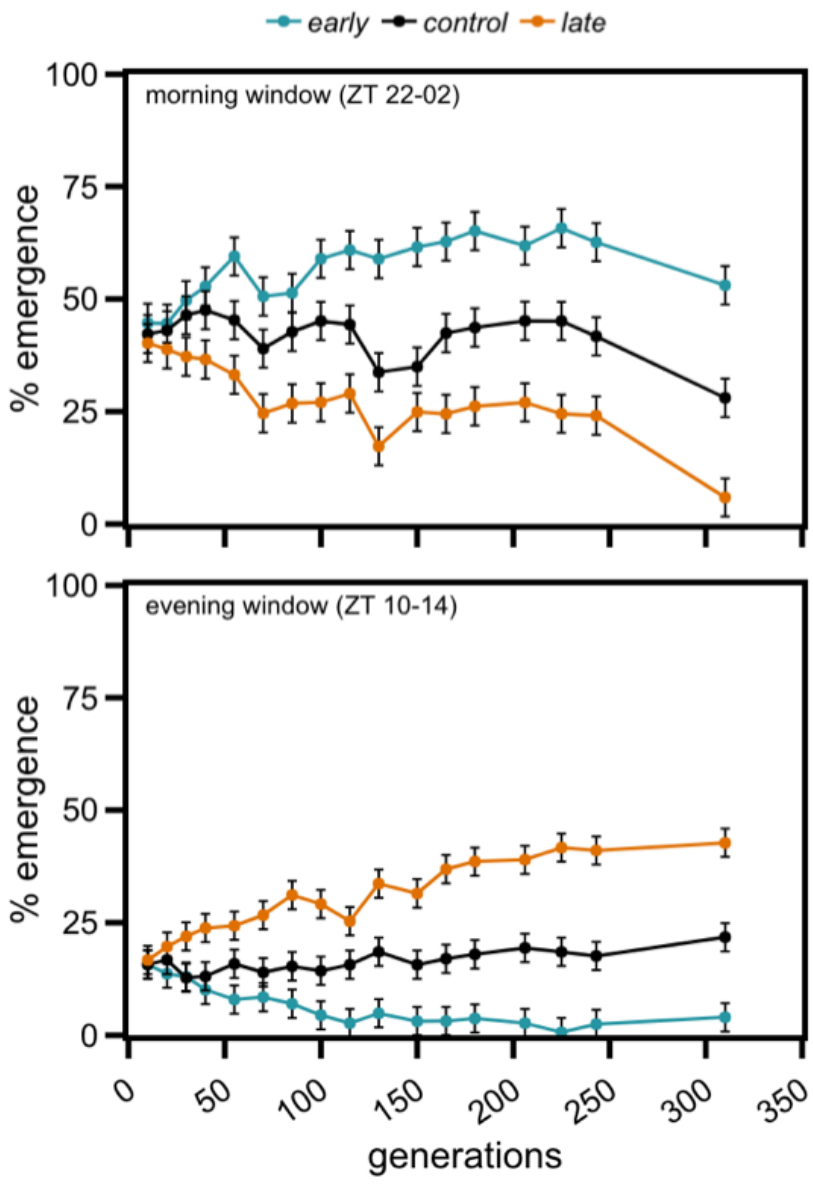

Figure 2.1: Direct responses of percentage emergence to selection in early and late stocks relative to control stocks in the morning window (top) and the evening window (bottom). Error bars represent 95% CI from a Tukey's HSD post-hoc test, to facilitate visual hypothesis testing. Therefore, means with overlapping error bars are not significantly different from each other and means with non-overlapping error bars are significantly different from each other.

Table 2.1: ANOVA table summarising the effects of selection, generation and their interaction on percentage emergence in the morning window. Italicised effects are significant.

Summary of all effects	df Effect	MS Effect	df Error	MS Error	F	p
Selection (Sel)	*2*	*14527.8508*	*6*	*19.7041*	*737.30*	*0.00*
Generation (Gen)	*16*	*219.1046*	*48*	*47.6492*	*4.60*	*0.00*
Block (B)	3	15.2262	0	0.0000	--	--
Sel × Gen	*32*	*176.0581*	*96*	*10.9749*	*16.04*	*0.00*
Sel × B	6	19.7041	0	0.0000	--	--
Gen × B	48	47.6492	0	0.0000	--	--
Sel × Gen × B	96	10.9749	0	0.0000	--	--

Table 2.2: ANOVA table summarising the effects of selection, generation and their interaction on percentage emergence in the evening window. Italicised effects are significant.

Summary of all effects	df Effect	MS Effect	df Error	MS Error	F	p
Selection (Sel)	*2*	*10274.0826*	*6*	*20.2349*	*507.74*	*0.00*
Generation (Gen)	*16*	*63.9819*	*48*	*13.5159*	*4.73*	*0.00*
Block (B)	3	34.1295	0	0.0000	--	--
Sel × Gen	*32*	*153.8043*	*96*	*6.0036*	*25.62*	*0.00*
Sel × B	6	20.2349	0	0.0000	--	--
Gen × B	48	13.5159	0	0.0000	--	--
Sel × Gen × B	96	6.0036	0	0.0000	--	--

2.4. Evolution of eclosion waveforms

Waveforms are simply the shape of the oscillation over the entire length of one cycle. As a consequence of evolution of percentage eclosion in the morning and evening windows, the *early* and *late* chronotypes have also evolved to exhibit very divergent eclosion waveforms (Figure 2.2a) under standard maintenance conditions described above. As a consequence of the direct effects of selection, there appear to be

concomitant evolution of phases of the behaviour, height of the emergence peak and gate-width ('allowed' zone of emergence; see Saunders, 2002). To analyse these parameters of the waveform after 310 generations of selection, I used block means of three phase-markers: (i) phase of onset of emergence (ψ_{ONSET}; time-of-day when emergence exceeds 5% for the first time in a cumulative distribution), (ii) phase of peak of emergence (ψ_{PEAK}; time of maximum percentage emergence), and (iii) phase of offset of emergence (ψ_{OFFSET}; time-of-day when emergence exceeds 95% for the first time in a cumulative distribution) separately in two way mixed model randomised block design ANOVAs wherein selection was treated as a fixed factor and block as the random factor, followed by post-hoc comparisons using the Tukey's HSD test. Similar analyses were also performed on height of emergence peak and the gate-width.

I found that selection has a main effect on all three phase-markers (ψ_{ONSET}: $F_{2,6} = 13.00$, $p < 0.05$; ψ_{PEAK}: $F_{2,6} = 102.30$, $p < 0.05$; ψ_{OFFSET}: $F_{2,6} = 102.60$, $p < 0.05$; see Tables 2.3, 2.4 and 2.5). The *early* stocks evolved an advanced ψ_{ONSET} relative to both *control* and *late* stocks, while the latter two did not differ from each other (Figure 2.2b). In case of ψ_{PEAK}, the *early* and *control* did not differ from each other, but the *late* stocks evolved a delayed phase relative to both (Figure 2.2b). Further, the *early* stocks evolved a significantly advanced ψ_{OFFSET} relative to *control* stocks, whereas the *late* stocks evolved a delayed phase (Figure 2.2b). I also found that the *early* stocks evolved a significantly higher peak of emergence compared to the *control* populations and the *late* stocks evolved a diminished peak ($F_{2,6} = 807.40$, $p < 0.05$; Figure 2.2c, left; Table 2.6). In accordance with the emergence profiles (Figure 2.2a), we find that the *early* stocks show highly narrow gate width relative to the *late* stocks, which showed a much wider allowed zone for emergence ($F_{2,6} = 21.00$, $p < 0.05$; Figure 2.2c, right; Table 2.7).

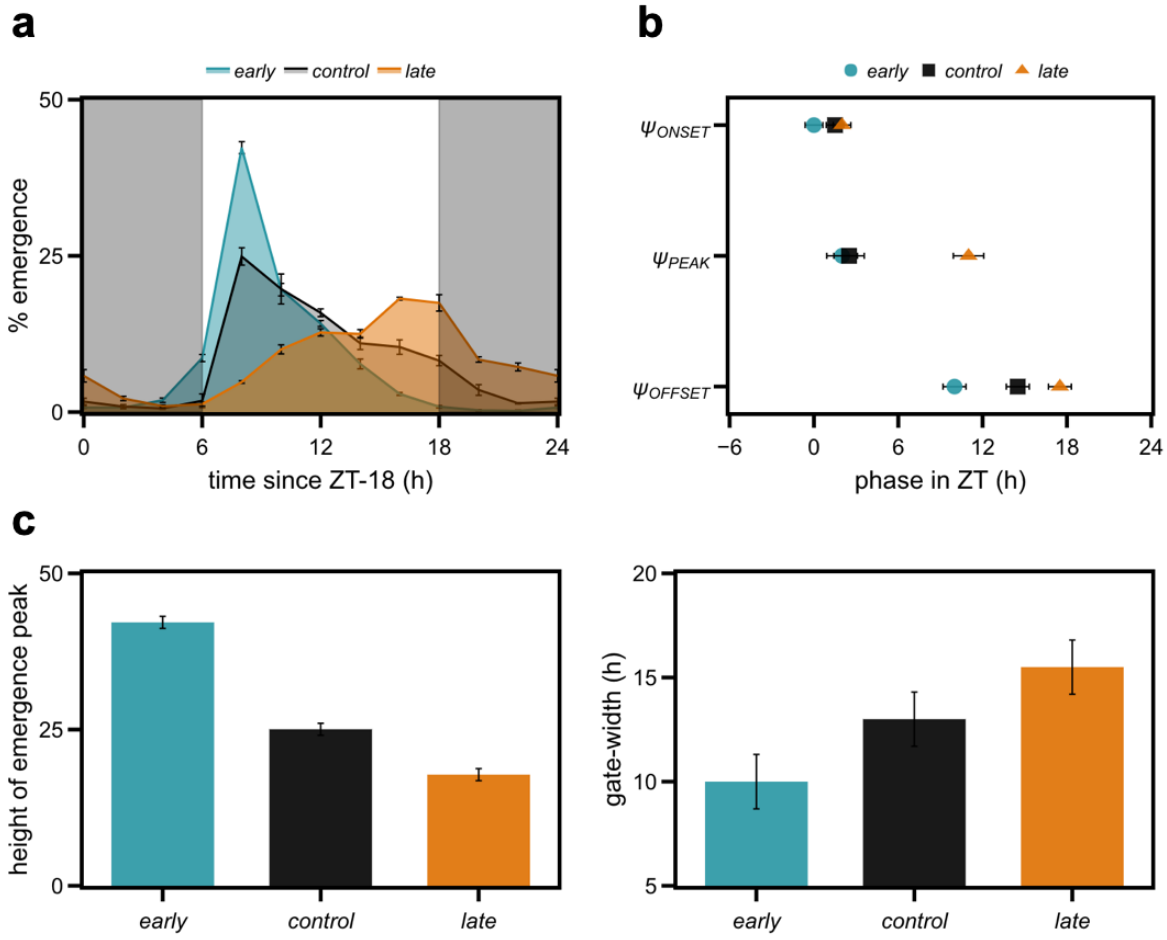

Figure 2.2: (a) Evolved eclosion waveforms of *early*, *control* and *late* stocks at 310th generation after selection. Error bars represent standard error of mean (SEM). (b) Depicted are phases of onset, peak and offset of emergence for the three stocks. (c) Also shown are height of emergence rhythm (left) and the gate-width of rhythm (right) for all three stocks. Error bars in panels (b) and (c) represent 95% CI from a Tukey's HSD post-hoc test, to facilitate visual hypothesis testing. Therefore, means with overlapping error bars are not significantly different from each other and means with non-overlapping error bars are significantly different from each other.

Table 2.3: ANOVA table summarizing the effects of selection regime on ψ_{ONSET} of the eclosion rhythm. Italicised effects are significant.

Summary of all effects	df Effect	MS Effect	df Error	MS Error	F	p
Selection (Sel)	*2*	*4.3330*	*6*	*0.3330*	*13.01*	*0.01*
Block (B)	3	0.3333	0	0.0000	--	--
Sel × B	6	0.3330	0	0.0000	--	--

Table 2.4: ANOVA table summarizing the effects of selection regime on ψ_{PEAK} of the eclosion rhythm. Italicised effects are significant.

Summary of all effects	df Effect	MS Effect	df Error	MS Error	F	p
Selection (Sel)	*2*	*102.3000*	*6*	*1.0000*	*102.30*	*0.00*
Block (B)	3	0.3333	0	0.0000	--	--
Sel × B	6	1.0000	0	0.0000	--	--

Table 2.5: ANOVA table summarizing the effects of selection regime on ψ_{OFFSET} of the eclosion rhythm. Italicised effects are significant.

Summary of all effects	df Effect	MS Effect	df Error	MS Error	F	p
Selection (Sel)	*2*	*57.0000*	*6*	*0.5600*	*102.60*	*0.00*
Block (B)	3	0.8889	0	0.0000	--	--
Sel × B	6	0.5600	0	0.0000	--	--

Table 2.6: ANOVA table summarizing the effects of selection regime on height of eclosion peak. Italicised effects are significant.

Summary of all effects	df Effect	MS Effect	df Error	MS Error	F	p
Selection (Sel)	*2*	*625.7000*	*6*	*0.8000*	*807.40*	*0.00*
Block (B)	3	6.5630	0	0.0000	--	--
Sel × B	6	0.8000	0	0.0000	--	--

Table 2.7: ANOVA table summarizing the effects of selection regime on gate-width of the eclosion rhythm. Italicised effects are significant.

Summary of all effects	df Effect	MS Effect	df Error	MS Error	F	p
Selection (Sel)	*2*	*30.3330*	*6*	*1.4440*	*21.01*	*0.00*
Block (B)	3	2.1110	0	0.0000	--	--
Sel × B	6	1.4440	0	0.0000	--	--

2.5. Brief review of associated changes in circadian clock properties in the *early* and *late* strains

In the first published study describing our populations and associated changes in clock properties underlying such divergent evolution of emergence waveforms, the authors found that the free-running period (FRP; τ) of the emergence rhythm under constant conditions also evolved in divergent directions in the *early* and *late* populations (Kumar et al., 2007). While the *early* stocks showed shorter than 24-h τ, the *late* stocks showed longer than 24-h τ, a result expected from the non-parametric model of entrainment (see previous chapter). However, this relationship between entrained phase under LD cycles and τ is, strictly speaking, expected under the assumption that the photic PRCs of these stocks are of similar shape. Incidentally, Kumar et al. (2007) found that the photic PRCs of these stocks had also evolved such that the *early* stocks showed larger phase advances and the *late* stocks, larger phase delays. This implied that temporal light utilisation by the two stocks to achieve their characteristic evolved phases, must be different. To test this, another study was carried out, wherein emergence waveforms were assessed under a skeleton photoperiod regime with a 15-min light pulse given starting at the time of lights-ON to indicate dawn and another 15-min light pulse given starting 15-min before lights-OFF to indicate dusk (the regime is referred to as skeleton photoperiod owing to its role in providing a skeleton to a full photoperiod, with one pulse indicating dawn and the other indicating dusk; Vaze, Nikhil et al., 2012). We found from this experiment that the evolved emergence waveforms under LD 12:12 was not replicated under the skeleton photoperiod

for any stock. Waveforms under the two regimes are expected, from theory, to be similar under the assumptions of the non-parametric model of entrainment. This result suggested that perhaps parametric effects of light contribute to entrainment and therefore characteristic waveform shape under LD 12:12. To test this, we provided our populations with two asymmetric skeleton photoperiods, i.e., one regime wherein the first half of the day had light as usual but the second half was in darkness until 15-min before the scheduled lights-OFF when a light pulse was provided; and the other regime was the exact opposite, lights were off during the first half of the day except the 15-min pulse at the beginning of the day phase and the second half of the day had light as usual. Interestingly, we found that the *early* stocks showed waveforms identical to those under LD 12:12 when lights were ON during the second half of the day, whereas the *late* stocks showed similar waveforms to those under LD 12:12 when lights were ON during the first half of the day. Owing to the fact that the *early* stocks need delays to entrain and had smaller delay shifts in their PRC, we argue that they must require light for a longer duration in the second half of the day (part of the day corresponding to phase delays). Reciprocally, we argue that the *late* stocks must require longer duration of light during the first half of the day when they will incur phase advances, owing to the fact that they have smaller advance zones. These results provided evidence suggestive of the dominant role of parametric effects of light on entrained behaviour of the emergence rhythm in *early* and *late* stocks.

Further, Kumar et al. (2007) showed that in addition to changes in the τ of the adult emergence rhythm, τ of the activity/rest rhythm also evolved such that τ_{early} was shorter than τ_{late}. This result was also observed in another study performed much later along the course of selection (Nikhil, Abhilash et al., 2016) and persists even today after 310 generations of selection (Figures 2.3 and 2.4). It is interesting here to note that while such differences in the clock period exist for the activity/rest rhythm (Figure 2.3; Table 2.8), these rhythms do not show any difference in the entrained phase of their rhythm under LD 12:12 (Figure 2.3).

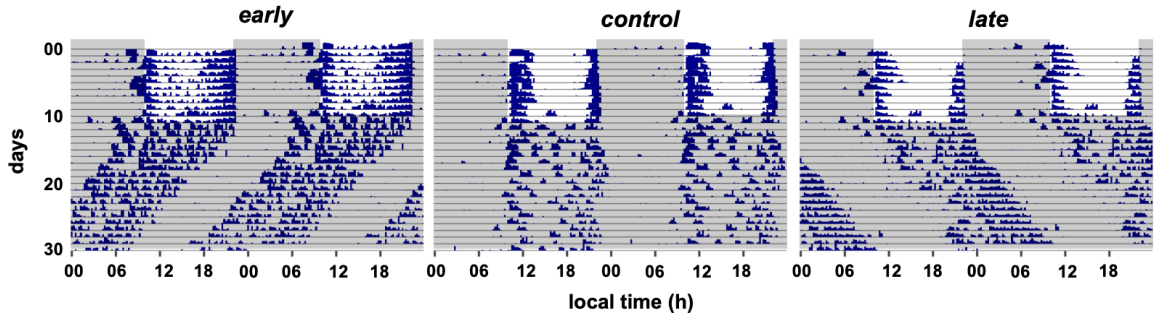

Figure 2.3: Representative actograms of individual flies from each of the three stocks. The flies were exposed to LD 12:12 for 10 days after which they were transferred to constant darkness (DD) for estimation of free-running period. The gray shaded regions indicate dark phases.

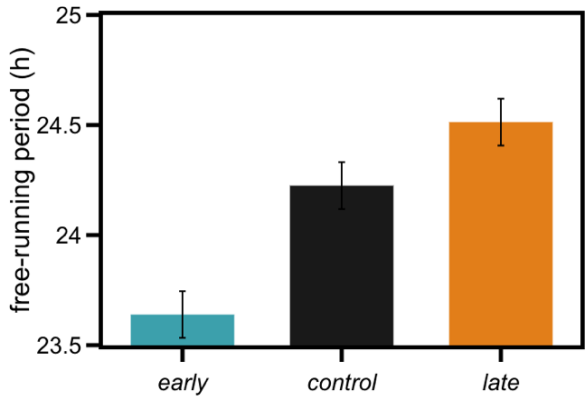

Figure 2.4: Mean free-running period of the activity/rest rhythm of *early*, *control* and *late* flies. Error bars represent 95% CI estimated from a Tukey's HSD post-hoc test to enable visual hypothesis testing. Therefore, means with non-overlapping error bars are significantly different from each other.

Table 2.8: ANOVA table summarizing the effects of selection regime on free-running period of the activity/rest rhythm after 310 generations of selection. Italicised effects are significant.

Summary of all effects	df Effect	MS Effect	df Error	MS Error	F	p
Selection (Sel)	*2*	*0.7935*	*6*	*0.0096*	*82.52*	*0.00*
Block (B)	3	0.0069	0	0.0000	--	--
Sel × B	6	0.0096	0	0.0000	--	--

This was suggestive of divergent photic PRCs of the activity/rest rhythm. Therefore, yet another study from our laboratory assayed phase-responses of the activity/rest rhythm and found that there was no difference in the PRCs of *early* and *late* stocks (Nikhil, Vaze et al., 2016). This indicated that perhaps, the activity/rest rhythm, like that of the emergence rhythm, also predominantly utilised parametric effects of light to entrain to LD cycles. This idea also gained anecdotal evidence from other experiments that examined light sensitivity of the activity/rest rhythm clock using a wide repertoire of experiments. These experiments also suggested that the *late* flies co-evolved a circadian organisation with weak oscillators and stronger *E*-oscillators within the context of the activity/rest rhythm.

Along a different line of investigation to examine the sensitivity of *early* and *late* stocks to different zeitgebers, we examined the emergence waveform of these populations under an outdoor enclosure, wherein light and temperature cycled as in nature (referred to as semi-natural conditions). We found that the divergence between the emergence rhythm of the two populations drastically increased under semi-natural conditions, relative to divergence under laboratory LD 12:12 (Vaze, Kannan et al., 2012). To further understand the role of light and temperature, other experiments in our laboratory were performed, wherein emergence waveforms were observed under temperature cycles alone, and light and temperature cycles in-phase and out-of-phase. It was found that while light reduced chronotype divergence, temperature enhanced the same. Further, light appeared to have an overall phase-delaying effect and temperature, a phase-advancing effect (Nikhil et al., 2014). The authors, based on these results, argue that under natural conditions, optimal phase-relationships are driven by a synergistic effect of light and temperature, thereby giving rise to observed chronotype divergence.

Further, to study if the molecular clockwork has also diverged between *early* and *late* populations, mRNA expression profiles of core clock genes such as *per*, *tim* and *clk* (Hardin, 2011), and two more circadian clock components representing input (circadian photoreceptor, *cry*) and output (*vri*) pathways (Hardin, 2011) were assessed. Pigment Dispersing Factor (PDF) levels (neuropeptide orchestrating circadian rhythms; Helfrich-Förster, 2017) were also assessed to test for the hypothesis of weakly coupled oscillator

network in *late* populations. It was found that, in accordance with their emergence chronotypes, the phase of *per, tim, clk, vri* and PDF oscillation in *early* and *late* populations have diverged with the mRNA and neuropeptide levels peaking earlier in *early* populations relative to *late* populations (Nikhil, Abhilash et al., 2016). Furthermore, amplitude and levels of mRNA and PDF oscillations have also diverged between these two populations (Nikhil, Abhilash et al., 2016). These results were taken to suggest that since *vri* apart from being an output molecule, also regulates *per* and *tim* mRNA expression (Hardin, 2011), selection on timing of eclosion probably drove the divergence of *vri* oscillation which in turn may have caused the divergence of the core molecular clockwork between *early* and *late* populations (Nikhil, Abhilash et al., 2016); thus, highlighting the possible ways in which selection on ψ_{ENT} of a circadian behaviour might drive the evolution of underlying circadian clocks.

The above discussed studies highlight that features such as τ, amplitude, PRC and network level properties of circadian clocks co-evolve in response to selection on timing of behaviour; therefore implying that various aspects of circadian organisation and their relative responses to different zeitgebers may, in principle, affect the ways in which organisms entrain to light and temperature, thereby influencing timing of behaviour (also discussed in the previous chapter).

2.6. Summary of present study

To further understand the relationships between circadian organisation and mechanisms of entrainment that may underlie different timings of behaviour, I used the *early*, *control* and *late* populations in a series of experiments, which will be discussed in the following paragraphs.

In the third chapter of my thesis, I report results from experiments that attempt to understand if and how the hierarchical organisation of the circadian network regulating adult emergence rhythm has changed in *early* and *late* stocks. To do this, I monitored the adult emergence rhythm in these stocks under different constant ambient temperatures in an otherwise LD 12:12 regime, and under both LD 12:12 and different amplitudes of TC 12:12 (thermophase/cryophase). I found, unequivocally, that while the *early* stocks

evolved attenuated temperature sensitivity of the clock, the *late* stocks were highly sensitive to different temperature regimes.

Results of experiments carried out to understand the difference (if any) in the *M-E* oscillator organisation regulating activity/rest rhythms between the *early* and *late* stocks are reported in the fourth chapter. I, first, established the use of high frequency LD cycles (12-h periodicity) as a tool to probe into the *M-E* organisation, and used this to understand the behavior of *early* and *late* flies. I found evidence in support of stronger *E*-oscillators in the *late* chronotypes.

Subsequently, I examined the temperature sensitivity and properties of entrainment to temperature cues of the activity/rest rhythms in our *early*, *control* and *late* stocks. Interestingly, I found that the *late* stocks show significantly enhanced temperature responsiveness of the activity/rest rhythm. Additionally, the evening bout of activity in the *late* stocks appears more sensitive to temperature and most properties of entrainment are in agreement with predictions made from the non-parametric model. These results are described in the fifth chapter.

In the sixth chapter I examine properties of entrainment of these stocks to light cues and found that predictions from the non-parametric model are not met. Further, parametric effects of light seem to be able to explain phases of entrainment of our stocks to light very well, especially for the *late* chronotypes.

In my seventh chapter, I discuss the implications of results from all the previous chapters and make some general remarks and propose a hypothesis regarding how as a consequence of selection, different aspects of organisation may evolve thereby determining different extents of parametric and non-parametric contributions to entrainment. I also discuss future experiments that could be done to further understand the inter-relationship between timing of behaviour, circadian organisation and mechanisms of entrainment.

In addition to the work discussed above, I have also been involved in a large experiment wherein the whole genomes of all our *early*, *control* and *late* stocks have been sequenced to understand genetic signatures

associated with timing of behaviour. This study is ongoing in collaboration with other researchers in our laboratory. The eighth chapter of my thesis is that of appendices, where I first describe results of the part of the genome sequencing project that I have been involved in.

Further, many analyses described above are difficult or cumbersome to perform using existing rhythms analyses software. This prompted me to develop an open-source software for facilitating a wide range of rhythm analyses that have been widely used by me for my work reported here, and I hope would be useful to the chronobiology community. This is described in the second section of the appendices chapter.

Chapter 3. Selection for timing of eclosion results in co-evolution of temperature responsiveness in *Drosophila melanogaster*

Parts of this chapter have been published in the following research article:

Abhilash L, Ghosh A and Sheeba V (2019) Selection for timing of eclosion results in co-evolution of temperature responsiveness in Drosophila melanogaster. Journal of Biological Rhythms, 34(6): 596–609.

3.1. Introduction

Restricting behaviour to specific phases of the cyclic external environment is associated with enhanced Darwinian fitness and is known to improve physical and mental well-being in humans (Roenneberg et al., 2012; Vaze and Sharma, 2013). Thus, the study of behavioural phases under entrainment (ψ_{ENT}; also referred to as chronotypes) and their regulation is essential. Early studies have postulated that between-group differences in ψ_{ENT} (chronotype divergence) is predominantly driven by different free-running periods (FRP) and/or the phase/velocity responses (PRC/VRC) of the clock to zeitgebers (Daan and Pittendrigh, 1976; Pittendrigh and Daan, 1976a; Swade, 1969). Additional factors that regulate ψ_{ENT} also include inter-oscillator coupling, amplitude of the zeitgeber and intrinsic amplitude of the circadian clock (Aschoff and Pohl, 1978; Bordyugov et al., 2015; Granada et al., 2013; Johnson et al., 2003b; Roenneberg, Hut et al., 2010). While there are many studies that look at the effect of period on ψ_{ENT} in great detail (for instance, Rémi et al., 2010; Srivastava et al., 2019), there are relatively few experimental studies that have analysed the effect of other factors such as zeitgeber strength and coupling on ψ_{ENT} (Abraham et al., 2010; Aschoff and Pohl, 1978). Moreover, each such study has been performed on a different model system and therefore, gaining a unifying understanding of clock features that regulate phasing and their inter-relationships is difficult.

I have used sets of populations of *Drosophila melanogaster* (described in the previous chapter) that have evolved in our laboratory to exhibit divergent phases of the adult eclosion rhythm (Kumar et al., 2007) to ask questions regarding (i) the clock properties that have evolved to facilitate divergent timing, and (ii) the inter-relationships between said clock properties.

As a consequence of selection on phasing, earlier studies from our laboratory have found that flies of the morning eclosing (*early*) stocks and evening eclosing (*late*) stocks have shorter and longer FRP, respectively (Kumar et al., 2007; Nikhil, Abhilash et al., 2016). Although this is expected, the between-stock difference in phasing of the eclosion rhythm under standard laboratory conditions (4 to 5-h; Nikhil et al., 2014) exceeds the between-stock differences in period (~1.35-h for the eclosion rhythm and ~0.75-h for activity/rest rhythm; Nikhil, Abhilash et al., 2016). This suggests that, in our populations, variation in ψ_{ENT} cannot be explained by differences in FRP alone. Moreover, although light pulse PRCs of the eclosion rhythm of the *early* stocks show relatively larger phase advances and that of the *late* stocks show larger phase delays (Kumar et al., 2007), these differences do not explain ψ_{ENT} of the two sets of populations (Vaze, Nikhil et al., 2012).

Therefore, I reasoned that differences in the inter-oscillator coupling between circadian clocks (also referred to as circadian network/organization, hereafter) regulating eclosion rhythm may explain chronotype divergence in our stocks. This notion stems from a model of circadian organisation that was proposed by Pittendrigh and Bruce (1959) to explain phasing of eclosion rhythms in insects (described in Chapter 1, Section 1.4.2.1). The authors proposed that the phase of eclosion rhythm follows immediately from the phase of a peripheral/slave/*B*-oscillator, which is entrained by a central/master/*A*-clock. Further, the authors proposed that the master clock is light sensitive, and its period is temperature compensated, whereas the peripheral clock is light insensitive, and its period is temperature sensitive. This implies that when the *B*-clock is entrained by the *A*-clock, different periodicities of the *B*-clock (under different temperatures) will entrain with different phases relative to the light cycle thereby regulating the phase of overt behaviour.

However, the extent of this regulation depends on the strength of coupling between the *A*- and *B*-clocks (Oda and Friesen, 2011; Pittendrigh et al., 1958; Pittendrigh and Bruce, 1959).

A previous study from our laboratory found that the phase divergence between *early* and *late* stocks was enhanced under semi-natural conditions wherein the culture vials were exposed to multiple zeitgebers, predominantly light and temperature (Vaze, Kannan et al., 2012). This prompted me to hypothesise that temperature plays an important role in phase divergence in the context of the aforementioned model of circadian organization. Subsequently, Nikhil et al. (2014) assayed the eclosion rhythms of the *early* and *late* stocks under rectangular and ramped light/dark (LD) and thermophase/cryophase (TC) cycles either in-phase or out-of-phase. Overall, the authors observed that phases of the eclosion rhythm were delayed in all populations under LD cycles relative to phases under semi-natural conditions, when temperature was constant; whereas all populations showed similar phases under TC cycles + constant darkness and semi-natural conditions. The authors argued that ψ_{ENT} in natural environments is likely to be regulated by both zeitgebers together for "optimal" phasing, such that TC cycles can compensate for delayed phase under LD cycles. However, in the experiments conducted by Nikhil et al. (2014), the nature of LD cycles i.e., rectangular versus ramped, and the altered phase-relationship between LD and TC cycles could have acted differentially on the light sensitive pacemaker (or *A*-clock) of the *early* and *late* stocks. Therefore, although the authors attributed different extents of phase-divergence/convergence in their study to differences in the circadian organization, the individual role of temperature sensitive *B*-clock in mediating such differences remains unclear. Additionally, I hypothesised that the phase advancing effect of TC cycles must be dependent on the absolute value of temperatures of the TC cycle. I was also interested in examining eclosion rhythms in our populations under different constant ambient temperatures and amplitudes of temperature cycles

because (i) from an ecological perspective, temperature is expected to be a major zeitgeber in the wild, especially for insects (Rensing and Ruoff, 2002), and (ii) mean temperature and amplitude of daily temperature cycles vary by a large amount across latitudes and significantly across seasons even at lower latitudes (Figure 3.1, top and bottom, respectively) where photoperiod does not change much. For instance, in Colombo, Sri Lanka (latitude: 6.93 °N) mean temperature varies annually between 26 °C to 29 °C, and the amplitude of temperature cycles varies annually between ~3 °C to ~8 °C (Figure 3.2, top); however, photoperiod only varies by less than an hour (Figure 3.2, bottom). Owing to the fact that smaller fluctuations in temperature can entrain circadian clocks in organisms (see Das and Sheeba, 2017 for a review), aforementioned changes may be imposing selective pressures on insect clocks in the wild, thereby influencing chronotype divergence.

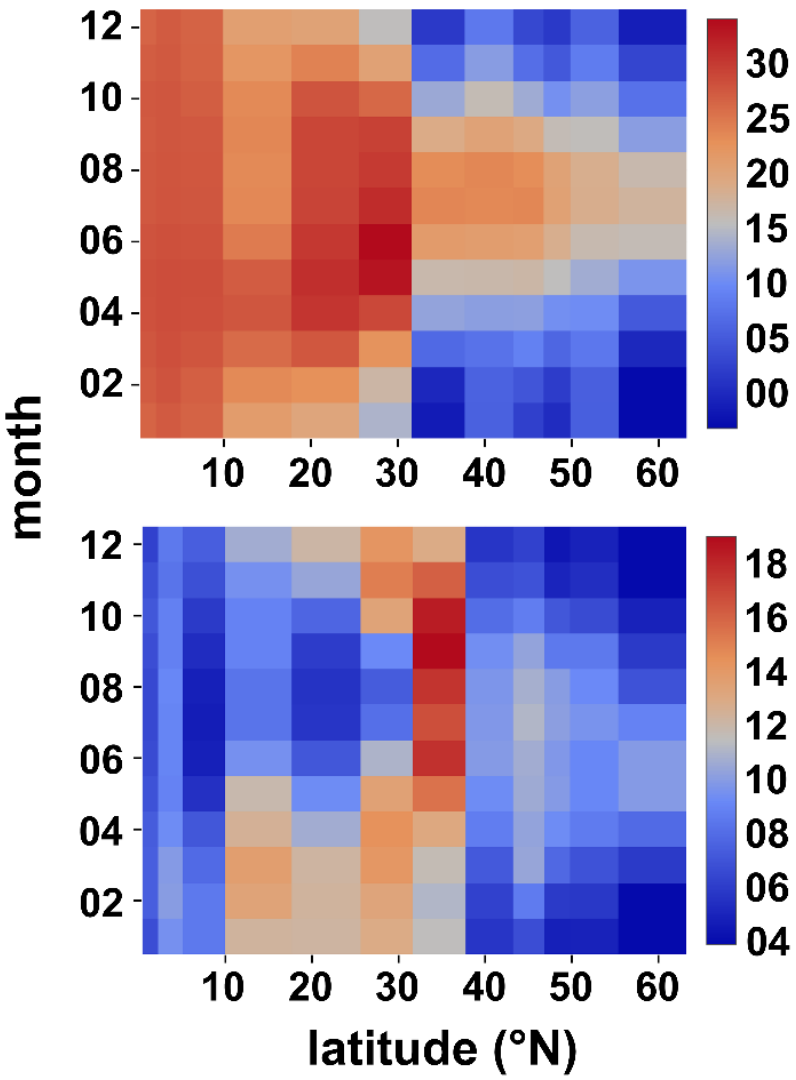

Figure 3.1: Heat map of mean daily temperature across latitudes and months (top), and amplitude of daily temperature cycles across latitudes and months (bottom). Data for this figure was collected from 12 independent locations across longitudes from http://worldweather.wmo.int/. The places include Singapore, Kuala Lumpur, Colombo, Bangalore, Kolkata, Delhi, Kabul, Istanbul, Milan, Vienna, London and Stockholm. Values obtained for each month is an average value over 30 years. I chose them to represent well-known places at different latitudes. However, we are aware that temperature values could be strongly affected depending on the altitude of these locations. Therefore, we collected altitude values for each of these locations and performed a correlation analysis with the latitude. There was no significant correlation between latitude and altitude in our case (Spearman's $\rho = 0.03$, $p > 0.05$). This implies that temperature variations reported here are largely latitude dependent.

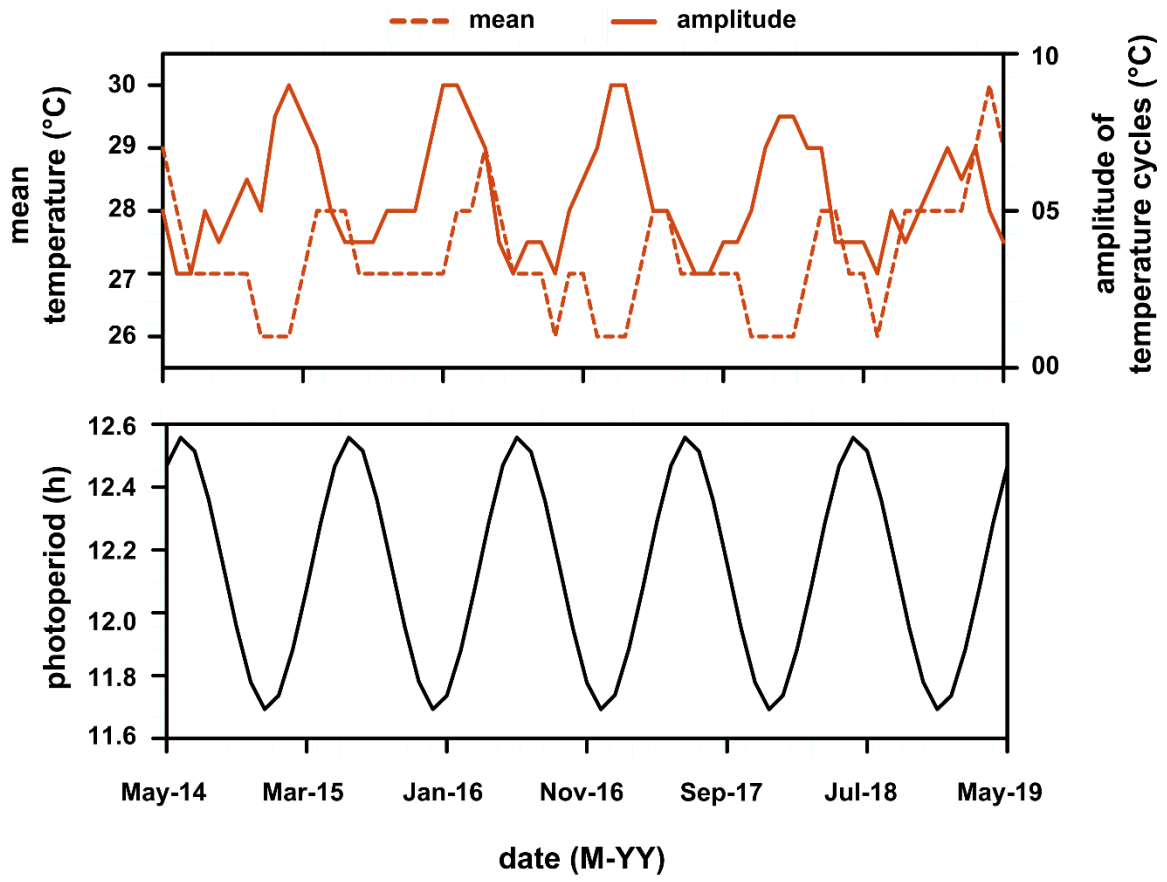

Figure 3.2: Depicted here is annual variation in mean ambient temperature and amplitude of temperature cycles (top) and photoperiod (bottom) over 5 consecutive years in Colombo, Sri Lanka. It is clear that although amplitude of temperature cycles varies annually by ~8 °C, in latitudes as low as ~6 °N, photoperiod varies only by less than 1-h (see text). Data for temperature was collected from https://www.worldweatheronline.com/, and data for photoperiod was collected from https://www.timeanddate.com/.

To test my aforementioned hypotheses, and gain clarity regarding differences in the circadian organization of the clock regulating eclosion rhythms in our flies, I asked the following questions:

1. Do the *early* and *late* stocks respond differently to low and high constant ambient temperatures in the presence of an LD cycle, relative to standard 25 °C?

2. How do phases of the eclosion rhythm in our stocks behave under LD+TC cycles with increasing amplitude of TC cycles under overall cool temperature?

3. Do the relationships seen above change when the overall temperature is warm?

In addition to these very specific questions related to our stocks, I think that these experiments are important because they allow us to assess broader questions regarding how chronotype divergence is affected by different temperature regimes. Additionally, while Nikhil et al. (2014) demonstrated that the phase-relationship of temperature and light cycles is an important regulator of chronotype divergence, my study focusses on aspects of temperature cycles that contribute to the regulation of such divergence. Furthermore, the fact that magnitude of chronotype divergence is subject to the environment provided suggests that all chronotypes do not respond in a similar manner to such changes in the environment. My study allows one to understand the contribution of two extremes of the chronotype distribution to the overall regulation of divergence between them. I feel that such studies are important to fuel further theoretical and mechanistic studies that can allow us to understand how chronotypes are regulated under realistic environmental conditions.

3.2. Materials and Methods

3.2.1. Adult eclosion rhythm assay

In all my experiments, I had a fixed LD schedule of LD 12:12 (12-h light and 12-h darkness) with ~70-lux light intensity during the photophase. I also fixed the phase-relationship between the LD cycles and different TC cycles such that warm temperature onset happened 4-h after onset of light. I fixed these aspects of the light cycle to ensure that during all temperature manipulations input to the light sensitive *A*-clock was held constant. In this way, variations in the rhythm could be predominantly attributed to the effects of temperature on the *B*-clock and any other light-temperature integrator within the clock circuit.

~300 eggs from each of the 12 populations were collected and dispensed into 10 vials, each with banana-jaggery medium, for all the assays. Initially, eclosion of *early* and *late* chronotypes was monitored under LD 12:12 at constant 19, 25 and 28 °C. The LD 12:12 under 25 °C experiment was done by me, and a part of those results are published elsewhere (Nikhil, Abhilash et al., 2016). Further, I performed eclosion assays under LD 12:12 along with a temperature cycle TC 12:12 of low amplitude (3 °C) or high amplitude (6 °C). These LD+TC assays with different amplitudes of temperature cycles were performed under two different mean ambient temperatures, first at 19 °C (17.5-20.5 °C, LA_{19} and 16-22 °C, HA_{19}), and subsequently at 28 °C (26.5-29.5 °C, LA_{28} and 25-31 °C, HA_{28}). These temperatures were chosen so that the lower limit of temperature during TC cycles with low mean was not too low and the upper limit of temperature during TC cycles with high mean was not too high for our flies (for a detailed note on temperature tolerance of *Drosophila*, please see Ashburner et al., 2005). Further, it ensured that the temperature values were not overlapping between the two regimes. Under all conditions, I started the assay a day after most pupae were black and recorded the number of flies emerging in every vial at 2-h intervals until most flies in each culture vial had emerged. For more details regarding temperature profiles inside our incubators please see Figure 3.3.

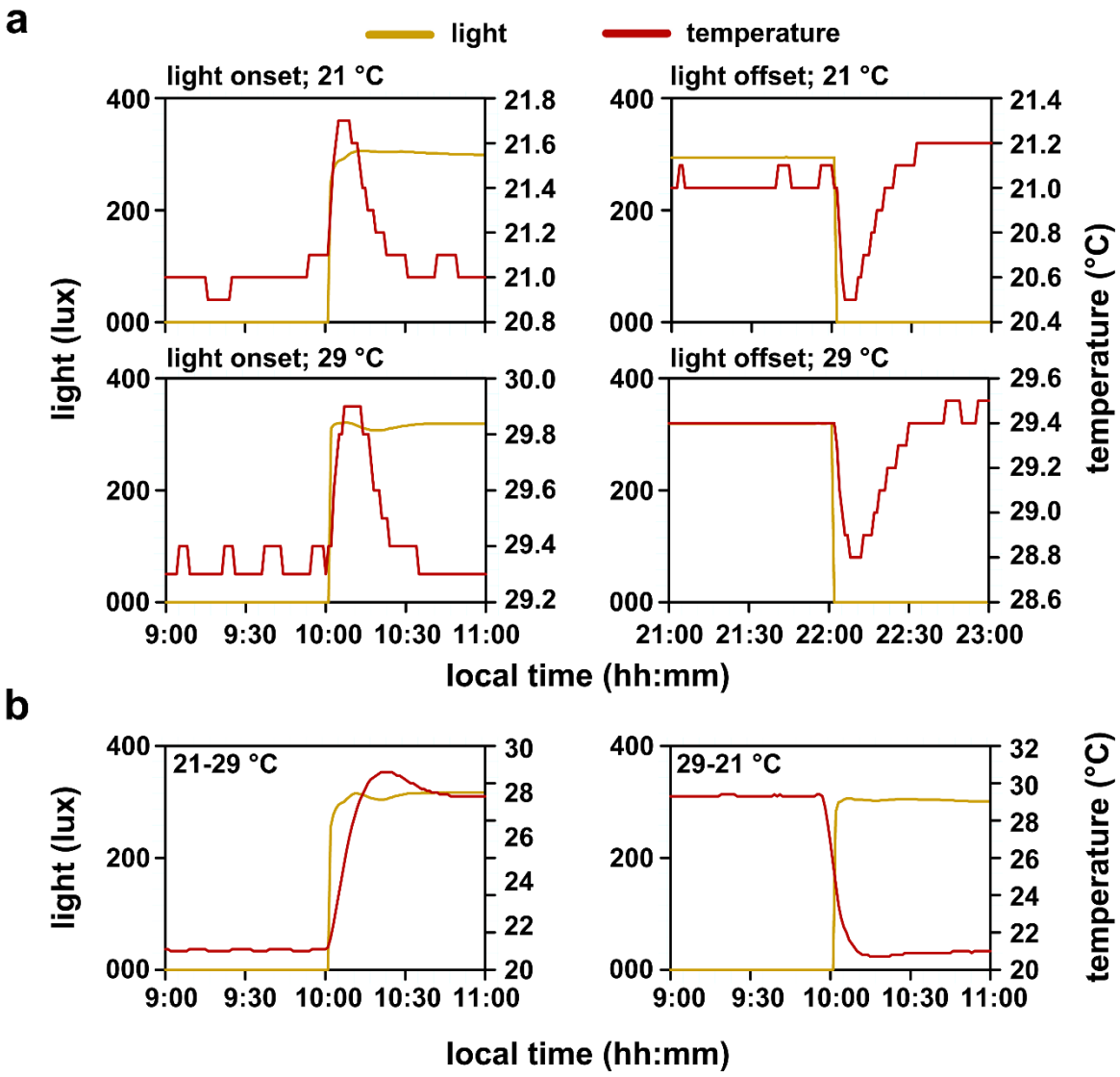

Figure 3.3: Light and temperature traces recorded from a different experiment to exemplify the accuracy and stability of temperature maintenance in our Percival incubators. Shown in the top panel of (a) are temperature fluctuations during lights-ON transition (left) when the temperature regime inside the incubator was constant 21 °C, while on the right is the same but during the lights-OFF transition. Shown in the bottom panel of (a) are the same features when the incubator was set at a constant temperature of 29 °C. Also shown in (b) are times taken for the temperature to change from 21 to 29 °C (left) and from 29 to 21 °C. All my experiments were carried out in the same Percival incubator (Percival Scientific, Inc.). Given that all my manipulations were changes either in the constant ambient temperature or under cycling temperature environments where the cycles were rectangular, environmental monitors were not placed inside the incubator for monitoring temperature values. Additionally, from several past records we were aware that temperature fluctuations in response to light/dark or dark/light transitions are minimal and stabilize

soon. However, just to exemplify, here I have shown traces of light and temperature recorded inside the incubator during a different, unrelated experiment. Under constant 21 °C, during the dark/light transition, temperature spikes up by only ~0.5 °C and stabilizes back to 21 °C within 30-min (top-left). Similarly, during the light/dark transition, temperature falls by ~0.6 °C and stabilizes within 30-min (top-right). Effects are similar when the constant ambient temperature is 29 °C (a, bottom). In the traces shown here, light intensity is ~300-lux, whereas in my case light intensity was 70-lux and therefore the effects on temperature perceived by the culture vials are likely to be even smaller. We also show the time taken for the temperature to change from 21 to 29 °C and vice versa during one of the light/dark transitions (b). It is clear that temperature changes fairly quickly (typically within 30- to 45-min). It is important to note that in all cases, the temperature changes required were much smaller and are likely to have occurred sooner than depicted in the figures above.

3.2.2. Quantifying rhythm parameters and chronotype divergence

To estimate features of the rhythm that change under each of the assay conditions, I quantified 6 rhythm parameters. In a cumulative distribution of eclosion over one cycle/vial, I defined phase-of-onset (ψ_{ONSET}) of eclosion as the time at which the proportion of emerging flies exceeded 0.05 and phase-of-offset (ψ_{OFFSET}) as the time at which the proportion of emerging flies exceeded 0.95. I also computed phase-of-peak (ψ_{PEAK}) as the time at which maximum flies emerged, over a cycle/vial (same as in Chapter 2). If there were two subsequent time-points with the same maximum number of eclosing flies, then ψ_{PEAK} was calculated as the average time between the two time-points. Further, if there appeared to be bimodality in the eclosion rhythm, I considered the phase of the higher peak to carry out further analyses. Additionally, gate-width was calculated as the time duration between the phases of onset and offset ($\psi_{OFFSET} - \psi_{ONSET}$). I also calculated circular mean phase of entrainment (phase-of-Centre of Mass; ψ_{CoM}), which is a measure of the centrality of emergence on the time-axis. Amplitude of the eclosion rhythm is also a key feature describing the pattern of emergence and has also been used earlier to describe the emergence rhythm waveform (Vaze, Nikhil et al., 2012). However, amplitude of the emergence rhythm is dependent on the gate-width of emergence, and hence, I used distance from the center (r) in polar

coordinates as a measure of normalized amplitude (or in other words, consolidation) of the oscillation. Chronotype divergence was measured as ${}^{late}\psi_{CoM} - {}^{early}\psi_{CoM}$.

3.2.3. Data analyses and statistical tests

First, the proportion of flies eclosing at a time-point under each temperature regime was separately analysed using a mixed model four-way randomized block design ANOVA where selection, temperature regime and time-point were treated as fixed factors and blocks were treated as random factors.

A separate mixed model three-way randomized block design ANOVA with block means was used for analyzing each rhythm characteristic, wherein selection and temperature regime were treated as fixed factors and blocks as a random factor. Chronotype divergence under different constant ambient temperatures was analysed using a two-factor mixed model randomized block design ANOVA with temperature regime as a fixed factor and block as a random factor. On the other hand, chronotype divergence under TC cycles was analysed using a three-way mixed model randomized block design ANOVA with mean temperature and amplitude of temperature cycles as fixed factors and block as a random factor. All post-hoc multiple comparisons were performed using Tukey's Honestly Significant Difference (HSD) tests. All statistical tests were performed using STATISTICA v5.0 (StatSoft, Tulsa, OK), and results were considered significant at $\alpha = 0.05$.

3.3. Results

In each of the temperature regimes that I used, the first level of analysis was performed to infer if the rhythm of one stock differed from any other under different temperature regimes through a four-way randomized block design ANOVA. A significant interaction between selection × time-

point × temperature regime implied that the waveform's response to temperature regime was stock dependent, therefore enabling downstream analyses. Each of the rhythm descriptors that I have looked at further is analysed using a three-way randomized block design ANOVA, wherein a significant selection × temperature regime interaction implied that the temperature response of the waveform descriptor was stock dependent.

3.3.1. Eclosion rhythms under different constant ambient temperatures

The statistically significant effect of selection × temperature regime × time-point interaction on the proportion of eclosion for *early*, *control* and *late* stocks indicated that the stocks responded differently to presented temperature regimes ($F_{44,132} = 11.09$, $p < 0.05$; Figure 3.4a; Table 3.1).

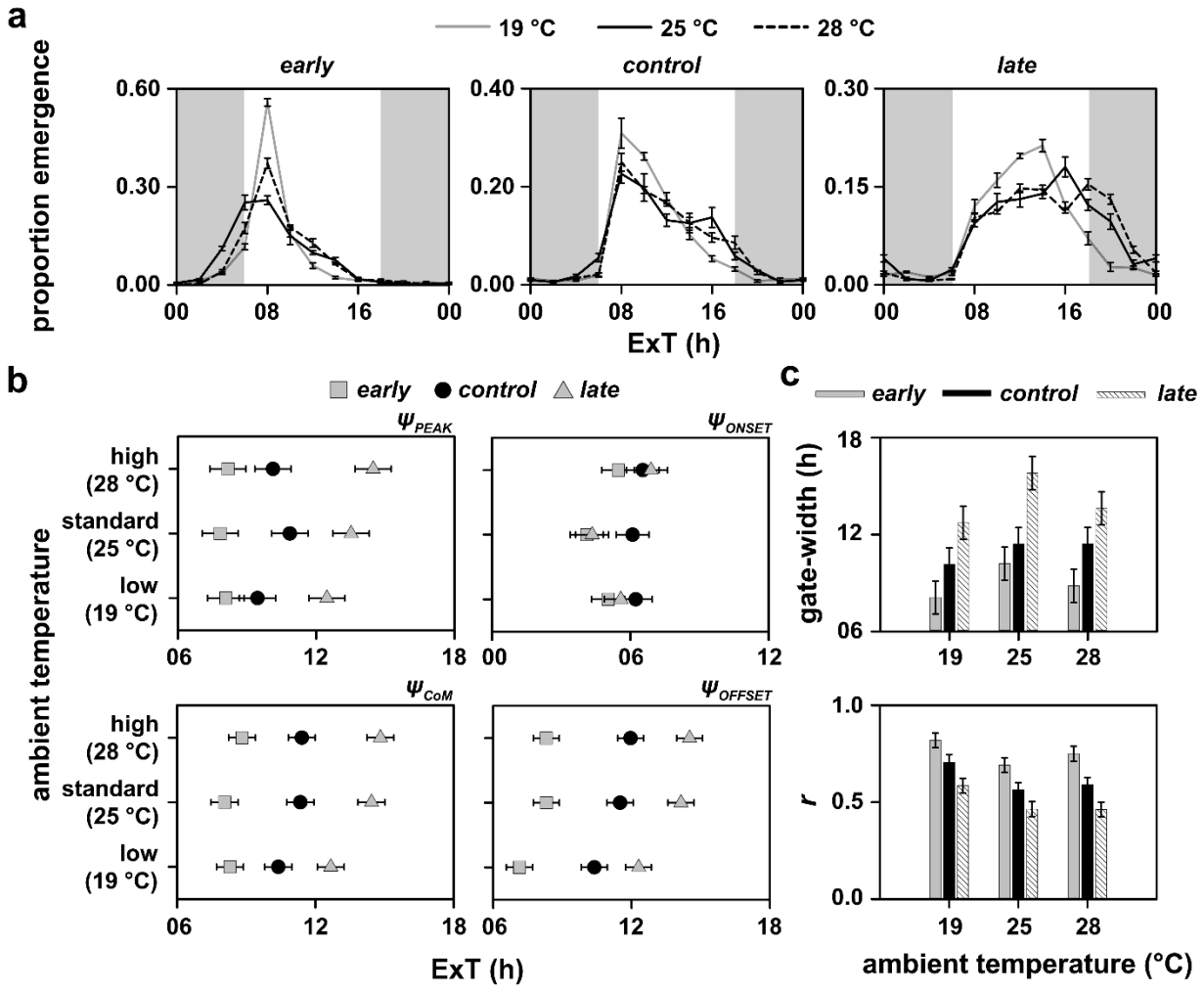

Figure 3.4: Depicted here are (a) eclosion rhythm profiles averaged over four replicate populations for *early*, *control* and *late* stocks, (b) phase-of-peak (ψ_{PEAK}), phase-of-centre of mass (ψ_{CoM}), phase-of-onset (ψ_{ONSET}) and phase-of-offset (ψ_{OFFSET}), and (c) gate-width and normalized amplitude (r) under LD 12:12 and constant low (19 °C), standard (25 °C) and high (28 °C) temperatures. 25 °C is referred to as standard temperature owing to it being the maintenance temperature for the populations. The shaded regions in (a) represent the scotophase. Error bars in (a) are SEM, and in (b) and (c) are 95% CI calculated using the Tukey's HSD critical values. Therefore, all means in (b) and (c) with non-overlapping error bars are statistically significantly different from each other. In all plots data points were obtained by averaging values, first over all cycles, then over all vials and finally across four replicate populations.

Table 3.1: Summary of all effects of a four-way mixed model randomized block design ANOVA on the proportion of flies eclosing at any given time-point of *early*, *control* and *late* populations under LD 12:12 and different constant ambient temperatures.

Summary of all effects	***df* Effect**	**MS Effect**	***df* Error**	**MS Error**	***F***	***p***
Selection (Sel)	*2*	*0.0000*	*6*	*0.0000*	*6.20*	*0.03*
Temperature (Temp)	2	0.0000	6	0.0000	0.26	0.78
Time-Point (TP)	*11*	*0.2005*	*33*	*0.0002*	*959.17*	*0.00*
Block (B)	3	0.0000	0	0.0000	--	--
Sel × Temp	4	0.0000	12	0.0000	0.66	0.63
Sel × TP	*22*	*0.0497*	*66*	*0.0004*	*114.76*	*0.00*
Temp × TP	*22*	*0.0089*	*66*	*0.0003*	*27.96*	*0.00*
Sel × B	6	0.0000	0	0.0000	--	--
Temp × B	6	0.0000	0	0.0000	--	--
TP × B	33	0.0002	0	0.0000	--	--
Sel × Temp × TP	*44*	*0.0044*	*132*	*0.0004*	*11.09*	*0.00*
Sel × Temp × B	12	0.0000	0	0.0000	--	--
Sel × TP × B	66	0.0004	0	0.0000	--	--
Temp × TP × B	66	0.0003	0	0.0000	--	--
Sel × Temp × TP × B	132	0.0004	0	0.0000	--	--

It is clear that the ψ_{PEAK}, while invariant in response to different temperatures in the *early* and *control* stocks, was significantly delayed in case of the *late* populations under warm temperatures ($F_{4,12}$ = 4.60, $p < 0.05$; Figure 3.4b, top-left; Tables 3.2 and 3.3). Further in the *late* stocks, although there was no significant difference in ψ_{PEAK} between 19 and 25 °C and 25 and 28 °C, the phase was significantly delayed under 28 °C relative to 19 °C (Figure 3.4b, top-left; Table 3.3). In case of the ψ_{CoM}, the patterns were similar to those observed with ψ_{PEAK}. There was no difference in the phases of *early* and *control* stocks with change in temperature but there was a

significant advance of ψ_{CoM} in the *late* populations under 19 °C relative to both 25 and 28 °C ($F_{4,12}$ = 6.20, $p < 0.05$; Figure 3.4b, bottom-left; Tables 3.3 and 3.4).

Table 3.2: ANOVA table summarising the effects of selection, different constant ambient temperatures and their interaction on ψ_{PEAK}. Italicised effects are significant.

Summary of all effects	***df* Effect**	**MS Effect**	***df* Error**	**MS Error**	***F***	***p***
Selection (Sel)	*2*	*90.8233*	*6*	*0.1334*	*680.93*	*0.00*
Temperature (Temp)	*2*	*2.8529*	*6*	*0.0952*	*29.96*	*0.00*
Block (B)	3	0.3053	0	0.0000	--	--
Sel × Temp	*4*	*1.6328*	*12*	*0.3546*	*4.60*	*0.02*
Sel × B	6	0.1334	0	0.0000	--	--
Temp × B	6	0.0952	0	0.0000	--	--
Sel × Temp × B	12	0.3546	0	0.0000	--	--

Table 3.3: Phase values (in ExT), gate-width and normalized amplitude/consolidation of eclosion rhythms in *early*, *control* and *late* populations under LD 12:12 and different constant ambient temperatures and amplitudes of temperature cycles under overall cool and warm environments. The columns with similar shades of gray are comparable.

		constant temperature			temperature cycles			
					mean=19 °C		mean=28 °C	
					amp		amp	
		19 °C	25 °C	28 °C	3 °C	6 °C	3 °C	6 °C
early	ψ_{ONSET}	5.04	4.10	5.47	6.48	7.39	6.50	6.73
	ψ_{PEAK}	8.08	7.83	8.17	8.12	8.61	8.62	8.11
	ψ_{OFFSET}	13.14	14.31	14.30	13.65	14.28	13.22	11.84
	ψ_{CoM}	8.29	8.06	8.82	8.80	9.63	9.04	8.60
	gate-width	8.11	10.20	8.83	7.16	6.89	6.72	5.12
	r	0.82	0.69	0.75	0.84	0.82	0.82	0.90
control	ψ_{ONSET}	6.24	6.10	6.54	7.41	8.41	8.02	7.87
	ψ_{PEAK}	9.45	10.85	10.12	10.23	12.14	10.38	8.40
	ψ_{OFFSET}	16.39	17.51	17.96	17.02	17.29	16.84	14.56
	ψ_{CoM}	10.39	11.35	11.41	10.93	12.42	11.25	9.75
	gate-width	10.15	11.41	11.42	9.61	8.88	8.83	6.69
	r	0.71	0.56	0.59	0.73	0.76	0.64	0.82
late	ψ_{ONSET}	5.58	4.34	6.90	6.93	8.93	8.15	8.53
	ψ_{PEAK}	12.46	13.51	14.47	13.47	14.42	13.90	10.73
	ψ_{OFFSET}	18.31	20.15	20.52	19.45	19.45	19.59	18.24
	ψ_{CoM}	12.67	14.43	14.82	13.75	14.95	13.90	12.08
	gate-width	12.72	15.81	13.63	12.52	10.52	11.44	9.72
	r	0.58	0.46	0.46	0.62	0.72	0.53	0.71

Table 3.4: ANOVA table summarising the effects of selection, different constant ambient temperatures and their interaction on ψ_{CoM}. Italicised effects are significant.

Summary of all effects	*df* Effect	MS Effect	*df* Error	MS Error	*F*	*p*
Selection (Sel)	*2*	*93.5897*	*6*	*0.1789*	*523.07*	*0.00*
Temperature (Temp)	*2*	*4.7466*	*6*	*0.1974*	*24.04*	*0.00*
Block (B)	3	0.0158	0	0.0000	--	--
Sel × Temp	*4*	*1.2197*	*12*	*0.1966*	*6.20*	*0.01*
Sel × B	6	0.1789	0	0.0000	--	--
Temp × B	6	0.1974	0	0.0000	--	--
Sel × Temp × B	12	0.1966	0	0.0000	--	--

The *early* and *control* stocks showed no change in ψ_{ONSET} under different temperature regimes, whereas the ψ_{ONSET} was advanced by ~2.5-h under 25 °C relative to its value under 28 °C in the *late* populations ($F_{4,12} = 3.97$, $p < 0.05$; Figure 3.4b, top-right; Tables 3.3 and 3.5). However, there was no difference in the way any population responded to different temperatures with respect to ψ_{OFFSET} ($F_{4,12} = 1.82$, $p > 0.05$; Figure 3.4b, bottom-right; Tables 3.3 and 3.6). All populations appeared to advance their eclosion offset by similar amounts in response to cool temperatures (Figures 3.4a and 3.4b, bottom-right; Table 3.3).

Table 3.5: ANOVA table summarising the effects of selection, different constant ambient temperatures and their interaction on ψ_{ONSET}. Italicised effects are significant.

Summary of all effects	***df* Effect**	**MS Effect**	***df* Error**	**MS Error**	***F***	***p***
Selection (Sel)	*2*	*6.0488*	*6*	*0.1635*	*37.00*	*0.00*
Temperature (Temp)	*2*	*6.3586*	*6*	*0.1579*	*40.26*	*0.00*
Block (B)	3	0.0147	0	0.0000	--	--
Sel × Temp	*4*	*1.1655*	*12*	*0.2937*	*3.97*	*0.03*
Sel × B	6	0.1635	0	0.0000	--	--
Temp × B	6	0.1579	0	0.0000	--	--
Sel × Temp × B	12	0.2937	0	0.0000	--	--

Table 3.6: ANOVA table summarising the effects of selection, different constant ambient temperatures and their interaction on ψ_{OFFSET}. Italicised effects are significant.

Summary of all effects	***df* Effect**	**MS Effect**	***df* Error**	**MS Error**	***F***	***p***
Selection (Sel)	*2*	*99.9039*	*6*	*0.6572*	*152.02*	*0.00*
Temperature (Temp)	*2*	*9.3728*	*6*	*0.4235*	*22.13*	*0.00*
Block (B)	3	0.1225	0	0.0000	--	--
Sel × Temp	4	0.3337	12	0.1831	1.82	0.19
Sel × B	6	0.6572	0	0.0000	--	--
Temp × B	6	0.4235	0	0.0000	--	--
Sel × Temp × B	12	0.1831	0	0.0000	--	--

Under cool temperatures, gating of the eclosion rhythm was tighter and normalized amplitude was higher (Figure 3.4c, top and bottom; Table 3.3). However, all three stocks behaved similarly (gate-width: $F_{4,12}$ = 1.50, p > 0.05; Tables 3.3 and 3.7; normalized amplitude: $F_{4,12}$ = 2.36, p > 0.05; Tables 3.3 and 3.8).

Table 3.7: ANOVA table summarising the effects of selection, different constant ambient temperatures and their interaction on gate-width. Italicised effects are significant.

Summary of all effects	***df* Effect**	**MS Effect**	***df* Error**	**MS Error**	***F***	***p***
Selection (Sel)	*2*	*0.1876*	*6*	*0.0008*	*249.41*	*0.00*
Temperature (Temp)	*2*	*0.0567*	*6*	*0.0018*	*31.29*	*0.00*
Block (B)	3	0.0007	0	0.0000	--	--
Sel × Temp	4	0.0013	12	0.0008	1.50	0.26
Sel × B	6	0.0008	0	0.0000	--	--
Temp × B	6	0.0018	0	0.0000	--	--
Sel × Temp × B	12	0.0008	0	0.0000	--	--

Table 3.8: ANOVA table summarising the effects of selection, different constant ambient temperatures and their interaction on *r* (a proxy for normalised amplitude of the oscillation). Italicised effects are significant.

Summary of all effects	***df* Effect**	**MS Effect**	***df* Error**	**MS Error**	***F***	***p***
Selection (Sel)	*2*	*76.4098*	*6*	*0.9805*	*77.93*	*0.00*
Temperature (Temp)	*2*	*13.8516*	*6*	*0.4353*	*31.82*	*0.00*
Block (B)	3	0.1209	0	0.0000	--	--
Sel × Temp	4	1.4247	12	0.6026	2.36	0.11
Sel × B	6	0.9805	0	0.0000	--	--
Temp × B	6	0.4353	0	0.0000	--	--
Sel × Temp × B	12	0.6026	0	0.0000	--	--

The phases of our *control* populations under cool and warm temperatures were largely similar and this result is in contrast with a previously reported study, under similar conditions, albeit on *D. pseudoobscura* (Pittendrigh, 1954), thereby highlighting the importance of context/species-specificity of such results (Figures 3.4a, middle and 3.4b). It is also important to mention here that ψ_{PEAK} of *late* populations under 25 and 28 °C in the profiles (Figure 3.4a, right) appear to be different compared to the values reported in Table 3.3 and depicted in Figure 3.4b (top-left). This is due to higher replicate-to-replicate variation in the phase-value, as can be clearly seen in Figure 3.5.

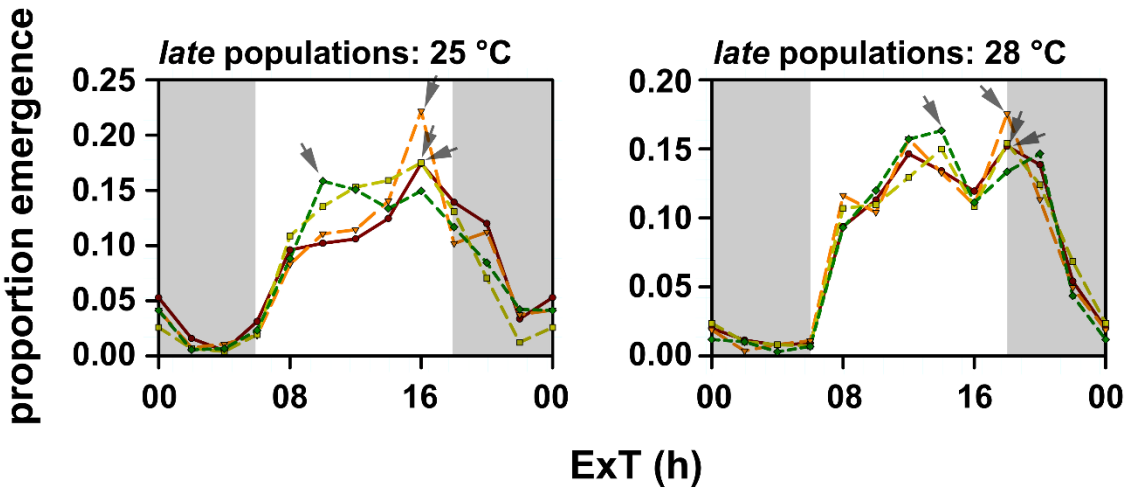

Figure 3.5: Block-wise profiles of the eclosion rhythm of *late* populations under LD 12:12 and constant temperatures of 25 °C (left) and 28 °C (right). Each trace in the figures represents the average eclosion profile for a replicate population. In both figures gray shaded regions represent the scotophase of the light/dark cycle. Arrowheads in both figures mark the phase of peak for each block. Such variation in the phases across blocks is likely the reason for apparent discrepancy between the peak timing observed in the average profile in Figure 3.4a, right and the values reported in Table 3.3.

In summary, the major bout of eclosion in *early* and *control* populations happened around the same time across different constant ambient temperatures. However, the *late* populations phase advanced their eclosion bout under lower temperatures relative to higher temperatures, thereby suggesting enhanced temperature sensitivity of the circadian network in these populations.

3.3.2. Eclosion rhythms under overall cool temperature cycles

Although I saw that under constant ambient temperatures, the divergence between *early* and *late* populations was driven by the response of *late* populations, to claim that such responses are driven by differences in the temperature sensitive slave oscillator, I must study their behaviour under conditions wherein temperature can act as a zeitgeber. Therefore, I first studied the eclosion rhythms of *early*, *control* and *late* stocks that were subjected to LD+TC_{19} (TC cycles with a mean

temperature of 19 °C) with low or high amplitudes – 3 °C or 6 °C, and compared them with constant cool (19 °C) temperature (cryophase:cryophase or CC, analogous to DD for constant darkness).

Visually, while the *early* chronotypes did not differ much across the provided regimes (Figure 3.6a, left), the *control* populations seemed to widen their eclosion distribution under TC19 with 3 °C amplitude, and delay the peak under 6 °C amplitude such that majority eclosion occurred during the thermophase (Figure 3.6a, middle). The *late* chronotypes suppressed eclosion even after lights-ON until the thermophase began, under both low and high amplitude temperature cycles (LA_{19} and HA_{19}, respectively) relative to its eclosion pattern under constant 19 °C (Figure 3.6a, right). That the three stocks respond to these zeitgeber regimes differently is supported by a statistically significant effect of selection × temperature regime × time-point interaction on proportion eclosion ($F_{44,132} = 18.36$, $p < 0.05$; Table 3.9).

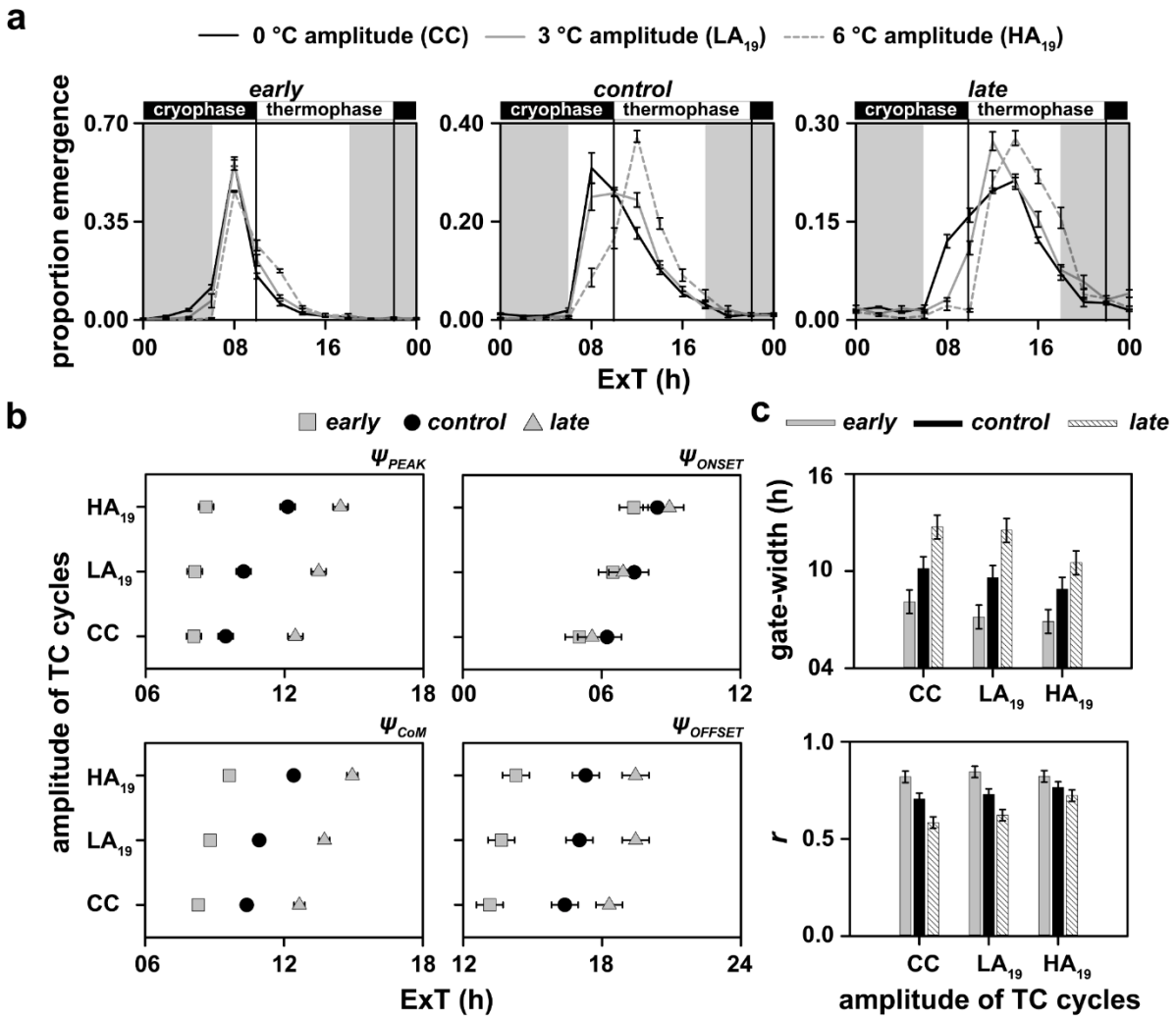

Figure 3.6: Depicted here are (a) eclosion rhythm profiles, (b) phase-markers, and (c) gate-width and normalized amplitude (*r*) for all stocks under LD 12:12 and varying amplitudes of TC 12:12 with an overall cool temperature. Temperature during the cryophase is 17.5 °C and 16 °C and that during the thermophase is 20.5 °C and 22 °C under the low and high amplitude TC, respectively. Note that the eclosion profiles of *early*, *control* and *late* populations under 0 °C amplitude (CC-regime) are data obtained from experiments reported in Figure 3.4. They are re-plotted here to facilitate appropriate analyses and visual comparisons. All other details are same as in Figure 3.4.

Table 3.9: Summary of all effects of a four-way mixed model randomized block design ANOVA on the proportion of flies eclosing at any given time-point of *early*, *control* and *late* populations under LD 12:12 and different amplitudes of TC 12:12 with an overall cool temperature.

Summary of all effects	***df* Effect**	**MS Effect**	***df* Error**	**MS Error**	***F***	***p***
Selection (Sel)	2	0.0000	6	0.0000	2.49	0.16
Temperature (Temp)	2	0.0000	6	0.0000	0.05	0.95
Time-Point (TP)	*11*	*0.2869*	*33*	*0.0004*	*720.27*	*0.00*
Block (B)	3	0.0000	0	0.0000	--	--
Sel × Temp	4	0.0000	12	0.0000	0.52	0.72
Sel × TP	*22*	*0.0959*	*66*	*0.0007*	*144.14*	*0.00*
Temp × TP	*22*	*0.0126*	*66*	*0.0002*	*61.47*	*0.00*
Sel × B	6	0.0000	0	0.0000	--	--
Temp × B	6	0.0000	0	0.0000	--	--
TP × B	33	0.0004	0	0.0000	--	--
Sel × Temp × TP	*44*	*0.0046*	*132*	*0.0002*	*18.36*	*0.00*
Sel × Temp × B	12	0.0000	0	0.0000	--	--
Sel × TP × B	66	0.0007	0	0.0000	--	--
Temp × TP × B	66	0.0002	0	0.0000	--	--
Sel × Temp × TP × B	132	0.0002	0	0.0000	--	--

I found that while the ψ_{PEAK} of *early* populations were invariant to different TC cycles, the *control* and *late* populations progressively delayed their phases with increasing amplitude of the TC cycles ($F_{4,12} = 21.94$, $p < 0.05$; Figure 3.6b, top-left; Tables 3.3 and 3.10). Interestingly, there were subtle changes in the waveform modulation of the *late* populations as compared to *early* and *control* populations that were observed when I analysed the ψ_{CoM}. Although all three stocks showed delayed ψ_{CoM} under HA_{19}, relative to their values under CC, only the *late* populations significantly delayed their phase under LA_{19} ($F_{4,12} = 10.12$, $p < 0.05$; Figure 3.6b, bottom-left; Tables 3.3 and 3.11). The apparent delay in ψ_{CoM} of *early* chronotypes under HA_{19} despite the profiles looking similar, I think, could be due to increased eclosion during the thermophase, which is visibly absent under CC (Figure 3.6a, left).

Table 3.10: ANOVA table summarising the effects of selection, amplitude of temperature cycles (low mean) and their interaction on ψ_{PEAK}. Italicised effects are significant.

Summary of all effects	***df* Effect**	**MS Effect**	***df* Error**	**MS Error**	***F***	***p***
Selection (Sel)	*2*	*80.8701*	*6*	*0.4032*	*200.55*	*0.00*
Temperature (Temp)	*2*	*9.1481*	*6*	*0.0631*	*145.09*	*0.00*
Block (B)	3	0.2158	0	0.0000	--	--
Sel × Temp	*4*	*1.3209*	*12*	*0.0602*	*21.94*	*0.00*
Sel × B	6	0.4032	0	0.0000	--	--
Temp × B	6	0.0631	0	0.0000	--	--
Sel × Temp × B	12	0.0602	0	0.0000	--	--

Table 3.11: ANOVA table summarising the effects of selection, amplitude of temperature cycles (low mean) and their interaction on ψ_{CoM}. Italicised effects are significant.

Summary of all effects	*df* Effect	MS Effect	*df* Error	MS Error	*F*	*p*
Selection (Sel)	*2*	*71.4611*	*6*	*0.2996*	*238.56*	*0.00*
Temperature (Temp)	*2*	*10.8815*	*6*	*0.0462*	*235.37*	*0.00*
Block (B)	3	0.1575	0	0.0000	--	--
Sel × Temp	*4*	*0.3026*	*12*	*0.0299*	*10.12*	*0.00*
Sel × B	6	0.2996	0	0.0000	--	--
Temp × B	6	0.0462	0	0.0000	--	--
Sel × Temp × B	12	0.0299	0	0.0000	--	--

Both, ψ_{ONSET} and ψ_{OFFSET} delayed with increasing amplitude of TC cycles, but all three stocks responded similarly (ψ_{ONSET}: $F_{4,12} = 2.38$, $p > 0.05$; Figure 3.6b, top-right; Tables 3.3 and 3.12; ψ_{OFFSET}: $F_{4,12} = 0.81$, $p > 0.05$; Figure 3.6b, bottom-right; Tables 3.3 and 3.13).

Gate-width narrowed with increasing amplitude of TC cycles, in a similar manner across all three stocks ($F_{4,12} = 2.71$, $p > 0.05$; Figure 3.6c, top; Tables 3.3 and 3.14). However, the normalized amplitude significantly increased under HA_{19} compared to its value under LA_{19} and CC only in the *late* populations ($F_{4,12} = 11.54$, $p < 0.05$; Figure 3.6c, bottom; Tables 3.3 and 3.15).

Table 3.12: ANOVA table summarising the effects of selection, amplitude of temperature cycles (low mean) and their interaction on ψ_{ONSET}. Italicised effects are significant.

Summary of all effects	*df* Effect	MS Effect	*df* Error	MS Error	*F*	*p*
Selection (Sel)	*2*	*3.7203*	*6*	*0.2596*	*14.33*	*0.01*
Temperature (Temp)	*2*	*20.6407*	*6*	*0.1029*	*200.65*	*0.00*
Block (B)	3	0.1493	0	0.0000	--	--
Sel × Temp	4	0.5231	12	0.2201	2.38	0.11
Sel × B	6	0.2596	0	0.0000	--	--
Temp × B	6	0.1029	0	0.0000	--	--
Sel × Temp × B	12	0.2201	0	0.0000	--	--

Table 3.13: ANOVA table summarising the effects of selection, amplitude of temperature cycles (low mean) and their interaction on ψ_{OFFSET}. Italicised effects are significant.

Summary of all effects	*df* Effect	MS Effect	*df* Error	MS Error	*F*	*p*
Selection (Sel)	*2*	*87.9500*	*6*	*0.9347*	*94.10*	*0.00*
Temperature (Temp)	*2*	*3.5760*	*6*	*0.2823*	*12.67*	*0.01*
Block (B)	3	0.2636	0	0.0000	--	--
Sel × Temp	4	0.1556	12	0.1924	0.81	0.54
Sel × B	6	0.9347	0	0.0000	--	--
Temp × B	6	0.2823	0	0.0000	--	--
Sel × Temp × B	12	0.1924	0	0.0000	--	--

Table 3.14: ANOVA table summarising the effects of selection, amplitude of temperature cycles (low mean) and their interaction on gate-width. Italicised effects are significant.

Summary of all effects	*df* Effect	MS Effect	*df* Error	MS Error	*F*	*p*
Selection (Sel)	*2*	*61.7331*	*6*	*1.8556*	*33.27*	*0.00*
Temperature (Temp)	*2*	*7.5321*	*6*	*0.1314*	*57.31*	*0.00*
Block (B)	3	0.4317	0	0.0000	--	--
Sel × Temp	4	0.8340	12	0.3075	2.71	0.08
Sel × B	6	1.8556	0	0.0000	--	--
Temp × B	6	0.1314	0	0.0000	--	--
Sel × Temp × B	12	0.3075	0	0.0000	--	--

Table 3.15: ANOVA table summarising the effects of selection, amplitude of temperature cycles (low mean) and their interaction on *r*. Italicised effects are significant.

Summary of all effects	*df* Effect	MS Effect	*df* Error	MS Error	*F*	*p*
Selection (Sel)	*2*	*0.1034*	*6*	*0.0021*	*49.49*	*0.00*
Temperature (Temp)	*2*	*0.0135*	*6*	*0.0005*	*29.35*	*0.00*
Block (B)	3	0.0001	0	0.0000	--	--
Sel × Temp	*4*	*0.0057*	*12*	*0.0005*	*11.54*	*0.00*
Sel × B	6	0.0021	0	0.0000	--	--
Temp × B	6	0.0005	0	0.0000	--	--
Sel × Temp × B	12	0.0005	0	0.0000	--	--

In summary, the *early* populations were robust under different amplitudes of cool temperature TC cycles. However, although the *control* and *late* populations altered their phases in response to different regimes in a similar manner, the *late* populations were more sensitive compared to both *early* and *control* stocks and could alter their phases in response to a mere 3 °C amplitude in TC cycles. Moreover, the amplitude/consolidation of only the *late* populations increased under HA_{19}.

These results suggest the evolution of attenuation of temperature response in the *early* populations and reinforces the notion of the evolution of enhanced temperature sensitivity of the clock in *late* populations.

3.3.3. Eclosion rhythms under overall warm temperature cycles

Subsequently, I analysed the eclosion rhythm profiles of our populations under LD+TC_{28} (TC cycles with a mean temperature of 28 °C). I found a statistically significant effect of selection × temperature regime × time-point interaction on proportion eclosion ($F_{44,132} = 18.59$, $p < 0.05$; Table 3.16). The waveform of *control* populations was not altered under LA_{28} as compared to constant 28 °C (thermophase:thermophase or TT, analogous to LL for constant light; Figure 3.7a, middle). However, the *control* populations had sharper peak and tighter gating under HA_{28}. The *early* chronotypes showed sharper peaks and narrower gate-width under both LA_{28} and HA_{28} relative to TT (Figure 3.7a, left). The *late* chronotypes, overall, showed the most distinct changes in waveform - a phase advance under LA_{28} such that emergence occurred during the early hours of the thermophase. Importantly, under HA_{28}, the *late* chronotypes showed a very sharp peak and phase advance by ~5-6-h relative to TT and most emergence occurred just before the transition to the thermophase (~31 °C; Figure 3.7a, right).

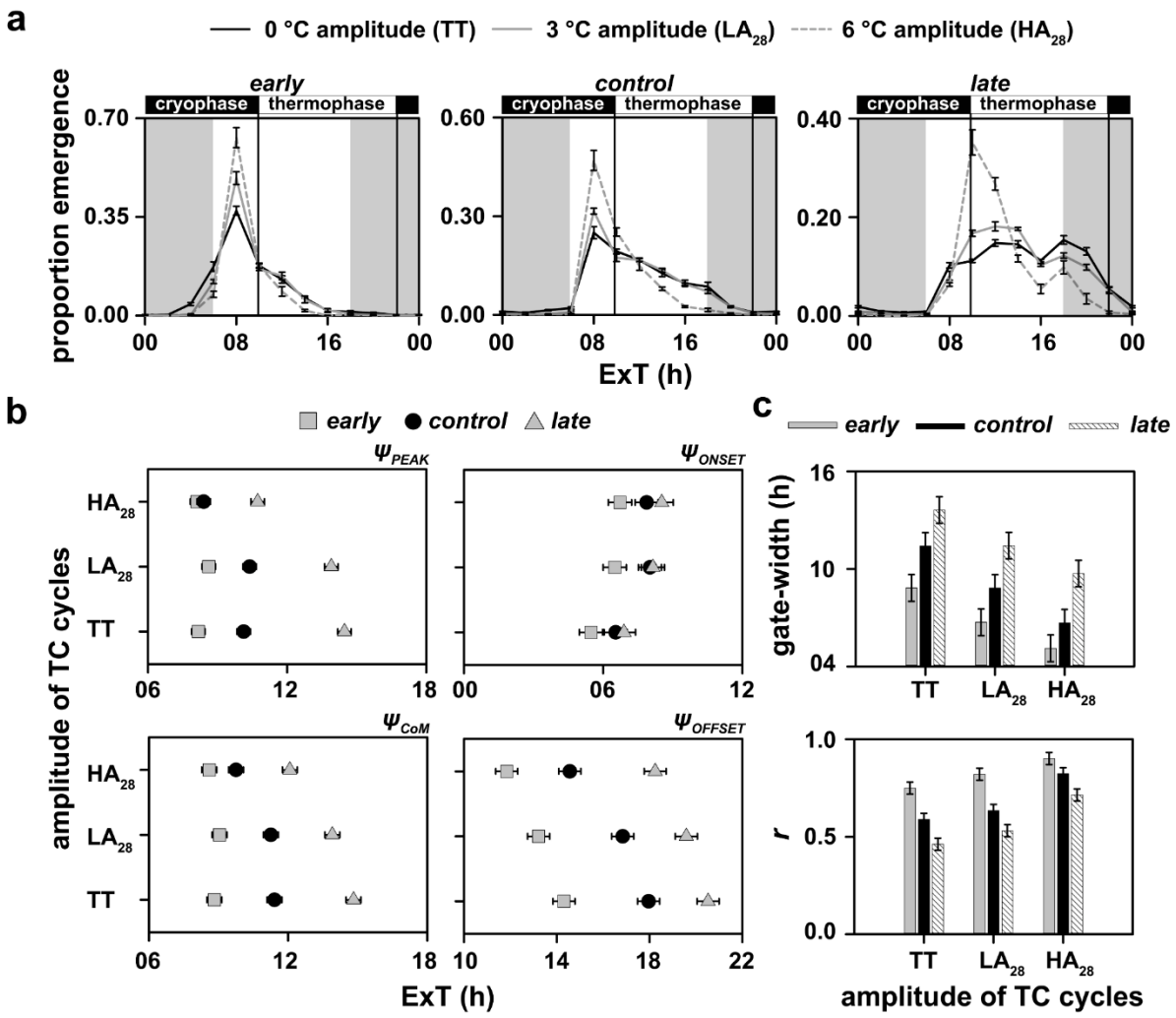

Figure 3.7: Depicted here are (a) eclosion rhythm profiles, (b) phase-markers, and (c) gate-width and normalized amplitude (*r*) for all stocks under LD 12:12 and varying amplitudes of TC 12:12 with an overall warm temperature. Temperature during the cryophase is 26.5 °C and 25 °C and that during the thermophase is 29.5 °C and 31 °C under the low and high amplitude TC, respectively. Note that the eclosion profiles of *early*, *control* and *late* populations under 0 °C amplitude (TT-regime) are data obtained from experiments reported in Figure 3.4. All other details are same as in Figure 3.6.

Table 3.16: Summary of all effects of a four-way mixed model randomized block design ANOVA on the proportion of flies eclosing at any given time-point of *early*, *control* and *late* populations under LD 12:12 and different amplitudes of TC 12:12 with an overall warm temperature.

Summary of all effects	***df* Effect**	**MS Effect**	***df* Error**	**MS Error**	***F***	***p***
Selection (Sel)	*2*	*0.0000*	*6*	*0.0000*	*6.14*	*0.04*
Temperature (Temp)	2	0.0000	6	0.0000	1.00	0.42
Time-Point (TP)	*11*	*0.3173*	*33*	*0.0003*	*1051.38*	*0.00*
Block (B)	3	0.0000	0	0.0000	--	--
Sel × Temp	4	0.0000	12	0.0000	0.27	0.89
Sel × TP	*22*	*0.0662*	*66*	*0.0005*	*134.50*	*0.00*
Temp × TP	*22*	*0.0129*	*66*	*0.0002*	*60.20*	*0.00*
Sel × B	6	0.0000	0	0.0000	--	--
Temp × B	6	0.0000	0	0.0000	--	--
TP × B	33	0.0003	0	0.0000	--	--
Sel × Temp × TP	*44*	*0.0056*	*132*	*0.0003*	*18.59*	*0.00*
Sel × Temp × B	12	0.0000	0	0.0000	--	--
Sel × TP × B	66	0.0005	0	0.0000	--	--
Temp × TP × B	66	0.0002	0	0.0000	--	--
Sel × Temp × TP × B	132	0.0003	0	0.0000	--	--

I found that the ψ_{PEAK} of *early* populations were again robust; whereas both the *control* and *late* populations phase advanced their peak under HA_{28} relative to LA_{28} and TT ($F_{4,12} = 75.74$, $p < 0.05$; Figure 3.7b, top-left; Tables 3.3 and 3.17). In case of the ψ_{CoM}, while the *early* populations held similar phases under LA_{28} and HA_{28}, the *control* and *late* populations phase advanced under HA_{28} relative to LA_{28} and TT. However, only the *late* populations phase advanced significantly even under LA_{28} compared with TT ($F_{4,12} = 27.87$, $p < 0.05$; Figure 3.7b, bottom-left; Tables 3.3 and 3.18).

Table 3.17: ANOVA table summarising the effects of selection, amplitude of temperature cycles (high mean) and their interaction on ψ_{PEAK}. Italicised effects are significant.

Summary of all effects	*df* Effect	MS Effect	*df* Error	MS Error	*F*	*p*
Selection (Sel)	*2*	*71.4779*	*6*	*0.0759*	*941.24*	*0.00*
Temperature (Temp)	*2*	*13.9333*	*6*	*0.2452*	*56.83*	*0.00*
Block (B)	3	0.1720	0	0.0000	--	--
Sel × Temp	*4*	*3.6558*	*12*	*0.0483*	*75.74*	*0.00*
Sel × B	6	0.0759	0	0.0000	--	--
Temp × B	6	0.2452	0	0.0000	--	--
Sel × Temp × B	12	0.0483	0	0.0000	--	--

Table 3.18: ANOVA table summarising the effects of selection, amplitude of temperature cycles (high mean) and their interaction on ψ_{CoM}. Italicised effects are significant.

Summary of all effects	*df* Effect	MS Effect	*df* Error	MS Error	*F*	*p*
Selection (Sel)	*2*	*69.2731*	*6*	*0.1489*	*465.23*	*0.00*
Temperature (Temp)	*2*	*8.0814*	*6*	*0.1820*	*44.40*	*0.00*
Block (B)	3	0.0467	0	0.0000	--	--
Sel × Temp	*4*	*1.6419*	*12*	*0.0589*	*27.87*	*0.00*
Sel × B	6	0.1489	0	0.0000	--	--
Temp × B	6	0.1820	0	0.0000	--	--
Sel × Temp × B	12	0.0589	0	0.0000	--	--

Unlike in the cool temperature TC cycles, ψ_{ONSET} and ψ_{OFFSET} delayed and advanced, respectively, with increasing amplitude of TC cycles when overall temperature was warm. This change, however, was similar for all populations (ψ_{ONSET}: $F_{4,12} = 0.76$, $p > 0.05$; Figure 3.7b, top-right; Tables 3.3 and 3.19; ψ_{OFFSET}: $F_{4,12} = 3.35$, $p = 0.05$; Figure 3.7b, bottom-right; Tables 3.3 and 3.20).

Table 3.19: ANOVA table summarising the effects of selection, amplitude of temperature cycles (high mean) and their interaction on ψ_{ONSET}. Italicised effects are significant.

Summary of all effects	*df* Effect	MS Effect	*df* Error	MS Error	*F*	*p*
Selection (Sel)	*2*	*8.6462*	*6*	*0.1109*	*77.94*	*0.00*
Temperature (Temp)	*2*	*7.1296*	*6*	*0.1322*	*53.93*	*0.00*
Block (B)	3	0.0666	0	0.0000	--	--
Sel × Temp	4	0.1085	12	0.1429	0.76	0.57
Sel × B	6	0.1109	0	0.0000	--	--
Temp × B	6	0.1322	0	0.0000	--	--
Sel × Temp × B	12	0.1429	0	0.0000	--	--

Table 3.20: ANOVA table summarising the effects of selection, amplitude of temperature cycles (high mean) and their interaction on ψ_{OFFSET}. Italicised effects are significant.

Summary of all effects	*df* Effect	MS Effect	*df* Error	MS Error	*F*	*p*
Selection (Sel)	*2*	*120.2974*	*6*	*1.1740*	*102.47*	*0.00*
Temperature (Temp)	*2*	*22.4639*	*6*	*0.3593*	*62.53*	*0.00*
Block (B)	3	0.2252	0	0.0000	--	--
Sel × Temp	4	0.4349	12	0.1299	3.35	0.05
Sel × B	6	1.1740	0	0.0000	--	--
Temp × B	6	0.3593	0	0.0000	--	--
Sel × Temp × B	12	0.1299	0	0.0000	--	--

Gating of rhythms were affected to similar extents in all three sets of populations under TT, LA_{28} and HA_{28} ($F_{4,12} = 0.75$, $p > 0.05$; Figure 3.7c, top; Tables 3.3 and 3.21). Additionally, the relative difference in *r* between chronotypes was significantly lower under HA_{28} relative to TT ($F_{4,12} = 8.17$, $p < 0.05$; Figure 3.7c, bottom; Tables 3.3 and 3.22).

Table 3.21: ANOVA table summarising the effects of selection, amplitude of temperature cycles (high mean) and their interaction on gate-width. Italicised effects are significant.

Summary of all effects	***df* Effect**	**MS Effect**	***df* Error**	**MS Error**	***F***	***p***
Selection (Sel)	*2*	*66.7302*	*6*	*1.5464*	*43.15*	*0.00*
Temperature (Temp)	*2*	*51.1091*	*6*	*0.3200*	*159.73*	*0.00*
Block (B)	3	0.1185	0	0.0000	--	--
Sel × Temp	4	0.2915	12	0.3876	0.75	0.58
Sel × B	6	1.5464	0	0.0000	--	--
Temp × B	6	0.3200	0	0.0000	--	--
Sel × Temp × B	12	0.3876	0	0.0000	--	--

Table 3.22: ANOVA table summarising the effects of selection, amplitude of temperature cycles (high mean) and their interaction on *r*. Italicised effects are significant.

Summary of all effects	***df* Effect**	**MS Effect**	***df* Error**	**MS Error**	***F***	***p***
Selection (Sel)	*2*	*0.1954*	*6*	*0.0021*	*93.59*	*0.00*
Temperature (Temp)	*2*	*0.1439*	*6*	*0.0010*	*146.63*	*0.00*
Block (B)	3	0.0004	0	0.0000	--	--
Sel × Temp	*4*	*0.0045*	*12*	*0.0006*	*8.17*	*0.00*
Sel × B	6	0.0021	0	0.0000	--	--
Temp × B	6	0.0010	0	0.0000	--	--
Sel × Temp × B	12	0.0006	0	0.0000	--	--

It is important to note here, the apparent discrepancy in the phase-values for the peak in *control* populations in Figure 3.7a (middle) and 3.7b (top-left). Although it appears as if the peak occurred at the same phase for TT, LA_{28} and HA_{28}, it is clear that the eclosion profiles of the *control* populations after the peak were flatter in TT and LA_{28}. In order to gain clarity on this issue, I examined block-wise profiles and the raw time-series values of all vials within a block and found

high degree of across-cycle and across-vial variation (Figure 3.8). This I believe contributed to the flatter profile under TT and LA_{28}, and to the mean phase-values that appear delayed as compared to what one would infer from the profiles.

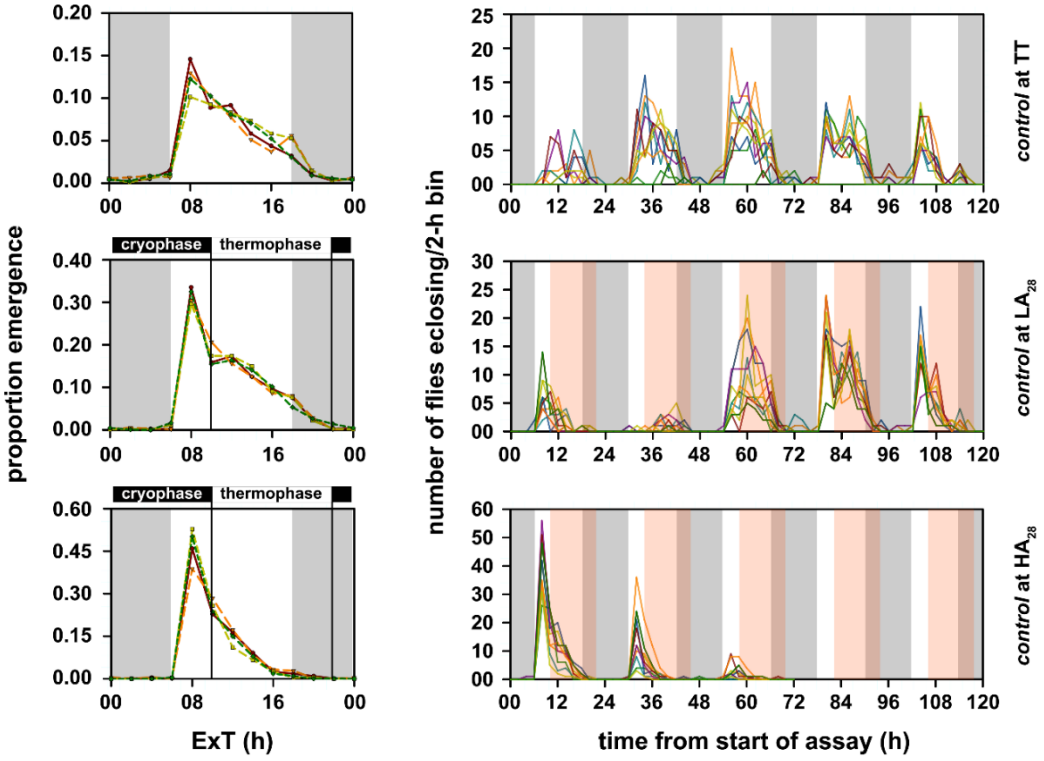

Figure 3.8: Block-wise profiles of the eclosion rhythm of *control* populations under TT (top), LA_{28} (middle) and HA_{28} (bottom) regimes. The left panel for all three regimes represents the average eclosion profile for each replicate block. Although the ψ_{PEAK} appears to be at the same time for all three regimes, the fall of the waveform after the peak in TT and LA_{28} appeared flatter than the one under HA_{28}. This prompted me to look at the raw data for each of these regimes. Shown on the right are time-series traces for each regime for Block-3. Each line in the figures on the right side represents a single culture vial. It is abundantly clear that there is higher cycle-to-cycle and vial-to-vial variation under TT and LA_{28} as compared with HA_{28}. This, I argue, is the reason why phases in the profiles of Figure 3.7a, middle and plots in Figure 3.7b, top-left do not match. In all the figures, gray shaded region represents the scotophase of the LD cycle and the red shaded region represents the thermophase of the TC cycle.

In summary, I again found that the *early* populations were robust, and the *late* populations were more labile than the *control* populations, in response to changes in constant ambient temperatures. Additionally, I found that chronotype divergence is finely regulated depending on ambient temperature values and was largely brought about by the response of our *late* populations.

3.3.4. Chronotype divergence

To understand the degree of difference in chronotype divergence/convergence that is brought about by different temperature regimes, I analysed divergence values using ψ_{CoM}. I found that the phase divergence between *early* and *late* stocks under LD 12:12 and constant 19 °C (~4.37-h) was statistically, significantly lower than the divergence under both, 25 (~6.37-h) and 28 °C (~6-h; $F_{2,6} = 11.66$, $p < 0.05$; Figure 3.9, left; Table 3.23).

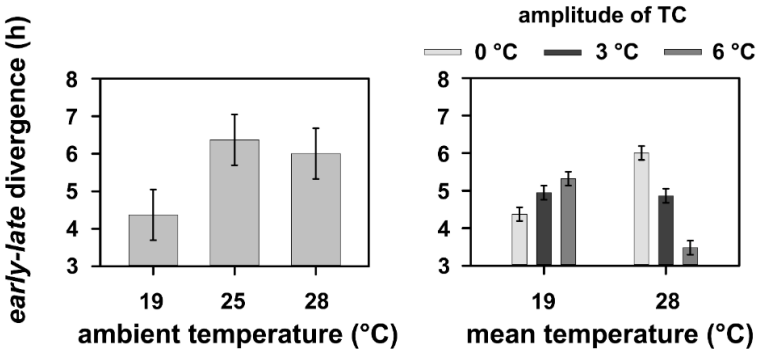

Figure 3.9: The phase divergence between *early* and *late* chronotypes estimated using the phase-of-centre of mass (ψ_{CoM}) under LD 12:12 and different constant ambient temperatures (left) and LD 12:12 and varying amplitudes of TC 12:12 with different mean temperatures (right). Error bars denote 95% CI calculated using the Tukey's HSD critical values. Therefore, all means with non-overlapping error bars are statistically significantly different from each other. Please note that the data for divergence between *early* and *late* chronotypes under LD+TC with 0 °C amplitude in the right panel is the same data as that in the 19 and 28 °C category in the left panel. They are re-plotted here to facilitate appropriate analyses and visual comparisons. All mean values were derived as described in Figure 3.4.

Moreover, my analysis revealed a statistically significant interaction of mean temperature × amplitude of temperature cycle on *early-late* divergence using ψ_{CoM} ($F_{2,6} = 345.01$, $p < 0.05$; Figure 3.9, right; Table 3.24). Under an overall cool temperature, the divergence between *early* and *late* stocks increased by ~1-h with increasing amplitudes of temperature cycles (Figure 3.9, right). On the other hand, the divergence significantly reduced by ~2.5-h with increasing amplitude of temperature cycles under an overall warm temperature environment (Figure 3.9, right).

Table 3.23: Summary of all effects of a two-way mixed model randomized block design ANOVA on the divergence between *early* and *late* populations under LD 12:12 and different constant ambient temperatures.

Summary of all effects	***df* Effect**	**MS Effect**	***df* Error**	**MS Error**	***F***	***p***
Temperature (Temp)	*2*	*4.5286*	*6*	*0.3883*	*11.66*	*0.01*
Block (B)	3	0.5303	0	0.0000	--	--
Temp × B	6	0.3883	0	0.0000	--	--

Table 3.24: Summary of all effects of a three-way mixed model randomized block design ANOVA on the divergence between *early* and *late* populations under LD 12:12 and different amplitudes of TC 12:12 with different mean temperatures.

Summary of all effects	***df* Effect**	**MS Effect**	***df* Error**	**MS Error**	***F***	***p***
Mean temperature (MT)	1	0.0559	3	0.3837	0.15	0.73
Amplitude of temperature cycle (Amp)	*2*	*1.2761*	*6*	*0.1913*	*6.67*	*0.03*
Block (B)	3	0.5669	0	0.0000	--	--
MT × Amp	*2*	*6.0235*	*6*	*0.0175*	*345.01*	*0.00*
MT × B	3	0.3837	0	0.0000	--	--
Amp × B	6	0.1913	0	0.0000	--	--
MT × Amp × B	6	0.0175	0	0.0000	--	--

While earlier work from our laboratory showed that chronotype divergence enhances when presented with both LD and TC cycles simultaneously (Nikhil et al., 2014), here I show that (i) divergence increases depending on the overall temperature regime, (ii) change in entrained phase that contributes to divergence is affected at amplitudes of temperature cycles as low as 3 °C, and (iii) this difference in divergence is brought about only by the *late* chronotypes' response to different temperature regimes. These results, along with results under constant 19° and 28 °C ambient temperature, are suggestive of the fact that the *late* chronotypes have evolved enhanced temperature responsiveness in response to selection on timing of behavior under light cycles, perhaps via a change in their circadian clock structure/properties that is responsible for temperature sensing/entrainment. This, I speculate, may allow the *late* populations to restrict emergence to 'favourable' times of the day by tracking temperature cycles, even in the presence of standard LD cycles. Additionally, my results suggest the evolution of attenuated temperature sensitivity in the *early* populations, at least in the presence of LD cycles.

3.4. Discussion

While studies have been performed to understand the association between circadian clock properties, and chronotype regulation and divergence, barring a few (Liu et al., 1998; Nikhil et al., 2014; Pittendrigh, 1960), these studies have probed circadian clock properties using only one zeitgeber at a time (Bordyugov et al., 2015; Granada et al., 2013; Nikhil, Vaze et al., 2016; Roenneberg, Tan et al., 2005). Moreover, these studies have not explicitly attempted to understand the relative roles of light and temperature sensitive components of the circadian clock network in mediating chronotype divergence. In view of these observations, and to understand the contributions of mean environmental temperature, amplitude of temperature cycles and temperature sensitive modalities of the clock to chronotype divergence in a realistic environmental

regime, I assayed the eclosion rhythm of *early*, *control* and *late* stocks under different temperature regimes in the presence of standard LD cycles.

I found that (i) phases of *early* populations were fairly robust and did not change much under different temperature regimes (Figures 3.4, 3.6 and 3.7), (ii) phases of *late* populations appear to be more flexible and changed readily (Figures 3.4, 3.6 and 3.7), and (iii) as a consequence, chronotype divergence was different under different temperature regimes (Figure 3.9). In my experiments, under overall cool TC cycles, the highest temperature reached was 22 °C, whereas the minimum was 16 °C; and under warm temperature TC cycles, while the highest was 31 °C, the lowest was 25 °C. I think that the *late* populations delayed their phase to avoid eclosing at times of the day when temperature was too low and thereby enhanced chronotype divergence under cool mean temperatures, and on the other hand, advanced their phase to avoid eclosing at times of the day when temperature was too high and reduced chronotype divergence under warm mean temperatures. Moreover, I also found that while ψ_{PEAK} and ψ_{CoM} behaved similarly, they differed from ψ_{ONSET} and ψ_{OFFSET} in terms of their response, suggesting differential functional constraints on each phase-marker (Figures 3.4b, 3.6b and 3.7b; discussed later).

3.4.1. Why are timing of eclosion and temperature responsiveness associated? - Reflections on how the circadian timekeeper is wired

Circadian programs are believed to have evolved in response to the complex "time structure of the environment" (Daan, 1981). This implies that behavioural routines, to enhance fitness in organisms, would require, in addition to a time-keeping device, adaptation at multiple levels that would enable individuals to capitalize on a specific temporal niche. For instance, adopting diurnality as a strategy would require adaptations to enable vision and/or to avoid desiccation in

insects with thin integuments under high temperatures during the day as opposed to nocturnality (see Daan, 1981 and references therein).

I believe that evidence of co-evolution of traits from experimental evolution studies such as ours significantly enhances our understanding of which adaptations accompany the evolution of a different timing of behaviour. Despite selection acting on these populations under a constant temperature of 25 °C, enhanced sensitivity to temperature evolved in *late* populations and attenuated sensitivity evolved in the *early* populations, implying a genetic correlation between timing of eclosion and temperature sensitivity of the clock. A few previous studies have also shown a relationship between timing of eclosion and temperature sensitivity, albeit not in a similar way as mine. Kureck (1979) showed that midges (*Chironomus thummi*, Diptera) in cold water emerge during early hours of the afternoon, but midges in warm water emerge only after dusk. Another study done on the zygaenid moth (*Pseudopidorus fasciata*, Lepidoptera) showed that under natural conditions, these moths eclose predominantly during mid-day and in the laboratory their eclosion rhythm phase advances under warm temperature, in a manner somewhat similar to the behaviour of our *late* populations (Fig. 3.7a; Wu et al., 2014). Such results strengthen our notion that the circadian network evolves as an ensemble, reflecting how they may have been shaped in the evolutionary past. There are other insect species that show eclosion predominantly in the evening or night, such as the flour moth and some chironomids (Saunders, 2002), but there is no specific information on the temperature sensitivity of their circadian clocks. Studies that probe into the temperature responses in these insects will prove to be a useful resource in understanding the relationship between temperature sensitivity and the timing of adult eclosion.

I think that it is crucial here to also ask why the *early* chronotypes do not seem to respond to such a wide range of temperature regimes. One reason for this could be that there is inadvertent

selection on the masking response to light in the *early* populations (see Chapter 2). During my assays, we count flies in 2-h intervals, and at the time-point at which lights turn ON, we count flies just before the transition. However, for the next time-point, all flies that eclose after lights turned ON are counted; therefore, a large component of the number of flies that eclose in the time-point after lights-ON could be because of masking response to this transition. Indeed, some preliminary results from our laboratory indicate that the *early* populations may have evolved higher masking responses (*Arijit Ghosh and Vasu Sheeba, unpublished data*). This may lead to higher propensity of the *early* chronotypes to follow the dark-to-light transition and therefore be phase-locked to dawn. Alternatively, the fact that ψ_{ENT} of *early* populations are robust across different temperature regimes could imply that there is evolution of attenuated temperature responses in the *early* populations. There are some indications from prior studies in our laboratory that suggest *early* populations have enhanced light sensitivity compared to the *late* populations (Abhilash and Sharma, 2020; Nikhil, Vaze et al., 2016). Based on this result one could speculate that there is perhaps a trade-off between light sensitivity and temperature sensitivity of the circadian clock.

3.4.2. How are the *late* chronotypes more temperature responsive?

3.4.2.1. From a molecular mechanistic perspective

The behaviour of ψ_{ENT} of the *late* chronotypes under constant ambient temperatures is reminiscent of the behaviour of the evening peak of activity/rest rhythms in *D. melanogaster,* that phase-delays under warm temperatures, and advances under cool temperatures in an otherwise regular light/dark cycle (Helfrich-Förster, 2017; Majercak et al., 1999). We now know that cool and warm temperatures promote splicing of *per* (period) and *tim* (timeless), respectively. Moreover, we understand that full-length TIM has increased affinity towards CRY, and therefore promotes earlier degradation of TIM. While cool temperatures lead to faster accumulation of *per* mRNA,

and reduced splicing of *tim* and such conditions phase advance the activity/rest rhythms, the opposite occurs under warm temperatures. It is thought that such temperature sensitive splicing events in core clock genes contribute to different phases under a wide range of constant and cycling temperature cues (Helfrich-Förster, 2017; Montelli et al., 2015). Given similar behaviour of the phase of eclosion rhythm of *late* chronotypes in my experiments, I hypothesise that differential propensity to splice *per* and/or *tim* may have evolved to facilitate enhanced phase-lability in the face of temperature changes in the *late* flies. More recently, other studies have also revealed the importance of splicing events in regulating period and phase of circadian rhythms, and also entrainment under different temperature regimes (Evantal et al., 2018; Foley et al., 2018; Shakhmantsir et al., 2018), thereby providing substrate for my hypothesis that phase-lability could be driven by changes in these intra-cellular mechanisms. However, it is important to note that it is not possible to directly comment on the exact role these mechanisms will have on phase-lability of the eclosion rhythm, without first establishing that differential splicing events may indeed regulate phases of the eclosion rhythm under different temperatures. Nevertheless, I feel that this is an open question and merits further investigation.

3.4.2.2. From an organisational perspective

Many studies on moths and *Drosophila* have indicated that adult eclosion timing is regulated by two processes, the developmental stage and the circadian clock (Newby and Jackson, 1991; Pittendrigh and Skopik, 1970; Qiu and Hardin, 1996). Subsequently, work in *D. melanogaster* has shown that the prothoracic gland (PG) has a self-sustained oscillation of PER and TIM, suggesting the presence of a second 'clock', which is regulated by the central brain clock, thereby yielding physiological correlates of Pittendrigh's *A-B* oscillator model (Emery et al., 1997; Morioka et al., 2012; Myers et al., 2003). More recently, Selcho et al. (2017) showed that the s-LNvs (small

ventral lateral neurons) communicate timing information via the inhibitory sNPF (*Drosophila* short neuropeptide F) to the PTTH neurons, which then relay this information to the PG clock. This information inhibits steroidogenesis, and the ecdysone titers drop below the threshold, which then leads to the commitment to emerge in the next available "gate." Owing to the fact that the *B*-oscillator must be temperature sensitive to facilitate optimal phasing and temperature entrainment, I think that phases of processes downstream of the LNvs, such as sensitivity of PTTH neurons to sNPF, or the period of the PG clock, are what have changed in the *late* chronotypes, thereby yielding flexible ψ_{ENT}. It is also possible that changes in the PG clock in response to a variety of temperatures may render them more or less susceptible to temporal signals coming from the PTTH neurons. Although speculative, the circuitry downstream of the s-LNvs provides putative targets for further experiments to understand the mechanisms by which ψ_{ENT} of the *late* chronotypes is made highly flexible and that of the *early* chronotypes highly rigid.

3.4.2.3. From a theoretical perspective

One can understand high phase lability in the *late* populations using either the slope of the temperature pulse PRC (Pittendrigh and Daan, 1976a) or the amplitude model of limit-cycle oscillators (Lakin-Thomas et al., 1991). Although abstract, the limit-cycle model postulates that amplitude of the limit cycle shrinks and expands under cool and warm temperatures, respectively, to maintain the periodicity of the circadian time-keeper, and has found validation from phase-response based studies performed in *Neurospora* and *Drosophila* (Lakin-Thomas et al., 1991; Ruoff et al., 1999; Varma et al., 2013). Additionally, slope of the PRC contributes a great deal to the flexibility of ψ_{ENT} (Pittendrigh and Daan, 1976a). My results suggest that high lability of phases in the *late* populations may stem from larger amplitude of the PRC or higher sensitivity of

the amplitude of the limit-cycle state variable to temperature, thereby yielding testable predictions for future experiments.

I have integrated these mechanisms at different organizational levels into a speculative model for clarity and refer the reader to Figure 3.10.

3.4.3. On the differential response of different phase-markers to temperature regimes

The importance of the choice of phase-marker is highlighted by studies that showed opposite effects of light intensity on precision of phases of the onset and offset of activity (Aschoff et al., 1971). Hence, I used multiple phase-markers in our experiments to analyse the overall response of rhythms to different temperature regimes. In all my experiments, different phase-markers respond to different extents, either in the same direction or in the opposite direction (see Figures 3.4b, 3.6b and 3.7b). This pattern of differential response of phase-markers suggests that optimal phasing and gating of eclosion rhythm is brought about by the modulation of different phase-markers, such that majority eclosion happens around 'favourable' times of the day.

In summary, I argue that low and high flexibility in the ψ_{ENT} of the *early* and *late* chronotypes, respectively, is perhaps, a result of the genetic correlation between temperature responsiveness and timing of behaviour. Additionally, regulation of flexibility in ψ_{ENT} in our populations can occur at different levels of biological organization which may be explored in future studies.

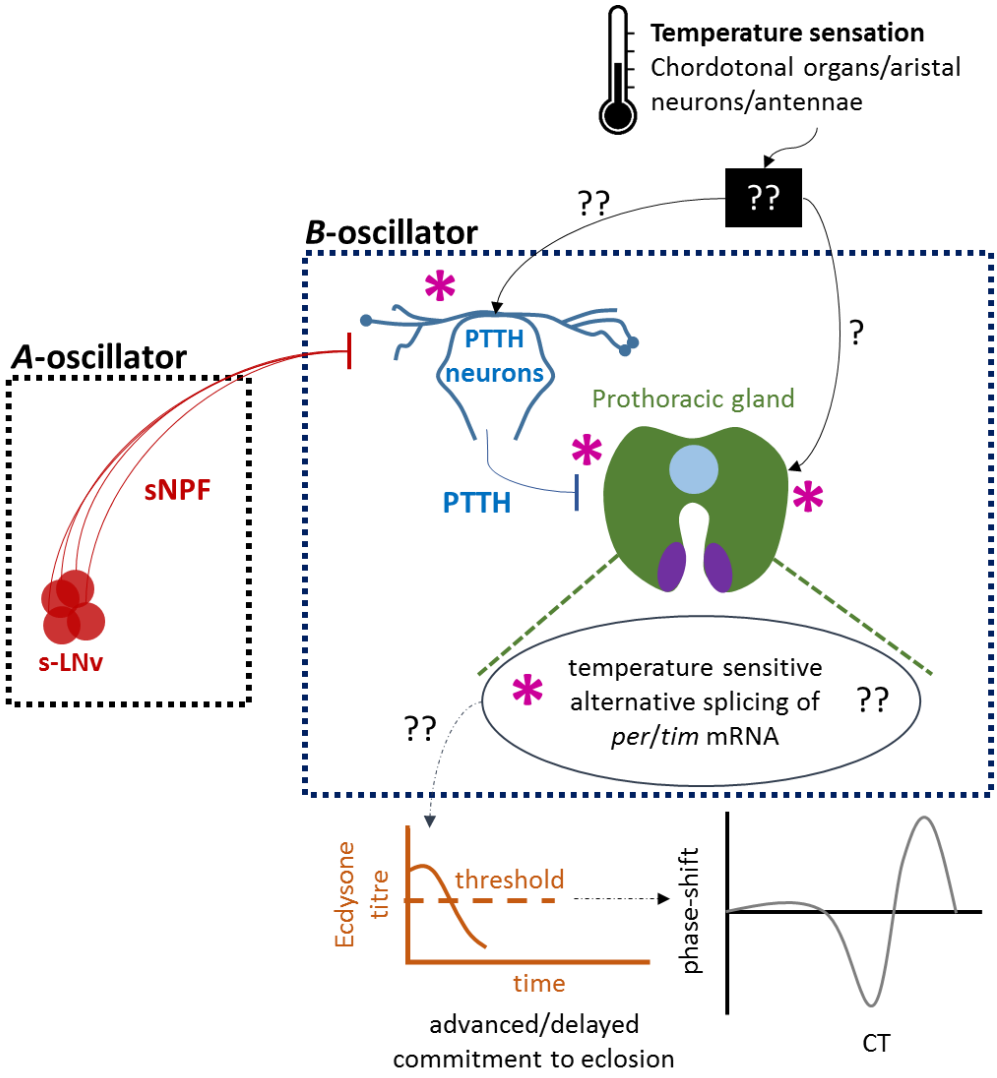

Figure 3.10: A speculative model integrating intra-cellular and organizational level circuitry regulating the eclosion rhythm in *Drosophila*. Also shown are putative pathways to relay temperature information to the clock regulating gating. Asterisks indicate potential areas of the control centre that may have evolved differently in the *early* and *late* populations. See text for more details. The question marks indicate a lack of information regarding those arms in the model. Additionally, the dash-dot-dash arrows indicate putative indirect regulation. We think that s-LNvs owing to their role as the central/*A*-clock are unlikely to be temperature sensitive. Moreover, Selcho et al. (2017) argue that timing information to the PG clock comes via the PTTH neurons. Additionally, because PER and TIM levels cycle in the PG clock (Myers et al., 2003), it is possible that temperature input to PG clock enables alternative splicing of these genes that may result in phase-advanced or phase-delayed behaviour. Such differences in the coupling of the circuit could also be invoked to understand bimodality of eclosion rhythm in the *late* populations under warm temperatures (Figure 3.4a, right; Figure 3.7a, right).

Chapter 4. Waveform plasticity under entrainment to 12-hour *T*-cycles in *Drosophila melanogaster*: behaviour, neuronal network and evolution

Parts of this chapter are accepted for publication in the following research article:

Abhilash L, Ramakrishnan A, Priya S and Sheeba V (2020) Waveform plasticity under entrainment to 12-hour T-cycles in Drosophila melanogaster: behavior, neuronal network and evolution. Journal of Biological Rhythms 35(2): 145–157.

4.1. Introduction

Circadian clocks are time-keeping mechanisms that drive near 24-h rhythms in behaviour and physiology, under constant conditions, across the living world. They synchronise to the environmental day and night, and restrict activity to specific times of the day via a process referred to as entrainment (Dunlap et al., 2004). Such temporal restriction is believed to be adaptive to organisms (Vaze and Sharma, 2013). Over and above timing, clocks are also known to alter the rhythm waveform (also referred to as waveform plasticity, henceforth) in response to various environmental pressures, in ways that have ecological relevance (De et al., 2013; Menegazzi et al., 2012; Vanin et al., 2012; Vaze, Nikhil et al., 2012).

Plasticity in response to varying light conditions has been extensively studied in rodents over the last several decades (Gorman et al., 2017; Gorman and Elliott, 2003, 2004; Harrison et al., 2016; Pittendrigh and Daan, 1976b). Few such studies have revealed that two LD cycles of short periodicity (e.g., 12-h) within one 24-h day is perceived by nocturnal rodents as an opportunity to bifurcate their activity patterns into two bouts, one in each of the dark phases. Moreover, studies show that such behavioural bifurcation is accompanied by anti-phasic oscillations of *Per1* in the core and shell of the Suprachiasmatic Nucleus (SCN; site of the circadian pacemaker for sleep/wake behaviour in mammals) in hamsters (Yan et al., 2010), and anti-phasic oscillations of *Per1* and *Bmal1* in the core and shell of the SCN in mice (Watanabe et al., 2007). Additionally, the ability of organisms to show such bifurcation is thought to be dependent on the rigidity or lability of the circadian clock network (Gorman et al., 2017), thereby illustrating the utility of such unique, albeit unnatural environments in understanding the physiological regulation of plasticity. However, such studies have been restricted only to rodents, and I concur with the idea that understanding the functional significance of the clock's ability to show such patterns of plasticity

can be comprehensive only if we examine such behaviours in organisms from diverse taxa (as also discussed in Gorman et al., 2017).

Therefore, as a first step to understanding the effects of such environmental regimes on entrained activity/rest behaviour of *Drosophila melanogaster*, I examined the behaviour of our lab-reared wild-type flies (*control* stocks) under LDLD 5:7:5:7. I also monitored the molecular clocks in the circadian pacemaker circuit along with the most well studied output molecule, Pigment Dispersing Factor (PDF) to further understand how this entrainment behaviour is physiologically regulated.

I found that the LDLD (two light/dark cycles each with 12-h period) regime does not induce bifurcation in *control* flies. Instead, flies display a behaviour similar to but significantly different from that under a long photoperiod, suggesting that flies interpret LDLD as a 'skeleton' to a long day. To the best of my knowledge, this is the first report that describes the neuronal circuit level phenotype reflective of such behaviour in flies, and the circuit response is distinct from what is known under regular entrainment to LD 12:12 or to long photoperiods. Previous experiments have suggested that the evening oscillators (part of the dual oscillator framework known to regulate activity/rest rhythms) in *Drosophila* are dominant under long photoperiods (Stoleru et al., 2007). Results from our *control* flies indicated that comparing behaviours between LDLD and long photoperiod is a useful approach to probe into inherent differences in the organization of the dual oscillator network in flies.

I was, therefore, additionally interested in addressing three major questions.

1. Is there any utility of such a unique regime in behaviourally assessing the differences between strains that have inherently divergent networks?

2. To what extent is the hypothesis generalizable, that waveform plasticity is dependent on the rigidity or flexibility of the clock network?
3. Can aspects of waveform plasticity evolve? If they do, we gain insights into the adaptive significance of such plasticity.

To answer these questions, I used our *early* and *late* stocks (see Chapter 2; Kumar et al., 2007; Vaze, Nikhil et al., 2012). Earlier experiments from our laboratory have hinted at correlated evolution of dominant evening oscillators and flexible clock network in the *late* chronotypes (Nikhil, Vaze et al., 2016). Therefore, these lines are ideal to address the aforementioned questions and additionally understand evolutionary constraints under which different aspects of plasticity can evolve.

I found that our *early* and *late* stocks showed differing degrees of waveform plasticity contingent upon the parameter examined, thereby providing further evidence for the utility of such regimes in probing the neuronal network organization underlying entrained behaviour.

4.2. Materials and Methods

4.2.1. Activity/rest recording

Two sets of 32 virgin male flies aged 3-5 days each were sampled from each of the 12 populations and were used in the behaviour experiments. These flies were loaded into 5mm activity tubes with corn-sucrose-yeast medium for the recording of locomotor activity using the *Drosophila* Activity Monitoring system (DAM; Trikinetics, Waltham, MA, USA) at 25±0.5 ˚C. For both sets, recording of activity were performed under LDLD 5:7:5:7. For the first 9 days, the light intensity was maintained at ~70-lux during the photophase, following which on the 10th day, the flies were transferred to fresh tubes, and light intensity was set at ~0.1-lux. Flies were recorded under ~0.1-

lux for 7-8 days. Subsequently, each of the two sets of flies were transferred into constant darkness after the end of each photophase. Thus, one set of flies experienced DD 7-h later. Flies, from both sets were used in analysis of behaviour under entrainment. Recording was carried out for 4-5 days in constant darkness for each set to assess phase-control. Activity/rest data for the long day conditions of LD 18:06 with ~70-lux light intensity during the photophase was used from an experiment performed by me, preliminary results of which have been reported elsewhere (Nikhil, Abhilash et al., 2016).

4.2.2. Rationale for LDLD experimental regime

Recent experiments on mice revealed that bifurcation of activity occurs only in the presence of LDLD cycles only when the dark phase has dim illumination (Harrison et al., 2016). This has been attributed to the effect of constant light on the inter-neuronal coupling of the circadian network (Gorman et al., 2017). However, in my experiments I used LDLD to induce bifurcation in flies with complete darkness during the dark phase. This was because earlier studies in flies with dim night time illumination has revealed that the effects of this dim light at night were predominantly clock independent (Kempinger et al., 2009). Additionally, I used an LDLD 5:7:5:7 regime such that the duration of the light/dark regime that allows for activity for a diurnal animal (i.e., 5-h for each photophase) is the same as that provided to nocturnal rodents in Harrison et al. (2016; i.e., 5-h for each scotophase), only to maintain consistency.

4.2.3. Immunohistochemistry

Adult flies of the four *control* populations alone were pooled and subjected to LDLD 5:7:5:7 for ~10 days (~70-lux). These flies were then sampled at six different phases, i.e., ZT03, ZT07, ZT11, ZT15, ZT19 and ZT23 while they were entrained to LDLD 5:7:5:7 for immunohistochemistry. The protocol I used is a slight modification of the method that has been published in a previous

study (Prakash et al., 2017). I used *control* flies only, to first gain insights into the behaviour of the network under this novel short *T*-cycle regime. Briefly, their brains were dissected in ice cold Phosphate-Buffered Saline (PBS) and immediately fixed with 4% Paraformaldehyde solution for 30-min at room temperature (RT). The brain samples were then blocked with 10% horse serum for 1-h at RT and for 6-h at 4 °C followed by incubation with primary antibody cocktail for 48 hours at 4°C. The primary antibodies used were anti-PER (Rabbit 1:20,000; a gift from Jeffrey C Hall, Brandeis University) and anti-PDF (Mouse 1:5000; DSHB, PDF C7). Subsequently, 6-7 washes of 10-mins each were given with 0.5% PBT. Incubation with appropriate secondary antibodies was performed for 24-h at 4 °C. The secondary antibodies used were Alexa fluor conjugated goat anti-rabbit 488 (1:3000; Invitrogen) and goat anti-mouse 647 (1:3000; Invitrogen). The brains were further cleaned after the immunostaining and were mounted on a glass slide in 7:3 glycerol:PBS mounting medium.

4.2.4. Data acquisition and analysis

4.2.4.1. Behavioural analysis

The first part of my analysis was to test if our flies underwent waveform bifurcation under an LDLD regime or frequency demultiplication. Frequency demultiplication is the phenomenon wherein a circadian rhythm entrains to zeitgebers with periodicity that are multiples of 24-h with an exactly 24-h period (see Saunders, 2002). In other words, under such circumstances the circadian component dominates over the light/dark cycle's periodicity. I examined the actograms and the amplitude of periodograms at 12- and 24-h periodicities under both light intensities. I quantified for each fly, the amplitude of the chi-squared (χ^2) periodogram. The estimates of power were obtained using the open-source rhythm analysis software, RhythmicAlly (Abhilash and Sheeba, 2019). Owing to the fact that measurements for the periodogram power at different

periodicities for each fly comes from the same time-series data, they are likely to be dependent on each other. Therefore, paired *t*-tests were performed using block means to compare if power at 12-h was significantly different from that at 24-h, individually for all comparisons. These comparisons were made only for data obtained from flies exposed to LDLD 5:7:5:7 and not for those that experienced LD 18:06. Importantly, I assess and comment upon the presence or absence of behavioural bifurcation based on visual inspection of the activity profiles and phases under constant conditions immediately post entrainment, in addition to the periodogram power.

Second, I quantified phase and amplitude of the activity waveform under different regimes. For both these estimates I defined a 5-h window coinciding with each of the photophase under LDLD. To estimate phase, I used phase of Centre of Mass for the morning and evening activity separately (Batschelet, 1981). For amplitude, I calculated the activity maxima in the evening window and divided it by the maximum activity in the morning window and referred to it as the relative height of evening peak (RHEP). Phase and amplitude values in the same windows were computed for LD 18:06 regime as well.

I compared the relative height of evening peak in *control* flies under LDLD 5:7:5:7 (70-lux) and LD 18:06 using a two-way mixed model randomized block design ANOVA using block means, wherein regime was a fixed factor and block was treated as a random factor. Similarly, I analysed LDLD 5:7:5:7 (0.1-lux) versus LD 18:06. Post-hoc tests were done using the Tukey's HSD test, and all results were considered significant at $\alpha = 0.05$. I used similar two-way mixed model designs to analyse morning and evening phases as well. While comparing amplitude and phase of *early* and *late* flies, I used separate three-way mixed model randomized block design ANOVA, wherein genotype and regime were treated as fixed factors and block was treated as a random factor. Multiple comparisons following these ANOVAs were done using the Tukey's HSD test. All

results were considered statistically significant at α = 0.05. I point out that the LD 18:06 experiment was done once, and the same data has been used in different figures for facilitating appropriate visualization and statistical comparisons.

Additionally, to comment upon circadian entrainment of flies to LDLD regimes, phases under constant conditions, during and post-entrainment to LDLD 5:7:5:7 and LD 18:06 were analysed. Daily phases of offset (ψ_{OFFSET}) of activity for the entire duration of the experiment were subjectively marked for individual flies using RhythmicAlly. These values were averaged over all cycles under the presence of the zeitgeber as an estimate of ψ_{OFFSET}. Under constant conditions, the eye-fit ψ_{OFFSET} was used to fit a least-squares regression line to estimate free-running period. Using this extrapolated regression line ψ_{OFFSET} on the first day in DD was estimated and used for analyses. *D. melanogaster* activity/rest offset typically occurs around the time of dusk, and therefore we used the *V*-test at α = 0.05 to ask if ψ_{OFFSET} are significantly unimodal around the local time of dusk (Zar, 1999) under and post-entrainment to gain insights into phase-control. All these analyses were performed using custom written R-codes and the CircStats package for R (Lund and Agostinelli, 2018).

4.2.4.2. Image acquisition and analysis of intensities

All the slides prepared during the immunohistochemistry experiment were imaged using confocal microscopy on a Zeiss LSM 880 microscope with a 40-X (oil immersion) objective as described elsewhere (Prakash et al., 2017). I used a multiple component COSINOR based method (Cornelissen, 2014) to analyse aspects of rhythmicity in our intensity data, for both PER and PDF. I used a two-component model, with 12-h as one component and 24-h as the other. All these COSINOR analyses were implemented using custom scripts and the CATCosinor function from

the CATkit package written for R (Gierke and Cornelissen, 2016). All statistically significant contributions are based on a Type-1 error rate of 5%.

4.3. Results

4.3.1. *Drosophila* populations show frequency demultiplication under LDLD 5:7:5:7

Visual inspection of the actograms under LDLD 5:7:5:7 suggested that our *control* stocks show frequency demultiplication (Figure 4.1a, top and middle) and not a bifurcated activity pattern. To quantitatively verify if this pattern of activity/rest in our flies was indeed frequency demultiplication, I measured power of the χ^2 periodogram at 12-h and 24-h periods, with the expectation that higher power at 24-h would imply frequency demultiplication and higher power at 12-h would imply activity bifurcation (Harrison et al., 2016). We found that power at 24-h was statistically significantly higher than that at 12-h (Figure 4.1b; Table 4.1) under both high and low light intensities during the photophase (Figure 4.1b, left and right panels, respectively), thereby clearly indicating that our flies entrain with a periodicity of 24-h by treating two consecutive light/dark cycles as one day (high light intensity: paired $t_3 = -14.36$, $p < 0.05$; low light intensity: $t_3 = -34.92$, $p < 0.05$). I am confident that this behaviour is a bona fide entrainment state due to – (i) stable timing of activity bouts across days, (ii) major activity bouts not coinciding with any light/dark transition, and (iii) the phase at which activity starts under constant darkness (Figures 4.1a, top and middle and 4.2). It is critical to note here that periodogram power using the χ^2 periodogram is typically higher for longer periods and this happens to be a limitation of using the method. Therefore, I use the following additional criteria to comment upon the presence or absence of behavioural bifurcation; in addition to periodogram power, I consider rhythms to be

bifurcated only if (i) visual inspection of actograms and activity profiles show two distinctly separate activity bouts, and (ii) each of these different bouts of activity start free-running from phases dictated by the respective photophases they are restricted to, before transfer to DD (see Figures 4.1, 4.2 and subsequent paragraphs).

Additionally, the behaviour of our flies under LDLD 5:7:5:7 was similar to the behaviour of flies under long photoperiod (LD18:06; Figure 4.1a, bottom), thereby suggesting that the *control* flies may have perceived the provided LDLD regime as a 'skeleton' for a long day (Figure 4.1a). However, there were subtle differences in the activity waveform between LDLD 5:7:5:7 and LD 18:06 (Figure 4.1c). Under the long day regime, I found that the relative height of evening peak (RHEP) was close to 2, implying that maximum evening activity was almost twice as much as that of morning activity ($F_{1,3}$ = 88.86, p < 0.05; Figures 4.1c, bottom and 4.1d, top; Table 4.2). However, under LDLD 5:7:5:7 the two activity peaks were comparable (Figures 4.1c, top and 4.1d, top). This, I argue is not because of the masking response of morning activity to lights ON, as the same feature is also present when flies are subjected to 0.1-lux light intensity LDLD 5:7:5:7 ($F_{1,3}$ = 13.08, p < 0.05; Figures 4.1c, middle and 4.1d, top; Table 4.3). Such changes in the RHEP is predominantly brought about by increased amplitude of morning activity (Figure 4.1c).

Furthermore, there was no significant difference in the phase of centre of mass (ψ_{CoM}) of morning (Figure 4.1d, middle; high light intensity: $F_{1,3}$ = 3.95, p > 0.05; Table 4.4; low light intensity: $F_{1,3}$ = 7.75, p > 0.05; Table 4.5) or evening (Figure 4.1d, bottom; high light intensity: $F_{1,3}$ = 0.20, p > 0.05; Table 4.6; low light intensity: $F_{1,3}$ = 0.10, p > 0.05; Table 4.7) bouts of activity under either light intensity (see materials and methods). This suggests that LDLD induced amplitude plasticity in wild-type flies.

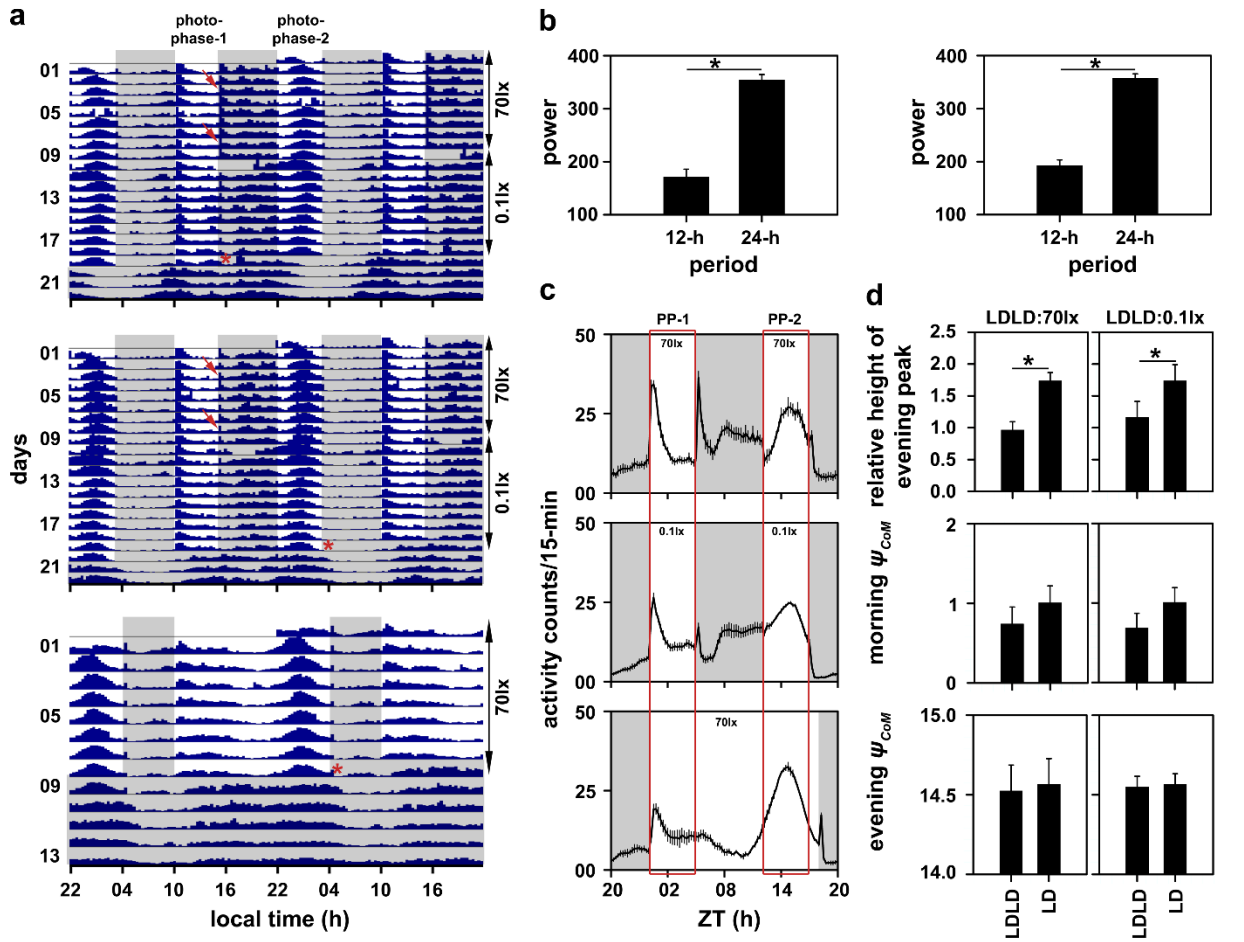

Figure 4.1: (a) Batch actograms displaying activity patterns of *control* flies under LDLD 5:7:5:7 (top and middle) and LD 18:06 (bottom). In case of the LDLD regime, flies were first exposed to 70-lux light intensity during the photophases and then to 0.1-lux light intensity during the photophases. One batch of flies were then transferred into constant darkness (DD) after the odd photophase (top) and the other batch were transferred to DD after the even photophase (middle). Flies were recorded under LD 18:06 for 8 days with 70-lux light intensity during the photophase after which they were transferred to DD. The gray shaded region on the actograms represent the scotophase of the light/dark cycle. Arrowheads represent the masking response to light transitions when 70-lux was provided during the LDLD regime. Asterisks on the actograms indicate the phases at which individuals were transferred to DD. The short interval during which data is not seen in the top and middle actograms indicate the duration when monitors were disconnected to transfer flies into tubes with fresh food. Shown also are power values extracted from the χ^2-periodogram at period values of 12- and 24-h (b) under LDLD with 70-lux during the photophase (left) and 0.1-lux during the photophase (right). Error bars in this panel are SEM and the asterisks indicate statistically significant differences. Depicted are activity profiles averaged over cycles and individuals under LDLD with 70-lux during the photophase (c, top), 0.1-lux during the photophase (c, middle) and long photoperiod (c, bottom). Gray shaded regions indicate the

scotophase. The red rectangular box spanning panel (c) on the left is the morning window and on the right is the evening window that I defined to calculate ψ_{CoM} of morning and evening activity, respectively. The error bars represent standard error of mean (SEM). PP-1 and PP-2 refer to photophases 1 and 2, respectively for the top and middle figures. (d) Relative height of the evening peak of activity under 70-lux during the photophase compared with its value under long photoperiod (top-left) and the same under 0.1-lux light intensity during the photophase of LDLD (top-right). Also shown are ψ_{CoM} of morning (middle-left and middle-right) and evening activity (bottom-left and bottom-right) under both light intensities. All the error bars in panel (d) are 95%CI estimated using the Tukey's HSD test to facilitate visual hypothesis testing. All means with non-overlapping error bars are statistically significantly different from each other (also indicated by asterisks). The LD 18:06 data in both the left and right sides of panel (d) are the same data that have been re-plotted to facilitate appropriate statistical comparisons.

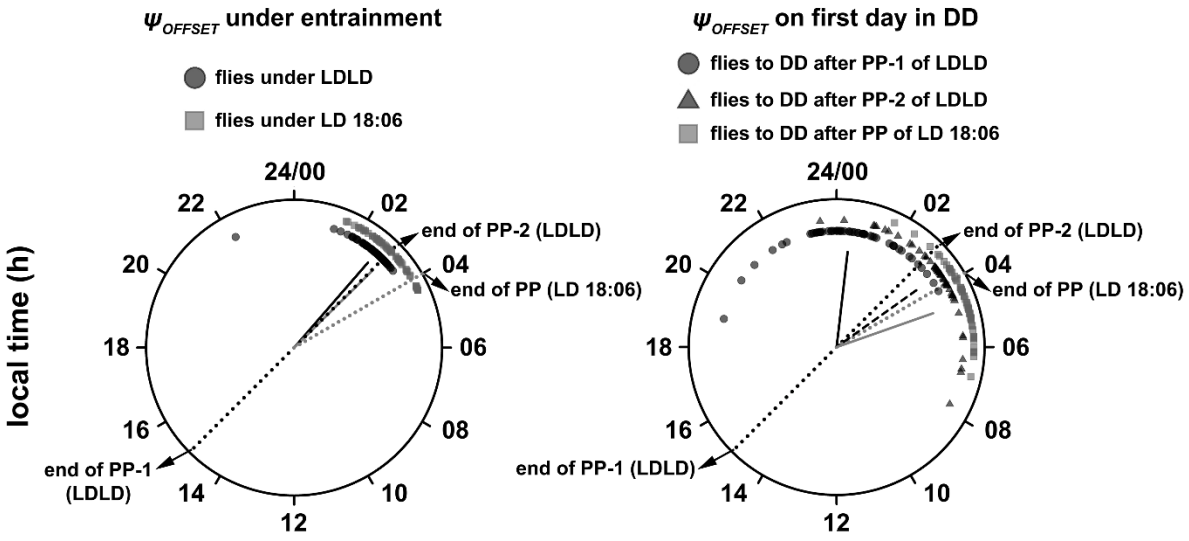

Figure 4.2: (left) ψ_{OFFSET} of flies under their respective zeitgeber regimes. The solid black and gray lines represent the mean angle and length of resultant vector (measure of angular dispersion) of flies under LDLD and LD 18:06 regimes, respectively. Also depicted here are ψ_{OFFSET} of flies on the first day of DD post entrainment (right). The solid and dashed black lines indicate the mean phase and angular dispersion of flies that were transferred to DD after the first and second photophases respectively. The gray line indicates the mean phase and angular dispersion of flies that were transferred to DD after a long day regime.

Table 4.1: Table summarizing the power values extracted from the χ^2-periodogram at 12- and 24-h periodicity values for the *early*, *control* and *late* populations.

Populations	Regime	Period	Power
early	LDLD 5:7:5:7 (70-lux)	12	173.05
		24	361.06
	LDLD 5:7:5:7 (0.1-lux)	12	192.78
		24	342.30
control	LDLD 5:7:5:7 (70-lux)	12	171.11
		24	354.54
	LDLD 5:7:5:7 (0.1-lux)	12	192.64
		24	357.47
late	LDLD 5:7:5:7 (70-lux)	12	192.69
		24	376.32
	LDLD 5:7:5:7 (0.1-lux)	12	217.09
		24	391.96

Table 4.2: ANOVA table summarizing the effects of light regime (LD 18:06 and LDLD 5:7:5:7 – ~70-lux) on RHEP. Italicised effects are significant.

Summary of all effects	***df* Effect**	**MS Effect**	***df* Error**	**MS Error**	***F***	***p***
Regime (Reg)	*1*	*1.1943*	*3*	*0.0134*	*88.86*	*0.00*
Block (B)	3	0.0270	0	0.0000	--	--
Reg × B	3	0.0134	0	0.0000	--	--

Table 4.3: ANOVA table summarizing the effects of light regime (LD 18:06 and LDLD 5:7:5:7 – ~0.1-lux) on RHEP. Italicised effects are significant.

Summary of all effects	*df* Effect	MS Effect	*df* Error	MS Error	*F*	*p*
Regime (Reg)	*1*	*0.6652*	*3*	*0.0508*	*13.08*	*0.04*
Block (B)	3	0.0047	0	0.0000	--	--
Reg × B	3	0.0134	0	0.0000	--	--

Table 4.4: ANOVA table summarizing the effects of light regime (LD 18:06 and LDLD 5:7:5:7 – ~70-lux) on phase of morning activity. Italicised effects are significant.

Summary of all effects	*df* Effect	MS Effect	*df* Error	MS Error	*F*	*p*
Regime (Reg)	1	0.1415	3	0.0358	3.95	0.14
Block (B)	3	0.0406	0	0.0000	--	--
Reg × B	3	0.0358	0	0.0000	--	--

Table 4.5: ANOVA table summarizing the effects of light regime (LD 18:06 and LDLD 5:7:5:7 – ~0.1-lux) on phase of morning activity. Italicised effects are significant.

Summary of all effects	*df* Effect	MS Effect	*df* Error	MS Error	*F*	*p*
Regime (Reg)	1	0.2087	3	0.0270	7.74	0.07
Block (B)	3	0.0537	0	0.0000	--	--
Reg × B	3	0.0270	0	0.0000	--	--

Table 4.6: ANOVA table summarizing the effects of light regime (LD 18:06 and LDLD 5:7:5:7 – ~70-lux) on phase of evening activity. Italicised effects are significant.

Summary of all effects	*df* Effect	MS Effect	*df* Error	MS Error	*F*	*p*
Regime (Reg)	1	0.0033	3	0.0209	0.16	0.72
Block (B)	3	0.0071	0	0.0000	--	--
Reg × B	3	0.0209	0	0.0000	--	--

Table 4.7: ANOVA table summarizing the effects of light regime (LD 18:06 and LDLD 5:7:5:7 – ~0.1-lux) on phase of evening activity. Italicised effects are significant.

Summary of all effects	*df* Effect	MS Effect	*df* Error	MS Error	*F*	*p*
Regime (Reg)	1	0.0005	3	0.0036	0.14	0.73
Block (B)	3	0.0127	0	0.0000	--	--
Reg × B	3	0.0036	0	0.0000	--	--

My claims regarding this behaviour of flies under LDLD being an entrained phenomenon and similar to that under long day regimes is validated by analyses of ψ_{OFFSET} on the first day in DD. Owing to the fact that *D. melanogaster* activity offset typically occurs around dusk, I wanted to ask whether offset under entrainment clustered around dusk in our flies for LDLD (i.e., end of the second photophase) and for LD 18:06. Moreover, I wanted to know if similar clustering is observed on the first day in DD, which would then indicate entrainment. I found that under LDLD mean ψ_{OFFSET} was ~2.73-h and this phase value was significantly clustered around 3-h which is when the second photophase ended, i.e., onset of perceived night-time (Figure 4.2, left; $\bar{r}$ = 0.987, $p < 0.05$). Under LD 18:06, the mean ψ_{OFFSET} was 3.03-h which was not significantly different from 4-h which is the onset of darkness in this regime (Figure 4.2, left; $\bar{r}$ = 0.947, $p < 0.05$). Similarly, I asked if phases clustered around the first photophase for flies that went into DD after it, and found that these flies clustered around 0.44-h and was significantly delayed from the end of first photophase (15-h; $\bar{r}$ = -0.710, $p > 0.05$). Interestingly, phases significantly cluster around the end of second photophase (3-h; $\bar{r}$ = 0.710, $p < 0.05$; Figure 4.2, right). Additionally, when flies were transferred into DD from the second photophase, ψ_{OFFSET} clustered significantly around the end of the second photophase and was much closer to the end of the second photophase (3.63-h; $\bar{r}$ = 0.913, $p < 0.05$; Figure 4.2, right). Furthermore, when flies were transferred into DD after exposure to long photoperiod of 18-h, ψ_{OFFSET} was clustered significantly around the end of the

photophase (4.71-h; $\bar{r}$ = 0.951, $p < 0.05$; Figure 4.2, right). The fact that phases on the first day under DD for both sets of flies under LDLD were similarly clustered around the end of the second photophase as were phases under entrainment, clearly implies phase-control and therefore, entrainment to such regimes and not behavioural bifurcation.

4.3.2. Levels of nuclear PER (PERIOD) in the circadian clock circuit

To examine the cellular underpinnings of frequency demultiplication in *Drosophila*, I analysed the oscillations in levels of nuclear PER protein in different cell types of the circadian neuronal network. Using a multiple component COSINOR based method I detected a significantly bimodal oscillation in the s-LNvs (small lateral ventral neurons). There was a significant 24-h component that explained 29.14% of the variation in PER levels, whereas the 12-h component, although significant, only explained 15.98% of the variation (Figures 4.3 and 4.4; Table 4.8). The dominant 24-h peak coincided with the dawn of photophase-1 (Figure 4.3). The lower 12-h peak of PER oscillation occurred just before the dawn of photophase-2 (Figure 4.3). We found that only ~11.2% of variation in PER in the l-LNvs (large lateral ventral neurons) is explained by the multiple component COSINOR, out of which neither the 24-h nor the 12-h components were statistically significant (24-h: 4.69%, $p > 0.05$; 12-h: 6.64%, $p > 0.05$; Figures 4.3 and 4.4; Table 4.8).

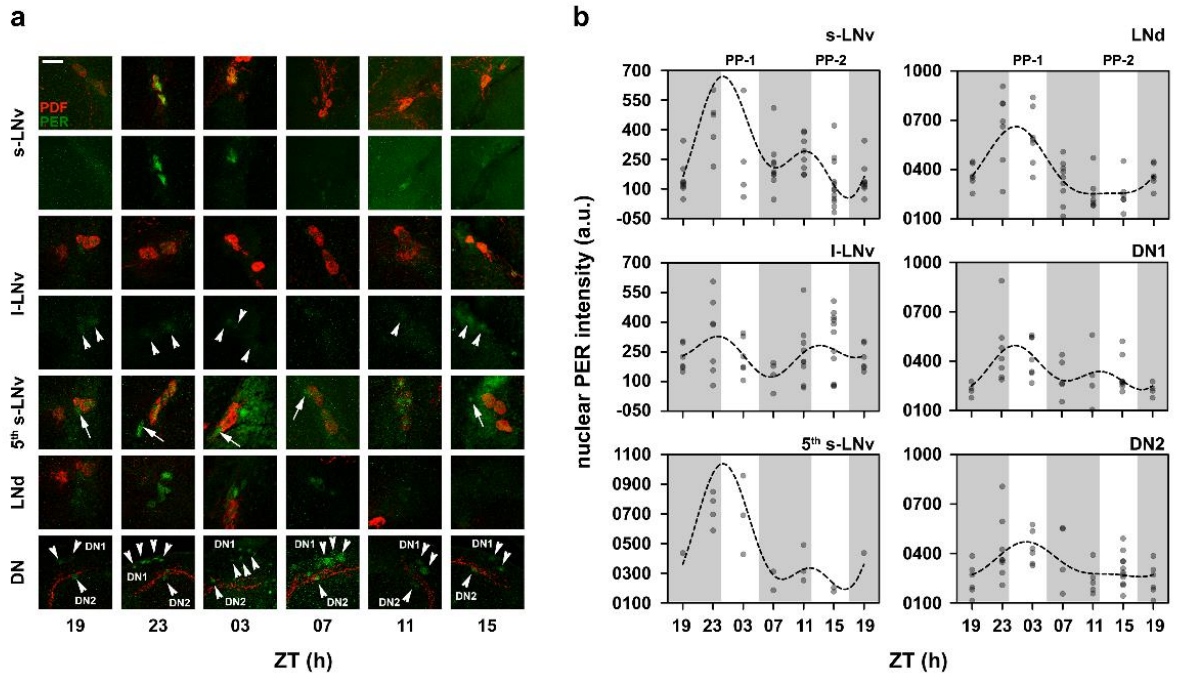

Figure 4.3: (a) Representative confocal images showing different cell types from which I estimated the level of nuclear PER under an LDLD regime with 70-lux light intensity during the photophase. Scale bar represents 20 microns. The arrowheads facilitate the visualization of cells. (b) Scatter plots of PER intensities in different cells of the circadian network. Each dot represents the mean PER value averaged over hemispheres of one brain. The dots are set at reduced opacity; therefore, darker shades of dots imply multiple values overlapping. The dashed line is the best fit COSINE curve from the parameters that were extracted from the multiple component COSINOR analysis. PP-1 and PP-2 refer to photophases 1 and 2, respectively.

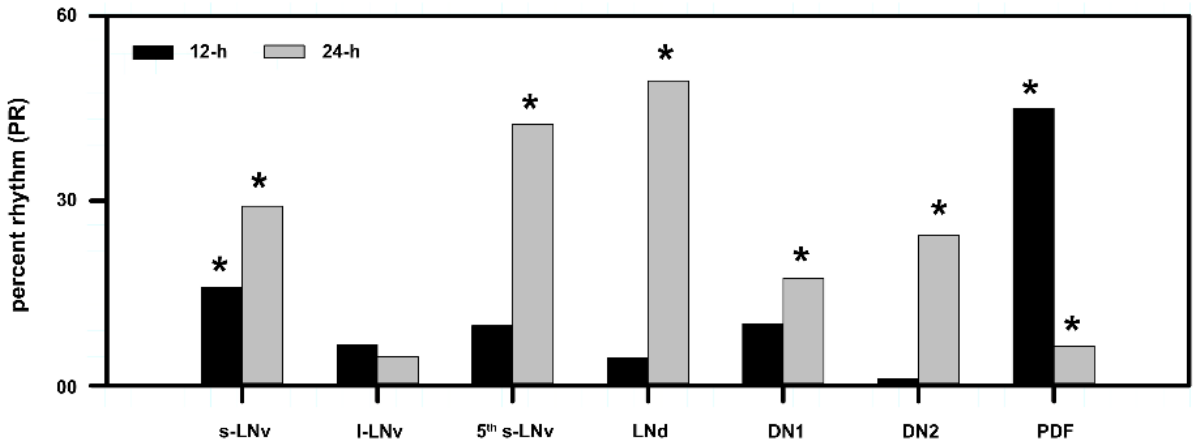

Figure 4.4: The percent rhythm (PR) for each periodic component that was tested in the multiple-component COSINOR for nuclear PER in each cell type and PDF in the dorsal projections. PR is analogous to R^2 (coefficient of determination) and describes what percent of variation in the data set is described by each periodicity. The asterisks above each bar indicate whether or not that periodic component had a statistically significant contribution towards explaining variation in the data set.

Table 4.8: Table summarizing the contribution of the 12-h and 24-h component to the multiple component COSINOR and their statistical significance for nuclear PER in all cell types and PDF in the dorsal projections. The strength of each periodicity is estimated using PR (percent rhythm). PR is essentially similar to an R^2 value (coefficient of determination). It is representative of the percentage of overall variation explained by each component of the fitted model.

Region	Protein	Period	PR	*p*
s-LNVs	PER	12	15.98	< 0.05
		24	29.14	< 0.05
l-LNVs	PER	12	6.64	> 0.05
		24	4.69	> 0.05
5th-s-LNv	PER	12	9.73	> 0.05
		24	42.45	< 0.05
LNds	PER	12	4.50	> 0.05
		24	49.46	< 0.05
DN1	PER	12	9.99	> 0.05
		24	17.42	< 0.05
DN2	PER	12	1.17	> 0.05
		24	24.33	< 0.05
Dorsal projections	PDF	12	44.97	< 0.05
		24	6.42	< 0.05

In case of the 5th s-LNv, the model explained ~52% of variation in PER, but majority of this was due to a statistically significant effect of the 24-h component (42.45%, $p < 0.05$; Figure 4.4; Table 4.8). The 12-h component was not significant and explained 9.73% of the variation (Figure 4.4; Table 4.8). The dominant peak of PER occurred at the same phase as that of the other s-LNvs (Figure 4.3). In case of the LNds (lateral dorsal neurons), I found a statistically significant contribution of only the 24-h component, which explained 49.46% of the variation in PER levels

(Figure 4.4; Table 4.8). The 12-h component, on the other hand, only explained 4.50% of the variation and was not statistically significant (Figure 4.4; Table 4.8). Furthermore, largely, the phase of PER oscillations in the LNds is in phase with those in the s-LNvs (Figure 4.3).

I also quantified the level of nuclear PER in two sets of dorsal neurons, i.e., DN1s and DN2s. In both these subsets, PER oscillation appeared to be highly damped, relative to PER oscillations in the s-LNvs (Figure 4.3). In case of the DN1s, the 24-h and 12-h components together explained ~27% of the variation in PER levels (Figure 4.4). While the 12-h component was not statistically significant, the 24-h component was marginally statistically significant ($p = 0.044$) and contributed to 17.42% of the variation in PER (Figure 4.4; Table 4.8). Moreover, the PER oscillation in DN1s was in-phase with that in the s-LNvs (Figure 4.3). The DN2s showed similar unimodal oscillation with a statistically significant 24-h component that explained 24.33% of the variation in PER levels. The 12-h component explained only 1.18% of the variation and was not statistically significant (Figure 4.4; Table 4.8). However, the phase of PER oscillation in DN2s appeared to be slightly delayed relative to PER oscillations in other neuronal clusters, such that the peak occurred during the first photophase and not the transition (Figure 4.3).

4.3.3. Pigment Dispersing Factor (PDF) oscillation in the dorsal projections shows bifurcation under LDLD 5:7:5:7

Owing to the fact that PDF is a core neuropeptide thought to have a role in regulating network synchrony and in mediating rhythmic output (Helfrich-Förster, 2017), I quantified its levels in the dorsal projections from the LNvs. My analysis revealed that a total of ~51% of variation in PDF levels in the dorsal projection can together be explained by the 24-h and 12-h components. The 12-h component was statistically significant and explained ~45% of this variation (Figure 4.4;

Table 4.8). Although the 24-h component was also statistically significant, it was not the dominant component in the model and explained only 6.42% of the total variation in PDF levels (Figure 4.4; Table 4.8). Therefore, I concluded that PDF in the dorsal projections showed 'bifurcation' instead of frequency demultiplication (Figures 4.5a and 4.5b). There were two peaks of PDF levels, one in each photophase, of comparable amplitude and appeared to coincide with the two major bouts of activity under the LDLD regime. Thus, I find that while the core clock in the circadian pacemaker circuit appears entrained with a significant 24-h period, the output molecule i.e., PDF seems to be bifurcated, implying a breakdown of synchrony between the core clock and the PDF oscillation.

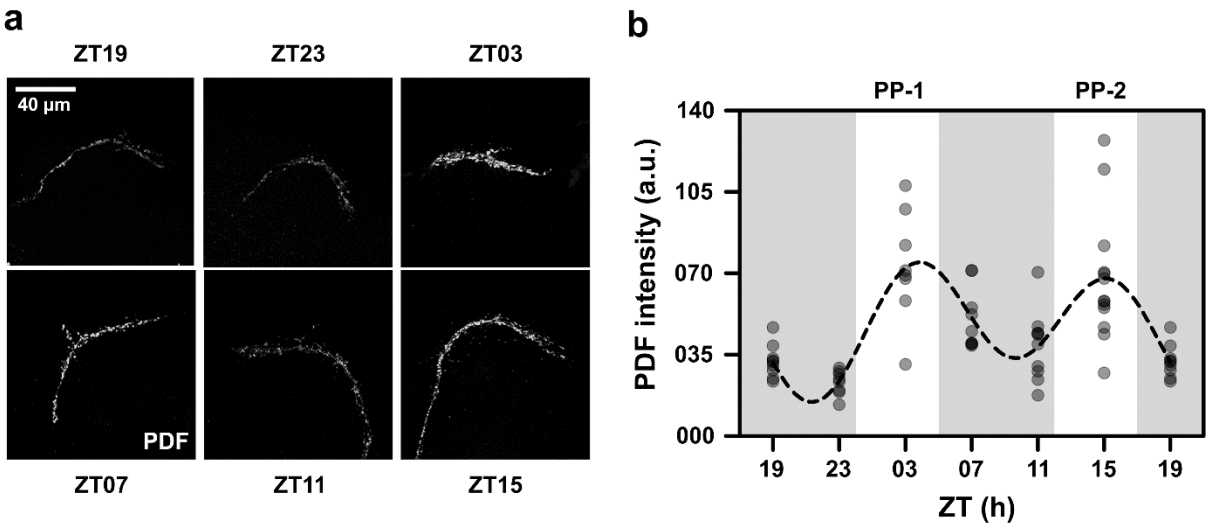

Figure 4.5: (a) Representative images showing parts of the dorsal projection for each time-point. (b) Scatter plot of PDF intensity in the dorsal projections. Each dot represents the mean PDF intensity value averaged over hemispheres of one brain. The dots are set at reduced opacity; therefore, darker shades of dots imply multiple values overlapping. The dashed line is the best fit COSINE curve from the parameters that were extracted from the multiple component COSINOR analysis. PP-1 and PP-2 refer to photophases 1 and 2, respectively.

4.3.4. The *early* and *late* chronotypes show higher amplitude and phase plasticity, respectively

Firstly, I found that both *early* and *late* chronotypes also showed frequency demultiplication like that of *control* stocks under both 70- and 0.1-lux light intensities during the photophase of the LDLD regime (Figures 4.6a, top and middle and 4.6b). Although significant, the power of periodogram at 12-h was significantly lower than the power at 24-h, confirming the notion that these flies treated two *T*-cycles as one day (Figure 4.6b; Table 4.1; For *early* chronotypes – high light intensity: paired $t_3 = -72.80$, $p < 0.05$; low light intensity: $t_3 = -17.12$, $p < 0.05$; For *late* chronotypes – high light intensity: paired $t_3 = -45.70$, $p < 0.05$; low light intensity: $t_3 = -12.42$, $p < 0.05$).

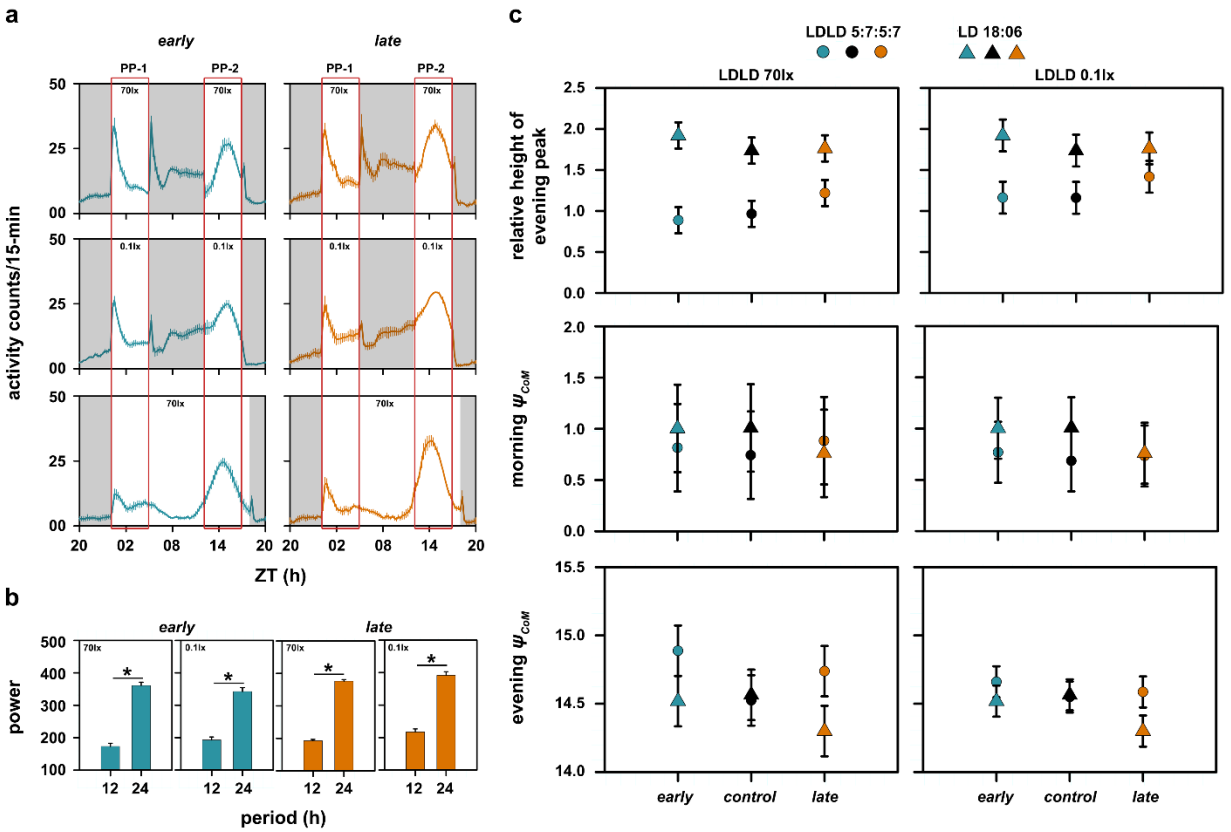

Figure 4.6: (a) The average activity profiles of *early* (left) and *late* (right) populations are shown for LDLD with 70-lux during the photophase (top), 0.1-lux during the photophase (middle) and under LD 18:06 (bottom). Gray shaded regions indicate the scotophase. The rectangular box spanning the left and right side of panel (a) depict the morning and evening windows as described in Figure 4.1. The error bars represent standard error of mean (SEM). PP-1 and PP-2 refer to photophases 1 and 2, respectively for the top and middle figures. (b) Shown also are power values extracted from the χ^2 periodogram at period values of 12- and 24-h for *early* and *late* populations under LDLD with both light intensities. The error bars represent SEM and asterisks indicate statistically significant difference. (c) Relative height of the evening peak of activity under 70-lux during the photophase compared with its value under long photoperiod for *early*, *control* and *late* populations (top-left) and the same under 0.1-lux light intensity during the photophase of LDLD (top-right). Also shown are ψ_{CoM} of morning (middle-left and middle-right) and evening activity (bottom-left and bottom-right) under both light intensities for all three populations. All the error bars in panel (c) are 95%CI estimated using the Tukey's HSD test to facilitate visual hypothesis testing. All means with non-overlapping error bars are statistically significantly different from each other. The LD 18:06 data in both the left and right sides of panel (c) are the same data that have been re-plotted to facilitate appropriate statistical comparisons.

Subsequently, I analysed the RHEP in our stocks, under the LDLD regime and long day condition. The ANOVA revealed a significant effect of selection × regime interaction on RHEP under high light intensity during the LDLD regime ($F_{2,6}$ = 9.37, p < 0.05; Table 4.9). While the RHEP of the *late* chronotypes under LDLD was closer to its value under the long day regime (Figure 4.6c, top-left), in case of the *early* chronotypes, the evening peak height was either comparable to the morning peak height or lower (RHEP value close to 1; Figure 4.6c, top-left). Although there was no statistically significant effect of the selection × regime interaction on the RHEP under low light intensity ($F_{2,6}$ = 4.52, p > 0.05; Table 4.10), there is a clear trend showing that the RHEP of *late* stocks under LDLD is closer to its value under long days (Figure 4.6c, top-right).

Table 4.9: ANOVA table summarizing the effects selection, light regime (LD 18:06 and LDLD 5:7:5:7 – ~70-lux) and their interaction on RHEP. Italicised effects are significant.

Summary of all effects	***df* Effect**	**MS Effect**	***df* Error**	**MS Error**	***F***	***p***
Selection (Sel)	2	0.0401	6	0.0271	1.48	0.30
Regime (Reg)	*1*	*3.6887*	*3*	*0.0110*	*334.63*	*0.00*
Block (B)	3	0.0076	0	0.0000	--	--
Sel × Reg	*2*	*0.1202*	*6*	*0.0128*	*9.37*	*0.01*
Sel × B	6	0.0271	0	0.0000	--	--
Reg × B	3	0.0110	0	0.0000	--	--
Sel × Reg × B	6	0.0128	0	0.0000	--	--

Table 4.10: ANOVA table summarizing the effects selection, light regime (LD 18:06 and LDLD 5:7:5:7 – ~0.1-lux) and their interaction on RHEP. Italicised effects are significant.

Summary of all effects	***df* Effect**	**MS Effect**	***df* Error**	**MS Error**	***F***	***p***
Selection (Sel)	2	0.0415	6	0.0565	0.73	0.52
Regime (Reg)	*1*	*1.8849*	*3*	*0.0666*	*28.29*	*0.01*
Block (B)	3	0.1015	0	0.0000	--	--
Sel × Reg	2	0.0858	6	0.0190	4.51	0.06
Sel × B	6	0.0565	0	0.0000	--	--
Reg × B	3	0.0666	0	0.0000	--	--
Sel × Reg × B	6	0.0190	0	0.0000	--	--

I, then, analysed ψ_{CoM} of the morning activity in our populations and found that all three stocks had similar ψ_{CoM} under both high ($F_{2,6} = 0.93$, $p > 0.05$; Table 4.11) and low ($F_{2,6} = 1.03$, $p > 0.05$; Table 4.12) light intensity LDLD (Figure 4.6c, middle). However, the ANOVA revealed that there was a significant effect of the selection × regime interaction on ψ_{CoM} of the evening activity under both light intensities (high light intensity: $F_{2,6} = 7.80$, $p < 0.05$; Table 4.13; low light intensity: $F_{2,6} = 7.00$, $p < 0.05$; Table 4.14). I found that the *early* chronotypes and *control* stocks had the same ψ_{CoM} under LDLD and long day conditions (Figure 4.6c, bottom). Importantly, the *late* chronotypes in both high and low light intensity LDLD showed a delayed ψ_{CoM} relative to its value under LD 18:06 (Figure 4.6c, bottom). These results imply that *late* chronotypes show reduced amplitude plasticity and increased phase lability across the two environmental regimes tested.

Table 4.11: ANOVA table summarizing the effects selection, light regime (LD 18:06 and LDLD 5:7:5:7 – ~70-lux) and their interaction on phase of morning activity. Italicised effects are significant.

Summary of all effects	*df* Effect	MS Effect	*df* Error	MS Error	*F*	*p*
Selection (Sel)	2	0.0156	6	0.0610	0.26	0.78
Regime (Reg)	1	0.0729	3	0.0389	1.87	0.26
Block (B)	3	0.0615	0	0.0000	--	--
Sel × Reg	2	0.0852	6	0.0.920	7.86	0.45
Sel × B	6	0.0610	0	0.0000	--	--
Reg × B	3	0.0389	0	0.0000	--	--
Sel × Reg × B	6	0.0920	0	0.0000	--	--

Table 4.12: ANOVA table summarizing the effects selection, light regime (LD 18:06 and LDLD 5:7:5:7 – ~0.1-lux) and their interaction on phase of morning activity. Italicised effects are significant.

Summary of all effects	*df* Effect	MS Effect	*df* Error	MS Error	*F*	*p*
Selection (Sel)	2	0.0416	6	0.1181	0.35	0.72
Regime (Reg)	1	0.2279	3	0.0325	7.00	0.08
Block (B)	3	0.0520	0	0.0000	--	--
Sel × Reg	2	0.0462	6	0.0448	1.03	0.41
Sel × B	6	0.1181	0	0.0000	--	--
Reg × B	3	0.0325	0	0.0000	--	--
Sel × Reg × B	6	0.0448	0	0.0000	--	--

Table 4.13: ANOVA table summarizing the effects selection, light regime (LD 18:06 and LDLD 5:7:5:7 – ~70-lux) and their interaction on phase of evening activity. Italicised effects are significant.

Summary of all effects	***df* Effect**	**MS Effect**	***df* Error**	**MS Error**	***F***	***P***
Selection (Sel)	*2*	*0.0797*	*6*	*0.0023*	*35.39*	*0.00*
Regime (Reg)	*1*	*0.3918*	*3*	*0.0044*	*89.97*	*0.00*
Block (B)	3	0.0085	0	0.0000	--	--
Sel × Reg	*2*	*0.1341*	*6*	*0.0172*	*7.79*	*0.02*
Sel × B	6	0.0023	0	0.0000	--	--
Reg × B	3	0.0044	0	0.0000	--	--
Sel × Reg × B	6	0.0172	0	0.0000	--	--

Table 4.14: ANOVA table summarizing the effects selection, light regime (LD 18:06 and LDLD 5:7:5:7 – ~0.1-lux) and their interaction on phase of evening activity. Italicised effects are significant.

Summary of all effects	***df* Effect**	**MS Effect**	***df* Error**	**MS Error**	***F***	***P***
Selection (Sel)	*2*	*0.0475*	*6*	*0.0073*	*6.53*	*0.03*
Regime (Reg)	*1*	*0.1131*	*3*	*0.0078*	*14.55*	*0.03*
Block (B)	3	0.0154	0	0.0000	--	--
Sel × Reg	*2*	*0.0458*	*6*	*0.0065*	*7.01*	*0.03*
Sel × B	6	0.0073	0	0.0000	--	--
Reg × B	3	0.0078	0	0.0000	--	--
Sel × Reg × B	6	0.0065	0	0.0000	--	--

4.4. Discussion

Although *Drosophila* has been a very useful model to understand the design principles of circadian behaviour, their neuronal circuits and molecular regulation (Helfrich-Förster, 2017), there have not been many studies that systematically analyzed the extent of waveform plasticity under varying environmental conditions. Therefore, I undertook, to the best of my knowledge, the first set of experiments to understand the behaviour and the underlying neuronal basis of entrainment to *T*-cycles as short as 12-h.

Our *control* flies showed frequency demultiplication, very similar to what was seen in mice under an LDLD regime when the dark phase was in complete darkness (Figure 4.1a; Harrison et al., 2016). This implied that the behaviour is similar to how flies behave under long photoperiod conditions. Therefore, I analysed and found that although similar, there were significant differences between the behaviour under LDLD and long day LD. In an earlier study (Stoleru et al., 2007), the authors discussed that the relative dominance of the morning and evening oscillators depends on the light regime, such that the evening oscillators are dominant under long days. Under long day condition where the photoperiod duration was 18-h, I found that the *control* stocks showed evening peak more than 1.5 times as high as the morning peak of activity (Figures 4.1c and 4.1d, top). However, the evening peak of activity became more comparable to the morning peak under LDLD of both high and low light intensity (Figure 4.1d, top). I interpret this to be a consequence of the reduction in dominance of the evening oscillator under the provided LDLD condition.

To examine the neuronal circuit underlying this behaviour, I quantified PER in different cell types and found that the non-s-LNv neurons show highly damped PER oscillations (Figure 4.3). The

peak to trough ratio in s-LNvs is 12.49, whereas it is only 2.62, 2.17 and 1.82 in the LNds, DN1s and DN2s, respectively (Figure 4.3), thereby supporting the idea of reduced evening oscillator dominance under LDLD. Furthermore, few earlier studies have implicated that the clock in the l-LNvs are important for the regulation of evening activity, especially under long days (Menegazzi et al., 2017; Potdar and Vasu, 2012; Schlichting et al., 2016). However, given that in my study the l-LNvs have no significant oscillation of PER, and I found no effect of the environmental regime on phase of evening activity, I conclude that similar phasing of behaviour can be brought about by distinct remodeling of the neuronal network.

Under long-day conditions, nuclear PER in the s-LNvs is bimodal with both peaks having comparable heights and a phase-difference of ~8-h between the peaks (Shafer et al., 2004). More recently, studies have revealed that PDF in the dorsal projections are also bimodal under long-day conditions with a phase-difference of ~9-h (*Charlotte Helfrich-Förster, personal communication, 1st August 2019*). In my experiment, PDF oscillates with a 12-h phase-difference between the two peaks thereby leading me to conclude that indeed bifurcation occurs under LDLD, and this is distinct from mere bimodality. While it is possible that the second PDF peak in my experiment (Figures 4.4 and 4.5b) is driven by the shorter peak of PER oscillation in the s-LNvs, alternatively, it is also possible that the provided LDLD regime desynchronized the nuclear PER oscillation and PDF oscillation in the dorsal projections, a phenomenon that appears to have occurred in at least two previous manipulations (Kula et al., 2006; Prakash et al., 2017). Yet another possibility is that light directly affects properties of the LNvs such that PDF levels increase during the second photophase (similar to hyperexcitability-induced constitutive PDF expression in Nitabach et al., 2006), but in my case, PER oscillations are not acutely affected. However, I must acknowledge here that a previous study has shown that increased neuronal firing reduces the expression of PDF

in the soma (Mezan et al., 2016) which may imply that in my experiment, light in the second photophase has an inhibitory effect on the membrane potential thereby increasing PDF levels. Additionally, this desynchrony could also explain highly damped PER oscillation in the LNds and DNs. Zhang et al. (2010) showed that altered speed of clock in the s-LNvs acutely affects PER oscillations in the DN1 and suggest that perhaps conflicting signals to the DN1 cluster from the s-LNvs and LNds may contribute to loss of rhythmicity. A recent study by Schlichting et al. (2019) has demonstrated a circuit that involves the direct communication of light information via l-LNvs through PDF to the evening oscillators, and regulates the phasing of evening activity. Given this circuit, I speculate that, in my case, damped oscillation in the LNds can be explained via an apparent decoupling of the molecular clocks in the l-LNvs and PDF in the dorsal projections. Additionally, de-synchrony between PDF and PER in the s-LNvs and LNds may contribute to damped oscillations in the dorsal set of neurons. Furthermore, since PDF is bimodal in the same way as that of the activity/rest behaviour, it suggests that the role of PDF may be more than just synchronizing the phase of molecular oscillations in the neuronal circuit. It is possible that PDF may have a more proximal role in directly regulating output, an idea that has received some evidence previously (Pírez et al., 2013).

The reduced difference in the RHEP between long day and LDLD in the *late* chronotypes (Figure 4.6c, top) suggests that these flies have retained the evening oscillator's dominance to a larger extent relative to the *early* chronotypes. Additionally, given the proposed role of evening oscillators in tracking dusk (Pittendrigh and Daan, 1976b), the *late* chronotypes having delayed phase of evening activity relative to its values under long photoperiod (Figure 4.6c, bottom) also point towards a robust evening oscillator in these flies. This, I hypothesise, will reflect in reduced damping of PER oscillations in the evening cells of the *late* chronotypes as opposed to the highly

damped oscillations that were observed in the *control* stocks, and provides leads for further studies. Therefore, I show that waveform plasticity can be brought about by different direction of changes in phase and amplitude. Previous speculations of the *late* chronotypes having weak oscillators (Nikhil, Vaze et al., 2016), and my study demonstrating high plasticity in these stocks, at least with respect to phase provides evidence partially in favour of the trade-off hypothesized by Gorman et al. (Gorman et al., 2017) between rigidity and plasticity, highlighting the complex nature of such relationships.

In summary, I show that activity/rest rhythms of fruit-flies display frequency demultiplication under LDLD. This is associated with weakly bimodal oscillation of PER in the morning cells (s-LNvs), highly damped unimodal PER oscillations in a subset of the evening cells (LNds and DNs), and strongly bimodal oscillations of PDF in the dorsal projections which perhaps directly acts on the output yielding the observed activity pattern. In addition, my experiments reveal that behaviour experiments under short *T*-cycles can be useful to infer inherent differences in the network hierarchy of the circadian neuronal network. Finally, I confirm that waveform plasticity is heritable and can evolve, suggesting an adaptive value for the ability to show such plasticity.

However, certain questions still remain. For instance, how plastic can fly waveforms be? What kind of manipulation of the environmental regime can induce plasticity in flies? Can dim light at night induce bifurcation as it did in rodents? Can temperature zeitgebers also induce bifurcation? Would these shed light on how the network is organised in flies? How does the molecular oscillation in the network get affected under such regimes? These are questions that warrant further research, some of which are being pursued currently, in our laboratory.

Chapter 5. Activity/rest rhythms of *Drosophila* populations selected for divergent eclosion timing under temperature cues

Parts of this chapter are uploaded as a bioRxiv preprint and are also under review:

Abhilash L, Kalliyil A and Sheeba V (2020) Activity/rest rhythms of Drosophila populations selected for divergent eclosion timing under temperature cues. Journal of Experimental Biology 223(11).

bioRxiv DOI: https://doi.org/10.1101/831347

5.1. Introduction

Many insects show rhythmic emergence of adults from their pupal cases. These rhythms persist in the wild and in the laboratory under both LD cycles and constant conditions (Saunders, 2002). Among them, a large proportion of species time this remarkable phenomenon to occur just after dawn. These include, for instance, the yellow dung fly (*Scopeuma stercoraria*), the Queensland fruit-fly (*Dacus tryoni*), moths (*Pectinophora gossypiella* and *Heliothis zea*) and many *Drosophila* species (Saunders, 2002). These observations have raised two interesting questions. What is the mechanism by which organisms restrict emergence to certain times of the day? Why is emergence predominantly restricted to dawn in so many insect species? These questions have been of interest for many decades, and we are now aware of the presence of circadian clocks that generate and drive rhythmicity in many aspects of behavior, and across almost all living beings (Dunlap et al., 2004). To the question of why emergence is restricted to dawn, Colin S Pittendrigh in the mid-1950s hypothesised that organisms must have evolved to time emergence to the time of the day when humidity is high, and temperature is low. This was thought to allow efficient wing expansion in pharate adults and therefore enable survival (Pittendrigh, 1954).

Pittendrigh's hypothesis implied that timing of emergence and modalities that allow sensation of and responses to temperature and/or humidity are intimately linked. Adaptations to capitalise on a temporal niche, in many other organisms, are also thought to be multi-tiered such that multiple aspects of behaviour, physiology and morphology evolve together (Daan, 1981). For instance, in addition to circadian clock properties, waxy cuticles to prevent water loss and enhanced vision are thought to have evolved in diurnal insects, while improved sound and olfaction are thought to have evolved in nocturnal birds and mammals (Daan, 1981; also discussed in Chapter 3). However, clear demonstration of the genetic association of various aspects of physiology and circadian clock

properties via the evolution of behavioural timing has been lacking. With the goal of understanding such relationships, our laboratory generated and currently maintains four large and outbreeding *Drosophila melanogaster* populations that are laboratory (artificially) selected for morning and evening adult emergence (first described in Kumar et al., 2007; also see Chapter 2).

In relation to Pittendrigh's 1954 hypothesis, I have recently demonstrated that laboratory selection for evening timing of emergence (as opposed to morning) is strongly associated with the co-evolution of enhanced temperature sensitivity of the circadian clock circuit regulating adult emergence rhythms (Abhilash et al., 2019; see Chapter 3). This clearly demonstrates a genetic correlation between behavioural phase and temperature responses and is in agreement with the above hypothesis. Although Pittendrigh's argument was made based on cycles of both temperature and humidity, due to technical limitations, there are barely any studies on the role of humidity in emergence rhythms. Effects of temperature, on the other hand, are fairly well studied in both adult emergence and locomotor activity rhythms (Das and Sheeba, 2017; Konopka, 1972; Pittendrigh, 1954; Selcho et al., 2017).

It is important to note here that (i) while the emergence rhythm is a population level phenomenon (each individual can emerge from its pupal case only once), locomotor activity is an individual level rhythm, (ii) further, adult emergence and adult locomotor activity are two very different physiological processes occurring at two entirely different life-stages of the fly life cycle. Despite that, interestingly, the first study that isolated and described the effects of (*per*) period mutation on behavioural rhythms in *Drosophila*, found that both emergence and activity/rest rhythms are affected in a similar manner for all alleles of the *per* locus (Konopka and Benzer, 1971). Subsequently, it was demonstrated that the small ventral lateral neurons (s-LNvs) are necessary to drive behavioural rhythms in eclosion and locomotor activity under constant conditions (Grima et

al., 2004; Myers et al., 2003; Stoleru et al., 2004), thereby illustrating the close overlap in the timing machinery regulating both rhythms. Additional evidence also comes from the fact that the free-running period estimated using eclosion and activity/rest rhythms are strongly positively correlated with each other in flies from our *early* and *late* selected populations (Kumar et al., 2007; Nikhil, Abhilash et al., 2016), again highlighting a common machinery regulating both behaviours. Considering these similarities in organisation of the circadian clock across rhythms spanning two very different behaviours, I asked if temperature sensitivity of the clock regulating the adult locomotor activity rhythm also evolved in the evening emerging flies. In reference to the way the circadian network is organised, what does this imply?

To address this question, I first subjected our flies to simulated jetlag of 6-h phase advance (equivalent to eastward travel, e.g., London to Bangkok) and 6-h phase delay (equivalent to westward travel, e.g., London to Chicago) using temperature cycles alone. I found that the *late* flies re-synchronise to phase-delayed temperature cycles much faster than the *early* and *control* populations. This result indicated differences in the temperature sensitive components of the circadian circuit in the *early* and *late* flies. To further understand the nature of differences in sensitivity, I explored their behaviour under temperature cycles with different durations of warm phase under otherwise constant darkness. I analysed various aspects of the activity/rest rhythm – phase, accuracy (day-to-day variation in phases), power of the rhythm (see material and methods) and consolidation of rhythm under entrainment. I also examined period of the rhythm and its amplitude under constant darkness post entrainment to the aforementioned temperature cycles. Subsequently, I also analysed the behaviour of these flies under LD cycles at two different constant ambient temperatures to understand the degree of waveform plasticity under different constant temperatures. My results suggest that selection for evening timing of emergence is also associated

with increased temperature sensitivity of the clock regulating activity/rest rhythms. Interestingly, I find that this increased sensitivity in the *late* chronotypes is brought about predominantly by the evening bout of activity.

5.2. Materials and Methods

5.2.1. Behavioural experiments

~300 eggs from each of the 12 populations were collected (as during maintenance) and dispensed into 5-10 vials and maintained under standard maintenance regime. Two sets of thirty-two 3- to 5-day old virgin males were collected, and under minimal CO_2 anaesthesia were transferred to 5mm locomotor tubes. These sets were then recorded using the *Drosophila* Activity Monitor (DAM) system under warm:cold cycles, TC 12:12 (thermophase: 28 °C; cryophase: 19 °C) for 4-5 cycles before simulating the jetlag. One of these sets was given a 6-h advance phase-shift, while the other set was given a 6-h delay phase-shift for 10 cycles before all the flies were transferred to constant darkness at 19 °C for a few cycles to judge phase-control (an essential property of circadian clocks wherein phase of activity on first day in constant darkness and temperature continues from the phase on last day of temperature cycles).

In the second batch of experiments, three sets of thirty-two 3- to 5-day old virgin male flies were collected in the same manner as described in the previous paragraph. One set each was then subjected to TC 06:18, TC 12:12 and TC 18:06, under constant darkness for 7 days (thermophase: 28 °C; cryophase: 19 °C). On the 8^{th} day, flies transitioned from TC to constant darkness (DD) at 19 °C for 6-8 days, so as to enable analyses of FRP.

In the third batch of experiments, two sets of thirty-two 3- to 5-day old virgin males were collected as described above. One set was recorded under LD 12:12 (~70 lux during the photophase) at 19

°C and the other at 28 °C. Both these sets were recorded under their respective conditions for 7-8 days, before being transferred to DD under their respective constant temperatures. Flies were maintained under free-running conditions for 6 days, so as to allow estimation of the FRP. I used FRP data of all our stocks to facilitate comparisons with the experiments reported here, from a previous experiment performed by me, entrained behaviour of which is published elsewhere (Nikhil, Abhilash et al., 2016).

5.2.2. Data analysis

5.2.2.1. Rates of re-entrainment

To estimate rates of re-entrainment to 6-h advance and delay, I marked phases of offset for each fly on each day for all 12 populations using RhythmicAlly (Abhilash and Sheeba, 2019). I then calculated the daily phase-relationship as phase of offset of activity – phase of offset of thermophase. For each pre-jetlag cycle, I calculated the average phase-relationship across flies. Next, I computed the average inter-individual variation in among-fly phase-relationships. Subsequently, I multiplied this measure by 1.96 to get a 95% confidence band around the mean inter-cycle phase-relationship. I did this for all populations and then examined the dynamics of phase-relationship change across days for each fly. A fly was considered re-entrained when its phase-relationship re-entered the confidence band and stayed inside the band for at least two subsequent cycles. The number of cycles taken for each fly to re-entrain was used as a measure of number of transients taken for re-entrainment. These values were averaged across flies for obtaining block means. Two separate two-factor mixed model randomised block design ANOVAs were used to analyse the effect of selection on number of transients taken for re-entrainment, each for the 6-h advance regime and 6-h delay regime. Selection was used as a fixed factor and block as a random factor.

5.2.2.2. Activity profiles under TC cycles

I analysed the activity profiles for all populations under TC 06:18, TC 12:12 and TC 18:06. Raw DAM data was scanned, and monitor files were saved in 20-min bins. These data files were analysed using RhythmicAlly (Abhilash and Sheeba, 2019). Individual profiles were downloaded and were re-organised to 1-h bins. Activity counts were then averaged across flies within each block to obtain population-wise profiles. As on multiple previous occasions (e.g., Nikhil et al., 2014; Srivastava et al., 2019), centre of mass (CoM) was used as a non-subjective phase marker (ψ_{CoM}) so that changes in the waveform under different regimes are captured reliably. Owing to the bimodality of activity profiles under TC 12:12 and TC 18:06, an angle doubling transformation was performed before computing ψ_{CoM} (Batschelet, 1981). For TC 06:18, ψ_{CoM} was computed without the angle doubling transformation. While activity/rest profiles of *Drosophila melanogaster* are typically bimodal with the morning and evening bouts of activity being regulated by different cells in the adult brain (Helfrich-Förster, 2017), we argue that in this particular case the ψ_{CoM} is a better phase marker. This is owing to two facts, i.e., under TC cycles (i) the morning activity has a sharp masking component, and (ii) the evening activity component is blunt (see Figure 5.1), as opposed to the sharp peaks under LD cycles. These make it difficult to identify the true peaks of activity, and hence measures of peak phase are certainly less reliable than the use of ψ_{CoM}. FRP of flies experiencing constant conditions post aforementioned entrainment regimes was quantified using the χ^2 periodogram implemented in RhythmicAlly (Abhilash and Sheeba, 2019).

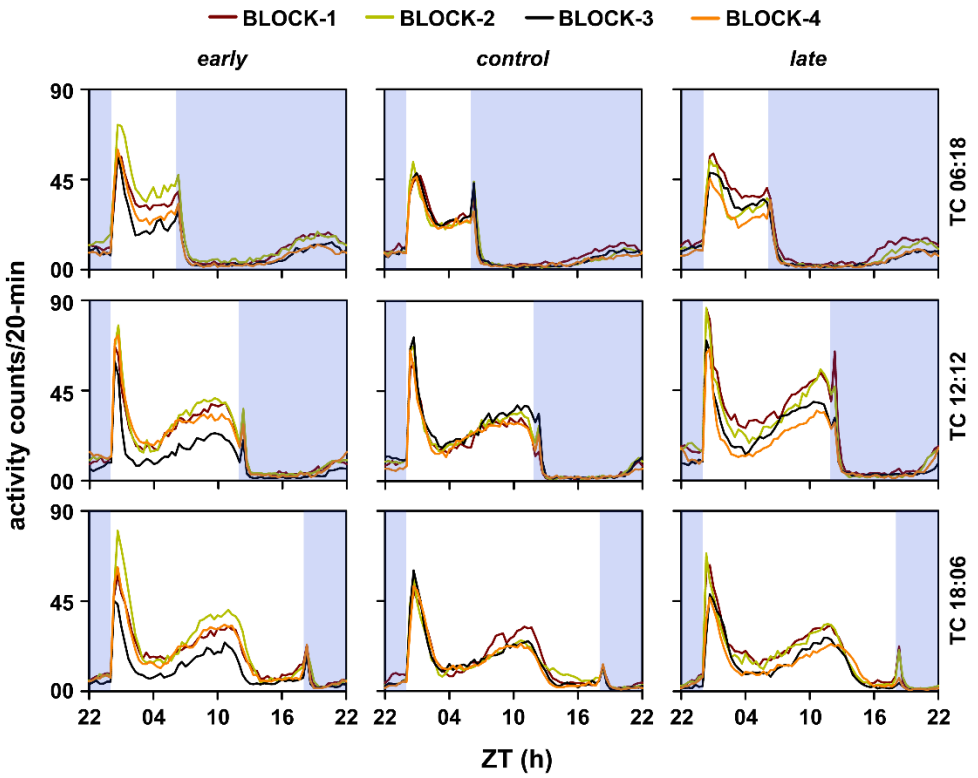

Figure 5.1: Depicted are block-wise activity/rest profiles of *early* (left), *control* (middle) and *late* (right) populations under TC 06:18 (top), TC 12:12 (middle) and TC 18:06 (bottom). The blue shaded regions depict the cryophase of the TC cycles. Note the distinct masking response of the morning peak and bluntness of the evening activity component.

I used circular *r* as a proxy measure of normalised amplitude (owing to its significance in describing the consolidation of a peak; see Abhilash et al., 2019). Similar to the computation of phase, angle doubling was performed on activity profiles under TC 12:12 and 18:06 only. Intrinsic amplitude of each of these stocks was estimated using ActogramJ (Schmid et al., 2011). First, average actograms for each block was generated using data post entrainment to their respective temperature cycles. Then a χ^2 periodogram analysis was done on each population to estimate the average FRP. Then activity profile was generated using modulo-FRP for each block. Amplitude was measured as the maximum activity count – minimum activity count in each of these profiles. To estimate accuracy (cycle to cycle variation in entrained phase), I calculated ψ_{CoM} for each fly

and each cycle during entrainment. Accuracy was defined as inverse of standard deviation in ψ_{CoM} across cycles for each fly. These values were then averaged across flies to obtain block means. Phases, FRP, intrinsic amplitude, amplitude and accuracy of entrainment were analysed using two-factor mixed model randomised block design ANOVAs, wherein selection was treated as a fixed factor and block as a random factor.

5.2.2.3. Activity profiles under constant ambient temperature regimes

To examine behaviour under LD 12:12 at different constant ambient temperatures, average profiles were obtained as described above. Using the population-wise profile data, I calculated a ratio of total activity during the day to the total activity during the night for each population (day/night ratio). These were quantified for profiles under both temperatures. Further, I was interested in asking if anything about the waveform in different temperatures changed differently across populations. For this, I used the 1-h binned activity profiles and computed difference in activity level at each time-point between two temperatures. This difference was squared and the sum of these squared differences (SSD) across the entire cycle was calculated as a measure of deviance of rhythm waveform in the two temperatures. From the 1-h binned profiles, I also computed total activity in a morning window (ZT01-06) and an evening window (ZT06-11) to assess the individual contributions of morning and evening bouts of activity to potential differences in temperature sensitivity. FRP for all these flies under constant darkness at 19 and 28 °C were assessed in RhythmicAlly (Abhilash and Sheeba, 2019) using the χ^2 periodogram. Similar analyses were performed to estimate FRP of flies under DD at 25 °C. The day/night ratio, total morning, total evening activity counts and FRP post entrainment to LD cycles under different temperatures were analysed using three-factor mixed model randomised block design ANOVAs using block means. In these ANOVAs, selection and temperature were treated as fixed factors and

block was treated as a random factor. The SSD values were analysed using a two-factor mixed model randomised block design ANOVA wherein selection was used as a fixed factor and block was used as a random factor. All statistical analyses were followed by a Tukey's HSD post-hoc test, to generate error bars that facilitate easy visual hypothesis testing. All results were considered significant at $\alpha = 0.05$.

5.3. Results

5.3.1. *late* stocks re-entrain faster to phase-delays, but not phase-advances

As a first step to understand if our *early* and *late* flies differ in sensitivity of their circadian clocks to temperature, I analysed their behaviours to simulated jetlag of 6-h phase-advance and 6-h phase-delay under TC 12:12. From the representative actograms, one can see that when flies were subjected to a 6-h phase-advance regime, all three stocks re-synchronised to the phase-shifted TC cycles fairly quickly and took about the same time (Figure 5.2a, top). On the other hand, it appears that all stocks took much longer to re-entrain to a 6-h phase-delay; however, the *late* stocks re-entrained sooner than the *early* and *control* stocks (Figure 5.2a, bottom). These patterns were clearly visible when we analysed the dynamics of phase-relationships for each stock across days for both phase-shifted regimes (Figure 5.2b). The traces in Figure 5.2b indicate average phase-relationships pre- and post-simulated jetlag for all three stocks; these traces are bound on either side by a mean 95% confidence interval estimated from all replicate blocks. The error bars on the lower and upper limits of the 95% interval are standard error of the mean across four replicate blocks. This trace is provided for visual inspection of how phase-relationships vary with days and was used to estimate entrainment (see methods), and therefore, number of transients, which have been used to statistically analyse differences in the rates of re-entrainment (Figure 5.2c).

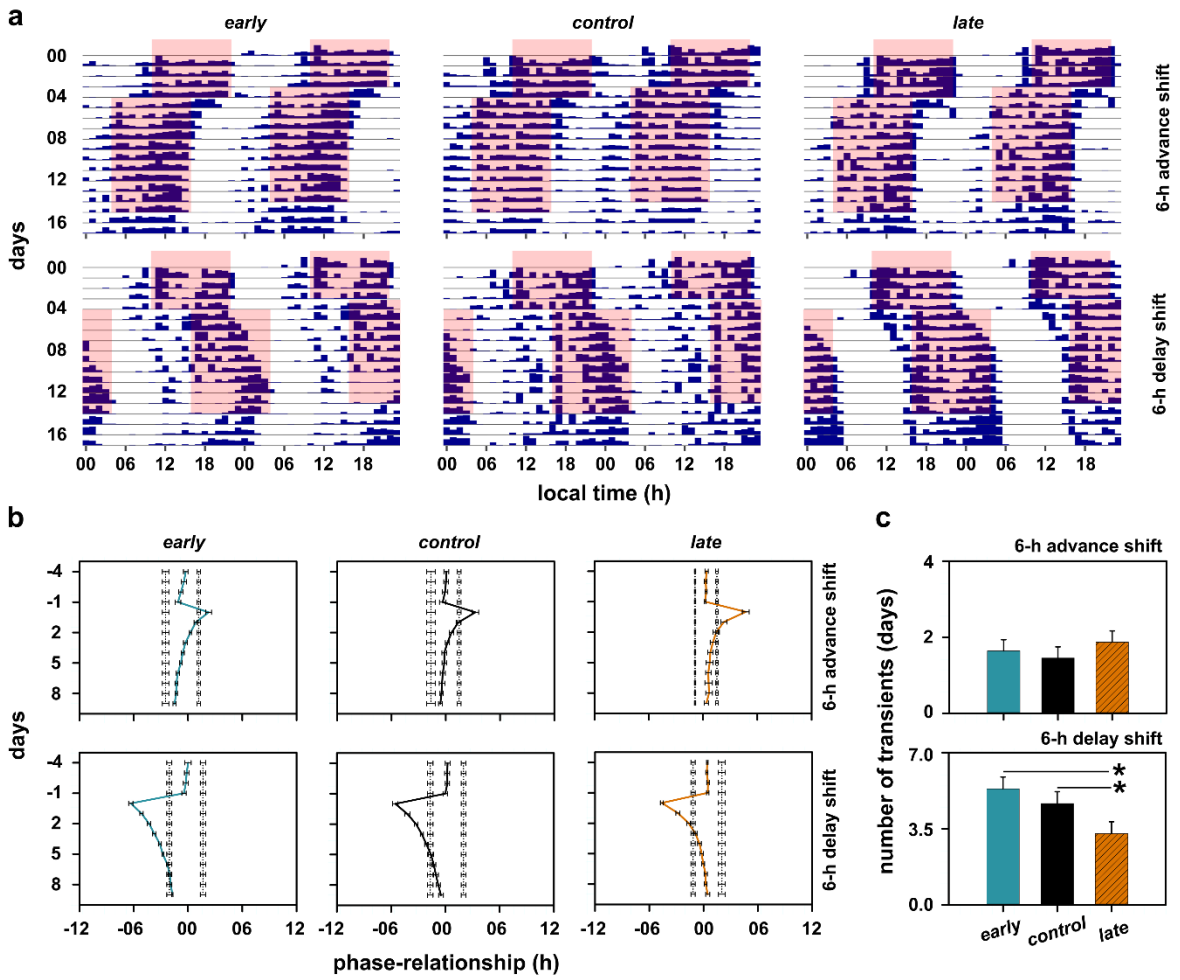

Figure 5.2: Representative actograms of flies experiencing 6-h advance (a, top) and 6-h delay (a, bottom) shift of TC cycles. Red shaded regions indicate the thermophase (28 °C) of the TC cycles (cryophase temperature was 19 °C). Also shown are phase-relationship resetting dynamics averaged over all 4 blocks for each population under 6-h advance (b, top) and 6-h delay (b, bottom) shifts. Error bars here are SEM. Day 0 on the *y*-axis represents the first day of simulated jetlag. Panel (c) shows the average number of transient cycles taken by each population to re-entrain to the 6-h advance (top) and 6-h delay (bottom) shifts. Error bars in this panel are 95% CI from a Tukey's HSD test at $\alpha = 0.05$. Therefore, means with non-overlapping error bars are statistically significantly different from each other. Additionally, asterisks are drawn to indicate means that are significantly different.

I found that all three stocks took fewer than 2 cycles to re-entrain to 6-h phase-advanced TC cycles and there were no among-stock differences in number of transient cycles ($F_{2,6}$ = 2.37, p > 0.05; Figures 5.2b, top and 5.2c, top; Table 5.1). On the other hand, under the 6-h phase-delayed TC cycles, while the *early* stocks took about 5.3 cycles and the *control* stocks took ~4.6 cycles, the *late* stocks only took ~3.2 cycles to re-entrain (Figures 5.2b, bottom and 5.2c, bottom). These among-stock differences were statistically significant as was revealed by the significant main effect of selection on number of transients ($F_{2,6}$ = 17.53, p < 0.05; Table 5.2). Results from this experiment suggest the presence of a circadian clock circuit with enhanced temperature sensitivity in the *late* stocks. I conclude this, as opposed to the *late* stocks being capable of faster re-entrainment to phase-delay regimes because of them having longer τ (Nikhil, Abhilash et al., 2016), owing to results from a similar jetlag experiment using light as a time-cue. Under 9-h delay paradigm, the *late* stocks took significantly longer time to re-entrain compared to the *early* stocks (Nikhil, Vaze et al., 2016), thereby implying that my results indeed indicate strong temperature sensitive components in the circadian network of the *late* stocks. Additionally, while it appears as though the *early* and *control* stocks showed anticipation to the onset of thermophase in the representative actograms (Figure 5.2a, bottom), this is not observed across all individuals as is clear from the averaged actograms (Figure 5.3).

Table 5.1: ANOVA table summarizing the effects of selection regime on number of transients in response to a 6-h advance phase-shift. Italicised effects are significant.

Summary of all effects	***df* Effect**	**MS Effect**	***df* Error**	**MS Error**	***F***	***p***
Selection (Sel)	2	0.1756	6	0.0740	2.37	0.17
Block (B)	3	0.1176	0	0.0000	--	--
Sel × B	6	0.0740	0	0.0000	--	--

Table 5.2: ANOVA table summarizing the effects of selection regime on number of transients in response to a 6-h delay phase-shift. Italicised effects are significant.

Summary of all effects	*df* Effect	MS Effect	*df* Error	MS Error	*F*	*p*
Selection (Sel)	*2*	*4.3895*	*6*	*0.2505*	*17.53*	*0.00*
Block (B)	3	0.2617	0	0.0000	--	--
Sel × B	6	0.2505	0	0.0000	--	--

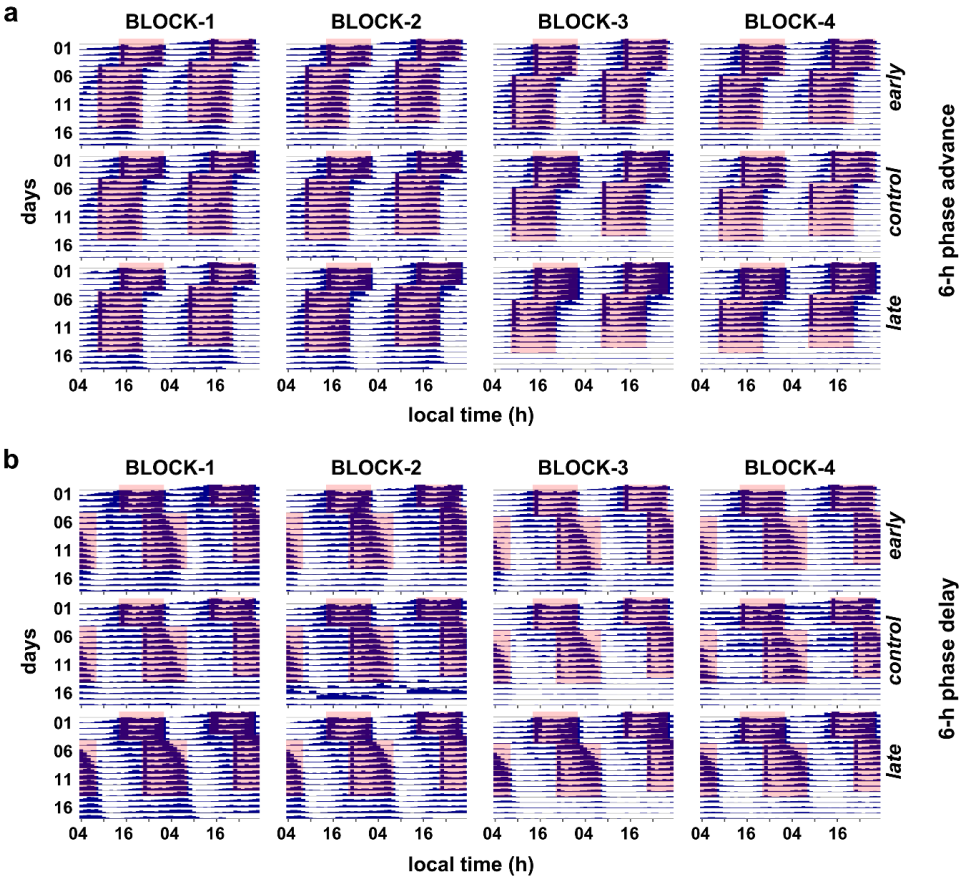

Figure 5.3: Depicted are average actograms of all four replicate blocks of the *early*, *control* and *late* stocks undergoing a 6-h advance shift (a) and a 6-h delay shift (b). The red shaded region indicates the thermophase of the TC 12:12 cycles. Note the distinctly quicker re-entrainment to advance jetlag compared with the delay jetlag in all stocks. Also note that the *late* stocks re-entrain significantly faster to the delay shift than the *early* and *control* stocks.

5.3.2. Activity/rest rhythms of *late* stocks under different thermoperiods are more plastic and entrainment is consistent with the non-parametric model

To further understand if underlying differences in clock sensitivity to thermal cues contribute to plasticity in phases under different durations of warmth in warm:cold cycles (TC cycles), I examined their behaviour under three different thermoperiods (TC 06:18, TC 12:12 and TC 18:06) under otherwise constant darkness. Across thermoperiods, most activity for both *early* and *late* stocks was restricted to the thermophase, as can be clearly seen in the actograms (Figure 5.4a and b). Moreover, it appears as though under TC 12:12 and TC 18:06, the *late* chronotypes have delayed evening activity compared to the *early* chronotypes (Figures 5.4a, middle and right and b, middle and right). Therefore, I quantified entrained phases and found that under TC 06:18 the ψ_{CoM} was not different among stocks ($F_{2,6}$ = 4.20, $p > 0.05$; Figure 5.4c, top-left; Table 5.3), whereas, as expected from the actograms, the ψ_{CoM} of *late* chronotypes was significantly delayed compared to that of *early* chronotypes under both TC 12:12 ($F_{2,6}$ = 7.10, $p < 0.05$; Table 5.4) and TC 18:06 ($F_{2,6}$ = 5.91, $p < 0.05$; Figure 5.4c, top-middle and top-right; Table 5.5). While under TC 06:18 the *early* stocks appear to start their activity earlier in the cryophase, I argue that it is not statistically significant. This is based on my use of CoM as a phase marker which incorporates changes in the entire waveform to describe the mean phase (Zar, 1999).

Table 5.3: ANOVA table summarizing the effects of selection regime on ψ_{CoM} under TC 06:18. Italicised effects are significant.

Summary of all effects	***df* Effect**	**MS Effect**	***df* Error**	**MS Error**	***F***	***p***
Selection (Sel)	2	0.1980	6	0.0471	4.20	0.07
Block (B)	3	0.0531	0	0.0000	--	--
Sel × B	6	0.0471	0	0.0000	--	--

Table 5.4: ANOVA table summarizing the effects of selection regime on ψ_{CoM} under TC 12:12. Italicised effects are significant.

Summary of all effects	*df* Effect	MS Effect	*df* Error	MS Error	*F*	*p*
Selection (Sel)	*2*	*1.1244*	*6*	*0.1577*	*7.13*	*0.03*
Block (B)	3	0.0391	0	0.0000	--	--
Sel × B	6	0.1577	0	0.0000	--	--

Table 5.5: ANOVA table summarizing the effects of selection regime on ψ_{CoM} under TC 18:06. Italicised effects are significant.

Summary of all effects	*df* Effect	MS Effect	*df* Error	MS Error	*F*	*p*
Selection (Sel)	*2*	*2.3421*	*6*	*0.3965*	*5.91*	*0.04*
Block (B)	3	0.0839	0	0.0000	--	--
Sel × B	6	0.3965	0	0.0000	--	--

Furthermore, earlier experiments from our laboratory have reported the presence of FRP differences among the stocks under DD at 25 °C (Kumar et al., 2007; Nikhil, Abhilash et al., 2016). My results, therefore, implied that entrainment to temperature cycles in these stocks can be explained within the framework of the non-parametric model of entrainment, a key prediction of which is that longer FRP is associated with delayed phase (Pittendrigh and Daan, 1976a). To test this, I first analysed FRP values of the flies that experienced the presented TC and were transferred to DD at 19 °C. I found that there was no statistically significant among-stock difference in FRP when flies were transferred to constant conditions after TC 06:18 ($F_{2,6}$ = 1.70, $p > 0.05$; Figure 5.4c, bottom-left; Tables 5.6 and 5.7). After exposure to TC 12:12, the *late* chronotypes showed significantly longer FRP in constant conditions compared to that of the *early* stocks ($F_{2,6}$ = 5.90, $p < 0.05$; Figure 5.4c, bottom-middle; Tables 5.6 and 5.8). However, although there were among-

stock differences in phase under TC 18:06, there was no among-stock difference in FRP ($F_{2,6}$ = 2.10, p > 0.05; Figure 5.4c, bottom-right; Tables 5.6 and 5.9). Typically, the difference in FRP between *early* and *late* stocks after entrainment to LD and different constant ambient temperatures varies from ~0.7 – ~0.9-h (Figure 5.4; Kumar et al., 2007; Nikhil, Abhilash et al., 2016). However, here there is no difference under short and long thermoperiods, and the difference persists under TC 12:12, but is greatly reduced (~0.38-h). This, I argue reflects differential response of the stocks' FRP to temperature as a zeitgeber (see discussion).

Table 5.6: Mean values of FRP post entrainment to LD 12:12 at different constant ambient temperatures and post entrainment to TC cycles with three different thermoperiods ± SEM for all three stocks are reported.

FRP post entrainment to	***early***	***control***	***late***
LD 12:12, 19 °C	23.34±0.06-h	23.62±0.07-h	23.98±0.08-h
LD 12:12, 25 °C	23.64±0.07-h	23.96±0.07-h	24.46±0.14-h
LD 12:12, 28 °C	23.91±0.05-h	24.39±0.09-h	24.88±0.05-h
TC 06:18, DD	23.12±0.05-h	23.27±0.24-h	23.56±0.09-h
TC 12:12, DD	22.80±0.06-h	22.95±0.10-h	23.18±0.05-h
TC 18:06, DD	23.35±0.07-h	23.42±0.07-h	23.54±0.04-h

Table 5.7: ANOVA table summarizing the effects of selection regime on FRP post entrainment to TC 06:18. Italicised effects are significant.

Summary of all effects	***df* Effect**	**MS Effect**	***df* Error**	**MS Error**	***F***	***p***
Selection (Sel)	2	0.1920	6	0.1153	1.67	0.27
Block (B)	3	0.0434	0	0.0000	--	--
Sel × B	6	0.1153	0	0.0000	--	--

Table 5.8: ANOVA table summarizing the effects of selection regime on FRP post entrainment to TC 12:12. Italicised effects are significant.

Summary of all effects	***df* Effect**	**MS Effect**	***df* Error**	**MS Error**	***F***	***p***
Selection (Sel)	*2*	*0.1475*	*6*	*0.0250*	*5.90*	*0.04*
Block (B)	3	0.0120	0	0.0000	--	--
Sel × B	6	0.0250	0	0.0000	--	--

Table 5.9: ANOVA table summarizing the effects of selection regime on FRP post entrainment to TC 18:06. Italicised effects are significant.

Summary of all effects	***df* Effect**	**MS Effect**	***df* Error**	**MS Error**	***F***	***p***
Selection (Sel)	2	0.0371	6	0.0179	2.07	0.21
Block (B)	3	0.0069	0	0.0000	--	--
Sel × B	6	0.0179	0	0.0000	--	--

Importantly, we have shown previously that similar experiments under three different photoperiods, i.e., LD 06:18, LD 12:12 and LD 18:06 yield very different results as compared to the results described above. We have found that while the *late* stocks show significantly delayed phase under short photoperiod relative to the *early* stocks, they are not different from the *early* stocks under LD 12:12, and are significantly advanced under long photoperiod (Abhilash and Sharma, 2020; Nikhil, Abhilash et al., 2016; *see also Chapter 6*). Further, post entrainment to all three photoperiods, there were significant differences in the FRP among these stocks with the *late* stocks exhibiting longer τ than the *early* stocks (see Chapter 6). We have discussed the implications of these results being that the non-parametric model of entrainment is unable to account for such patterns of period and phases in our populations (Abhilash and Sharma,*; also see next chapter*). However, results reported here of the patterns of period post entrainment and phases

under entrainment to different thermoperiods, we stress, are largely in agreement with the predictions made from the non-parametric model of entrainment.

Results from both previous sections were suggestive of among-stock differences in phase-dependent sensitivity of the circadian clock to temperature, typically characterised by the PRC (see Moore-Ede et al., 1982). However, there are inherent complexities of temperature pulse phase-resetting experiments and typically, only very small phase-shift values are obtained in response to long duration of pulses, as is discussed elsewhere (Chandrashekaran, 2005). Therefore, I tested predictions under the assumption of divergent temperature PRCs of the *early* and *late* stocks, without constructing the phase-response curves of these stocks to temperature pulses.

Figure 5.4: (a) Average actograms of *early* and *late* stocks under three different thermoperiods, i.e., TC 06:18 (Thermophase: 6-h, Cryophase: 18-h), TC 12:12 and TC 18:06. Also shown are activity profiles averaged over 4 blocks in panel (b) for all three thermoperiods. Error bars in panel (b) are SEM. The blue shaded region in panels (a) and (b) indicate the cryophase of the TC cycles. (c) Phases of center of mass (ψ_{CoM}) of the three stocks under all three thermoperiods (top panel). Phases for TC 12:12 and TC 18:06 were calculated after an angle doubling transformation was applied, due to the bimodality of the profiles. No such transformation was performed for calculating phase under TC 06:18. Also depicted are free-running periods (FRP) of each stock under constant conditions after being entrained to each of the thermoperiods for ~7 cycles (bottom panel). All error bars in panel (c) are 95% CI from a Tukey's HSD test at $\alpha = 0.05$. Therefore, means with non-overlapping error bars are statistically significantly different from each other. Additionally, asterisks are drawn to indicate means that are significantly different.

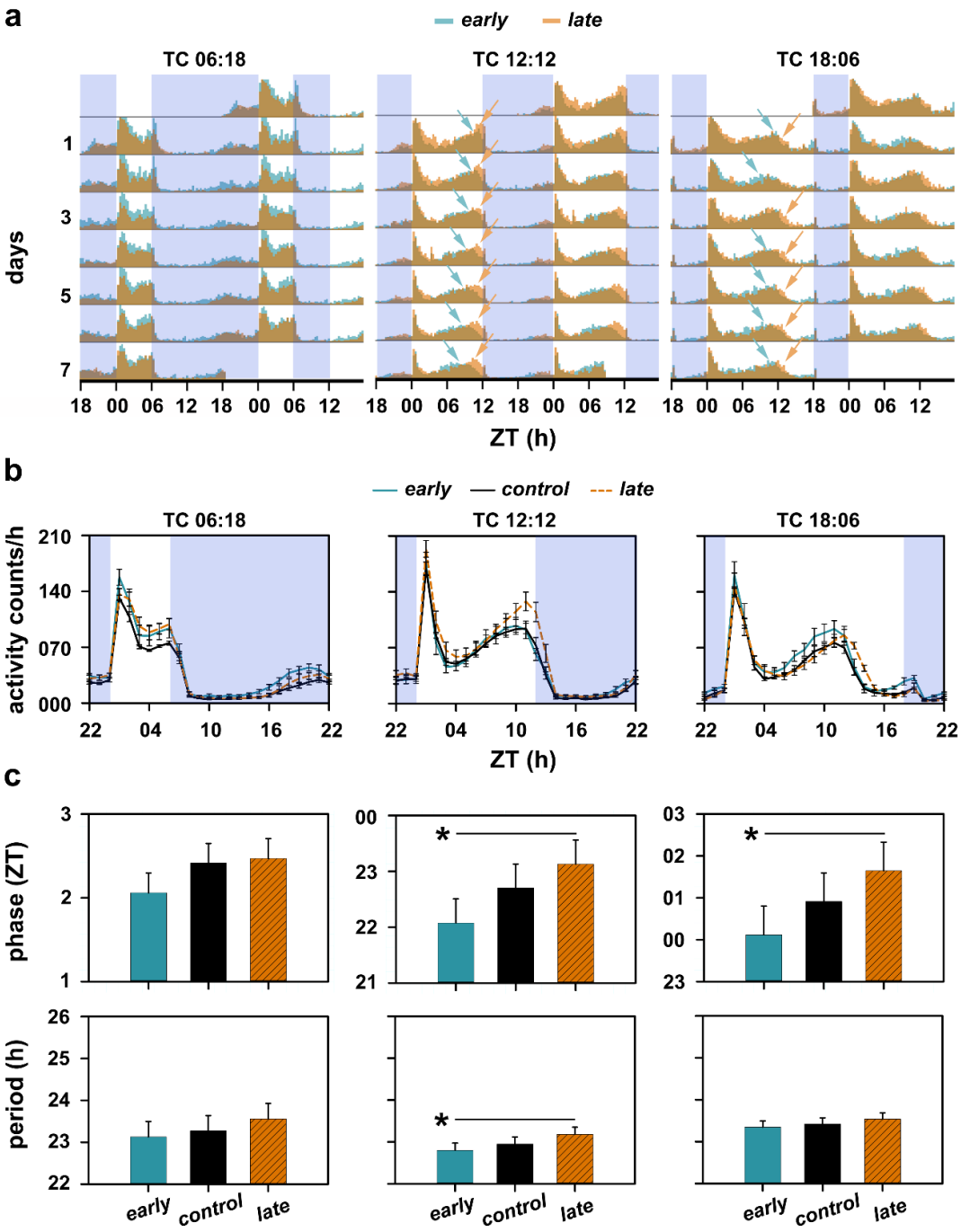

5.3.3. *late* stocks show higher robustness, amplitude and accuracy of entrainment, suggestive of evolution of high amplitude phase response curves

Previous studies have linked divergent PRCs to differences in intrinsic amplitude of the circadian oscillator, its amplitude under entrainment, power of periodogram and accuracy of entrainment

(Beersma et al., 1999; Brown et al., 2008; Nikhil, Vaze et al., 2016; Vitaterna et al., 2006). I examined these properties in flies that were exposed to TC and subsequently placed in DD, under constant temperatures. Firstly, I found that the *late* stocks had significantly higher amplitude of entrainment, estimated using circular *r* (a measure of how sharp the peak is; Figure 5.5a), under both the asymmetric thermoperiods TC 06:18 ($F_{2,6}$ = 20.77, $p < 0.05$; Table 5.10) and TC 18:06 ($F_{2,6}$ = 9.17, $p < 0.05$; Figure 5.6a, left and right; Table 5.11). However, there was no significant among-stock difference in the amplitude under entrainment to TC 12:12 ($F_{2,6}$ = 4.38, $p > 0.05$; Figure 5.6a, middle; Table 5.12). Further, there was no significant among-stock difference in intrinsic amplitude under DD post TC 06:18 ($F_{2,6}$ = 0.67, $p > 0.05$; Table 5.13) or post TC 18:06 ($F_{2,6}$ = 1.26, $p > 0.05$; Figure 5.6b, left and right; Table 5.14). However, the *late* stocks had significantly higher intrinsic amplitude, post entrainment to TC 12:12 ($F_{2,6}$ = 9.86, $p < 0.05$; Figure 5.6b, middle; Table 5.15). These results imply higher amplitude expansion of the *late* stocks under specific TC regimes, thereby suggesting stronger temperature sensitivity in these stocks. I reasoned that periodogram power during entrainment could provide additional evidence for enhanced temperature sensitivity in the *late* stocks. I found that power was significantly higher for *late* stocks only under entrainment to TC 12:12 ($F_{2,6}$ = 5.83, $p < 0.05$; Figures 5.5b and 5.6c; Tables 5.16, 5.17 and 5.18). Subsequently, I analysed the accuracy of entrainment under all three regimes and found that under short thermoperiod there was no among-stock differences in accuracy of entrainment ($F_{2,6}$ = 1.24, $p > 0.05$; Figures 5.5c and 5.6d, left; Table 5.19). Under both TC 12:12 and TC 18:06, there was a significant main effect of selection such that the *late* chronotypes showed significantly higher accuracy of entrainment (TC 12:12: $F_{2,6}$ = 9.20, $p < 0.05$; TC 18:06: $F_{2,6}$ = 6.46, $p < 0.05$; Figures 5.5c and 5.6d, middle and right; Tables 5.20 and 5.21).

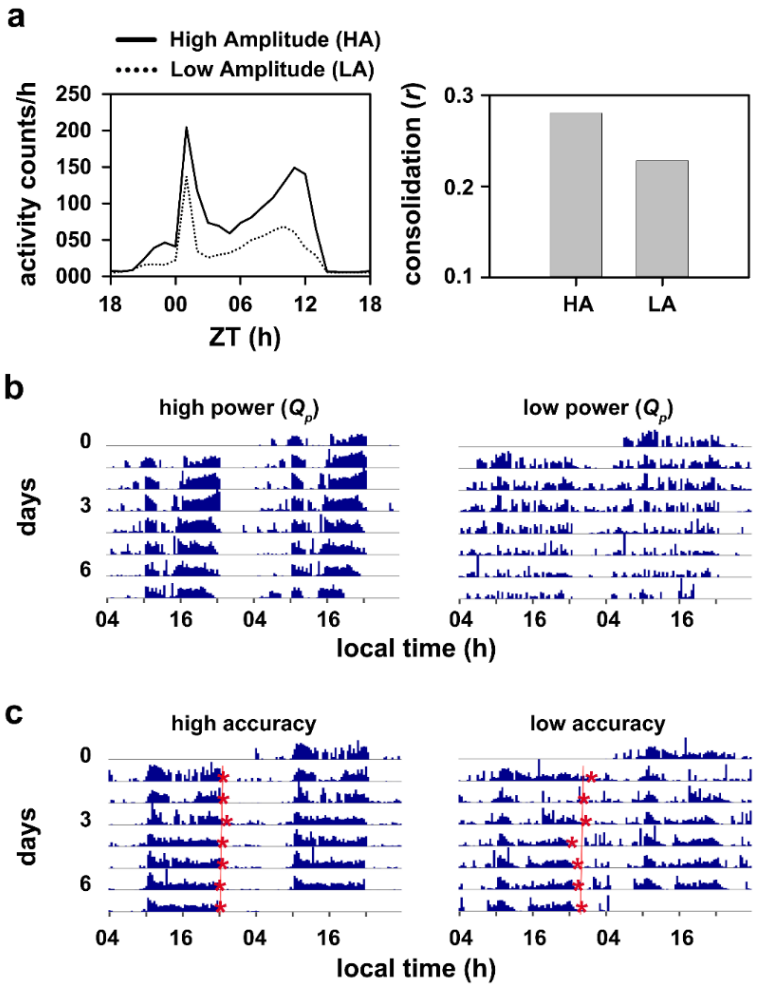

Figure 5.5: (a) Shown on the left are representative average profiles one with high and another with low amplitude under TC 12:12. Note that the flat/rounded nature of the peak makes it difficult to identify a distinct peak and compute the amplitude of the oscillation. Therefore, I use consolidation, a circular statistic, to estimate normalised amplitude of the oscillation (normalised by spread of activity, in this case; see also Zar, 1999). The values of consolidation for each of the profiles on the left, is plotted on the right. Note how this measure accurately captures differences in amplitude. (b) Example actograms of flies showing high power (left) of the periodogram and low power (right) of the periodogram. Note that power describes how tightly the rhythm is regulated. The actogram on the right is 'noisy', which leads to lower power. (c) Example actograms showing flies with high accuracy (left) and low accuracy (right). Accuracy is defined as inverse of day-to-day stability of entrained phases. One can clearly see here that day-to-day variability in phases of offsets (in this example; marked as red asterisks) is higher for the actogram

on the right. The red solid lines are eye-fitted regression lines, to enable the reader to visualise daily variability in phases.

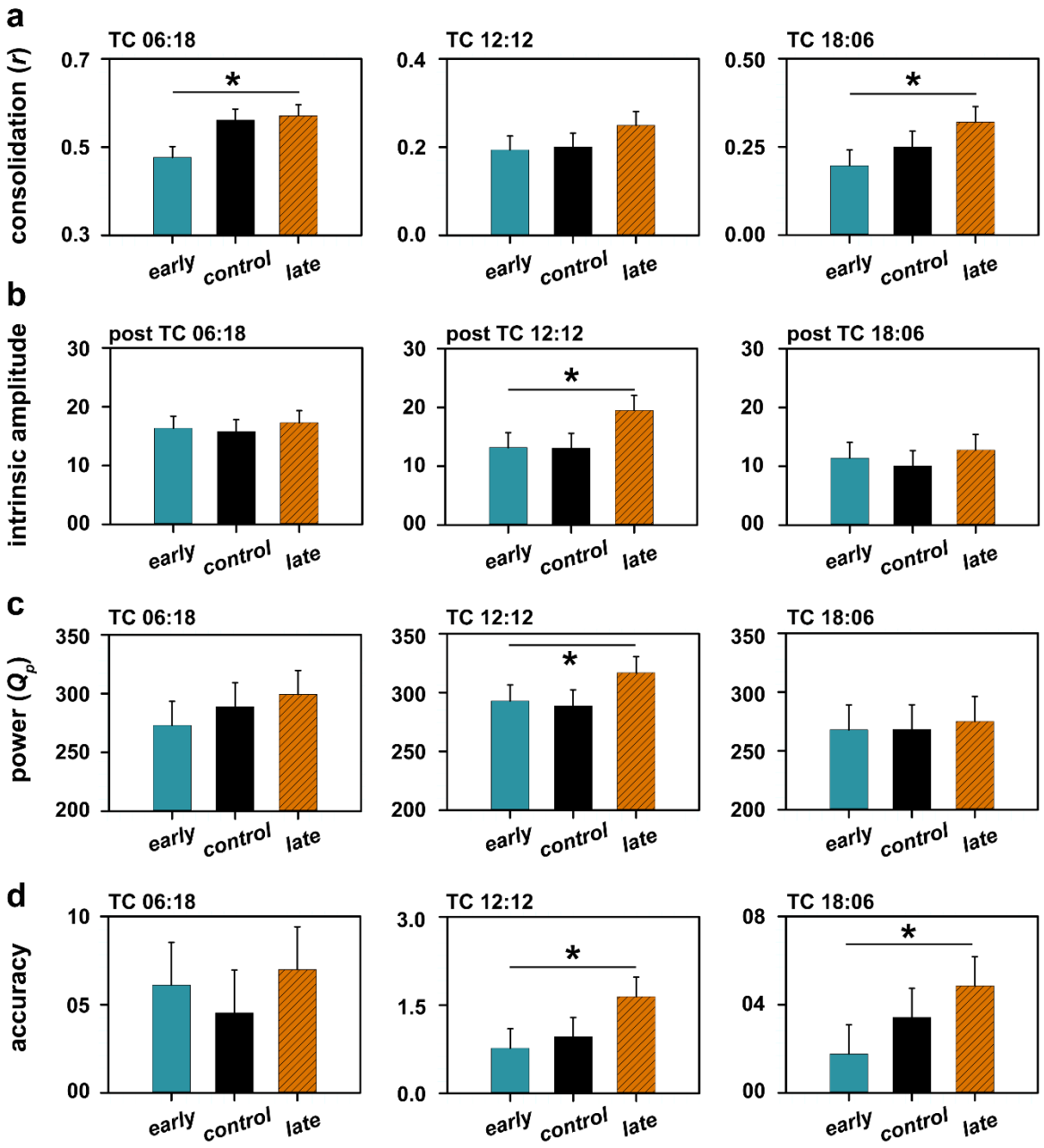

Figure 5.6: Depicted are consolidation as a measure of amplitude under TC cycles (a), intrinsic amplitude under constant conditions post entrainment (b), power of the χ^2 periodogram (c) and accuracy of entrainment (d) for all three stocks under all three thermoperiods. All error bars are 95% CI from a Tukey's HSD test at $\alpha = 0.05$. Therefore, means with non-overlapping error bars are statistically significantly different from each other. Additionally, asterisks are drawn to indicate means that are significantly different.

Table 5.10: ANOVA table summarizing the effects of selection regime on normalised amplitude (or consolidation) under entrainment to TC 06:18. Italicised effects are significant.

Summary of all effects	***df* Effect**	**MS Effect**	***df* Error**	**MS Error**	***F***	***p***
Selection (Sel)	*2*	*0.0108*	*6*	*0.0005*	*20.77*	*0.00*
Block (B)	3	0.0042	0	0.0000	--	--
Sel × B	6	0.0005	0	0.0000	--	--

Table 5.11: ANOVA table summarizing the effects of selection regime on normalised amplitude (or consolidation) under entrainment to TC 18:06. Italicised effects are significant.

Summary of all effects	***df* Effect**	**MS Effect**	***df* Error**	**MS Error**	***F***	***p***
Selection (Sel)	*2*	*0.0153*	*6*	*0.0017*	*9.17*	*0.01*
Block (B)	3	0.0006	0	0.0000	--	--
Sel × B	6	0.0017	0	0.0000	--	--

Table 5.12: ANOVA table summarizing the effects of selection regime on normalised amplitude (or consolidation) under entrainment to TC 12:12. Italicised effects are significant.

Summary of all effects	***df* Effect**	**MS Effect**	***df* Error**	**MS Error**	***F***	***p***
Selection (Sel)	2	0.0037	6	0.0008	4.38	0.07
Block (B)	3	0.0006	0	0.0000	--	--
Sel × B	6	0.0008	0	0.0000	--	--

Table 5.13: ANOVA table summarizing the effects of selection regime on intrinsic amplitude post entrainment to TC 06:18. Italicised effects are significant.

Summary of all effects	***df* Effect**	**MS Effect**	***df* Error**	**MS Error**	***F***	***p***
Selection (Sel)	2	2.4002	6	3.5603	0.67	0.54
Block (B)	3	5.1984	0	0.0000	--	--
Sel × B	6	3.5603	0	0.0000	--	--

Table 5.14: ANOVA table summarizing the effects of selection regime on intrinsic amplitude post entrainment to TC 18:06. Italicised effects are significant.

Summary of all effects	*df* Effect	MS Effect	*df* Error	MS Error	*F*	*p*
Selection (Sel)	2	7.5159	6	5.9720	1.26	0.35
Block (B)	3	6.2627	0	0.0000	--	--
Sel × B	6	5.9720	0	0.0000	--	--

Table 5.15: ANOVA table summarizing the effects of selection regime on intrinsic amplitude post entrainment to TC 12:12. Italicised effects are significant.

Summary of all effects	*df* Effect	MS Effect	*df* Error	MS Error	*F*	*p*
Selection (Sel)	*2*	*54.2285*	*6*	*5.5024*	*9.86*	*0.01*
Block (B)	3	4.3201	0	0.0000	--	--
Sel × B	6	5.5024	0	0.0000	--	--

Table 5.16: ANOVA table summarizing the effects of selection regime on periodogram power under entrainment to TC 12:12. Italicised effects are significant.

Summary of all effects	*df* Effect	MS Effect	*df* Error	MS Error	*F*	*p*
Selection (Sel)	*2*	*920.5348*	*6*	*157.8923*	*5.83*	*0.04*
Block (B)	3	317.0275	0	0.0000	--	--
Sel × B	6	157.8923	0	0.0000	--	--

Table 5.17: ANOVA table summarizing the effects of selection regime on periodogram power under entrainment to TC 06:18. Italicised effects are significant.

Summary of all effects	*df* Effect	MS Effect	*df* Error	MS Error	*F*	*p*
Selection (Sel)	2	698.1025	6	353.8381	1.97	0.22
Block (B)	3	107.2088	0	0.0000	--	--
Sel × B	6	353.8381	0	0.0000	--	--

Table 5.18: ANOVA table summarizing the effects of selection regime on periodogram power under entrainment to TC 18:06. Italicised effects are significant.

Summary of all effects	*df* Effect	MS Effect	*df* Error	MS Error	*F*	*p*
Selection (Sel)	2	66.9534	6	378.4583	0.18	0.84
Block (B)	3	214.4583	0	0.0000	--	--
Sel × B	6	378.4583	0	0.0000	--	--

Table 5.19: ANOVA table summarizing the effects of selection regime on accuracy under entrainment to TC 06:18. Italicised effects are significant.

Summary of all effects	*df* Effect	MS Effect	*df* Error	MS Error	*F*	*p*
Selection (Sel)	2	6.1742	6	4.9833	1.24	0.35
Block (B)	3	0.4486	0	0.0000	--	--
Sel × B	6	4.9833	0	0.0000	--	--

Table 5.20: ANOVA table summarizing the effects of selection regime on accuracy under entrainment to TC 12:12. Italicised effects are significant.

Summary of all effects	*df* Effect	MS Effect	*df* Error	MS Error	*F*	*p*
Selection (Sel)	*2*	*0.8484*	*6*	*0.0922*	*9.20*	*0.01*
Block (B)	3	0.0810	0	0.0000	--	--
Sel × B	6	0.0922	0	0.0000	--	--

Table 5.21: ANOVA table summarizing the effects of selection regime on accuracy under entrainment to TC 18:06. Italicised effects are significant.

Summary of all effects	*df* Effect	MS Effect	*df* Error	MS Error	*F*	*p*
Selection (Sel)	*2*	*9.5885*	*6*	*1.4847*	*6.46*	*0.03*
Block (B)	3	2.5772	0	0.0000	--	--
Sel × B	6	1.4847	0	0.0000	--	--

In summary, I found evidence for the evolution of temperature sensitivity in the activity/rest rhythms in populations selected for divergent timing of adult emergence rhythm. Additionally, these results also suggest that most features of entrainment can be well explained within the framework of the non-parametric model described above, which makes use of predictions using the FRP and the PRC of the clock.

5.3.4. Activity/rest rhythms under LD 12:12 and constant ambient temperatures are not different between the *early* and *late* chronotypes

Owing to the fact that selection for evening emergence contributed to enhanced phase plasticity of emergence rhythms even under LD and different constant ambient temperatures (Abhilash et al., 2019), I next analysed the activity/rest behaviour of our stocks under said regimes. Visual inspection of the activity/rest profiles of *early*, *control* and *late* stocks under 19 °C indicated higher evening activity in the *late* chronotypes (Figure 5.7a, left). On the other hand, profiles under 28 °C looked largely similar (Figure 5.7a, right), except the slightly increased morning activity in the *late* flies.

To quantify this, I calculated the ratio of total day-time activity to total night-time activity (day/night ratio, henceforth), and found that although there was a significant main effect of temperature-regime such that there was higher day-time activity under 19 °C as has earlier been shown ($F_{1,3} = 98.10$, $p < 0.05$; Table 5.22; Majercak et al., 1999), there was no significant effect of selection × temperature-regime interaction ($F_{2,6} = 0.54$, $p > 0.05$; Figure 5.7b, left; Table 5.22), thereby implying that the activity/rest rhythms of all three stocks responded similarly to cool and warm ambient temperatures.

I subsequently examined divergence in waveform across stocks and regimes by calculating SSD (see materials and methods) as a measure of extent of plasticity that *early*, *control* and *late* stocks show in response to different constant ambient temperatures. Although the SSD in *late* stocks is almost twice as much as that in *early* and *control* stocks (Figure 5.7b, right), the ANOVA did not detect a main effect of selection, thereby implying that the stocks respond similarly to change in ambient temperature ($F_{2,3} = 4.69$, $p = 0.059$; Table 5.23).

However, owing to the fact that the SSD difference among stocks was marginally non-significant and that there were trends of among stock differences, I quantified total activity in a morning window (ZT01-06) and an evening window (ZT06-11) for all three stocks under 19 and 28 ℃. I found that there was no significant effect selection × temperature-regime interaction on total morning ($F_{2,6} = 1.33$, $p > 0.05$; Figure 5.7c, left; Table 5.24) or total evening activity ($F_{2,6} = 2.56$, $p > 0.05$; Figure 5.7c, right; Table 5.25). But there is a clear trend of the *late* stocks suppressing evening activity more strongly under 28 ℃ relative to the *early* and *control* stocks (Figure 5.7c, right). These results are suggestive, although not strongly, of increased plasticity of the activity/rest waveform in the *late* chronotypes in response to different constant ambient temperatures under LD cycles.

Table 5.22: ANOVA table summarizing the effects of selection regime, temperature regime and their interaction on day/night ratio. Italicised effects are significant.

Summary of all effects	***df* Effect**	**MS Effect**	***df* Error**	**MS Error**	***F***	***p***
Selection (Sel)	2	0.0713	6	0.1081	0.66	0.55
Temperature (Temp)	*1*	*1.9558*	*3*	*0.0199*	*98.10*	*0.00*
Block (B)	3	0.5404	0	0.0000	--	--
Sel × Temp	2	0.0650	6	0.1212	0.54	0.61
Sel × B	6	0.1081	0	0.0000	--	--
Sel × B	3	0.0199	0	0.0000	--	--
Sel × Temp × B	6	0.1212	0	0.0000	--	--

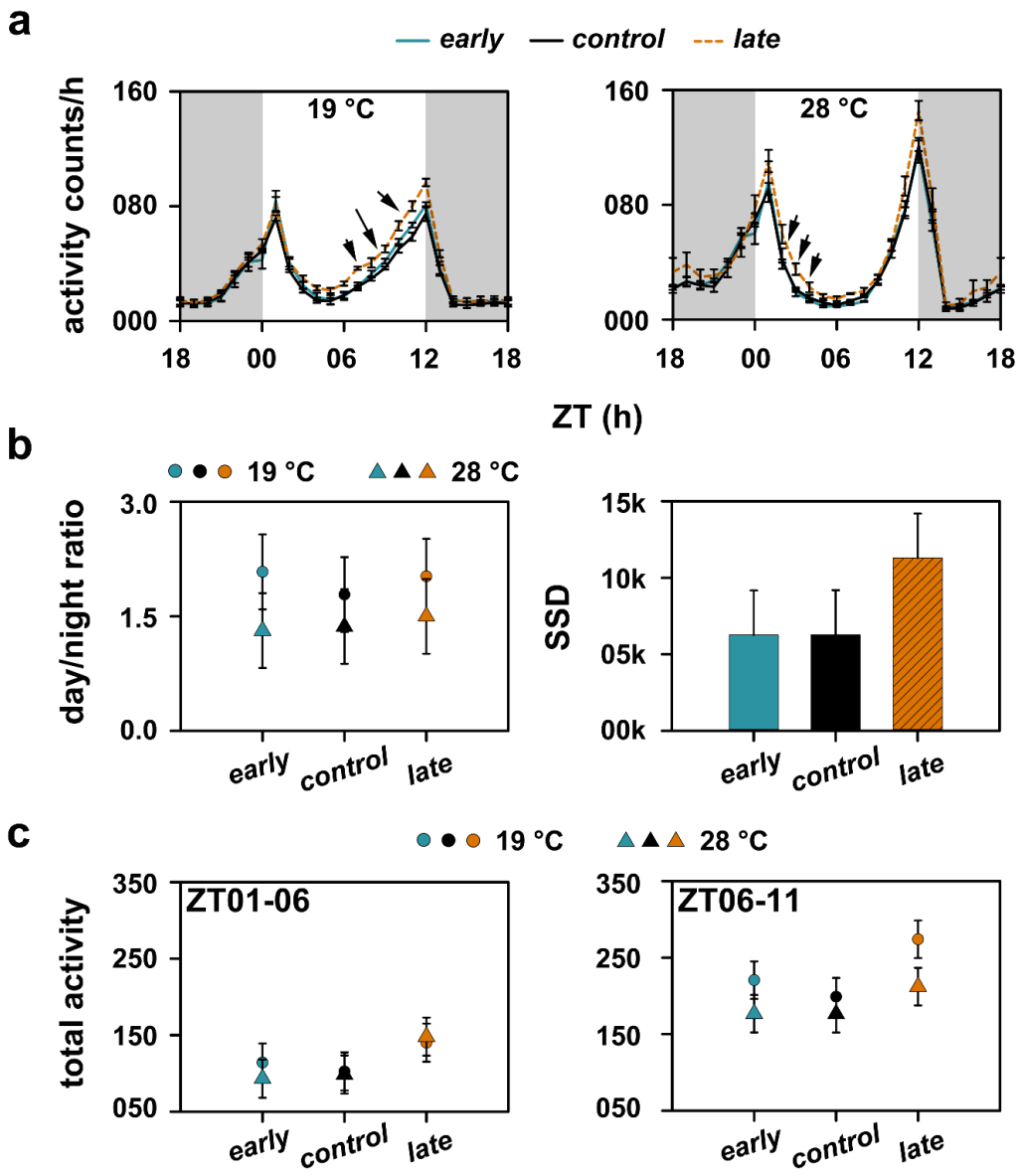

Figure 5.7: Depicted are locomotor activity profiles of *early*, *control* and *late* stocks under LD 12:12 at 19 °C (a, left) and 28 °C (a, right). The black arrowheads mark parts of the profiles where *late* stocks show higher activity. Gray shaded regions in panel (a) depict the dark phase of the LD cycle. Error bars in this panel are standard error of the mean (SEM). Also shown are day/night ratio of total activity under both temperatures for all three stocks (b, left) and the total sum of square difference between profiles under 19 and 28 °C for all three stocks (b, right). Panel (C) shows total activity in defined first (left) and second (right) halves of the light phase, ignoring the activity during the peak times. All error bars in panels (b) and (c) are 95% CI following a Tukey's HSD test at $\alpha = 0.05$. Therefore, means with non-overlapping error bars are significantly different from each other.

Table 5.23: ANOVA table summarizing the effects of selection regime on SSD between activity profiles under 19 and 28 °C. Italicised effects are significant.

Summary of all effects	*df* Effect	MS Effect	*df* Error	MS Error	*F*	*p*
Selection (Sel)	2	33628479.1192	6	7169608.0742	4.69	0.06
Block (B)	3	9634301.2839	0	0.0000	--	--
Sel × B	6	7169608.0742	0	0.0000	--	--

Table 5.24: ANOVA table summarizing the effects of selection regime, temperature regime and their interaction on activity between ZT01 and ZT06. Italicised effects are significant.

Summary of all effects	*df* Effect	MS Effect	*df* Error	MS Error	*F*	*p*
Selection (Sel)	*2*	*4708.3138*	*6*	*266.7263*	*17.65*	*0.00*
Temperature (Temp)	1	195.9317	3	250.8049	0.78	0.44
Block (B)	3	1474.8250	0	0.0000	--	--
Sel × Temp	2	418.9302	6	314.2764	1.33	0.33
Sel × B	6	266.7263	0	0.0000	--	--
Sel × B	3	250.8049	0	0.0000	--	--
Sel × Temp × B	6	314.2764	0	0.0000	--	--

Table 5.25: ANOVA table summarizing the effects of selection regime, temperature regime and their interaction on activity between ZT06 and ZT11. Italicised effects are significant.

Summary of all effects	*df* Effect	MS Effect	*df* Error	MS Error	*F*	*p*
Selection (Sel)	*2*	*6870.8318*	*6*	*438.1601*	*15.68*	*0.00*
Temperature (Temp)	*1*	*10960.2556*	*3*	*379.4805*	*28.88*	*0.01*
Block (B)	3	710.5806	0	0.0000	--	--
Sel × Temp	2	776.1551	6	303.4140	2.56	0.16
Sel × B	6	438.1601	0	0.0000	--	--
Sel × B	3	379.4805	0	0.0000	--	--
Sel × Temp × B	6	303.4140	0	0.0000	--	--

5.3.5. Temperature entrainment may induce stock dependent after-effects on FRP

While analysing features of the activity/rest rhythm under entrainment, one result that piqued my curiosity was the absolute scale on which FRP varied post entrainment to different thermoperiods (Figure 5.4c, bottom; Table 5.6), as compared with the FRP values post entrainment to LD cycles under different temperatures (Figure 5.8; Table 5.6). While period values ranged between 23.1-h (*early)* to 23.5-h (*late)* stocks and 23.3-h in the *early* stocks to 23.5-h in the *late* stocks post entrainment to TC 06:18 and TC 18:06 (Table 5.6), respectively, overall period values were much lower, post entrainment to TC 12:12 (Table 5.6). The period values ranged from 22.8-h in the *early* stocks to 23.2-h in the *late* stocks (see Figure 5.4c, bottom; Table 5.6). Moreover, the absence of statistically significant difference in FRP between *early* and *late* stocks post entrainment to TC 06:18 and 18:06, and the difference under TC 12:12 implies stock specific responses of FRP to cycling temperatures (Table 5.6).

I, then, examined the FRP of these stocks under DD at 19, 25 and 28 °C post entrainment to LD 12:12 at these respective temperatures. I found that there was a statistically significant main effect

of selection such that the *late* stocks had significantly longer FRP than the *early* stocks ($F_{2,6}$ = 189.70, $p < 0.05$; Figure 5.8; Tables 5.6 and 5.26). Also, there was a significant main effect of temperature such that FRP lengthened with increase in temperature ($F_{2,6}$ = 50.00, $p < 0.05$; Figure 5.8; Tables 5.6 and 5.26). Such overcompensation of FRP to changing temperatures in insects is an already established phenomenon (see Saunders, 2002). However, there was no statistically significant selection × temperature-regime interaction ($F_{2,6}$ = 1.10, $p > 0.05$; Figure 5.8; Table 5.26). These results indicate that temperature entrainment protocols may contribute to after-effects, despite the network being temperature compensated. This adds an additional dimension to the mechanisms of entrainment to temperature cues.

Table 5.26: ANOVA table summarizing the effects of selection regime, temperature regime and their interaction on FRP post entrainment to LD 12:12 under different constant ambient temperatures. Italicised effects are significant.

Summary of all effects	***df* Effect**	**MS Effect**	***df* Error**	**MS Error**	***F***	***p***
Selection (Sel)	*2*	*1.9860*	*6*	*0.0105*	*189.75*	*0.00*
Temperature (Temp)	*2*	*1.6722*	*6*	*0.0334*	*50.03*	*0.00*
Block (B)	3	0.0303	0	0.0000	--	--
Sel × Temp	4	0.0308	12	0.0277	1.11	0.40
Sel × B	6	0.0105	0	0.0000	--	--
Sel × B	6	0.0334	0	0.0000	--	--
Sel × Temp × B	12	0.0277	0	0.0000	--	--

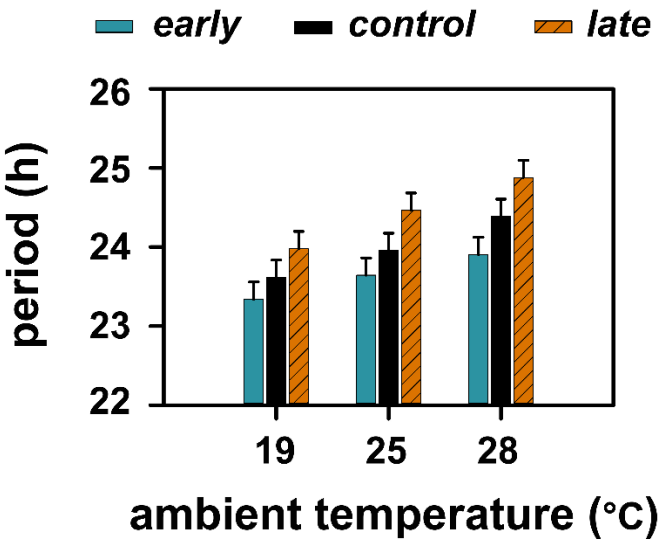

Figure 5.8: Free-running period of *early*, *control* and *late* stocks post entrainment to LD 12:12 at 19, 25 and 28 °C. All error bars are 95% CI following a Tukey's HSD test at $\alpha = 0.05$. Therefore, means with non-overlapping error bars are significantly different from each other.

5.4. Discussion

In this study, I was interested in examining features of entrained activity/rest behaviour of *early* and *late* stocks under a variety of temperature cues to (i) test responsiveness of the circadian clocks regulating activity/rest rhythms of these stocks to temperature cues, (ii) understand the mechanisms of entrainment that can account for such entrained behaviours, and (iii) as a consequence, understand the similarities, if any, in the organisational principles of the circuit regulating emergence rhythms and activity/rest rhythms.

In the case of our *early* and *late* flies, since all stocks re-synchronised quicker to 6-h phase-advances (Figures 5.2 and 5.3) compared to delays, I infer that the temperature pulse PRC of our stocks must have overall larger advance zones than delay zones. Further, my results demonstrated that *late* stocks re-synchronised significantly faster to 6-h phase-delay than *early* and *control* stocks (Figures 5.2 and 5.3), thereby implying that the *late* stocks have larger delay zone than the

other stocks. This would suggest the co-evolution of high amplitude temperature pulse PRCs of the circadian clock governing activity/rest rhythms in the *late* stocks in response to selection for evening adult emergence. High amplitude PRCs also imply increased phase variation (Pittendrigh and Daan, 1976a), higher amplitude and power of rhythm (Brown et al., 2008; Nikhil, Vaze et al., 2016; Vitaterna et al., 2006) and increased accuracy of entrainment (Beersma et al., 1999).

In relation to the aforementioned predictions, I obtained curious results when I analysed phases of entrainment in our stocks under TC cycles with three different durations of thermophase. I found that while there was no among-stock difference in phases of entrainment under short thermoperiod (Figure 5.4c, top-left), the *late* stocks showed significantly delayed phase compared to the *early* stocks under both, TC 12:12 and TC 18:06 (Figure 5.4c, top-middle and right). In both these cases, because the *early* and *late* stocks did not individually differ from the *control* stocks, it is not possible to comment upon the individual stock's contribution to phase lability under different temperature regimes. However, it is possible to still conclude that the small among-stock differences in lability, which may be present although not statistically detectable, could be due to among-stock differences in the PRCs.

Phase-difference among the stocks, however, can be explained using the non-parametric model of entrainment (Daan and Aschoff, 2001; Pittendrigh and Daan, 1976a). The model posits that the difference between FRP and the period of the external environment is adjusted, during entrainment, via phase-shifts due to the time-cue. This response is characterised using a PRC (discussed above; see also Chapter 1). Therefore, individuals with longer FRP are expected to show delayed phase under entrainment and vice versa, and this has found ample experimental evidence (Daan and Aschoff, 2001; Pittendrigh and Daan, 1976a; Rémi et al., 2010; Roenneberg, Dragovic et al., 2005; Sharma et al., 1998; Srivastava et al., 2019; Wright et al., 2005). This,

however, is thought to occur under the assumption that the PRC is a fixed entity in all these individuals. Therefore, if individuals have divergent PRCs they will not necessarily show such a relationship between FRP and entrained phase. I found that phases under entrainment to TC 06:18 were not different among stocks, and neither were the FRP of these stocks under constant conditions post entrainment to TC 06:18 (Figure 5.4c). In case of entrainment to TC 12:12, phases of the *late* stocks were delayed and their FRP was also longer under constant darkness post entrainment (Figure 5.4c). These two results are in agreement with the general rule outlined above. However, the absence of such a relationship between FRP and entrained phase under TC 18:06 reveal that although entrainment is in agreement with the non-parametric model, there is compelling support in favour of the co-evolution of divergent temperature pulse PRCs in our stocks.

To further garner support for divergent PRCs in our *early* and *late* stocks, I examined other features of entrainment to TC cycles. I found evidence for increased amplitude expansion, higher power of periodogram and higher accuracy in the *late* stocks, all of which are indicative of high amplitude PRCs. It is also interesting to note, at this point, that all the phase variations in the *late* stocks under different TC cycles is driven by the change in the evening bout of activity (see Figure 5.4b). This can be clearly seen when I examined phases of morning and evening peaks of activity under all three TC cycles (Figure 5.9; Tables 5.27, 5.28 and 5.29). I found that the phase of morning peak of activity was similar across all stocks under TC 06:18, and identical in all stocks under TC 12:12 and 18:06 (Figure 5.9, top). We could not perform statistical analyses to compare the phase of morning peak of activity across stocks owing to the lack of variance in all stocks in all regimes, except the *late* stocks under TC 06:18. Analysis of the phase of evening activity peak revealed results similar to those reported in Figure 5.4b; the *late* stocks were significantly delayed under

TC 12:12 and TC 18:06 compared to the *early* stocks (Figure 5.9, bottom). Importantly, analyses of the phase of evening peak of activity revealed that while the phase of *early* and *control* stocks do not differ from each other, the *late* stocks are phase delayed significantly from both, *early* and *control* stocks. This implies that plasticity in waveform in response to temperature regimes is predominantly brought about by the response of *late* stocks, consistent with the idea of high amplitude temperature PRCs in these populations. Differential response of the evening activity in response to temperature cues in our populations is further suggestive of possible temperature effects on period of the molecular clockwork regulating only evening activity. While an interesting possibility, this must await further experimentation.

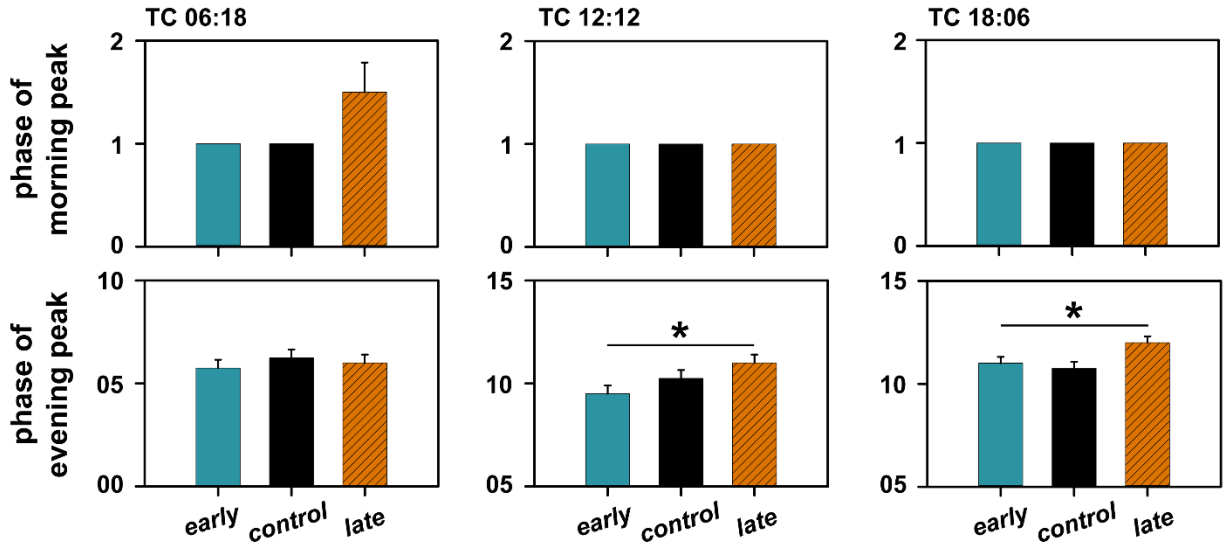

Figure 5.9: Phases of morning (top) and evening (bottom) peaks of activity (in units of ZT) of *early*, *control* and *late* under three different thermoperiods. Error bar in the top panel is SEM. All error bars in the bottom panel are 95% CI from a Tukey's HSD test at $\alpha = 0.05$. Therefore, means with non-overlapping error bars are statistically significantly different from each other. Additionally, asterisks are drawn to indicate means that are significantly different.

Table 5.27: ANOVA table summarizing the effects of selection regime on phase of evening peak of activity under entrainment to TC 06:18. Italicised effects are significant.

Summary of all effects	*df* Effect	MS Effect	*df* Error	MS Error	*F*	*p*
Selection (Sel)	2	0.2500	6	0.1389	1.80	0.24
Block (B)	3	0.2222	0	0.0000	--	--
Sel × B	6	0.1389	0	0.0000	--	--

Table 5.28: ANOVA table summarizing the effects of selection regime on phase of evening peak of activity under entrainment to TC 12:12. Italicised effects are significant.

Summary of all effects	*df* Effect	MS Effect	*df* Error	MS Error	*F*	*p*
Selection (Sel)	*2*	*2.2500*	*6*	*0.1389*	*16.20*	*0.00*
Block (B)	3	0.3056	0	0.0000	--	--
Sel × B	6	0.1389	0	0.0000	--	--

Table 5.29: ANOVA table summarizing the effects of selection regime on phase of evening peak of activity under entrainment to TC 18:06. Italicised effects are significant.

Summary of all effects	*df* Effect	MS Effect	*df* Error	MS Error	*F*	*p*
Selection (Sel)	*2*	*1.7500*	*6*	*0.0833*	*21.00*	*0.00*
Block (B)	3	0.0833	0	0.0000	--	--
Sel × B	6	0.0833	0	0.0000	--	--

My results, so far, are indicative of stronger temperature responsiveness of the activity/rest rhythms of *late* chronotypes compared to the *early* chronotypes, and this is predominantly due to the behaviour of the evening bout of activity; similar enhanced response of evening activity bout to temperature has been reported previously as well (Hall, 2003). In an earlier study, we have shown that temperature responsiveness of the eclosion rhythm of our *late* chronotypes is enhanced relative to the *early* chronotypes (Abhilash et al., 2019; see also Chapter 3). This enhanced

temperature sensitivity for the eclosion rhythm, we discuss, is perhaps due to the temperature sensitive oscillator (PG clock) regulating the eclosion rhythm. However, the evening bout of activity is known to be regulated by different cells (*E*-cells or evening oscillators) in the adult brain, i.e., the LNds (Lateral Dorsal Neurons) and DN1s (Dorsal neurons), and the DN1s are also known to be temperature sensitive (Gentile et al., 2013; Murad et al., 2007; Stoleru et al., 2004, 2007; Yadlapalli et al., 2018; Zhang et al., 2010). Therefore, my results indicate that while enhanced temperature responsiveness of both eclosion and activity/rest rhythms evolve in the *late* chronotypes, they perhaps do so, using distinct physiological mechanisms. To recapitulate previous discussions on circadian organization (see Chapter 1), the eclosion rhythm is thought to be driven by a hierarchically arranged set of two oscillators – one light sensitive master clock that drives a temperature sensitive slave oscillator (Oda and Friesen, 2011; Pittendrigh, 1974). The activity/rest rhythm on the other hand is described to be governed by a mutually coupled oscillator system, in which, historically, neither component is described to be sensitive to temperature (Helfrich-Förster, 2009; Pittendrigh and Daan, 1976b). Interestingly, the evolution of enhanced temperature sensitive components of the circadian clock network in the *late* stocks for both these rhythms is suggestive of remarkable conservation in organisation principles regulating the two rhythms with respect to the hierarchical system of organisation. Further, my results imply (i) a previously unrecognised role of the hierarchical model of organisation in regulating activity/rest rhythms, and (ii) potential overlap between temperature sensitive oscillators and the evening oscillators.

Plasticity of FRP under different temperature regimes pose an extremely interesting conundrum. In this regard, two key results are important to note; (i) FRP post entrainment to different TC cycles are shorter by > 1-h relative to the FRP post entrainment to LD cycles under different constant

temperatures (Figures 5.4c, bottom and 5.8; Table 5.6), and (ii) FRP post entrainment to short and long thermoperiod behaved similarly but differently from FRP post entrainment to TC 12:12 (Figure 5.4c, bottom; Table 5.6). Temperature compensation of the FRP is a crucial pre-requisite for calling an oscillatory physiological process a circadian clock (Dunlap et al., 2004; Moore-Ede et al., 1982; Saunders, 2002). Such compensatory mechanisms imply that in order for entrainment to occur in response to temperature time-cues, only phase-shifts must occur (as predicted by the non-parametric model) and not period changes (as predicted by the parametric model, which posits that the zeitgeber's effect is integrated over the cycle to constantly modulate the angular velocity of the clock, and therefore allow entrainment). However, I find that despite this being the case FRP post entrainment to different thermoperiods varied (Figure 5.4c, bottom). While the period value averaged over all stocks post entrainment to TC 12:12 was ~22.98-h, FRP post entrainment to TC 06:18 and TC 18:06 lengthened and was ~23.32-h and ~23.43-h, respectively (Table 5.6). If these responses were due to compensatory mechanisms, one would expect opposite effects on FRP post entrainment to short and long thermoperiods. Therefore, I think that these reflect some form of after-effects due to entrainment to TC cycles. Additional support for this also comes from the result that FRP values shortened greatly after being under the influence of different TC cycles relative to values after being under the influence of LD cycles and different constant ambient temperatures. Importantly, I find that *late* stocks show significantly longer FRP post entrainment to TC 12:12, while there is no among-stock difference under the two other thermoperiods (Figure 5.4c, bottom; Table 5.6). This suggests, although weakly, that the FRP of *late* stocks are less likely to change in response to temperature cycles relative to *early* stocks. While there have been many reports of after-effects of light regime on FRP (Dunlap et al., 2004), there are very few on after-effects of temperature cycles (Balzer and Hardeland, 1988). Results reported here, to the best of

my knowledge, provides first hints of temperature after-effects on FRP in *Drosophila* activity/rest rhythms, implying that temperature may also contribute to entrainment via parametric means, warranting further, more detailed documentation of effects of temperature cycles on FRP.

In conclusion, I find enhanced temperature sensitivity of the activity/rest rhythm in *late* chronotypes. Interestingly, altered rhythm phase under different temperature regimes of the *late* stocks is driven by changes in the evening bout of activity. Further, analyses of properties of entrainment and FRP implied that results can be explained under the assumption of the evolution of divergent temperature pulse PRCs, a matter worthy of further study.

Chapter 6. Mechanisms of photic entrainment of activity/rest rhythms in populations of *Drosophila* selected for divergent timing of eclosion

Parts of this chapter are accepted for publication in the following research article:

Abhilash L and Sharma VK (2020) Mechanisms of photic entrainment of activity/rest rhythms in populations of Drosophila selected for divergent timing of eclosion. Chronobiology International 37(4): 469–484.

6.1. Introduction

Stable daily timing of behaviour (ψ_{ENT}) of circadian rhythms, relative to environmental time-cues (zeitgebers) is brought about as a consequence of entrainment (Roenneberg et al., 2003). It is believed that the ψ_{ENT} is adaptive in that it facilitates optimal timing of physiological, behavioural and metabolic events so as to enhance fitness (as has been discussed several times before in this thesis; Vaze and Sharma, 2013). Thus, studies of entrainment mechanisms are central towards understanding the functional significance of circadian clocks, as has been discussed multiple times previously in my thesis.

Several generalist models of entrainment have been proposed in the past (Aschoff, 1960; Pittendrigh and Daan, 1976a; Roenneberg, Hut, et al., 2010; Swade, 1969). The earliest and most successful of them, the non-parametric (also called the discrete or phasic) model proposed that entrainment occurs via discrete phase-shifts elicited by the zeitgeber (Pittendrigh and Daan, 1976a). This model stemmed from the early discovery of phase response curves (PRC) in a variety of organisms including *Gonyaulax* (Hastings and Sweeney, 1958), *Drosophila* (Pittendrigh and Bruce, 1959), rodents (reviewed in Daan, 2000) and flying squirrels (DeCoursey, 1960b) which showed that phase-shifts elicited by the zeitgeber is a function of time of the day such that phase-delays are observed during early night and phase-advances during late night. The second, a parametric (also known as continuous or tonic) model proposed that entrainment occurs via net change in the angular velocity of phase progression of the circadian clock, and consequently the clock period (τ; Aschoff, 1960; Swade, 1969), such that zeitgebers decrease and increase angular velocity during early night and late night, respectively (Daan and Pittendrigh, 1976). This model gained anecdotal evidence from the observation that light had direct effect on τ such that with increasing light intensities, the τ of diurnal animals decreased and that of nocturnal animals

increased (Aschoff, 1960). A third and more recent model of entrainment made use of a Circadian Integrated Response Characteristic (CIRC) according to which entrainment is achieved by time-of-day dependent compression and expansion of the "internal cycle length" such that the internal cycle expands in response to zeitgebers during early night and compresses itself during late night (Roenneberg, Hut et al., 2010). Although this model is an elegant combination of phasic and tonic effects of the zeitgeber and provides a quantitative approach to estimate the tonic effects of any zeitgeber on the clock, what properties of the circadian clock contribute to such compression and expansion of the internal cycle length is unclear.

Based on theoretical considerations stemming from the non-parametric model, Pittendrigh and Daan (1976) proposed that under entrainment, clocks with shorter τ phase-lead those with longer τ for a given T (period of the zeitgeber). This prediction gained validation in case of white-footed mice (Pittendrigh and Daan, 1976a), *Drosophila* (Hamblen-Coyle et al., 1992; Srivastava et al., 2019), *Neurospora* (Roenneberg, Dragovic et al., 2005) and humans (Duffy and Czeisler, 2002; Wright et al., 2005). Additionally, several earlier experiments on chaffinches (Aschoff and Wever, 1966) and lizards (see Pittendrigh and Daan, 1976) also seemed to conform to this prediction wherein it was observed that for a given T, ψ_{ENT} of a rhythm leads less or lags more relative to the zeitgeber if $\tau > T$. The apparent ubiquity and acceptance of the τ and ψ_{ENT} relationship seems to suggest that the association between them is a functional and an ecologically relevant one.

In order to understand the functional relevance of ψ_{ENT} and the evolutionary correlates between them and other circadian clock properties, earlier work from our laboratory has raised fruit fly *Drosophila melanogaster* populations by imposing laboratory selection on morning and evening timing of eclosion (Kumar et al., 2007), henceforth referred to as *early* and *late* stocks/chronotypes, respectively. These populations (currently ~320 generations of selection, ~18

years) exhibit clear divergence in the ψ_{ENT} and τ of their eclosion rhythms such that *early* populations have advanced ψ_{ENT} and shorter τ relative to *late* populations (Kumar et al., 2007), as predicted by the non-parametric model of entrainment (see also Chapter 2). However, subsequently we showed that *early* and *late* chronotypes require longer duration of light to entrain their eclosion rhythms in the evening and morning, respectively (Vaze, Nikhil et al., 2012). This suggested the action of longer durations of light in aiding entrainment as opposed to phasic effects proposed by the non-parametric model. Intriguingly, even though the τ of activity/rest rhythm also evolved in the same direction (τ_{early} = 23.36-h; $\tau_{control}$ = 23.69-h; τ_{late} = 24.28-h) as that of the eclosion rhythm (Nikhil, Abhilash et al., 2016), the two stocks do not differ in the mean ψ_{ENT} of their activity/rest rhythm under LD 12:12 (12 hours of light and dark each, as under maintenance conditions; Nikhil, Abhilash et al., 2016). Although, this result is in contrast with the prediction from theories of entrainment, such a lack of difference in ψ_{ENT} of the activity/rest rhythm between the *early* and *late* stocks could be mediated via either divergent PRCs or divergent circadian photosensitivities (as measured using Dose Response Curves; DRC). Nikhil, Vaze et al. (2016) showed that there is no significant difference in either the photic-PRC or DRC between the *early* and *late* stocks, thereby suggesting that the non-parametric model is insufficient to explain the lack of divergent ψ_{ENT} between the two. Additionally, the authors also showed that the *late* stocks have a wider range of entrainment relative to the *early* stocks and suggested that this may be mediated by the larger area under the PRCs in case of the *late* stocks (tonic/parametric effect of light). It was also observed that the *late* stocks had larger amplitude expansion under entrainment to LD 12:12 (Nikhil, Vaze et al., 2016), suggesting that differential amplitude responses (characterised by an amplitude response curve or ARC) could contribute to entrainment in these stocks. This possibility stems from some previous studies on *Kalanchoe* flowers (Johnsson et al., 1973) and

Drosophila eclosion rhythms (Winfree, 1973) that have shown that amplitude of circadian rhythms also change in response to light pulses depending on the time-of-day when the light pulse is administered, and have been discussed as possible contributors to entrainment of circadian rhythms, such that there happens to be an amplitude expansion during early night and compression during late night (Johnsson et al., 1973).

The suggestion that, for the adult locomotor activity rhythm in the *early* and *late* stocks, (i) the non-parametric model is insufficient to explain several features of entrainment, (ii) that tonic/parametric effects of light may contribute to entrainment, (iii) that amplitude responses may facilitate entrainment, and (iv) the fact that mechanisms of photic entrainment of the emergence rhythms in these stocks have been fairly well studied (Kumar et al., 2007; Vaze, Nikhil et al., 2012), motivated this study, wherein I examine mechanisms of photic entrainment of the activity/rest rhythm in these stocks. Further, long-term monitoring of activity/rest rhythms in *Drosophila* populations is practically feasible thereby making this a good system to study and calculate the several parameters utilised here to understand photic entrainment. I systematically test the predictions from the theory of entrainment using activity/rest rhythms of *early* and *late* eclosion chronotypes. Additionally, I attempt to understand the entrainment of this rhythm in these populations using the CIRC, assess the role of transient amplitude responses to light at different phases of the circadian cycle and the contribution of duration DRCs to phase-shifts that may facilitate entrainment in these populations.

6.2. Materials and Methods

6.2.1. Activity/rest assay

To quantitatively examine predictions from the non-parametric model, I used activity/rest rhythms of *early* and *late* stocks, as read-outs of the underlying circadian clocks of the two respective chronotypes. For all activity/rest rhythm experiments, I used at least thirty-two 3- to 5-day old male flies from each replicate of the *early*, *control* and *late* stocks. Firstly, I recorded their activity/rest behaviour during and post exposure to a single white light pulse of the same intensity (~70-lux) and duration (5-min) that was used to construct the photic PRC (Nikhil, Vaze et al., 2016). Whether flies entrained to this regime or not was determined by (i) the period values estimated using the χ^2 periodogram implemented in ClockLab (Actimetrics, IL, USA; period must be exactly 24-h if entrained), and (ii) phase-control estimated by subjectively assessing individual actograms on first day in DD post subjecting flies to a single pulse. Additionally, I also recorded activity/rest behaviour of flies from these populations under different intensities (LD 12:12 with ~1-lux and ~70-lux during the photophase) and photoperiods (LD 06:18 and LD 18:06 with ~70-lux during the photophase) as these are the two factors that would determine strength of the zeitgeber *vis-à-vis* intensity and duration. These activity/rest data sets were collected by me; preliminary results of some of these runs are published elsewhere (Nikhil, Abhilash et al., 2016). Activity/rest behaviour was recorded using *Drosophila* Activity Monitors (Trikinetics, Waltham, MA, USA) under the aforementioned conditions at ~25 °C and ~70% RH prior to assaying their behaviour under DD. Data from 5-7 cycles under entrainment were used to estimate the phase of centre of mass (CoM) of the rhythm (Zar, 1999). I use CoM as the phase marker as it incorporates differences in the overall shape of the waveform, and therefore can also be used as a consistent marker across different zeitgeber conditions. Because the activity/rest rhythm in *Drosophila* is

typically bimodal, an angle-doubling transformation was performed for the analyses (Zar, 1999; Figure 6.1), and was back-transformed and rescaled for plotting (as in Nikhil, Abhilash et al., 2016). On the 8th day of recording, flies were transferred into locomotor activity tubes with fresh food and were recorded under DD. The flies were kept in this condition for at least 7 days, and data collected thereon was used for estimating the post entrainment τ (or τ_E; see 'predicting the CIRC' section; Roenneberg et al., 2010). We used the χ^2 periodogram implemented in ClockLab (Actimetrics, IL, USA) for estimating τ_E. For other actogram based analyses, I used either ActogramJ (Schmid et al., 2011) or RhythmicAlly (Abhilash and Sheeba, 2019).

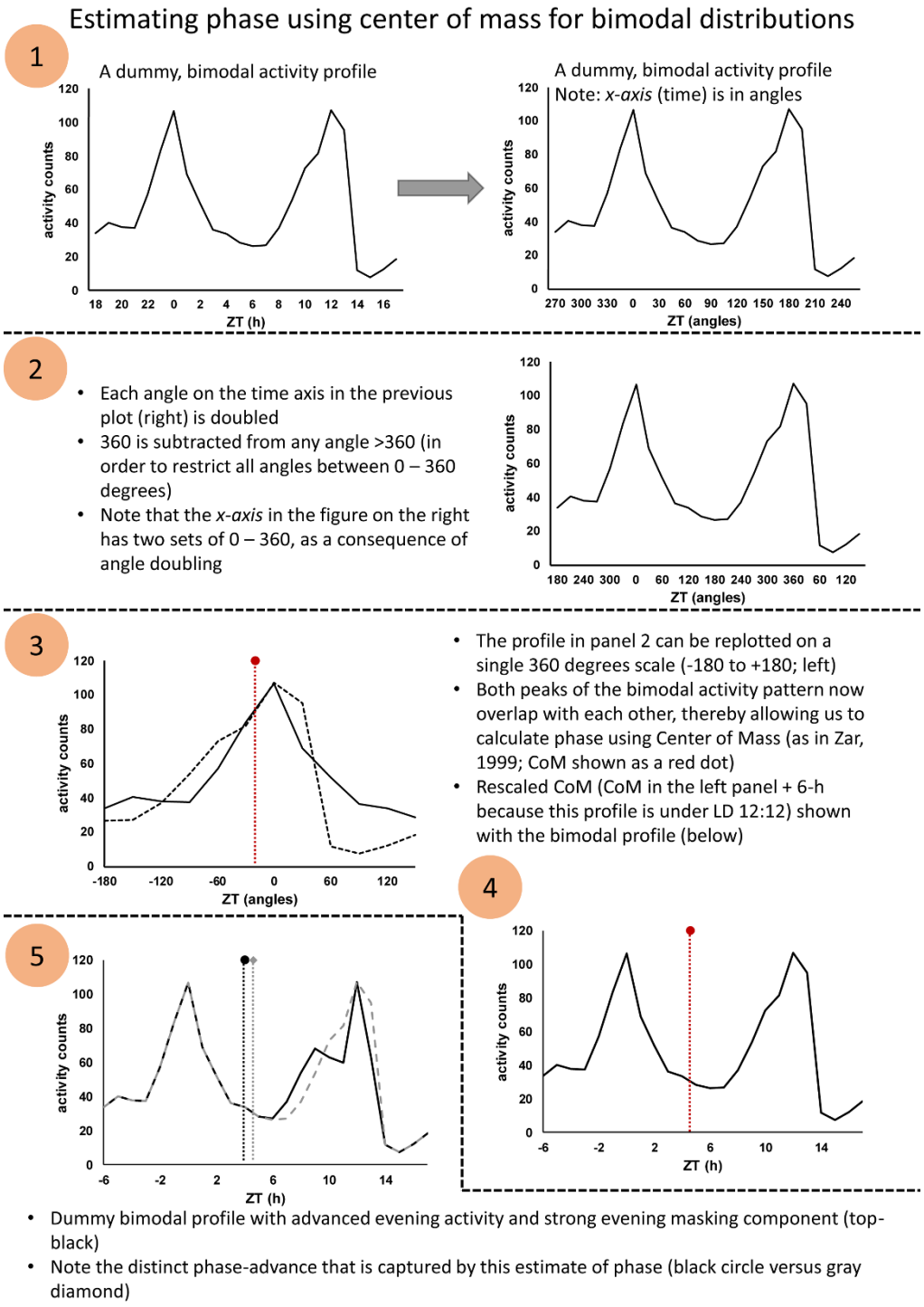

Figure 6.1: A schematic to describe the estimation of CoM when the distribution of activity is bimodal. Also, shown is a representation of how such an estimate is useful when there are subtle differences in the phase of activity and strong masking components.

In the experiments wherein flies were exposed to different photoperiods, freshly eclosed male flies of age ~3-5 days were recorded for ~10 days under DD to estimate the mean population τ (or τ_{DD}; see 'predicting the CIRC' section) at ~25 °C and ~70% RH before they were transferred to the respective photoperiods. In this case, I used the more statistically powerful Lomb-Scargle periodogram implemented in ClockLab (Actimetrics, IL, USA), because I had a longer stretch of continuous data.

To study the degree of association between τ_{DD} and ψ_{ENT}, circular-linear correlation analyses were performed (Mardia, 1976). A circular-linear correlation was performed in this case because one variable in our study is a linear random variable (τ_{DD}) and the other variable is a circular random variable (ψ_{ENT}). These correlation analyses were carried out using the CircStats toolbox written for MATLAB (Berens, 2009). Further, to analyse the effect of stock on proportion of individuals that entrain to cyclic brief light pulses, a mixed model two-factor analysis of variance (ANOVA) was carried out (using STATISTICA v7.0) using population as a fixed factor and blocks as a random factor. Tukey's HSD was used for post-hoc comparisons, and all results were considered statistically significant at $\alpha = 0.05$.

6.2.2. Predicting the CIRC for *early*, *control* and *late* populations

The CIRC model of entrainment suggests that daily correction for differences in τ is modelled by $\tau_E - T = \int C \times I \times c_{ZG}$ (Roenneberg, Hut et al., 2010), where τ_E is the τ under entrainment which is generally reflected as after-effects (the period of the individual in the first few days on transfer to DD), T is the zeitgeber period, C is the CIRC response i.e., time-of-day compression or expansion of the internal cycle length, I is the zeitgeber intensity, and c_{ZG} is the calibration factor that is a measure of the impact of the zeitgeber on the clock or in other words, the clock's sensitivity to the

zeitgeber. The basic CIRC is modelled using a sine curve and its first harmonic with certain conditions as specified below (from Roenneberg, Rémi et al., 2010).

$C_{0\text{-}2\pi} = \sin\varphi + s\,(\sin 2\varphi)$,

where φ is time of the day in radians and s is the shape factor.

Condition 1a: *For* $C_{0\text{-}\pi}$, *if* $C < 0$, *then* $C = 0$

Condition 1b: *For* $C_{0\text{-}\pi}$, *if* $a < 1$, *then* $C = C \times a$

Condition 2a: *For* $C_{\pi\text{-}2\pi}$, *if* $C > 0$, *then* $C = 0$

Condition 2b: *For* $C_{\pi\text{-}2\pi}$, *if* $a > 1$, *then* $C = C/a$

where a is the asymmetry factor (Roenneberg, Hut et al., 2010; Roenneberg, Rémi et al., 2010).

The shape factor is a measure of 'dead zone' of the CIRC (time of the day when the clock is insensitive to zeitgeber impulses) whereas the asymmetry factor is a measure of the relative differences between the compression and expansion zones of the CIRC. When $a = 1$, both, the compression and expansion zones are of the same magnitude; when $a > 1$, the compression is larger than the expansion zone and when $a < 1$, the expansion zone is larger than the compression zone. Using this equation and its ensuing conditions, I generated CIRC responses as a function of time of the day for all combinations of a and s and normalised it such that the maximum or minimum CIRC response is +1 or –1, respectively. I varied s from 0 to 1.5, and a from 0.3 to 2.5 in increments of 0.1. I then numerically simulated rectangular zeitgeber cycles of LD 12:12, LD 18:06 and of LD 06:18 with 1 depicting photophase and 0 the scotophase (as in Roenneberg, Rémi et al., 2010). These cycles were then shifted in phase by 6-min. This led to 240 scenarios of different phase-relationships with all the CIRCs for each photoperiod. We had experimental values of τ_E for all the three photoperiods for all four blocks, and in all cases T = 24-h. So, for different populations and photoperiods, I obtained different ($\tau_E - T$) values. I then computed the

area under the curve for each CIRC under each photoperiod for all the phases of entrainment. Given the number of combinations and loops it would have been tedious to integrate under the curve algorithmically. Thus, I computed the area under the curve as the sum of all the products of corresponding values of the zeitgeber and the CIRC responses (as in Roenneberg, Rémi et al., 2010). The area under the curve for each phase-relationship of the CIRCs with the zeitgeber was then subtracted from $\tau_E - T$. This difference was squared, and the minimum was then used to find the corresponding phase-relationship that yielded this minimum difference between $\int CIRC$ and $\tau_E - T$. I, therefore, obtain 3 modelled phase-relationships for each of the 12 populations, one for each photoperiod for each combination of *a* and *s*. I then subtracted these predicted phase-relationships for each photoperiod for all the combinations of *a* and *s* from the corresponding experimental phase-relationship (see Figure 6.2 for how phase-relationship was estimated from experimental data). I squared these differences and added them across all the three photoperiods. Thus, I get one Sum of Squared Difference (SSD) for each combination of *a* and *s*. The combination of *a* and *s* that yield the minimum SSD across the three photoperiods for each population is then thought to be the representative parameters of the CIRC for that population. I used custom written *R* scripts to perform this computation and the code was run separately for each population. Two separate two-way mixed model randomised block design ANOVAs were run to statistically compare between-stock difference in the asymmetry factor and shape factor, respectively. In both these cases, stock was treated as a fixed factor and block as a random factor. Post-hoc comparisons were performed using Tukey's HSD and differences were considered significant at $\alpha = 0.05$.

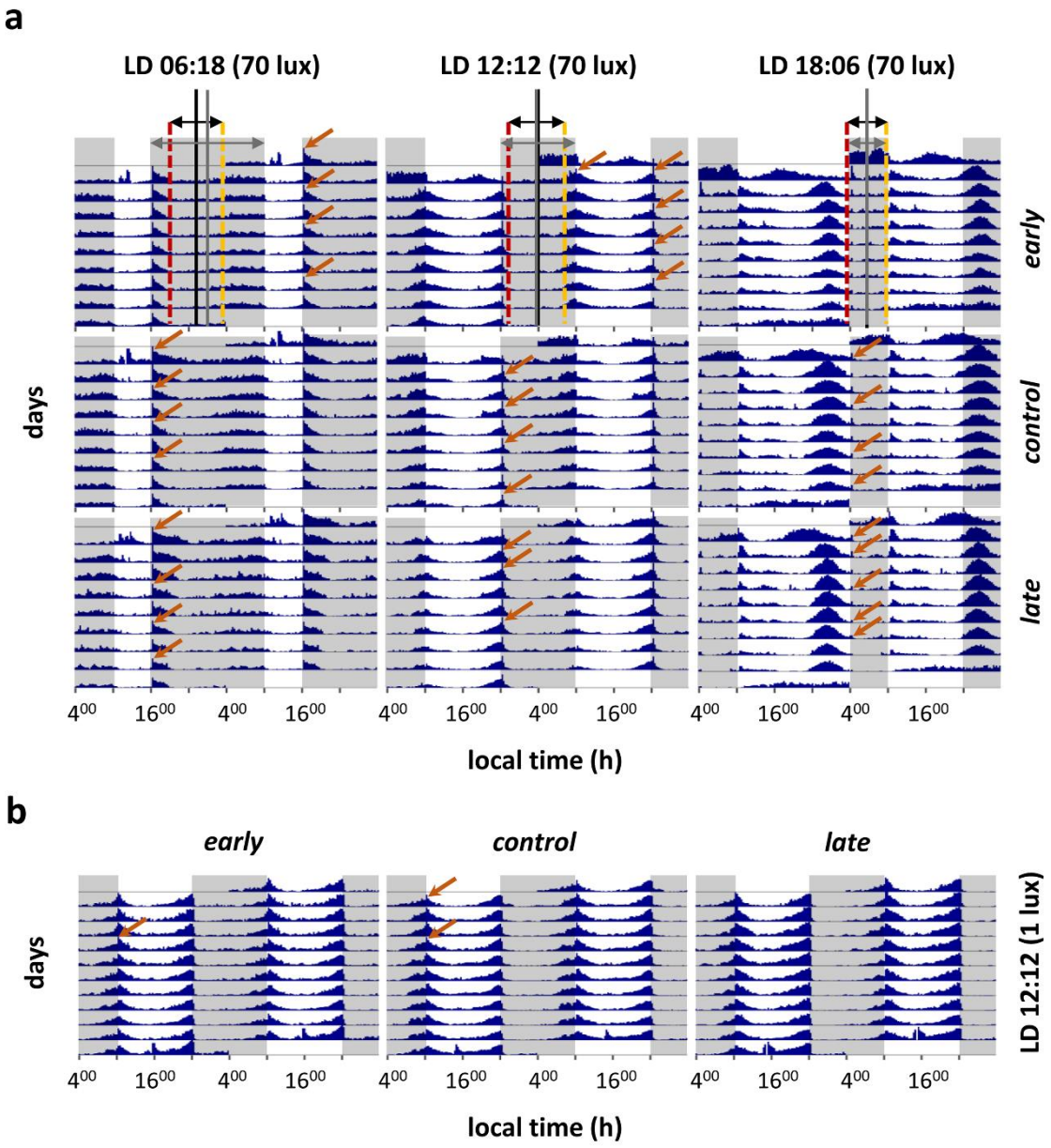

Figure 6.2: (a) Representative batch actograms of *early* (top), *control* (middle) and *late* (bottom) stocks under LD 06:18 (left), LD 12:12 (middle) and LD 18:06 (right) with 70-lux light intensity during the photophase. The gray shaded region indicates the dark phase of the LD cycle. Red dashed line indicates phases of activity offsets, the yellow dashed line indicates phases of activity onsets. The difference between the two (indicated by two-headed black arrow) is the rest phase, mid-point of which is considered as Internal Time (InT) 00 (black solid line). The two-headed gray arrow indicates the duration of dark phase of the respective LD cycles, mid-point of which is considered as External Time (ExT) 00 (gray solid line). The difference between ExT00 and InT00 is used as the experimental phase-relationship values against which all simulated phase-relationship values are compared. Please note that for LD 12:12 and LD 18:06, ExT00 and InT00 coincide to a large extent, thereby yielding phase-relationship values very close to 0. Also, marked are bouts of masking effects of light (orange arrows). (b) Representative batch actograms of *early*

(left), *control* (middle) and *late* (right) stocks under LD 12:12 (1-lux during the photophase). Orange arrows indicate masked components of activity, as before. Please note, the significantly lower bouts of masking components in the activity profiles under 1-lux light intensity.

6.2.3. Assessing amplitude response curves for *early*, *control* and *late* stocks

Data for the photic amplitude response curves (ARC) was extracted from the experiments from Nikhil, Vaze et al. (2016) which were done to estimate the photic PRCs for *early, control* and *late* stocks. It is thought that effects of light on amplitude of the clock may be transient and therefore, a phase only model may be a good approximation of the mechanism of entrainment (*Serge Daan, personal communication*). Hence, to address if transient amplitude responses may contribute to entrainment of *early* and *late* stocks, I estimated the amplitude of activity/rest rhythm in the cycle immediately following the brief light pulse of ~70-lux for 5-min administered at CT02, 06, 10, 14, 18 and 22 for all the three stocks. The amplitude response for each time-point was calculated by subtracting the amplitude of the pulsed population from the amplitude of the unpulsed disturbance control of the same population such that negative and positive values represent expansion and compression of the limit cycle, respectively (as is the case in CIRCs). A mixed model three-way ANOVA was carried out (using STATISTICA v7.0) to test the effect of selection, time-point and population × time-point interaction on amplitude responses. Selection and time-point were treated as fixed factors and blocks was treated as a random factor. Post-hoc analyses were carried out using Tukey's HSD, and all results were considered statistically significant at $\alpha = 0.05$.

6.2.4. Estimating net expansion and compression of photic amplitude response curves

Previous studies suggest that longer durations of light are important to entrain the emergence and activity/rest rhythms of *early* and *late* stocks (Nikhil, Vaze et al., 2016; Vaze, Nikhil et al., 2012). Therefore, I estimated area under the ARC of *early, control* and *late* stocks to serve as a proxy for

the effect of prolonged durations of light on the expansion and compression of limit cycles of circadian clocks in these populations. To do so, all the negative and positive values of the ARC were summed across time-points to represent the net expansion and net compression zones, respectively.

To test if net expansion and compression zones were different among populations, two respective mixed model two-way ANOVAs were carried out (using STATISTICA v7.0) with population as a fixed factor and blocks as a random factor. Post-hoc multiple comparisons were manually carried out using Tukey's HSD, and all results were considered statistically significant at $\alpha = 0.05$.

6.2.5. Duration dose response curves (duration DRC)

To understand if divergent parametric effects of light in our stocks could manifest via different degrees of phase-resetting in response to duration of light pulse, I assayed their duration DRC (as in Comas et al., 2006). Freshly eclosed male flies, aged 3-5 days were recorded under LD 12:12 at 25 °C for 7 days and then are transferred to DD on the 8th day. On the first day in DD, light pulse of two durations i.e., 25-min and 50-min, was given to all populations at CT14 and CT22 (CT00 is the onset of subjective day). Phase-shifts were calculated in the *early*, *control* and *late* stocks relative to their unpulsed, disturbance controls. Statistical comparisons for each time-point were done using a mixed model three-way randomised block design ANOVA wherein stock and duration were treated as fixed factors and block as a random factor. Post-hoc analyses were carried out using Tukey's HSD, and all results were considered significant at $\alpha = 0.05$.

6.3. Results

6.3.1. Testing predictions from the non-parametric model of entrainment

The first prediction from the non-parametric model is that, for a given zeitgeber, organisms/populations with longer τ will have delayed ψ_{ENT} (see introduction). Circular-linear correlation analyses revealed that τ and ψ_{ENT} of activity/rest rhythm was not significantly correlated when entrained to cyclic single brief light pulses of ~70-lux for 5-min (r = +0.65, p > 0.05; Figure 6.3) and to LD 12:12 (~70-lux; r = +0.06, p > 0.05; Figure 6.3). Additionally, to avoid effects of masking, when the experiment was done under LD 12:12 (~1-lux), τ and ψ_{ENT} were still not significantly correlated (r = +0.44, p > 0.05; Figures 6.2b and 6.3). However, τ and ψ_{ENT} of activity/rest rhythm were significantly positively correlated under LD 06:18 (~70-lux; r = +0.81, p < 0.05; Figure 6.3) such that *late* stocks had delayed ψ_{ENT}. Remarkably, the τ and ψ_{ENT} of activity/rest rhythm were significantly negatively correlated under LD 18:06 (~70-lux; r = –0 .85, p < 0.05; Figure 6.3) such that *late* stocks although have significantly longer period, had advanced ψ_{ENT} (also see Table 6.1 for compiled values to facilitate comparisons). Analysis of mean phase values using a randomised block design ANOVA revealed the same, and is published elsewhere (Nikhil, Abhilash et al., 2016). Thus, while I did not detect significant correlations under either standard 12:12 LD regimes or with single light pulses, both long and short photoperiods reveal significant, though opposite correlations between phase and period. These results imply that the non-parametric model alone is insufficient to explain this relationship between τ and ψ_{ENT}. To facilitate comparisons between calculated data and actual activity profiles, I have provided representative batch actograms of all stocks under these regimes (Figure 6.2).

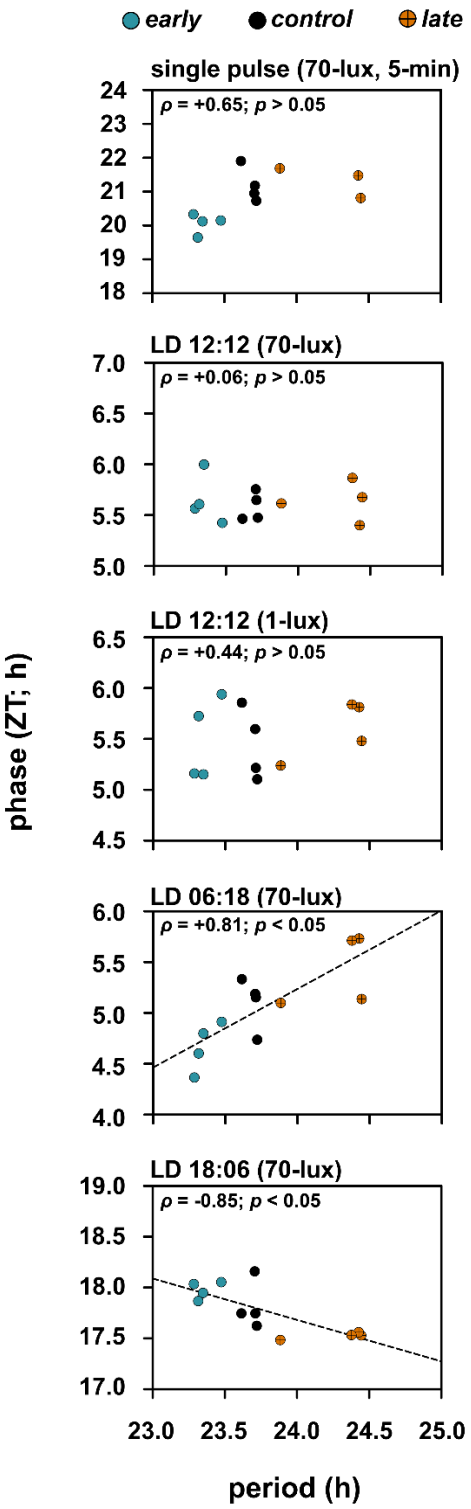

Figure 6.3: Correlations between circadian period and phase of entrainment under a wide variety of zeitgeber regimes. Under LD 06:18 there was a significant positive correlation between period and phase of entrainment and under LD 18:06 there was a significant negative correlation between the two. Dashed lines indicate regression lines that best fit the scatter. Each dot represents the mean period and phase of each replicate block. Period values from 18 – 29 flies were used to obtain block means, except in the case of two populations wherein 10 flies each were used, and phases under LD 12:12 (1-lux) from 31 – 63 flies. Mean phases for blocks under single light pulse experiment was highly variable, owing to differences in the proportion of flies that entrained. For phase estimation, number of flies per replicate block ranged from 21 – 31 in most cases, except two populations wherein 13 flies each were used to obtain block means under LD 06:18. Under LD 12:12 and LD 18:06, number of flies per replicate block in most cases ranged from 19 – 23 and 19 – 29, respectively. It is important to note here that in all cases, even where number of flies/block are relatively small, there is remarkable consistency between replicate blocks (as can be clearly seen in experimental phase-relationships in Figure 6.5a), which allows me to conclude that our estimates are not a consequence of biased sampling, but a true estimate of period and phase. This is true for all subsequent figures as well.

Table 6.1: Correlation coefficient values for all stocks under different zeitgeber regimes. Italicised entries are statistically significant.

Regime	**Correlation coefficient**	***p***
Single pulse (70-lux; 5-min)	+0.65	0.10
LD 12:12 (70-lux)	+0.06	0.98
LD 12:12 (1-lux)	+0.44	0.31
LD 06:18 (70-lux)	*+0.81*	*0.02*
LD 18:06 (70-lux)	*-0.85*	*0.01*

The second prediction from the non-parametric model of entrainment is that with known τ and PRC, one can quantitatively estimate the ψ_{ENT}. To test this prediction in the context of activity/rest rhythm of *early* and *late* stocks, I exposed flies from these populations to recurrent brief light pulses with the same intensity (~70-lux) and duration (5-min) every 24-h as that used to construct the photic PRC (Nikhil, Vaze et al., 2016). I found that while the light pulse fell at ~CT14.85-h in case of the *early* populations, it fell at CT13.38-h in case of the *late* populations (Figures 6.4a, top and 6.4b). A careful examination of the already published light pulse PRC of these stocks revealed that the average phase-shift obtained by the *early* and *late* stocks between CT10 and 14 would be ~2 – ~2.5-h for a light pulse with the same intensity and duration as that used to construct the PRC (Figure 6.4c). However, the *early* and *late* stocks need ~0.64 and ~0.28-h phase-delay and phase-advance, respectively to entrain to a 24-h zeitgeber. These results again suggest that the non-parametric model alone may be insufficient to quantitatively predict ψ_{ENT}.

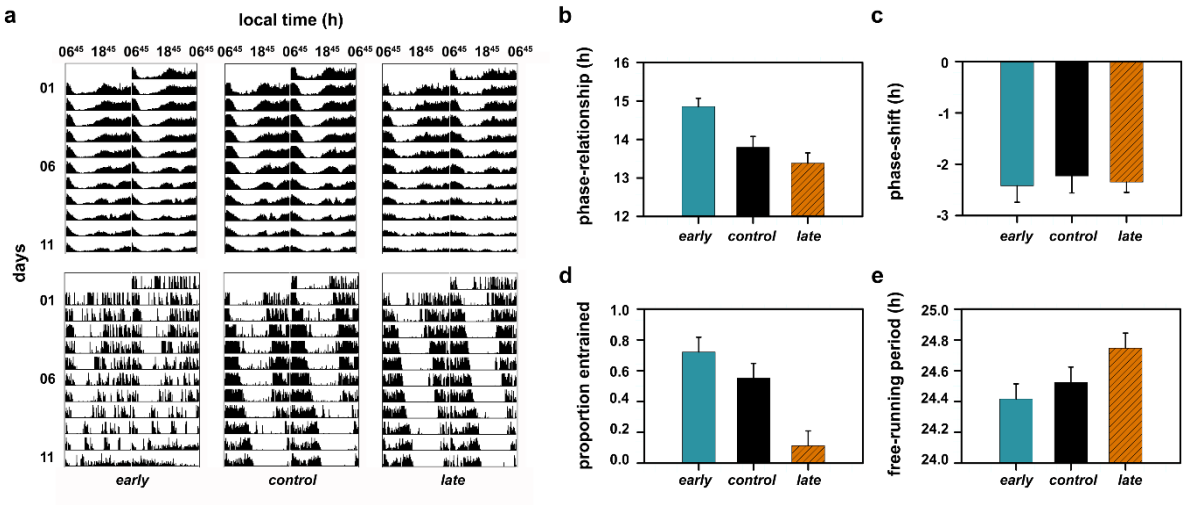

Figure 6.4: Entrainment to brief light pulses. (a, top) Average actograms of (left) *early*, (middle) *control* and (right) *late* stocks are depicted. The gray lines indicate the phase and duration of light pulse. These actograms are generated by averaging activity for only the flies that entrained to single light pulses (see materials and methods). (a-bottom) Representative actograms of flies that were free-running under recurrent light pulses for all three stocks. (b) The phase-relationships between onset of light pulse and onset of activity/rest rhythms of the three populations (also see Figure 6.2). (c) The phase-shift values averaged over CT10 and 14 elicited by the three stocks; data for this taken from Nikhil, Vaze et al. (2016). Panel (d) depicts proportion of individuals from each stock that entrain to the given regime. Whether they are entrained or not is judged by the phase of their activity on the first day in constant darkness (DD). Panel (e) depicts the circadian period of individuals that do not entrain to the given condition. Error bars in panels (b), (c) and (d) denote standard error of the mean. Error bars in panel (e) are 95% CI calculated using Tukey's HSD, hence, non-overlapping error bars indicate significantly different mean values. For each replicate block, 32 individuals were loaded into locomotor tubes and out of those, flies were either categorised as entrained or free-running. Proportion values of these were averaged over all 4 replicate blocks and that mean is represented here.

The non-parametric model also suggests that with the knowledge of τ and PRC, one can quantitatively predict entrainability of circadian clocks. The photic PRC of *early* and *late* stocks reveal that neither of them have statistically significant advance zones (Nikhil, Vaze et al., 2016). The mean τ_{early} and τ_{late} are ~23.35-h and ~24.28-h, respectively, and this implies that majority of flies from *early* stocks would have τ < 24-h and from *late* stocks would have τ > 24-h. This

suggests that most flies from *early* stocks need a phase-delay to entrain and a majority of flies from the *late* stocks need a phase-advance, thereby yielding the expectation that a greater proportion of *early* stocks can entrain to the brief light pulse than *late* stocks. Our results show that significantly higher percentage of *early* flies (~70%) entrain to cyclic brief light pulses than *late* flies (~10%; $F_{2,6} = 50.73$, $p < 0.05$; Figure 6.4d; Table 6.2). However, the percentage of entrained flies from *control* stocks was intermediate (~50%) and not different from that of *early* stocks (Figure 6.4d). Moreover, all the flies from all the stocks that do not entrain exhibited a free-running rhythm of τ > 24-h (Figure 6.4e). Representative actograms of free-running flies under the single light pulse regimes are shown in Figure 6.4a (bottom).

Table 6.2: ANOVA table summarizing the effects of selection regime on proportion of entrained flies. Italicised effects are significant.

Summary of all effects	**df Effect**	**MS Effect**	**df Error**	**MS Error**	**F**	**p**
Selection (Sel)	*2*	*0.3946*	*6*	*0.0078*	*50.73*	*0.00*
Block (B)	3	0.0168	0	0.0000	--	--
Sel × B	6	0.0078	0	0.0000	--	--

These results collectively show that two out of three predictions from the non-parametric model of entrainment do not hold, therefore suggesting that the non-parametric model alone is insufficient to explain photic entrainment of activity/rest rhythm in *early* and *late* chronotypes.

6.3.2. CIRCs of *early*, *control* and *late* stocks

Given that instantaneous effects of light on the circadian clocks of *early* and *late* stocks cannot explain entrainment fully, I tried to estimate if our populations had divergent CIRCs that could explain entrainment of activity/rest rhythm in these populations. I predicted ψ_{ENT} using a wide range of CIRCs and compared them with experimental ψ_{ENT} under three photoperiods i.e., LD 06:18, LD 12:12 and LD 18:06. CIRCs for each population was picked based on the parameters of CIRC which yielded the best fit between experimental and predicted ψ_{ENT} across all three photoperiods and these parameters were averaged over all four blocks to yield the stock specific CIRC (Figure 6.5a). I found that there was a significant main effect of selection on the asymmetry factor ($F_{2,6} = 6$, $p < 0.05$; Table 6.3) such that the *late* stocks had significantly larger compression zone than that of the *control* stocks (Figure 6.5b, left; Table 6.4). Further, I found that the shape factor was significantly higher in the *late* stocks than both *early* and *control* stocks ($F_{2,6} = 6$, $p < 0.05$; Figure 6.5b, right; Tables 6.4 and 6.5). Consequently, the *early* and *late* stocks showed distinct CIRCs wherein the *late* stocks had a larger 'dead' zone and higher maximum compression than the *early* and *control* stocks (Figure 6.5c).

The divergent CIRCs between *early* and *late* stocks, therefore, provide a basis to understand why differences in τ do not translate into differences in ψ_{ENT} under different LD regimes, thereby highlighting the importance of a holistic model in understanding entrained behaviour.

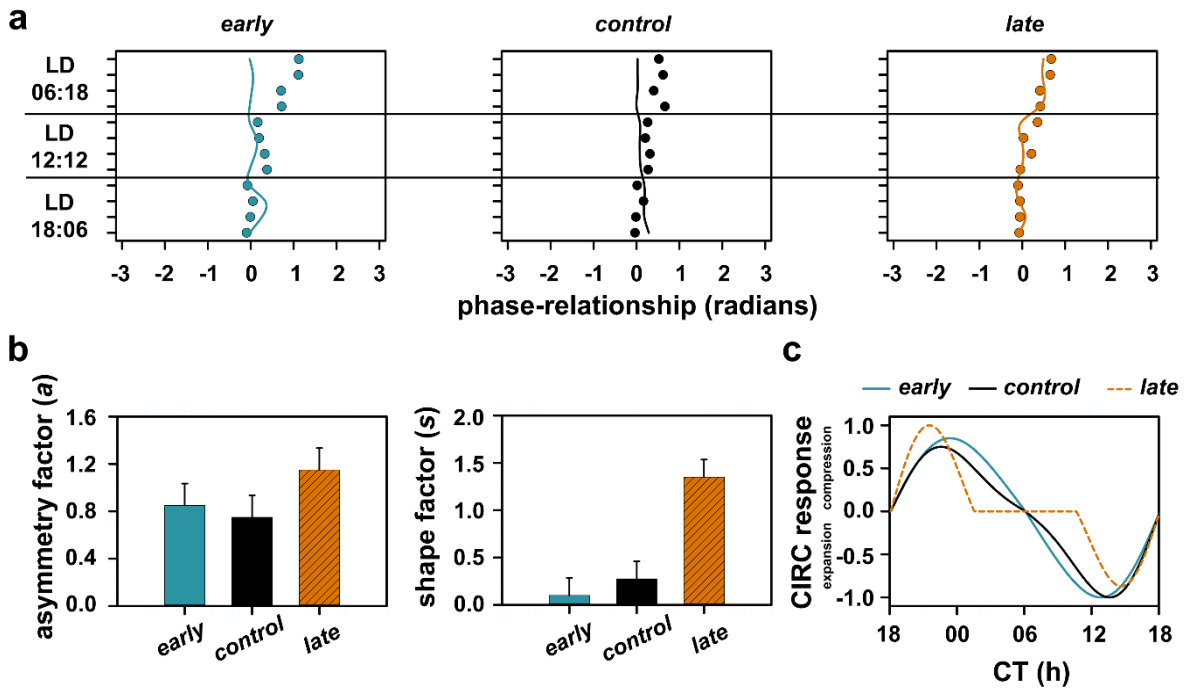

Figure 6.5: (a) Fits between experimental and predicted phases of entrainment from the best fitting CIRC for *early* (left), *control* (middle) and *late* (right) stocks. Each dot in the three panels represents the mean phase-relationship under entrainment for each replicate population under three different photoperiods. The line represents the predicted phase-relationships from the best-fitting CIRCs under all regimes. Each dot in panel (a) represents mean phase-relationship of each replicate block. See Figure 6.3 – legend for number of replicates within each block. Panels (b-left) and (b-right) depict the asymmetry factor (*a*) and shape factor (*s*) of the best fitting CIRCs of the *early*, *control* and *late* stocks, respectively. Panel (c) are the best fitting CIRCs for the three stocks. Error bars in panel (b) are 95% CI calculated using Tukey's HSD, hence, non-overlapping error bars indicate significantly different mean values.

Table 6.3: ANOVA table summarizing the effects of selection regime on asymmetry factor of the CIRC. Italicised effects are significant.

Summary of all effects	df Effect	MS Effect	df Error	MS Error	F	p
Selection (Sel)	*2*	*0.1733*	*6*	*0.0289*	*6.00*	*0.04*
Block (B)	3	0.0456	0	0.0000	--	--
Sel × B	6	0.0289	0	0.0000	--	--

Table 6.4: CIRC parameters and fit estimates for all populations. SSD represent values in square radians. It is clear that fits are much better for *control* and *late* stocks relative to *early* stocks.

		Block-1	Block-2	Block-3	Block-4
early	***a***	1.0	0.7	0.7	1.0
	s	0.0	0.1	0.3	0.0
	SSD	1.36	1.21	0.59	0.73
control	***a***	0.8	0.8	0.8	0.6
	s	0.2	0.2	0.2	0.5
	SSD	0.31	0.37	0.24	0.58
late	***a***	1.4	1.2	0.8	1.2
	s	1.5	1.4	1.3	1.2
	SSD	0.18	0.04	0.07	0.00

Table 6.5: ANOVA table summarizing the effects of selection regime on shape factor of the CIRC. Italicised effects are significant.

Summary of all effects	**df Effect**	**MS Effect**	**df Error**	**MS Error**	**F**	**p**
Selection (Sel)	*2*	*1.8325*	*6*	*0.0292*	*62.83*	*0.00*
Block (B)	3	0.0008	0	0.0000	--	--
Sel × B	6	0.0292	0	0.0000	--	--

6.3.3. Amplitude responses of *early*, *control* and *late* stocks

Although the CIRCs of *early* and *late* populations were found to be different, it is not clear what contributes to this difference in net compression and expansion of the CIRC waveform. As discussed in the introduction, I hypothesised that amplitude responses to light may contribute to this compression and expansion of circadian cycle lengths of *early* and *late* stocks, and to test this I analysed data from the experiment where brief light pulses were administered to these populations at different times of their circadian cycle and compared the amplitude with the

unpulsed control. The ANOVA revealed a statistically significant effect of selection ($F_{2,6} = 11.68$, $p < 0.05$; Table 6.6) but not of time-point ($F_{5,15} = 1.12$, $p > 0.05$; Table 6.6) or of selection × time-point interaction ($F_{10,30} = 1.9$, $p > 0.05$; Figure 6.6a; Table 6.6).

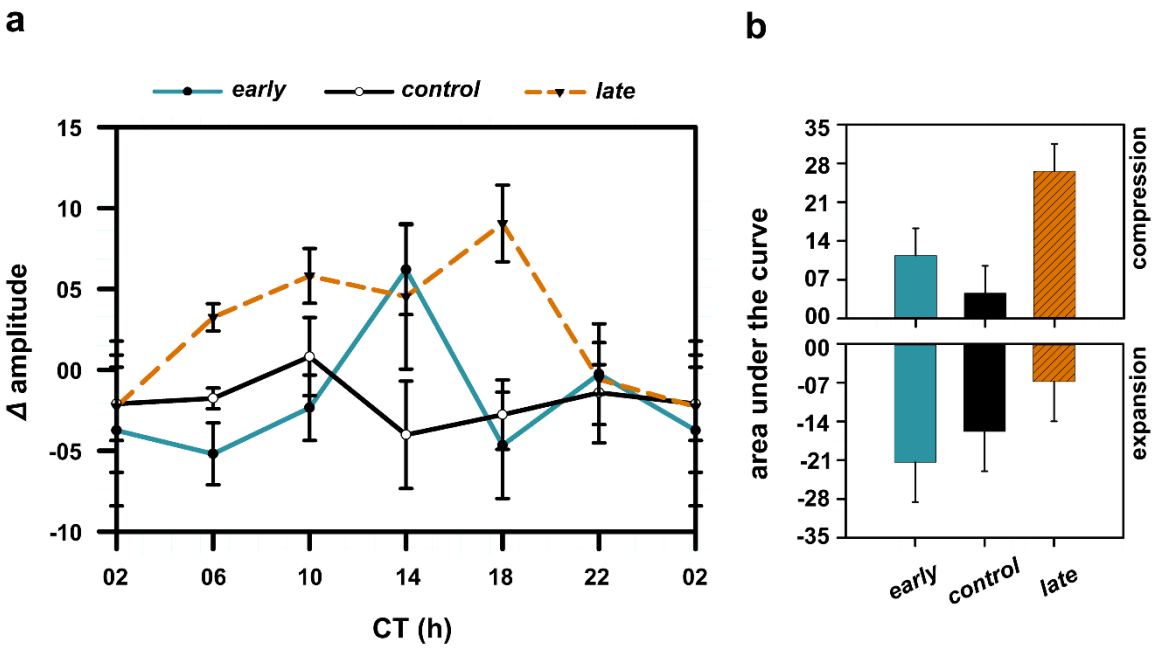

Figure 6.6: (a) Amplitude response curves for *early*, *control* and *late* stocks. Negative amplitude change values indicate amplitude expansion and positive changes indicate amplitude compression. Panel (b-top) shows the net amplitude compression and (b-bottom) shows the net amplitude expansion of the rhythm for all the three stocks as estimated using areas under the curve (AUC). Error bars are 95% CI calculated using Tukey's HSD, hence, non-overlapping error bars indicate significantly different mean values. Average values of amplitude change for each replicate block is obtained from 26 – 31 flies.

Table 6.6: ANOVA table summarizing the effects of selection, time-point and selection × time-point interaction on amplitude responses. Italicised effects are significant.

Summary of all effects	df Effect	MS Effect	df Error	MS Error	F	p
Selection (Sel)	*2*	*205.9862*	*6*	*17.6316*	*11.68*	*0.01*
Time-Point (TP)	5	40.2196	15	35.7541	1.12	0.39
Block (B)	3	55.1034	0	0.0000	--	--
Sel × TP	10	55.9899	30	29.5097	1.90	0.09
Sel × B	6	17.6316	0	0.0000	--	--
TP × B	15	35.7541	0	0.0000	--	--
Sel × TP × B	30	29.5097	0	0.0000	--	--

Given that stock had a significant main effect and owing to the fact that earlier studies have suggested the relevance of longer durations of light to entrainment (Nikhil, Vaze et al., 2016; Vaze, Nikhil et al., 2012), I assessed if longer durations of light have differential effects on the amplitude responses as estimated by area under the amplitude response curves (ARCs). The ANOVA revealed a statistically significant effect of selection on net compression ($F_{2,6} = 24.59$, $p < 0.05$; Table 6.7). Post-hoc comparison using Tukey's HSD revealed that *late* stocks undergo significantly higher net compression than both *early* and *control* stocks (Figure 6.6b, top). ANOVA done to test the effect of stock on net expansion revealed no significant effect although the *late* stocks showed a trend of reduced expansion relative to *early* stocks ($F_{2,6} = 4.95$, $p = 0.05$; Figure 6.6b, bottom; Table 6.8).

Table 6.7: ANOVA table summarizing the effects of selection regime on net amplitude compression. Italicised effects are significant.

Summary of all effects	df Effect	MS Effect	df Error	MS Error	F	p
Selection (Sel)	*2*	*508.7179*	*6*	*20.6877*	*24.59*	*0.00*
Block (B)	3	41.7660	0	0.0000	--	--
Sel × B	6	20.6877	0	0.0000	--	--

Table 6.8: ANOVA table summarizing the effects of selection regime on net amplitude expansion. Italicised effects are significant.

Summary of all effects	df Effect	MS Effect	df Error	MS Error	F	p
Selection (Sel)	2	216.5476	6	43.7036	4.95	0.05
Block (B)	3	179.7525	0	0.0000	--	--
Sel × B	6	43.7036	0	0.0000	--	--

6.3.4. Duration DRC of *early*, *control* and *late* stocks

In addition to differential, transient amplitude responses, I intended to ask if the velocity of phase progression is different between our stocks. One way to estimate this is via examining phase-shifts in response to different durations of light pulses (see Beersma et al., 2009; Comas et al., 2006). I performed such an experiment using two durations i.e., 25-min and 50-min of light pulses administered at CT14 (delay zone) and CT22 (advance zone), and examined them in relation to previously published values of phase-shifts in response to 5-min light pulses (Nikhil, Vaze et al., 2016). I found that there was a significant interaction between stock × duration of light pulse in the advance zone i.e., CT22 ($F_{2,6} = 6.04$, $p < 0.05$; Table 6.9). Phase-shifts obtained through a 25-min pulse was significantly lower in the *control* and *late* stocks relative to the *early* stocks. However, in response to a 50-min light pulse, both *early* and *late* stocks showed similar extents of phase-shifts, while *control* stocks showed lower phase-shift than the *early* stocks. Moreover, there

was no significant difference in phase-shifts of the *early* stocks with the 25-min or 50-min pulse (Figure 6.7, top). Importantly, the phase-shifts obtained in response to both 25-min and 50-min light pulses were higher than those in response to a 5-min pulse (Figure 6.7, top). This implies that the *late* stocks require longer durations of light to elicit phase-shifts of equal magnitude as that of the *early* stocks. This is suggestive of differential rates of phase-progression in the *early* and *late* stocks. However, there was no significant stock × duration of light pulse interaction effect on phase-shift of these stocks in the delay zone ($F_{2,6} = 2.69$, $p > 0.05$; Table 6.10; Figure 6.7, bottom), implying that the extent of velocity of phase progression in the delay zone is not different between stocks.

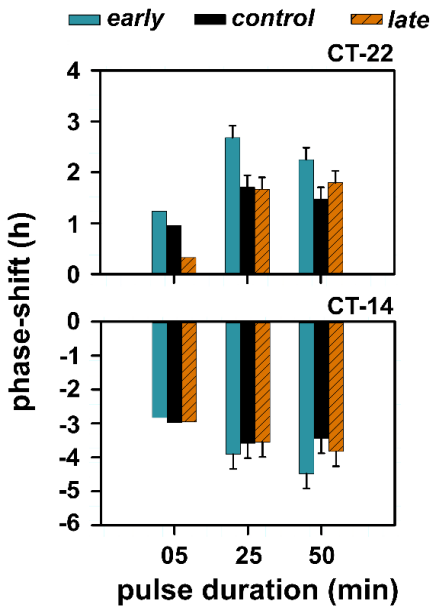

Figure 6.7: Duration DRC for *early*, *control* and *late* stocks for light pulses administered at CT22 (top) and CT14 (bottom). Error bars are 95% CI calculated using Tukey's HSD, hence, non-overlapping error bars indicate significantly different mean values. Phase-shift values for CT22 and CT14 for 5-min duration was obtained from Nikhil, Vaze et al. (2016). These values are depicted here for comparison purposes only and have not been used in the analyses. Block means of phase-shifts were estimated by averaging values from 19 – 32 flies.

Table 6.9: ANOVA table summarizing the effects of selection, duration of light pulse administered starting at CT22 and selection × duration interaction on phase-shifts. Italicised effects are significant.

Summary of all effects	df Effect	MS Effect	df Error	MS Error	F	p
Selection (Sel)	2	1.7665	6	1.4584	1.21	0.36
Time-Point (TP)	*1*	*0.1923*	*3*	*0.0065*	*29.38*	*0.01*
Block (B)	3	1.2575	0	0.0000	--	--
Sel × TP	*2*	*0.1562*	*6*	*0.0259*	*6.04*	*0.04*
Sel × B	6	1.4584	0	0.0000	--	--
TP × B	3	0.0065	0	0.0000	--	--
Sel × TP × B	6	0.0259	0	0.0000	--	--

Table 6.10: ANOVA table summarizing the effects of selection, duration of light pulse administered starting at CT14 and selection × duration interaction on phase-shifts. Italicised effects are significant.

Summary of all effects	df Effect	MS Effect	df Error	MS Error	F	p
Selection (Sel)	2	0.9921	6	0.9758	1.02	0.42
Time-Point (TP)	1	0.3320	3	0.0820	4.05	0.14
Block (B)	3	0.3478	0	0.0000	--	--
Sel × TP	2	0.2569	6	0.0956	2.69	0.15
Sel × B	6	0.9758	0	0.0000	--	--
TP × B	3	0.0820	0	0.0000	--	--
Sel × TP × B	6	0.0956	0	0.0000	--	--

In summary, I conclusively demonstrate that two out of three major predictions from the non-parametric model of entrainment are not withheld, thereby allowing me to conclude that the ψ_{ENT} of the activity/rest rhythm of *early* and *late* stocks cannot be fully explained by this model. I also show that a holistic model incorporating both phasic and tonic effects is better able to explain

differences in entrained phase of our stocks. This, I show can be brought about by tonic effects on transient amplitude of behaviour and on velocity of phase progression. Future experiments to address the differences in the effects of light on the clocks of *early* and *late* stocks must include detailed analyses of after-effects to various light regimes and, perhaps, the physiology of the visual system in them.

6.4. Discussion

My study was motivated by the results that *early* and *late* populations differ in the τ of their activity/rest rhythm by ~0.93-h, but do not differ in their photic PRC (Nikhil, Vaze et al., 2016) and mean ψ_{ENT} under LD 12:12 (Nikhil, Abhilash et al., 2016). This, in addition to some previous results (see introduction), suggested that phasic/non-parametric effects of light alone may be insufficient in explaining the entrainment of activity/rest rhythm in these populations.

To rigorously test the extent to which phasic effect of light contribute to entrainment of the activity/rest rhythm in *early* and *late* stocks, I tested the predictions from the non-parametric model. Firstly, I find that when subjected to brief light pulses of ~70-lux for 5-min administered once every 24-h, and to LD 12:12 (light intensity ~70-lux), there was no correlation between τ and ψ_{ENT} (Figure 6.3). Moreover, the steady state phase-relationship between onset of activity and light pulse yields phase-shifts that are more than what is required for entrainment of all our stocks (Figures 6.4b and 6.4c). However, proportion of individuals entraining to single pulses in all our stocks can be predicted using the non-parametric model alone (Figures 6.4d and e).

The absence of correlations between τ and ψ_{ENT}, one may argue, could be due to masking effects of the zeitgeber (Aschoff, 1960), which has indeed been shown to influence ψ_{ENT} of eclosion rhythms in *Drosophila* (McNabb et al., 2008). To test this, I exposed flies from *early* and *late*

stocks to LD cycles with varying intensity and durations i.e., LD 12:12 (light intensity ~1-lux during the photophase), LD 06:18 (light intensity ~70-lux during the photophase) and LD 18:06 (light intensity ~70-lux during the photophase). I did not find a significant correlation between τ and ψ_{ENT} when flies from the *early* and *late* populations were entrained to LD 12:12 with ~1-lux intensity (Figure 6.3), and even LD 12:12 with ~0.1-lux intensity (Nikhil, Vaze et al., 2016). However, there was a significant positive correlation between the two under LD 06:18 as expected, and surprisingly a significant negative correlation under LD 18:06 (Figure 6.3). These results allow me to conclude that the absence of a correlation between τ and ψ_{ENT} is perhaps not due to masking effects of the zeitgeber. The significant negative correlation between τ and ψ_{ENT} under summer-like long photoperiod is primarily driven by advanced evening peak of activity in *late* stocks (Nikhil, Abhilash et al., 2016). A rather successful model of circadian organisation regulating activity/rest behaviours in a wide range of organisms is the Morning (*M*) – Evening (*E*) dual oscillator model (Helfrich-Förster, 2009). I hypothesise, as previously (Nikhil, Abhilash et al., 2016; Nikhil, Vaze et al., 2016), that differential coupling of the *M*- and *E*-oscillators via PDF (Pigment Dispersing Factor) and/or dominance of the *E*-oscillator in the *late* stocks contributes to an advanced phase of evening activity under long photoperiods. However, I must stress that the difference in phasing of evening activity between the *early* and *late* stocks under LD 18:06 is small, and therefore these hypotheses are difficult to test, at the moment. One may further argue that the reason for the absence of a correlation between τ and ψ_{ENT} in case of activity/rest rhythm of *early*, *control* and *late* stocks may also be due to the range of period values sampled. The period values I sampled in my study ranges from 23-h to 24.5-h. Although some of the studies have indeed sampled wider range of period values and found significant correlations between τ and ψ_{ENT} (Aschoff and Wever, 1966; Hamblen-Coyle et al., 1992; Rémi et al., 2010; Srivastava et al., 2019),

other studies have found correlations with smaller ranges as well (Pittendrigh and Daan, 1976a; Wright et al., 2005). Moreover, results from our laboratory have revealed that within the same range of period values, there are correlations between τ and ψ_{ENT} for eclosion rhythm when entrained to LD 12:12 (Kumar et al., 2007; Nikhil, Abhilash et al., 2016). These allow me to conclude that in our stocks, phasic effect of light alone may be insufficient to explain entrainment of the activity/rest rhythm.

Although intriguing that there is no change in ψ_{ENT} with differences in τ as a consequence of entrainment, it is now well established that phase-relationship with the zeitgeber is of immense significance in terms of being adaptive (reviewed in Vaze and Sharma, 2013). Studies done previously have reported that phasing activity to certain times of the day is adaptive in terms of finding mates, avoiding predation and finding food, avoiding competition (Dodd et al., 2005; Fleury et al., 2000; Ouyang et al., 1998), and parasites' in-host survival and between host transmission potential (O'Donnell et al., 2011). All these studies indicate that the primary role of possessing circadian clocks is to time behaviour and physiology appropriately. If this were the case, then it does seem intuitive that relatively small differences in circadian period may not translate into corresponding differences in ψ_{ENT} as predicted by the non-parametric model of entrainment, suggesting that distinct regulatory components may be influencing τ and ψ_{ENT}. Furthermore, a recent study described that the miRNA, miR-124 advances ψ_{ENT} of activity/rest behaviour without affecting τ in *Drosophila* (Zhang et al., 2016). Other studies in mice have identified distinct miRNAs that lengthen τ and affect the entraining effects of light (Cheng et al., 2007). The miR-219 lengthens τ and miR-132 is induced by light cues and attenuates the entraining effects of light. Such results, along with ours, raise the very interesting possibility of τ

and ψ_{ENT} being regulated by distinct but coupled entities/components of the circadian clock network, a problem that I think is worth pursuing further.

As mentioned earlier, there is indirect evidence for the parametric model of entrainment (Aschoff, 1979) and the model seems to be adequate in predicting steady state entrainment under a wide range of zeitgeber conditions (Comas et al., 2006, 2007; Daan, 1977; Taylor et al., 2010). However, there are very few experiments done to study this model and additionally, velocity response curves (VRC) are derived from PRCs (Daan, 1977; Daan and Pittendrigh, 1976), thereby suffering from the same assumptions made in case of the non-parametric approach. Although evidence is relatively scanty, the parametric model is certainly thought to contribute to entrainment of circadian clocks, and hence newer approaches were taken to incorporate both phasic and tonic effects of light to understand the mechanism of entrainment. Among the initial approaches was that of Beersma et al. (1999), where the authors showed that maximal accuracy (minimum day-to-day variation in ψ_{ENT}) under entrainment is achieved when both phase and velocity respond to light signals. This study unequivocally showed that in nature entrainment is likely to occur via both parametric and non-parametric modes. However, this model was largely pedagogical and cannot be used to predict phases of entrainment in organisms or understand how phasic and tonic mechanisms contribute to phases. In a step towards building a generalist model of entrainment incorporating both phasic and tonic effects of light, came the CIRC model (Roenneberg, Hut et al., 2010; Roenneberg, Rémi et al., 2010). This model talks about time-of-day dependent compression and expansion of the internal cycle length. The authors discussed how this model can quantitatively predict phases and limits of entrainment. Furthermore, Roenneberg, Rémi et al. (2010) have also shown that the CIRC can predict ψ_{ENT} under 162 different conditions with varying T, τ and photoperiod, thereby highlighting the remarkable success of the model.

I subsequently hypothesised that a more holistic model such as the CIRC may aid our understanding of entrained activity/rest rhythm in *early* and *late* stocks. I predicted ψ_{ENT} for each of the 12 populations across three photoperiods and found that the CIRCs can predict ψ_{ENT} reasonably well for all populations under most environmental conditions, especially for the *late* chronotypes (Figure 6.5a). I found that the best fitting CIRCs are indeed different for *early* and *late* stocks, such that the compression and expansion zones of *late* populations were larger and smaller than *early* populations, respectively (Figures 6.5b and c). Intriguingly, the *late* stocks show best fits between experimental and predicted phase-relationships (Figure 6.5a, right), and this appears to be driven by the evolution of both, the compression/expansion ratio and the extent of dead zone of the CIRC (Figures 6.5b and c), thereby highlighting the importance of both features to entrainment. It is important to note that, for some reason, the model does not predict ψ_{ENT} under short photoperiod for the *early* and *control* stocks, and I think that the following could be reasons for it – (i) τ_E used in the model are based on actual values of free-running period post entrainment to the respective regimes as opposed to simulations in (Roenneberg, Rémi et al., 2010), and the nature of differential change of period and phase across stocks may influence fits (see Table 6.11 for the period values I empirically estimated); and/or (ii) we have assumed, for simplicity, that the calibration factor is unity for all stocks. This may not be true and the relative sensitivity of the zeitgeber in our stocks may be fundamentally different, thereby yielding poorer fits for *early* and *control* stocks. I think that accounting for these and parameterising the model may also improve fits in addition to use of more photoperiods under different *T*-cycles. In light of the current model and parameter space explored, I propose that the lack of fit under short photoperiod in the *early* and *control* stocks as opposed to the almost perfect fit for the *late* stocks, is evidence that, at least for *late* stocks, parametric effects of light explain photic entrainment better.

Table 6.11: Free-running periods of *early*, *control* and *late* stocks before (τ_{DD}) and after entrainment (τ_E) to three different photoperiods.

	early		***control***		***late***	
	τ_{DD}	τ_E	τ_{DD}	τ_E	τ_{DD}	τ_E
LD 06:18	23.61±0.03	23.52±0.04	23.86±0.04	23.81±0.08	24.25±0.08	24.17±0.08
LD 12:12	23.29±0.04	23.64±0.07	23.64±0.03	23.96±0.07	24.03±0.11	24.46±0.14
LD 18:06	23.27±0.04	23.71±0.07	23.77±0.09	24.10±0.09	24.14±0.03	24.48±0.06

As mentioned earlier, the mechanisms by which internal cycle length expands or compresses in the CIRC model has not been discussed so far. However, if the circadian clock is perceived as a limit cycle oscillator (as in Johnson et al., 2003), then it becomes evident that internal cycle lengths can change by modulating amplitude of the state variables, a proxy for which could be the overt behaviour's amplitude (see Johnsson et al., 1973; Winfree, 1973). To understand the contributions of such phase-dependent transient amplitude changes to entrainment of the activity/rest rhythm in response to brief light pulses, I calculated the ARCs of *early*, *control* and *late* stocks. Although I could not detect a time-dependent response, I found a significant effect of stock on instantaneous amplitude responses to brief light pulses (Figure 6.6a). Interestingly, I found that *late* stocks showed a significantly larger net compression than *early* stocks, thereby indicating that, longer durations of light may render *late* populations more sensitive to the zeitgeber and thereby facilitate entrainment (Figure 6.6b). In addition to amplitude responses, I also examined phase-shifts using duration DRCs and found support for the idea that the *late* stocks significantly differ in the parametric usage of light (Figure 6.7).

All results reported in this chapter indicate that entrainment of activity/rest rhythms of our *early*, *control* and *late* stocks can be predominantly explained by differences in the parametric effects of

light on amplitude and velocity of phase progression under long durations of light. Such saturation of the input system to the clock to longer durations of light are thought to contribute to divergent phase progression dynamics (Comas et al., 2006). In view of all these results and survey of literature, I think that future experiments must be targeted towards examining after-effects of entraining programmes on both τ and amplitude in our *early* and *late* stocks. Moreover, plasticity of τ and amplitude after rearing under various environmental conditions may also provide additional support for our claims. On an anatomical and physiological level, I think that the visual system must be probed to further understand how photic information is processed and relayed to the clock to facilitate entrainment in our stocks.

Chapter 7. Discussion – General remarks, hypotheses and future directions

Here I will summarise all my results so far (Chapters 3-6) and attempt to make a few general comments, build a hypothesis regarding the association between timing of behavior, circadian organization and mechanisms of entrainment, and discuss avenues for further studies. More specific future experiments with reference to each chapter are described in the respective discussion sections and will not be elaborated upon here.

(i) In the third chapter, I examined the adult eclosion behavior of *early*, *control* and *late* stocks under a wide variety of temperature regimes with a fixed LD schedule, in order to understand differences in the hierarchical organization of the circadian clock network, if any, in our populations. I found that under LD cycles and constant ambient temperatures, phases of the eclosion rhythm were invariant across different ambient temperatures in the *early* and *control* populations, while they were highly labile in the *late* chronotypes. Further, eclosion rhythm experiments under LD + TC cycles revealed that the *late* chronotypes progressively delayed their phase with increasing amplitude of TC cycles when the overall temperature was cool, thereby timing eclosion to occur at the relatively warmer phase of the day. Interestingly, the *late* chronotypes also progressively advanced their phase with increasing amplitude of TC cycles when the overall temperature was warm, thereby timing eclosion to relatively cooler times of the day. This showed remarkable phase lability in the *late* chronotypes. The *early* chronotypes, however, did not change their phase much under any temperature regime and was always phase-locked to dawn. These results, I argue, support the idea of a stronger *B*-oscillator (temperature sensitive components of the circadian clock network) in the *late* chronotypes, relative to the strength of the *B*-oscillator in the *early* chronotypes. Moreover, high phase-lability can be attributed to high amplitude temperature pulse PRCs in the *late* stocks.

(ii) Using the experimental paradigm reported in the fourth chapter, I first established that unnatural light regimes such as *T*-cycles as short as 12-h can be useful to understand the network organization regulating activity/rest rhythms in *Drosophila*. I found that wild-type flies treat two *T*-cycles as one day (referred to as LDLD) and therefore, I concluded that flies treat the two light phases within 24-h as a 'skeleton' to a long-day regime, but with significant differences. It is thought that the *E*-oscillator is dominant under long photoperiods in *Drosophila*; and owing to the fact that such dominance can be exerted via amplitude and/or phase of the evening peak of activity, I examined these properties in our *control* flies. I found that the relative height of evening peak was significantly reduced under LDLD as compared to its value under long-day LD cycles. This I argue reflects reduced *E*-oscillator dominance under LDLD and this is confirmed by my finding that the amplitude of PER oscillations in the *E*-cells in the *Drosophila* brain are highly damped compared to the oscillations in the *M*-cells. I subsequently examined phase and amplitude plasticity of the *early* and *late* stocks by analyzing behavior under LDLD and found that the *late* stocks show reduced amplitude plasticity and increased phase plasticity, both reflective of a dominant *E*-oscillator.

(iii) Owing to the (i) increased dominance of the *B*-oscillator regulating eclosion rhythms and increased dominance of the *E*-oscillator dominance regulating activity/rest rhythms in the *late* chronotypes, and (ii) the overlap between cells regulating evening activity and temperature sensitivity led me to ask how entrainment to temperature cues affect the activity/rest rhythm in the *early*, *control* and *late* stocks. In the fifth chapter of my thesis, I report that the *late* chronotypes re-entrained faster to jetlagged TC 12:12 cycles, indicative of high amplitude temperature pulse PRCs. As discussed above, high amplitude

temperature pulse PRCs are expected to lead to increased phase plasticity under entrainment to temperature cues. To examine this, I studied the activity/rest behavior of our flies under three different thermoperiods and found that the *late* stocks showed higher phase plasticity than the *early* and *control* stocks. Interestingly, this increased phase plasticity in the *late* stocks was predominantly driven by differences in the evening peak of activity, thereby indicating a previously unrecognized overlap between the hierarchical (*A-B* oscillator model) and mutual (*M-E* oscillator model) schemes of circadian organization. The *late* stocks also showed higher amplitude expansion, robustness and accuracy of entrainment; all of which are features associated with high amplitude temperature pulse PRCs. Importantly, the patterns of phase-relationship of the activity/rest rhythm of *early*, *control* and *late* stocks to the TC cycles are, to a large extent, consistent with predictions from the non-parametric model of entrainment; and the evidence pointing towards the evolution of high amplitude PRCs in the *late* stocks is also indicative of phasic contributions of temperature to entrainment.

(iv) In the sixth chapter of my thesis, I report results of studies that were carried out to identify the relative contributions of parametric and non-parametric effects of light to entrainment of our *early*, *control* and *late* stocks. I systematically tested predictions from the non-parametric model and found that most predictions are not met, therefore implying that in case of light, non-parametric effects of light cannot explain phases of entrainment of the activity/rest rhythm of our stocks under single recurrent light pulses and LD cycles with different photoperiods. However, phases of entrainment, especially of the *late* chronotypes, were to a large extent explained by a model incorporating parametric effects of light. Further, I found that tonic effects of light on amplitude of the rhythm and on phase

progression were different between the *early* and *late* stocks, suggesting that between stock differences in photic entrainment may be attributed to differences in the parametric effects of light.

As discussed in Chapter 1, under natural environments, both parametric and non-parametric effects of the zeitgeber contribute to entrainment. My experiments, results of which are reported in this thesis, indicate that the relative contributions of these effects may be different depending on the zeitgeber used to probe into features of entrainment. I found that while for temperature non-parametric mechanisms explain entrainment to a large extent, and in case of light, parametric effects are predominant. Fundamentally, the difference between parametric and non-parametric effects are that in case of the non-parametric effects, small stimuli (pulses in the order of minutes) leads to large effects (phase-shifts in the order of several hours); and in case of parametric effects, large stimuli (durations of light or temperature lasting for several hours) results in small effects (period change in the order of a few minutes). The fact that behavior of *late* chronotypes is consistent with the idea of differential phasic responses to temperature suggests that the component of the circadian network responsible for sensing and responding to temperature cues must be stronger in them than in the *early* chronotypes. This is precisely what I observe when I examine the organization wherein there is strong evidence for dominant *B*-oscillators in the *late* stocks. Interestingly, however, higher strength of the *B*-oscillator in the *late* stocks appears to be associated with stronger parametric contributions of light to entrained phase. Based on these arguments, I hypothesise that selection for timing of behavior leads to altered circadian organization. As a consequence of altered organization, the relative strengths of light and temperature sensitive components of the circadian clock network change and this determines the relative contributions of parametric and non-parametric effects of the zeitgeber to entrainment (see

Figure 7.1). Similar evolution of relative contributions of parametric and non-parametric effects of the zeitgeber are expected to occur in the wild as well, owing to the fact that a predominant selection pressure in nature must be on timing of behaviors.

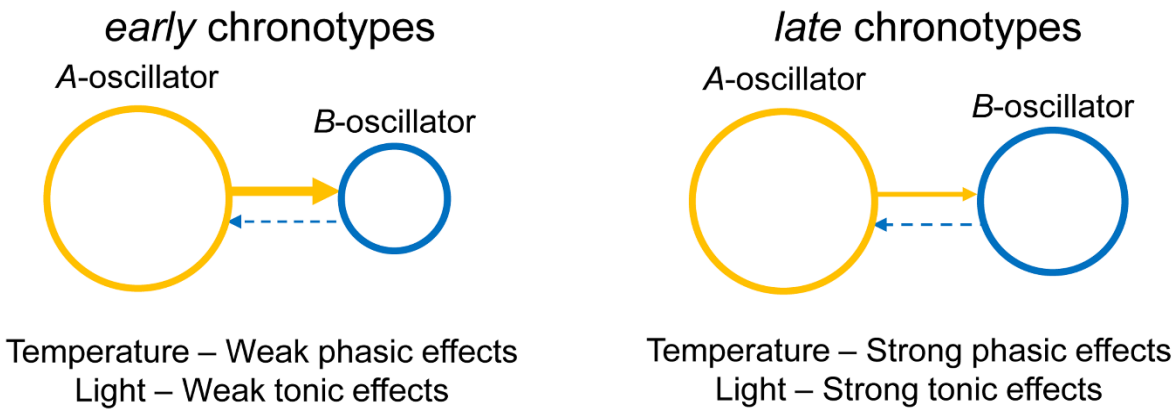

Figure 7.1: A schematic illustrating the hypothesis regarding the inter-dependence of timing of behavior, circadian organization and mechanisms of entrainment, specifically in the context of our *early* and *late* chronotypes.

To test the aforementioned hypothesis in the *early*, *control* and *late* stocks, it will be important to understand, in further detail, the organizational principles that differ between the stocks for different overt rhythms, the properties of entrainment, phase-responses, and effects of entrainment on different clocks properties. I propose that the following broad questions be pursued in the future:

(i) While plasticity of the eclosion waveform has been studied in fairly great detail, the activity/rest rhythm in our stocks have been less examined. Therefore, we must examine plasticity various aspects of the entrained waveform in response to a wide range of light and temperature regimes, in case of the activity/rest rhythm. In this

regard, specific questions regarding the overlap between hierarchical and mutual schemes of circadian organization regulating activity/rest rhythms can be better understood under conflicting light and temperature zeitgeber regimes. Further, studies probing into the extent of light sensitivity mediated waveform plasticity may be useful to ask if waveform bifurcation can at all happen in flies. If it can, are there specific differences between the early and late chronotypes, in the extent of such bifurcation may be worth examining. Further, are such bifurcation patterns only a light induced phenomenon, or can temperature cues also induce waveform bifurcation? Are there stock specific differences in the proportion of flies undergoing such light induced or temperature induced bifurcation?

(ii) To further understand properties/mechanisms of entrainment to light and temperature, we must construct a family of temperature pulse phase-response curves to cool and warm pulses of different durations. This will enable us to make quantitative predictions regarding phases of entrainment, re-entrainment rates, and range of entrainment for our stocks to different temperature zeitgebers, that can be tested.

(iii) Moreover, while my results show that period after-effects may exist post entrainment to different thermoperiods, it is now imperative to assess more elaborately the extent of after-effects to different thermoperiods and temperature *T*-cycles. Additionally, to further test the contribution of parametric effects of light, it is crucial to also estimate to what extent period is altered in response to different photoperiods and *T*-cycles in our stocks. Although it will be interesting to examine after-effects in both eclosion and activity/rest rhythms, due to technical limitations, at this point only activity/rest rhythms are feasible and must be examined.

(iv) A general point of interest that emerges also is the extent to which period is plastic in our stocks not only post entrainment but also to different rearing conditions. Analysis of period of our stocks under constant conditions post development under varying light and temperature zeitgeber frequencies will be interesting, to this end. This, unlike the after-effects can be performed for both the eclosion and activity/rest rhythms and is likely to give us an idea of the overall similarities in the organizational principles underlying the two rhythms in our stocks, and perhaps, in general.

Further studies to address the above discussed inter-dependence between timing of behavior, circadian organization and entrainment may include examining each of these in multiple insect species that have divergent timings of behavior. For instance, while many insects including a few *Drosophila* spp. predominantly eclose close to dawn, there are several insects, such as the flour moth (*Anagasta kühniella*) and Chironomids, that eclose later during the day, around dusk or even at night. It will be critical to examine light and temperature sensitivity of the circadian system in these insects to understand organizational principles and the mechanisms of entrainment and ask if they are similar to the relationship I have found here. Although in these insects, it is presumable that delayed phasing may not be a direct consequence of selection on timing, it is still behaviourally similar to our *late* stocks, and therefore such studies may be useful to conduct. It will also be important to examine if selection for evening timing of a behavior other than eclosion also leads to dominant *B*-oscillators and therefore determine the relative strengths of parametric and non-parametric mechanisms of entrainment contingent upon the zeitgeber used. It is important to note here that the nature of selection, the trait on which selection acts, and the organizational principles regulating the rhythmic behavior in question is likely to affect the way in which this inter-dependence evolves. In other words, picking evening chronotypes of a different behavior or

insects with night-time activity as opposed to insects with day-time activity and expecting changes in circadian organization and entrainment mechanisms is not fully warranted. However, it is nevertheless an interesting exercise to further understand the generalizability of my thesis and is bound to give us insights into this complex relationship.

Chapter 8. Appendices

8.1. Genetic architecture of *early* and *late* chronotypes

As mentioned in the synopsis and in Chapter 2, understanding the genetic signatures associated with early and late emergence chronotypes is an ongoing study that was initiated by a former student in the laboratory (Dr. Nikhil K.L.) and is currently being undertaken in part by me and in part by another student (Mr. Arijit Ghosh). In this thesis, I only report results from analyses of the genome data that I have performed.

8.1.1. Introduction

A chronotype distribution represents the inter-individual variation in timing of behaviour, such as sleep/wake in humans. While some individuals have an inherent propensity to wake up and sleep earlier in the day; referred to as 'early' chronotypes, 'late' chronotypes constitute individuals who inherently wake up and sleep later. Various studies have suggested that chronotypes are driven by differences in circadian clocks which not only drive rhythms in sleep/wake but also in other aspects of behaviour and physiology (Kumar, 2017). However, inter-individual differences in sleep/wake times are not characteristic of humans alone and is observed in timing of various circadian behaviours across species (Aschoff and Wever, 1962; Dominoni et al., 2013; Frías-Lasserre et al., 2019; García-Allegue et al., 1999; Helm and Visser, 2010; Ocampo-Garcés et al., 2006; Refinetti et al., 2016; Schwartz and Smale, 2005; V Sheeba et al., 2001; Stuber et al., 2015; Vivanco et al., 2009).

Chronotypes have attracted considerable attention in the recent past with various studies reporting the association of chronotype differences with a myriad of psychological, metabolic and other physiological dysregulations (Bullock, 2019; Kivelä et al., 2018; Koren et al., 2016; Manfredini et al., 2018; Roenneberg et al., 2019; Roenneberg and Merrow, 2016); thus, highlighting the

importance of understanding the functional underpinnings of chronotype regulation. Several studies exploring the genetic basis of chronotypes have reported varying degrees of heritability across human populations (Aguiar et al., 1991; Hur et al., 1998; Klei et al., 2005; Koskenvuo et al., 2007; Von Schantz et al., 2015); while others have reported association of chronotypes with various polymorphisms in clock genes such as *clock* (Katzenberg et al., 1998; Mishima et al., 2005), *per1-3* (Archer et al., 2003; Carpen et al., 2005, 2006; Ebisawa et al., 2001; Pereira et al., 2005), and *arntl2* (Parsons et al., 2014). However, some of these reports remain inconclusive as other studies either failed to replicate these findings or observed conflicting or no association of these polymorphisms with chronotypes (An et al., 2014; Barclay et al., 2011; Drake et al., 2015; Iwase et al., 2002; Kunorozva et al., 2012; Osland et al., 2011; Pedrazzoli et al., 2007; Perea et al., 2014; Pereira et al., 2005; Robilliard et al., 2002; Viola et al., 2007), possibly due to differences in statistical powers of detection because of variation in size and genetic backgrounds of sampling populations. In recent years, genome wide association studies on human cohorts have identified multiple circadian clock genes associated with chronotypes, and also several other genes known to be involved in neuronal signalling, sleep homeostasis, and light input pathways to the clock (Gottlieb et al., 2007; Hu et al., 2016; Jones et al., 2016, 2019; Lane et al., 2016). Interestingly, some of the identified genes have also been implicated with similar functions in mice and *Drosophila* thus suggesting that the genetic architecture underlying chronotype variation may be, at least partly, conserved across organisms. Although GWAS is a powerful strategy to identify genes that are unlikely to be identified by other approaches, the list of candidate genes may vary across studies due to multiple reasons (Kalmbach et al., 2017); therefore, necessitating further validation of the candidates which are often not possible in humans and requires a well-established model system.

Chronotypes essentially reflect differences in the entrained phase of the underlying circadian rhythm/clock; therefore, exploring mechanisms driving differential phases of entrainment can help us better understand chronotype regulation. To this end, our *early* and *late* populations are a unique resource (Kumar et al., 2007; also see Chapters 1 and 2). Over the course of ~18 years (>320 generations) we have reported that *early* and *late* emergence chronotypes in these populations are associated with differences in circadian period (Kumar et al., 2007; Nikhil, Abhilash et al., 2016), zeitgeber sensitivity (Abhilash et al., 2019; Nikhil et al., 2014; Vaze, Kannan et al., 2012; Vaze, Nikhil et al., 2012), amplitude, coupling, phase and period responses (Nikhil, Vaze et al., 2016) and also molecular clocks (Nikhil, Abhilash et al., 2016). These are in accordance with studies on other organisms including humans reporting that chronotypes are a complex trait that may stem from differences in various clock properties and their interaction with zeitgebers (Aschoff and Pohl, 1978; Duffy et al., 2001; Duffy and Wright, 2005; Kerkhof and Van Dongen, 1996; Lehmann et al., 2012; Vivanco et al., 2010).

Having established a well-characterized model of chronotypes that can serve as a system for further molecular-genetic studies, we sequenced the genomes of our *early* and *late* populations to identify putative loci that are likely to be associated with entrained phase/chronotype differences. The advancement of whole-genome sequencing has reinvigorated strategies for identifying genes undergoing adaptive change. One can scan along the genome to identify regions with patterns or signatures of polymorphism indicative of recent selection (Nielsen et al., 2007; Voight et al., 2006). Also, in recent years genome-wide scans of reduced heterozygosity have been identified as selective sweeps in many species including *Drosophila melanogaster* (Cassidy et al., 2013; Garud et al., 2015; Karasov et al., 2010). However, only in a few cases, it was possible to directly associate a phenotypic trait with adaptations at the molecular level.

Experimental evolution in laboratory populations followed by whole-genome sequencing, commonly called "Evolve and Re-sequence (E&R)" (Turner et al., 2011), is an attractive alternative for investigating the genetic basis of a selected trait (Kawecki et al., 2012). Evolve and Resequence has been applied in *Drosophila* with varying degrees of success to investigate the genetic basis of longevity and aging (Burke et al., 2010; Remolina et al., 2012), body size (Turner et al., 2011), hypoxia tolerance (Zhou et al., 2011), courtship song (Turner and Miller, 2012), bristle development (Cassidy et al., 2013), adaptation to novel environments (Orozco-Terwengel et al., 2012), temperature (Tobler et al., 2014), and diet (Reed et al., 2014). While there are advantages of using such a system to dissect the genetic regulation of complex traits, there are however a few limitations of such studies as well. "False positives" are likely to be caused by (i) linkage and hitchhiking, which can be exacerbated by linkage disequilibrium (LD) created by the investigator in the establishment of the artificial populations, (ii) genetic drift, and (iii) unintended natural selection in the laboratory populations.

To the best of my knowledge, there has been no other study where *Drosophila melanogaster* populations have been used as model system to understand genetic basis of chronotype divergence, except one in which the transcriptome of 'early' and 'late' flies were examined (Pegoraro et al., 2015). These 'early' and 'late' lines were identified through a screen for eclosion times using the *Drosophila* genetic reference panel (DGRP; MacKay et al., 2012). The DGRP lines are a set of isogenic lines created from the same wild-type population. However, in this study the authors do not show if the divergence between 'early' and 'late' lines persists under constant conditions, and it is not clear if these are merely a consequence of divergent development times. Further, changes (if any) in associated circadian clock properties (for instance, free-running period under constant darkness) are not reported in the paper. Additionally, owing to those fly lines being inbred, genetic

correlations as inferred from differentially expressing genes between their 'early' and 'late' strains may be spurious (see Abhilash and Sharma, 2016). Our outbred *early* and *late* populations with four replicates along with appropriate controls, with significantly diverged circadian phenotypes provide us a unique opportunity to study the underlying genetic correlates behind chronotype divergence in nature. Genome wide sequencing of genetic variation present in experimentally evolving sexual populations after many generations shed light on the relative importance of selective sweeps, particularly alleles being driven to fixation (Phillips et al., 2016). Though successive selective sweeps, along with continuous hitchhiking could possibly result in purging of genetic variation, Burke et. al. show there is no widespread purging of genetic variation in fly populations that have evolved in a laboratory for a few decades (Burke et al., 2010).

With recent advances in sophisticated algorithms, processing power of computers and mass scale high-depth sequencing techniques, pooled sequencing large number of individuals from a population in a high coverage (50X-100X) depth gives reliable variant identification (Burke et al., 2010, 2014; Cutler and Jensen, 2010; Futschik and Schlötterer, 2010; Phillips et al., 2016). We carried out pooled sequencing of the four replicate populations of *early*, *control* and *late* flies and analyzed the variants to identify the genetic correlates underlying chronotype divergence among these flies.

8.1.2. Materials and Methods

8.1.2.1. Sample preparation and reads generation

Approximately 250 male and 250 female flies (4-5 days old) were randomly sampled from each population (total 12 samples: $early_{1\text{-}4}$, $control_{1\text{-}4}$ and $late_{1\text{-}4}$). Total genomic DNA was extracted from them with the DNeasy Blood and Tissue Kit (#69504, QIAGEN, MD, USA). These DNA samples were subjected to quality check (Nanodrop QC and Qubit QC). Vast pair-end libraries of

each sample were prepared for sequencing with tags (Standard Illumina HiSeq protocol). The Illumina HiSeq generated 150 paired-end reads which were quality checked using FastQC (Andrews, 2010). These raw reads were processed by Cutadapt (Martin, 2011) to remove adapters and for low-quality base trimming. Depth of coverage was 100X to build more than standard significance as this was pooled sequencing experiment; this was done so that at least one read of each nucleotide from individuals having different genotypes are part of the library. The reads from the *early*, *control* and *late* stocks were then aligned to the reference *Drosophila* genome (Reference genome: BDGP6) using bowtie2 (Langmead et al., 2013) which is a variant of the famous Burrows-Wheeler Aligner (BWA) algorithm (Li and Durbin, 2010).

8.1.2.2. Variant identification and filtering

Variants were identified using SAMtools1.2 and BCFtools1.2 (Li et al., 2009). Potential variants were identified using read depth threshold as greater than 20 and mapping quality threshold as more than 30. The mpileup files were generated using SAMtools and were processed using Varscan2 (Koboldt et al., 2009) for identification of line specific markers between the samples in a group. Loci were treated as fixed if the minor allele frequency at any given location was less than 2% of the major allele frequency. This is an arbitrary measure but has no bearing on the list of differentiated loci that we identify because I examined both homozygous and heterozygous loci, albeit differently.

8.1.2.3. Analysis of variants

To identify the loci that got fixed in our *early* and *late* populations, I first filtered the VCF files such that the file only contained loci that were heterozygous in the *control* stocks. As described above, any locus was considered heterozygous if the minor allele had counts at least 2% or greater of the major allele counts. I matched the *early* and *late* VCF files to this list for each block and

chromosome arm separately and found the number and identity of loci that had been categorized as homozygous. This allowed me to identify percentage fixation for each chronotype population. I got one such list each for *early* and *late* chronotypes of one block. This was then used to identify block-to-block overlap in loci that were fixed. I used the loci that were fixed in all four blocks and examined extent of overlap between *early* and *late* chronotypes (see Figure 8.1.1 for a schematic).

To analyse heterozygous loci, I first created a list of all *control* loci that were heterozygous and all the ones out of those loci that were heterozygous in *early* or *late* chronotypes. A Fisher's Exact Test (FET) was performed to ask if the allelic diversity in each such locus was significantly different between *early* and *control* and *late* and *control* stocks. Due to the large number of loci for which FET were performed, I corrected for the inflated family-wise error rate by using a Benjamini-Hochberg correction to restrict the net Type I error to 5%. From these significantly differentiated loci, I only chose ones that showed significantly reduced allelic diversity. I was interested in loci with reduced diversity and the ones that were fixed because under directional selection (which is the case for our populations), variation at a locus is expected to reduce (Hartl and Clark, 1997). Using these loci that showed significantly reduced heterozygosity, as described above I examined block-to-block and *early-late* overlap (Figure 8.1.1). Subsequently, using these lists of fixed and reduced heterozygosity loci in the *early* and *late* chronotypes, I proceeded to analyse the predicted effects of these SNPs using the tool SnpEff (Cingolani et al., 2012); and then I performed gene ontology analyses to identify functional roles of these loci in different phenotypes of my interest using g:Profiler (Reimand et al., 2007). It is important to note here that percentage of SNPs that get categorized into different categories amount to more than 100%. There could be several reasons for this i.e., (i) several genes get categorized as having functional roles in more than one gene ontology categories, (ii) there may also be multiple SNPs in the same

gene, and (iii) I have manually curated the gene ontology categories and clubbed multiple categories into condensed functionally meaningful ones (Table 8.1.1). Therefore, sums of %SNPs in these condensed categories may add up to more than 100%, in some cases.

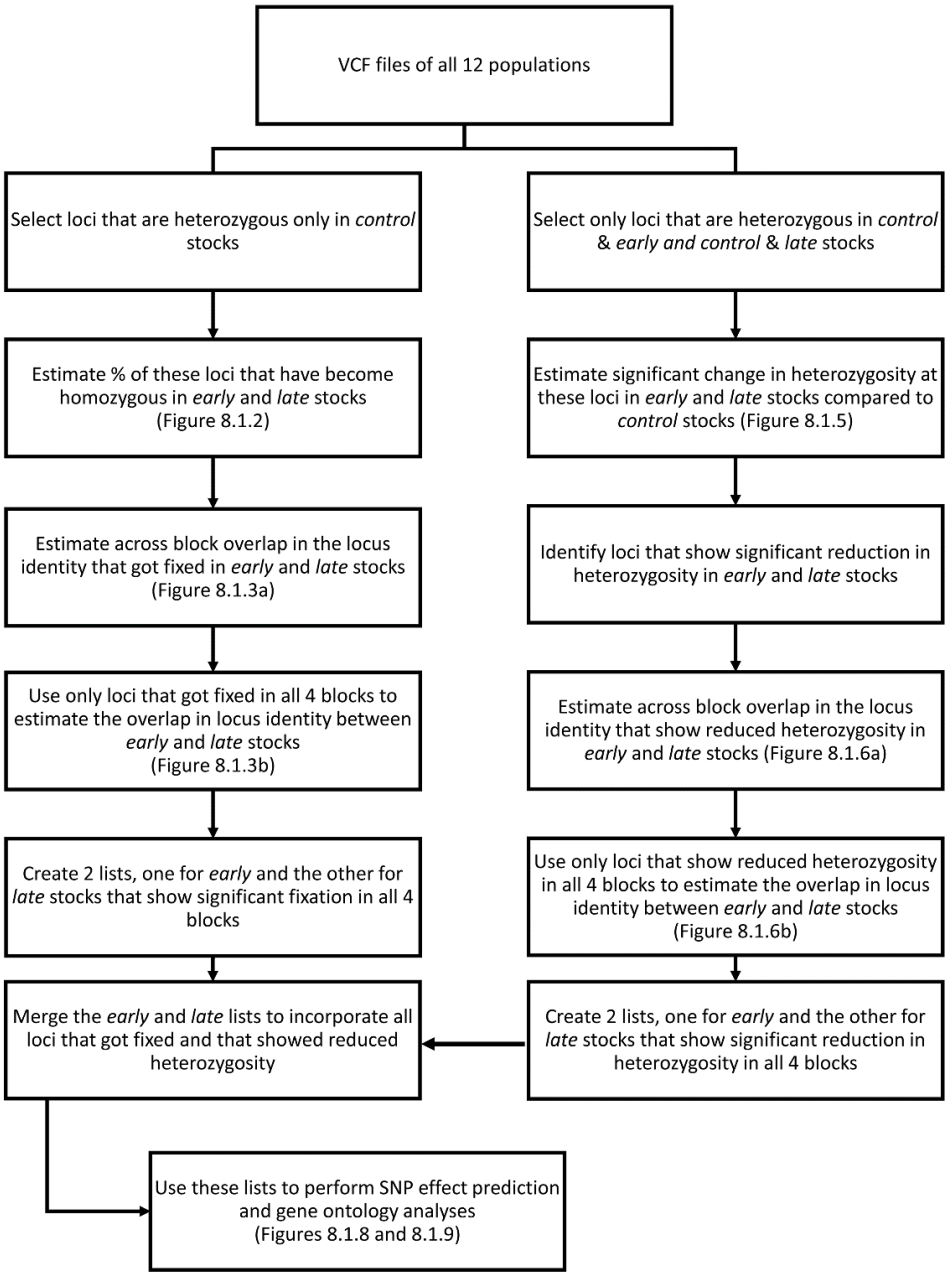

Figure 8.1.1: A schematic of the analysis workflow used to identify polymorphisms in loci associated with *early* and *late* adult eclosion chronotypes. See text for more details.

Table 8.1.1: Gene Ontology terms, the processes they are involved in and manual categories into which they are condensed.

GO Term	Process	Manual Categories
GO:0030048	actin filament-based movement	Cellular processes
GO:0043697	cell dedifferentiation	
GO:0048468	cell development	
GO:0030154	cell differentiation	
GO:0045165	cell fate commitment	
GO:0001709	cell fate determination	
GO:0001708	cell fate specification	
GO:0034330	cell junction organization	
GO:0045454	cell redox homeostasis	
GO:0198738	cell-cell signaling by wnt	
GO:0070887	cellular response to chemical stimulus	
GO:0071495	cellular response to endogenous stimulus	
GO:0104004	cellular response to environmental stimulus	
GO:0071496	cellular response to external stimulus	
GO:0031668	cellular response to extracellular stimulus	
GO:0033554	cellular response to stress	
GO:0007282	cystoblast division	
GO:0035234	ectopic germ cell programmed cell death	
GO:0035163	embryonic hemocyte differentiation	
GO:0050886	endocrine process	
GO:0045478	fusome organization	
GO:0035168	larval lymph gland hemocyte differentiation	
GO:1903046	meiotic cell cycle process	
GO:0051447	negative regulation of meiotic cell cycle	
GO:0009968	negative regulation of signal transduction	
GO:0097150	neuronal stem cell population maintenance	
GO:0016325	oocyte microtubule cytoskeleton organization	
GO:0008103	oocyte microtubule cytoskeleton polarization	
GO:0009967	positive regulation of signal transduction	
GO:0071805	potassium ion transmembrane transport	
GO:0001881	receptor recycling	
GO:0033628	regulation of cell adhesion mediated by integrin	
GO:0022407	regulation of cell-cell adhesion	
GO:0090287	regulation of cellular response to growth factor stimulus	
GO:1900076	regulation of cellular response to insulin stimulus	

GO:0035206	regulation of hemocyte proliferation	
GO:0010817	regulation of hormone levels	
GO:0051445	regulation of meiotic cell cycle	
GO:0001919	regulation of receptor recycling	
GO:0009966	regulation of signal transduction	
GO:0051037	regulation of transcription involved in meiotic cell cycle	
GO:0035019	somatic stem cell population maintenance	
GO:0017145	stem cell division	
GO:0008343	adult feeding behavior	Behavior
GO:0002118	aggressive behavior	
GO:0007635	chemosensory behavior	
GO:0030536	larval feeding behavior	
GO:2000253	positive regulation of feeding behavior	
GO:0060259	regulation of feeding behavior	
GO:0019098	reproductive behavior	
GO:0035176	social behavior	
GO:0042330	taxis	
GO:0008344	adult locomotory behavior	Locomotion
GO:0008345	larval locomotory behavior	
GO:0035641	locomotory exploration behavior	
GO:0090659	walking behavior	
GO:0097164	ammonium ion metabolic process	Metabolic processes
GO:1901135	carbohydrate derivative metabolic process	
GO:0005975	carbohydrate metabolic process	
GO:0018904	ether metabolic process	
GO:1901568	fatty acid derivative metabolic process	
GO:0006629	lipid metabolic process	
GO:0043170	macromolecule metabolic process	
GO:0032351	negative regulation of hormone metabolic process	
GO:1901360	organic cyclic compound metabolic process	
GO:1901615	organic hydroxy compound metabolic process	
GO:1901564	organonitrogen compound metabolic process	
GO:2001057	reactive nitrogen species metabolic process	
GO:0032350	regulation of hormone metabolic process	
GO:0044282	small molecule catabolic process	
GO:0006766	vitamin metabolic process	

GO:0048646	anatomical structure formation involved in morphogenesis	
GO:0071695	anatomical structure maturation	
GO:0030714	anterior/posterior axis specification, follicular epithelium	
GO:0048736	appendage development	
GO:0009798	axis specification	
GO:0010171	body morphogenesis	
GO:0040005	chitin-based cuticle attachment to epithelium	
GO:0007593	chitin-based cuticle sclerotization	
GO:0042335	cuticle development	
GO:0060560	developmental growth involved in morphogenesis	
GO:0071696	ectodermal placode development	
GO:0071697	ectodermal placode morphogenesis	
GO:0009790	embryo development	
GO:0009880	embryonic pattern specification	
GO:0007164	establishment of tissue polarity	
GO:0060322	head development	
GO:0035161	imaginal disc lineage restriction	
GO:0002165	instar larval or pupal development	Developmental processes
GO:0002164	larval development	
GO:0061138	morphogenesis of a branching epithelium	
GO:0010259	multicellular organism aging	
GO:0035264	multicellular organism growth	
GO:0061061	muscle structure development	
GO:0001748	optic lobe placode development	
GO:0035265	organ growth	
GO:0050931	pigment cell differentiation	
GO:0009886	post-embryonic animal morphogenesis	
GO:0031099	regeneration	
GO:0003002	regionalization	
GO:2000026	regulation of multicellular organismal development	
GO:0048608	reproductive structure development	
GO:0007379	segment specification	
GO:0009799	specification of symmetry	
GO:0048731	system development	
GO:0009888	tissue development	
GO:0048729	tissue morphogenesis	
GO:0035295	tube development	

GO:0048512	circadian behavior	Circadian
GO:0009649	entrainment of circadian clock	
GO:0045938	positive regulation of circadian sleep/wake cycle, sleep	
GO:0010841	positive regulation of circadian sleep/wake cycle, wakefulness	
GO:0042749	regulation of circadian sleep/wake cycle	
GO:1904059	regulation of locomotor rhythm	
GO:0060086	circadian temperature homeostasis	Temperature Homeostasis
GO:0001659	temperature homeostasis	
GO:0006952	defense response	Defense responses
GO:0006959	humoral immune response	
GO:0045087	innate immune response	
GO:0002251	organ or tissue specific immune response	
GO:0031349	positive regulation of defense response	
GO:1903036	positive regulation of response to wounding	
GO:0050776	regulation of immune response	
GO:0009611	response to wounding	
GO:0009582	detection of abiotic stimulus	Response to environmental stimulus
GO:0009593	detection of chemical stimulus	
GO:0009581	detection of external stimulus	
GO:0050906	detection of stimulus involved in sensory perception	
GO:0050921	positive regulation of chemotaxis	
GO:0032103	positive regulation of response to external stimulus	
GO:0050920	regulation of chemotaxis	
GO:0002831	regulation of response to biotic stimulus	
GO:0032101	regulation of response to external stimulus	
GO:0001101	response to acid chemical	
GO:0046677	response to antibiotic	
GO:0042493	response to drug	
GO:0051602	response to electrical stimulus	
GO:0043207	response to external biotic stimulus	
GO:0009991	response to extracellular stimulus	
GO:0009629	response to gravity	
GO:0055093	response to hyperoxia	
GO:0001666	response to hypoxia	

GO:0010035	response to inorganic substance	
GO:0009612	response to mechanical stimulus	
GO:1901698	response to nitrogen compound	
GO:0010033	response to organic substance	
GO:0006970	response to osmotic stress	
GO:0006979	response to oxidative stress	
GO:0070482	response to oxygen levels	
GO:1901700	response to oxygen-containing compound	
GO:0009268	response to pH	
GO:0009314	response to radiation	
GO:0042594	response to starvation	
GO:0009636	response to toxic substance	
GO:0009410	response to xenobiotic stimulus	
GO:0008069	dorsal/ventral axis specification, ovarian follicular epithelium	Reproductive Physiology
GO:0007306	eggshell chorion assembly	
GO:0007307	eggshell chorion gene amplification	
GO:0048135	female germ-line cyst formation	
GO:0007301	female germline ring canal formation	
GO:0007281	germ cell development	
GO:0008354	germ cell migration	
GO:0007294	germarium-derived oocyte fate determination	
GO:0030725	germline ring canal formation	
GO:0042078	germ-line stem cell division	
GO:0030718	germ-line stem cell population maintenance	
GO:0035262	gonad morphogenesis	
GO:0035188	hatching	
GO:0007320	insemination	
GO:0007618	mating	
GO:0007308	oocyte construction	
GO:0009994	oocyte differentiation	
GO:0048601	oocyte morphogenesis	
GO:0030707	ovarian follicle cell development	
GO:0007297	ovarian follicle cell migration	
GO:0030713	ovarian follicle cell stalk formation	
GO:0007277	pole cell development	
GO:0007315	pole plasm assembly	
GO:0019094	pole plasm mRNA localization	
GO:1905881	positive regulation of oogenesis	
GO:0007530	sex determination	

GO:0007548	sex differentiation	
GO:0048071	sex-specific pigmentation	
GO:0019953	sexual reproduction	
GO:0007338	single fertilization	
GO:0035092	sperm chromatin condensation	
GO:0046692	sperm competition	
GO:0048515	spermatid differentiation	
GO:0007289	spermatid nucleus differentiation	
GO:0048137	spermatocyte division	
GO:0007284	spermatogonial cell division	
GO:0018990	ecdysis, chitin-based cuticle	Eclosion
GO:0007562	eclosion	
GO:0007552	metamorphosis	
GO:0007591	molting cycle, chitin-based cuticle	
GO:0048069	eye pigmentation	Eye physiology
GO:0016318	ommatidial rotation	
GO:0048073	regulation of eye pigmentation	
GO:0045468	regulation of R8 cell spacing in compound eye	
GO:0050877	nervous system process	Neuronal processes
GO:0070050	neuron cellular homeostasis	
GO:0070997	neuron death	
GO:0050806	positive regulation of synaptic transmission	
GO:1990709	presynaptic active zone organization	
GO:0060004	reflex	
GO:0042391	regulation of membrane potential	
GO:0001505	regulation of neurotransmitter levels	
GO:0099177	regulation of trans-synaptic signaling	
GO:0050808	synapse organization	
GO:0051124	synaptic growth at neuromuscular junction	
GO:0099536	synaptic signaling	
GO:0019226	transmission of nerve impulse	
GO:0009409	response to cold	Response to temeprature
GO:0009408	response to heat	
GO:0009266	response to temperature stimulus	
GO:0001964	startle response	Startle

8.1.3. Results and Discussion

8.1.3.1. Analyses of homozygous loci in *early* and *late* chronotypes

Firstly, I found that the genome-wide percentage of fixation was higher in the *early* chronotypes (10.51%) than the *late* chronotypes (6.23%; Figure 8.1.2). Further, I found that in the *early* chronotypes percentage fixation was higher in the *X*-chromosome (16.18%) than in the other chromosomal arms (2L: 9.33%; 2R: 11.24%; 3L: 6.91%; 3R: 8.91%; Figure 8.1.2). Similarly, in the *late* chronotypes as well, percentage fixation was higher in the *X*-chromosome (9.75%), relative to the other arms (2L: 5.94%; 2R: 5.39%; 3L: 5.08%; 3R: 4.97%; Figure 8.1.2). With reference to autosomes, the uniformity in percentage fixation values across most chromosomal arms in the *late* chronotypes and the particularly higher percentage fixation in the right arm of the 2nd chromosome in the *early* chronotypes suggest that selection may have acted differently in this arm for *early* and *late* chronotypes.

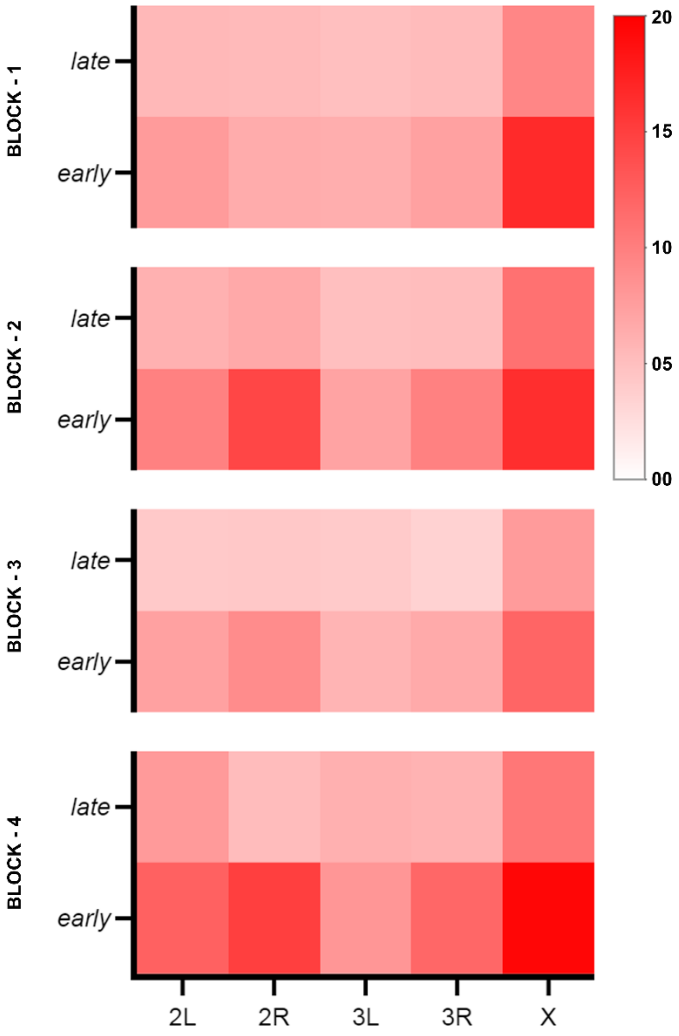

Figure 8.1.2: Percentage fixation of alleles across the major chromosome arms and all four replicate populations of *early* and *late* chronotypes. Darker the shade of red, higher the percentage of loci that got fixed.

Next, to assess the extent of similarity in genetic trajectories of replicate populations to achieve their *early* and *late* phenotypes, I examined block-to-block overlap in loci that were considered as fixed. It is clear that there is less than 1.5% overlap between all four replicate populations for both *early* and *late* chronotypes (Figures 8.1.3a and 8.1.4, right). After accounting for differences in the total number of loci that were considered fixed (Figure 8.1.4, left), I found that the percentage of overlap between all four replication populations was ~6 times lower in the *late* chronotypes than

that in the *early* chronotypes (Figure 8.1.4, right). These results raise three very interesting possibilities: (i) either stronger selection in the *late* chronotypes (as judged by the fact that the selection window is further away from the mean timing of eclosion of *control* populations, in the *late* flies as compared to the *early* flies; see Chapter 2) has driven increased divergence in the genetic trajectories taken by the *late* chronotypes to achieve the goal of delayed phase of entrainment or (ii) to begin with, the genetic targets of selection were different between the *early* and *late* chronotypes and therefore divergent trajectories appear to have been taken, or (iii) some combination of the above two. Subsequently, I analysed the extent of overlap in fixed loci between *early* and *late* chronotypes and found that across all chromosome arms, the extent of overlap between the two stocks was minimal suggesting that the second possibility may be true, i.e., targets of selection are perhaps different between *early* and *late* chronotypes (Figure 8.1.3b).

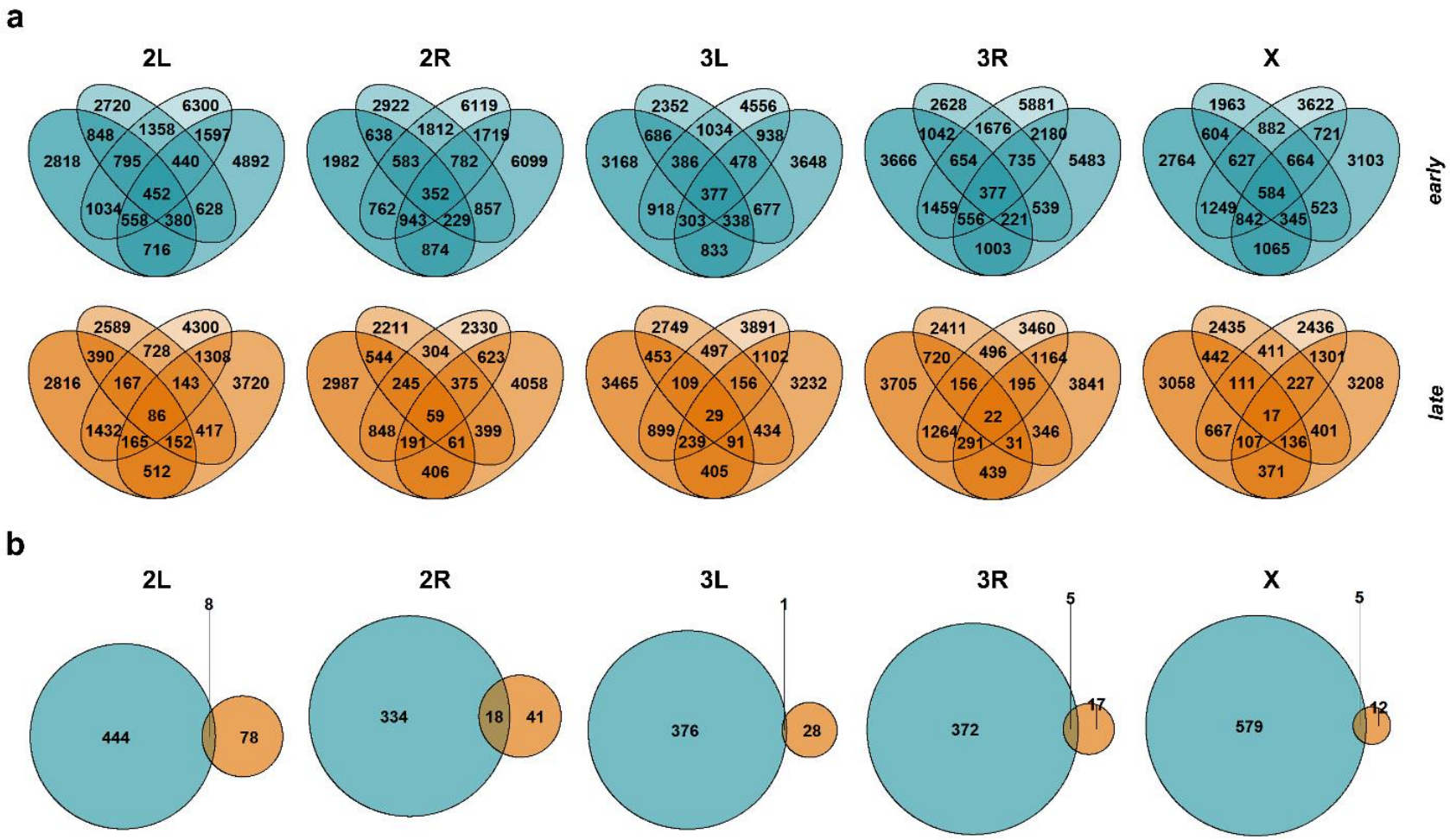

Figure 8.1.3: Panel (a) displays the extent of block-to-block overlap in loci that were considered fixed in comparison to *control* populations, in *early* stocks (top) and in the *late* stocks (bottom) for all major chromosome arms. Each ellipse represents one replicate block in both cases, and the number within each section is the number of fixed loci. Also shown is the extent of overlap between *early* and *late* chronotypes of loci that have been fixed in all four blocks (b).

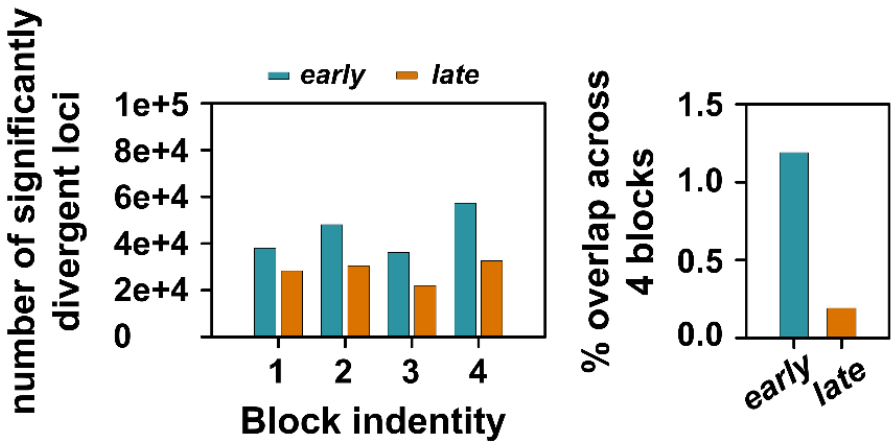

Figure 8.1.4: Number of loci that are fixed in each of the four replicate blocks of *early* and *late* chronotypes (left) and the percentage of all fixed loci that overlap between all four blocks (right).

8.1.3.2. Analyses of heterozygous loci in *early* and *late* chronotypes

Owing to the fact that my judgement of whether or not loci were fixed was based on an arbitrary cut-off, I used all loci that got categorised as heterozygous in my subsequent analyses of variants. Using the FET, I identified loci that showed significantly reduced heterozygosity (also referred to as allelic/nucleotide diversity, henceforth) in *early* and *late* chronotypes, compared to that in the *control* populations. The patterns of peaks of significantly differentiated loci are clearly different across *early* and *late* stocks, and also highly variable across replicate populations (Figure 8.1.5).

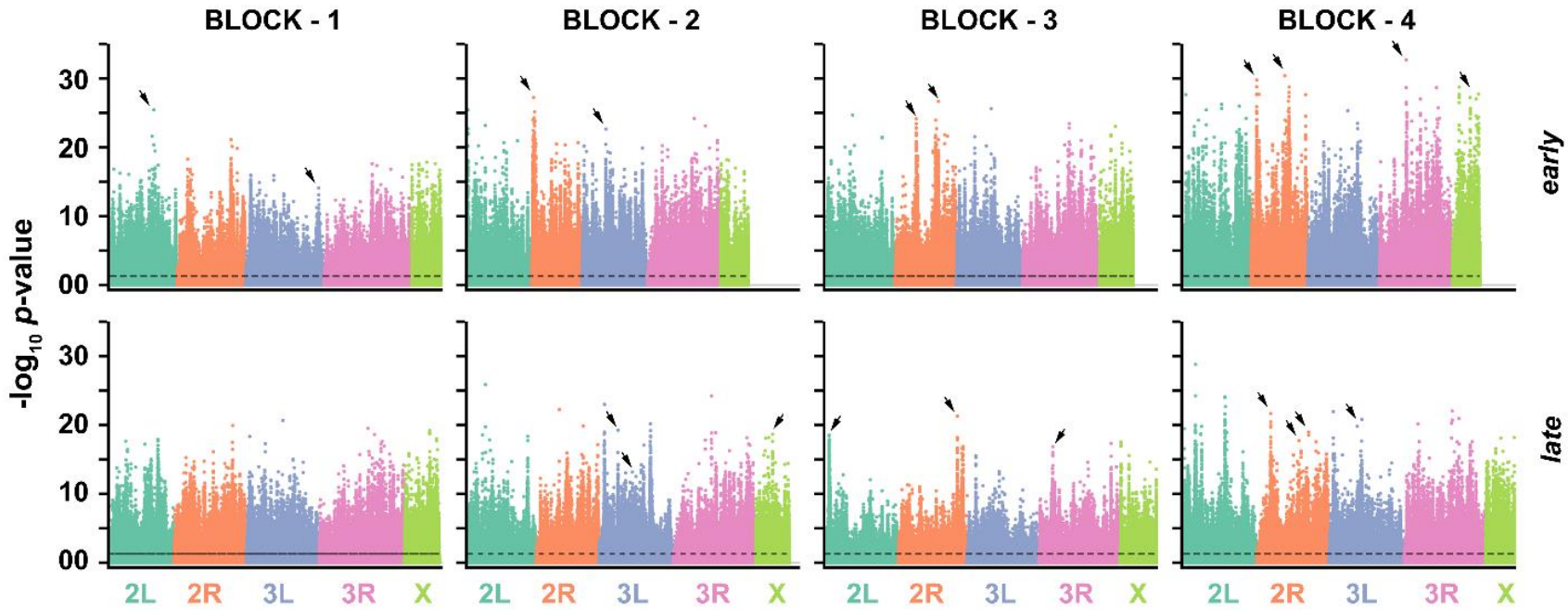

Figure 8.1.5: Manhattan plots for all replicate blocks of *early* and *late* chronotypes. The *p*-values are obtained from a Fisher's Exact Test and adjusted for the net Type-I error to be fixed at 5% using a Benjamini-Hochberg correction. Note the distinct block-to-block variation in the peaks and for the same block across *early* and *late* chronotypes. The black arrowheads are meant to point at peaks that are different compared to their counterparts in other replicate blocks.

In case of the *early* chronotypes, while the average number of loci with significantly reduced allelic diversity across blocks amounted to about 79,294 SNPs only 964 among them overlapped between the four blocks, making the overlap only 0.3% (Figures 8.1.6, top and 8.1.7). On the other hand, in case of the *late* chronotypes, while the across-block average number of significantly differentiated loci amounted to ~66,480 SNPs, only 0.09% (247 SNPs) of these overlapped in all four blocks (Figures 8.1.6, top and 8.1.7). These results are similar to the results presented in case of the fixed loci, in that there is greater divergence in the genomic trajectories taken by the *late* stocks to achieve their phenotype of delayed entrainment phase, in comparison to that of the *early* stocks. Further, when I examined the extent of overlap between *early* and *late* chronotypes of loci with reduced heterozygosity, I found that, again, there was minimal overlap between the two chronotypes. Results from both the fixed loci and the ones with reduced heterozygosity appear to suggest that selection on timing of behaviour acted on different targets, and therefore different standing genetic variation of the ancestral *control* populations.

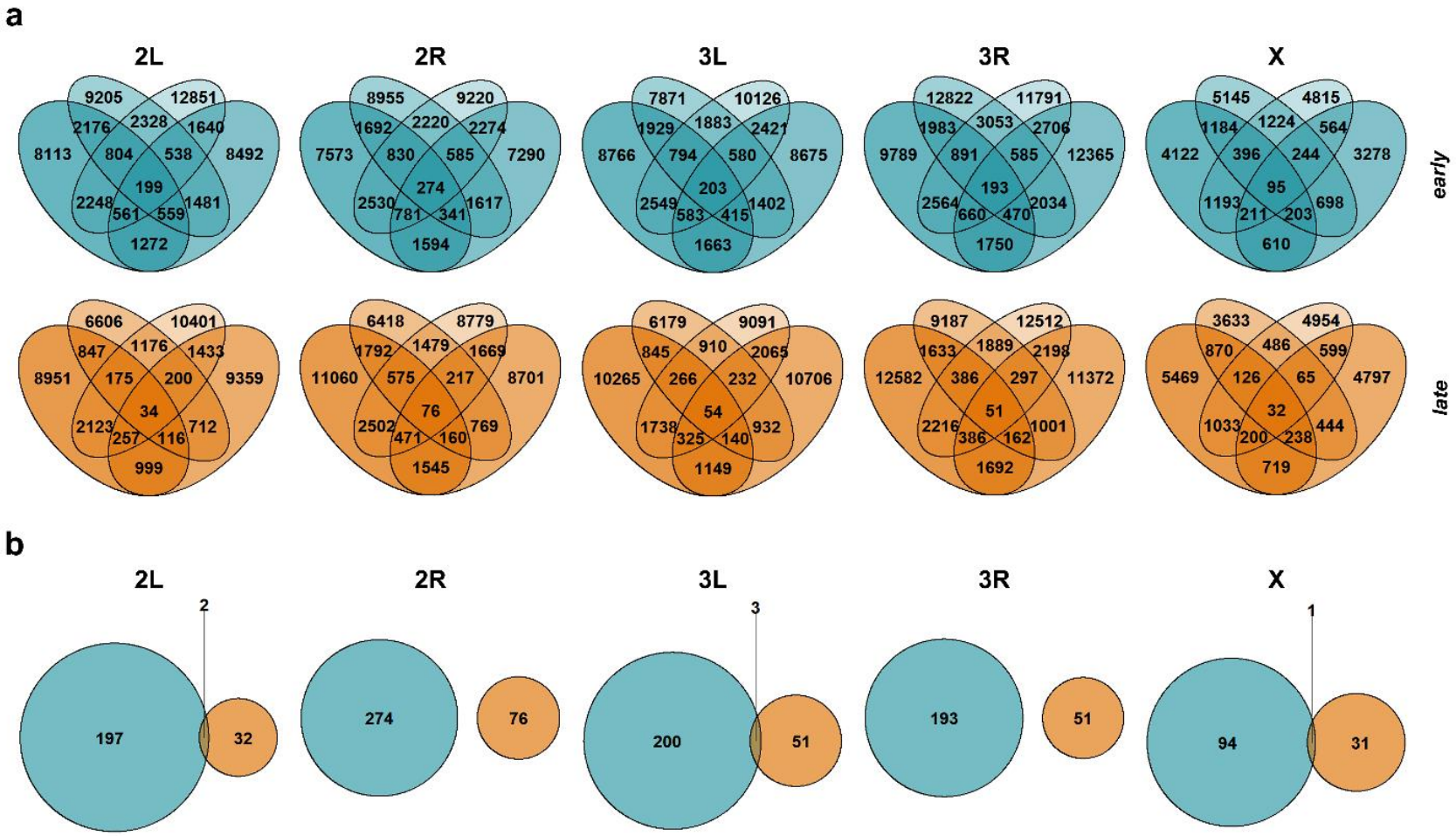

Figure 8.1.6: Panel (a) displays the extent of block-to-block overlap in loci that showed significantly reduced allelic diversity as compared to *control* populations, in *early* stocks (top) and in the *late* stocks (bottom) for all major chromosome arms. Each ellipse represents one replicate block in both cases, and the number within each section is the number of loci with reduced nucleotide variation. Also shown is the extent of overlap between *early* and *late* chronotypes of loci that show reduced diversity in all four blocks (b).

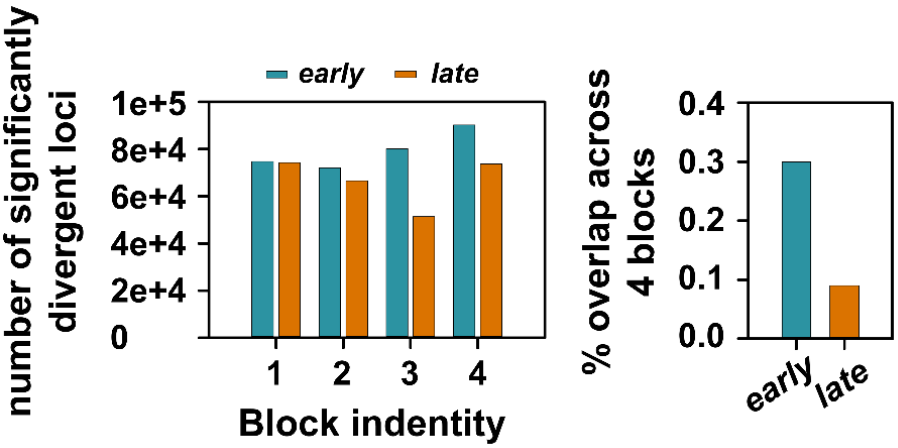

Figure 8.1.7: Number of loci that show significantly reduced nucleotide variation in each of the four replicate blocks of *early* and *late* chronotypes (left) and the percentage of all loci that show reduced diversity overlapping between all four blocks (right).

8.1.3.3. SNP effect prediction and gene ontology analyses

I pooled all the loci that were categorised as fixed and had significantly reduced nucleotide diversity that overlapped across all four blocks and created two lists, i.e., one that were exclusively altered in the *early* chronotypes and one in which they were exclusively differentiated in the *late* stocks. I used these to identify effects these variants have on, for instance, amino acid substitution leading to putative changes in protein structure and function. I found that the proportion of SNPs that have low, moderate or high effects on protein function are similar in the *early* and *late* chronotypes. Further, the percentage of SNPs that are categorised as modifiers (variants that may have regulatory effects on the protein function) were also similar between the two stocks (Figure 8.1.8). I subsequently, performed gene ontology analyses and found that a larger proportion of these SNPs were predicted to be involved in regulating developmental processes and eclosion in the *late* chronotypes than the *early* chronotypes (Figure 8.1.9, top and bottom; Table 8.1.2). There was significant reduction in allelic diversity at loci belonging to genes that regulate embryonic and larval morphogenesis, pattern formation, eye-antennal disc morphogenesis, neuronal remodelling,

axon pathfinding, wing vein, and tracheal and compound eye development in both the *early* and *late* chronotypes, albeit in different SNPs. Further, allelic differentiation in loci affecting chitin-based cuticle formation at different life-stages were higher in *early* than in *late* chronotypes. Moreover, while there were a few genes that trigger/regulate ecdysis signalling and/or response and play a role in the ecdysone biosynthetic process that showed differentiated allelic diversity in the *early* chronotypes, in the *late* chronotypes there were only two genes that showed some functional association with ecdysone. Interestingly, these two genes (*Kruppel homolog 1* and *Ecdysone-induced protein 74EF*) were the ones that also had a role to play in pupal photoreceptor maturation and pupa formation; none of the genes in the list of *early* chronotypes that affected eclosion have annotated functions in pupal stages (Table 8.1.2), although it may be possible that some genes in other categories have roles in pupariation.

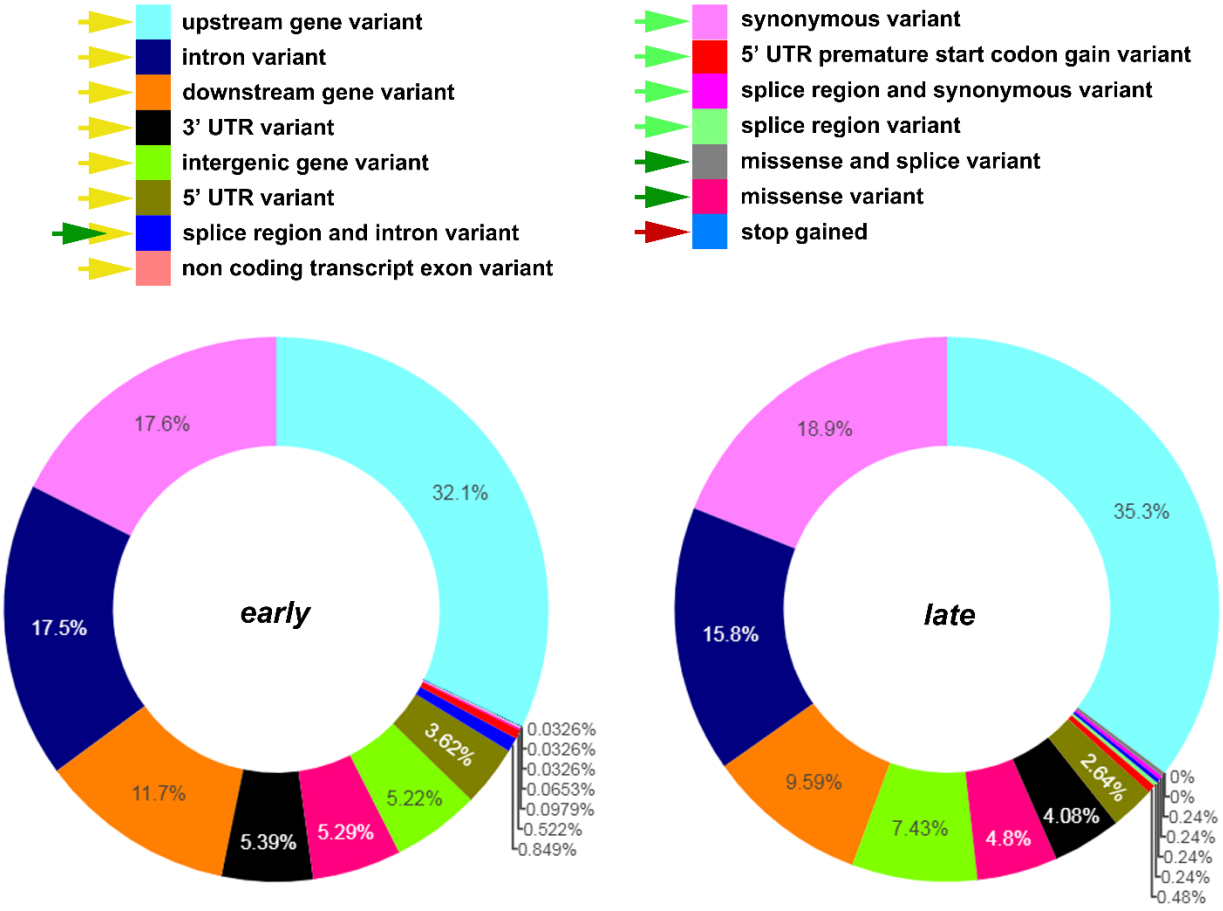

Figure 8.1.8: Percentages of SNP effects and the predicted strengths of these effects in the *early* (left) and *late* (right) chronotypes. Yellow arrowheads in the legend refer to variants that are predicted to have modifier effects; the light green, dark green and red arrowheads in the legend indicate variants that are predicted to have low, moderate and high effects, respectively.

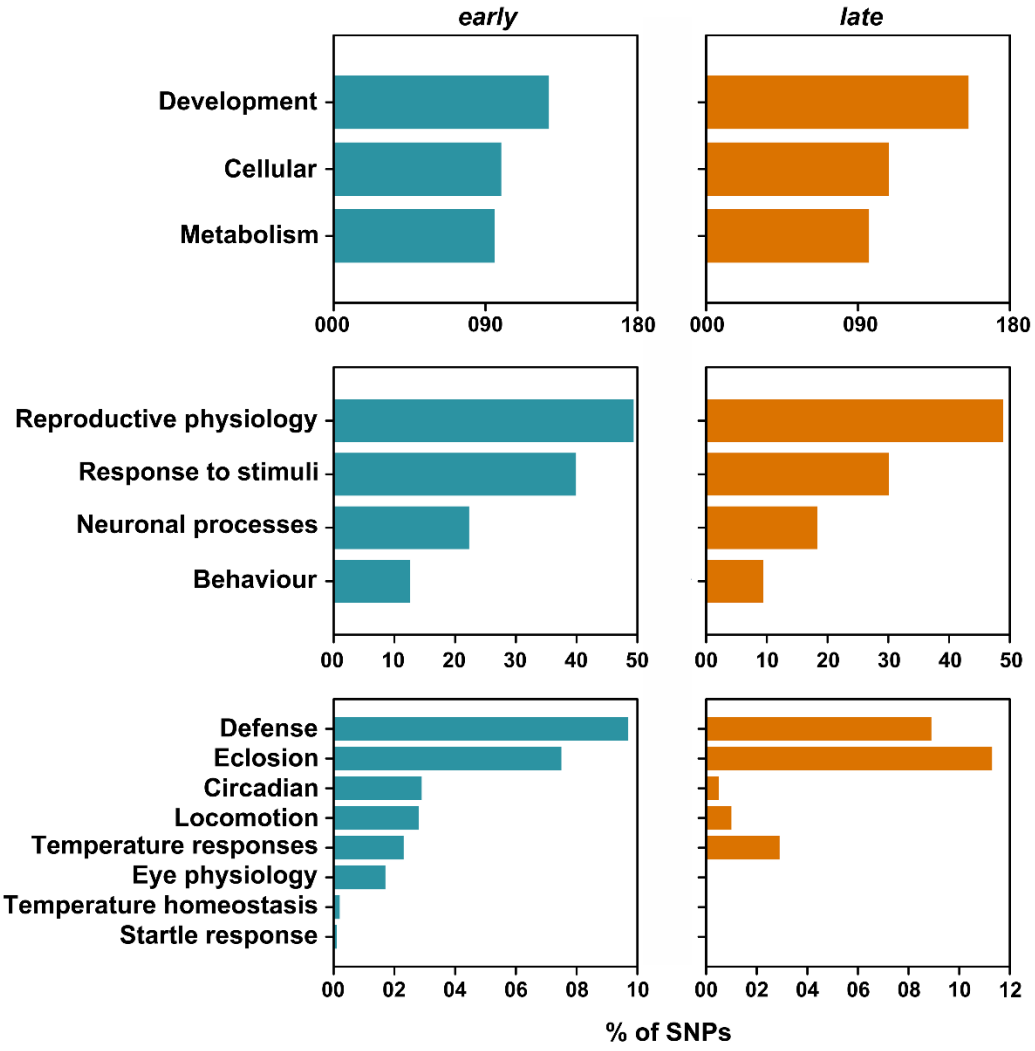

Figure 8.1.9: Percentage of SNPs that contribute to different biological processes in the *early* (left) and *late* (right) chronotypes.

Subsequently, I found that there was only one gene (*Casein kinase II beta subunit; CkII-β*) in the circadian category in which the SNP showed reduced diversity in the *late* stocks, as opposed to the *early* stocks wherein there were differentiated SNPs in about 13 genes (Figure 8.1.9; Table 8.1.2). *CkII-β* is known to contribute to long circadian period in *Drosophila* (Akten et al., 2003) and therefore, it is possible that differentiation of allelic frequency at this locus may be responsible for the longer circadian period in our *late* chronotypes relative to *control* and *early* stocks. In the

early chronotypes, on the other hand, several other genes that have a role in period length (*spaghetti*: Means et al., 2015; *shaggy*: Martinek et al., 2001), phasing of activity rhythm peaks (*Pigment-dispersing factor*: Lin et al., 2004; *Pigment-dispersing factor receptor*: Lear et al., 2005; *Ion transport peptide*: Johard et al., 2009), neuronal resting potential (*Mid1 ortholog*: Ghezzi et al., 2014; *Shaker*: Cirelli et al., 2005), levels of sleep (*5-hydroxytryptamine receptor 1A*: Yuan et al., 2006), and phase of sleep onset (*wide awake*: Liu et al., 2014) showed differentiation of allele frequencies. Importantly, several earlier studies from our laboratory (and this thesis) have shown that the circadian clock network in *late* chronotypes has differed in more than just period length (Abhilash et al., 2019; Nikhil, Vaze et al., 2016; Vaze, Nikhil et al., 2012). These results, therefore, imply that there must be undiscovered roles for many genes in regulating features of clock driven behaviours; and our dataset will serve as a resource for interested researchers to identify roles for genes in aspects of the clock network, such as inter-oscillator coupling, amplitude regulation etc.

Given that another important behaviour that we use to monitor the output of circadian systems in *Drosophila* is the locomotor activity rhythm, I examined SNPs that affect locomotion and found that a higher percentage of SNPs implicated in regulating locomotion differentiated in the *early* chronotypes, relative to that in the *late* chronotypes (Figure 8.1.9). While 21 genes had SNPs that differentiated in the *early* flies, only two were differentiated in the *late* chronotypes. Among these two, one is implicated in larval locomotion (*Calpain-A*) and the other in adult walking behaviour (*highwire*; Table 8.1.2). Interestingly, one of the genes implicated under locomotion was *TRPγ* (*Transient receptor potential cation channel gamma*). This gene, although got listed under locomotion, has general roles in detection of light stimulus involved in visual perception and response to light stimulus (Voets and Nilius, 2003; Xu et al., 2000). Owing to the window of selection (see Chapter 2), it is reasonable to think that light sensitivity in the *early* flies may have

evolved. Further, earlier experiments from our laboratory have suggested the clock photosensitivity may have differentially evolved in our *early* and *late* chronotypes (Nikhil, Vaze et al., 2016; Vaze, Nikhil et al., 2012; see also Chapter 6). To understand the genetic signatures of such phenotypes, in addition to the aforementioned *TRPγ*, I examined genes implicated in regulating eye physiology. Interestingly, I found that in the *early* chronotypes, 13 genes were implicated in eye physiology, whereas there were none in the *late* chronotypes (Figure 8.1.9; Table 8.1.2). These genes in the *early* flies have known roles to play in eye pigment biogenesis (*ruby*: Mullins et al., 2000), ommochrome biosynthesis (*cardinal, carmine*: Tearle, 1991) and ommatidial rotation (*scabrous*: Chou and Chien, 2002; *friend of echinoid*: Fetting et al., 2009), thereby suggesting that evolution of light sensitivity differences between *early* and *late* chronotypes may have occurred through allelic changes in these loci. However, this is only speculation and needs further validation. It is important to note here that *scabrous* also gets listed as a gene regulating eclosion in the *early* chronotypes (Table 8.1.2), thereby indicating that the eclosion rhythms of *early* chronotypes may show enhanced light sensitivity, perhaps via this gene as well. Moreover, *ninaC* (*neither inactivation nor afterpotential C*), a gene implicated in phototransduction and responses to light stimulus (Porter and Montell, 1993) also showed significant changes in allele diversity, in case of *early* chronotypes. Preliminary results from our laboratory indicate enhanced immediate responses to light in case of eclosion rhythms (*Arijit Ghosh and Vasu Sheeba, unpublished data*), and changes in the *ninaC* locus may underlie such differences.

Subsequently, due to my results of evolution of differential sensitivity of the clock to temperature cues in *early* and *late* chronotypes (Abhilash et al., 2019; and other results reported in this thesis), I analysed the genes listed under the responses to temperature category and found that although there is no difference in the percentage of SNPs that differentiated in terms of temperature

responses between *early* and *late* stocks, there were SNPs that affected temperature homeostasis in *early* chronotypes (*Pigment-dispersing factor receptor* or *Pdfr*: Head et al., 2015), while there were none in that category in the *late* chronotypes (Figure 8.1.9; Table 8.1.2). Although most of these genes are implicated in temperature responses in the adult fly, it may be possible that these genes may also play a role in the differential temperature responses in the eclosion rhythm of *early* and *late* chronotypes as reported in Chapter 3. In addition to the aforementioned categories, differences in the percentage of SNPs showing allelic differentiation in *early* and *late* chronotypes were also found in the response to stimulus, other behaviours, neuronal processes and defence categories, a detailed list of genes in each of which are appended below (Table 8.1.2).

Table 8.1.2: List of genes in which the allelic diversity is significantly differentiated in the *early* and *late* chronotypes.

early	***late***
Eclosion	
crossveinless 2 (cv-2)	Casein kinase II beta subunit (CkIIbeta)
Exchange factor for Arf 6 ortholog (*H. sapiens*) (Efa6)	short stop (shot)
alan shepard (shep)	Kruppel homolog 1 (Kr-h1)
absent, small, or homeotic discs 2 (ash2)	Death-associated inhibitor of apoptosis 1 (Diap1)
shotgun (shg)	CG9357 gene product from transcript CG9357-RA (Cht8)
mirror (mirr)	held out wings (how)
hephaestus (heph)	invected (inv)
Wnt oncogene analog 6 (Wnt6)	rutabaga (rut)
G protein-coupled receptor kinase 2 (Gprk2)	plexus (px)
debris buster (dsb)	Death-associated protein kinase related (Drak)
frizzled (fz)	Ecdysone-induced protein 74EF (Eip74EF)
Raf oncogene (Raf)	coracle (cora)
Hugin (Hug)	dumpy (dpy)
Calmodulin (Cam)	Gliotactin (Gli)
Rho GTPase activating protein at 54D (RhoGAP54D)	Cyclin E (CycE)
scribbled (scrib)	off-track (otk)
Autophagy-related 7 (Atg7)	Guanine nucleotide exchange factor in mesoderm (GEFmeso)
Imaginal disc growth factor 1 (Idgf1)	spaghetti-squash activator (sqa)
Distal-less (Dll)	hedgehog (hh)
mastermind (mam)	engrailed (en)
Ataxin-2 binding protein 1 (A2bp1)	dacapo (dap)
Guanine nucleotide exchange factor in mesoderm (GEFmeso)	
Imaginal disc growth factor 3 (Idgf3)	
Hormone receptor-like in 46 (Hr46)	
Protein kinase, cAMP-dependent, catalytic subunit 3 (Pka-C3)	
eyes absent (eya)	
slowdown (slow)	
shaggy (sgg)	
Dystrophin (Dys)	

Serrate (Ser)	
held out wings (how)	
plexus (px)	
Epidermal growth factor receptor (Egfr)	
four-jointed (fj)	
Death-associated protein kinase related (Drak)	
escargot (esg)	
piopio (pio)	
scabrous (sca)	
Fish-lips (Fili)	
Autophagy-related 6 (Atg6)	
ultraspiracle (usp)	
CG8201 gene product from transcript CG8201-RV (par-1)	
Protein tyrosine phosphatase 52F (Ptp52F)	
CG43658 gene product from transcript CG43658-RE (CG43658)	
Matrix metalloproteinase 1 (Mmp1)	
Ephexin (Exn)	
enhanced adult sensory threshold (east)	
frizzled 2 (fz2)	
blistered (bs)	
Ecdysone receptor (EcR)	
Pigment-dispersing factor (Pdf)	
roughex (rux)	
Notch (N)	
Lipin (Lpin)	
CG42674 gene product from transcript CG42674-RF (CG42674)	
off-track (otk)	
abrupt (ab)	
drumstick (drm)	
Rho guanine nucleotide exchange factor at 64C (RhoGEF64C)	
fruitless (fru)	
CG6831 gene product from transcript CG6831-RB (rhea)	
Circadian	
spaghetti (spag)	Casein kinase II beta subunit (CkIIbeta)
Pigment-dispersing factor receptor (Pdfr)	

shaggy (sgg)	
Ion transport peptide (ITP)	
5-hydroxytryptamine (serotonin) receptor 1A (5-HT1A)	
Mid1 ortholog (*S. cerevisiae*) (Mid1)	
Ecdysone receptor (EcR)	
Shaker (Sh)	
Adenosine deaminase acting on RNA (Adar)	
wide awake (wake)	
Pigment-dispersing factor (Pdf)	
dunce (dnc)	
Dopamine N acetyltransferase (Dat)	
Locomotion	
Myosuppressin receptor 1 (MsR1)	Calpain-A (CalpA)
Myosuppressin receptor 2 (MsR2)	highwire (hiw)
Shaker (Sh)	
Ecdysone receptor (EcR)	
alan shepard (shep)	
FMRFamide Receptor (FMRFaR)	
beethoven (btv)	
CG10671 gene product from transcript CG10671-RA (CG10671)	
kurtz (krz)	
bruchpilot (brp)	
jim lovell (lov)	
alpha actinin (Actn)	
CG1349 gene product from transcript CG1349-RB (dj-1beta)	
Excitatory amino acid transporter 1 (Eaat1)	
Sarco/endoplasmic reticulum Ca(2+)-ATPase (SERCA)	
G protein alpha q subunit (Galphaq)	
Adenosine deaminase acting on RNA (Adar)	
amontillado (amon)	
tiwaz (twz)	
Mitochondrial assembly regulatory factor (Marf)	
Transient receptor potential cation channel gamma (Trpgamma)	
Eye Physiology	
pebbled (peb)	frizzled (fz)

Epidermal growth factor receptor (Egfr)	escargot (esg)
shotgun (shg)	friend of echinoid (fred)
Cadherin-N (CadN)	
Cadherin-N2 (CadN2)	
escargot (esg)	
scabrous (sca)	
Notch (N)	
ruby (rb)	
cardinal (cd)	
carmine (cm)	
friend of echinoid (fred)	
frizzled (fz)	
Temperature Sensitivity and Homeostasis	
mustard (mtd)	lethal (2) essential for life (l(2)efl)
Neprilysin 3 (Nep3)	mustard (mtd)
CG34362 gene product from transcript CG34362-RI (CG34362)	CG34362 gene product from transcript CG34362-RI (CG34362)
CG34356 gene product from transcript CG34356-RF (CG34356)	highwire (hiw)
CG7409 gene product from transcript CG7409-RA (CG7409)	rutabaga (rut)
Turandot M (TotM)	CG11321 gene product from transcript CG11321-RG (CG11321)
G protein alpha q subunit (Galphaq)	
Adenosine deaminase acting on RNA (Adar)	
dunce (dnc)	
CG6492 gene product from transcript CG6492-RB (Ucp4A)	
Calcineurin B (CanB)	
brivido-3 (brv3)	
Activating transcription factor-2 (Atf-2)	
CG8778 gene product from transcript CG8778-RA (CG8778)	
CG42261 gene product from transcript CG42261-RB (CG42261)	
Pigment-dispersing factor receptor (Pdfr)	
Behaviours	
Dishevelled Associated Activator of Morphogenesis (DAAM)	Toll (Tl)
milkah (mil)	short stop (shot)
tramtrack (ttk)	Netrin-B (NetB)
Shaker (Sh)	rutabaga (rut)

alan shepard (shep)	plexus (px)
shotgun (shg)	roundabout 2 (robo2)
Protein tyrosine phosphatase 99A (Ptp99A)	sequoia (seq)
beethoven (btv)	jelly belly (jeb)
minibrain (mnb)	gryzun (gry)
mirror (mirr)	arrest (aret)
CG34387 gene product from transcript CG34387-RF (futsch)	NADH dehydrogenase (ubiquinone) 20 kDa subunit-like (ND-20L)
Ionotropic receptor 64a (Ir64a)	hu li tai shao (hts)
jim lovell (lov)	enoki mushroom (enok)
Fasciclin 3 (Fas3)	off-track (otk)
Accessory gland protein 36DE (Acp36DE)	Abelson interacting protein (Abi)
hattifattener (haf)	hedgehog (hh)
chromosome bows (chb)	engrailed (en)
Tachykinin-like receptor at 86C (TkR86C)	CG33197 gene product from transcript CG33197-RP (mbl)
dunce (dnc)	
Wnt oncogene analog 4 (Wnt4)	
lamina ancestor (lama)	
Netrin-A (NetA)	
frizzled (fz)	
Protein tyrosine phosphatase 4E (Ptp4E)	
Ejaculatory bulb protein (Ebp)	
Multiplexin (Mp)	
Hugin (Hug)	
caskin (ckn)	
Mid1 ortholog (*S. cerevisiae*) (Mid1)	
doublesex (dsx)	
Calmodulin (Cam)	
Sec15 ortholog (*S. cerevisiae*) (Sec15)	
scribbled (scrib)	
arrest (aret)	
Tiggrin (Tig)	
Distal-less (Dll)	
fra mauro (frma)	
smooth (sm)	
Na channel protein 60E (NaCP60E)	
boule (bol)	
eyes absent (eya)	

CG3638 gene product from transcript CG3638-RJ (CG3638)	
Juvenile hormone esterase (Jhe)	
shaggy (sgg)	
Neurotactin (Nrt)	
pou domain motif 3 (pdm3)	
pebbled (peb)	
Esterase 6 (Est-6)	
Tenascin major (Ten-m)	
plexus (px)	
Gustatory receptor 93b (Gr93b)	
Epidermal growth factor receptor (Egfr)	
CG15138 gene product from transcript CG15138-RB (beat-IIIc)	
CG18405 gene product from transcript CG18405-RE (Sema-1a)	
escargot (esg)	
Glutactin (Glt)	
Pigment-dispersing factor receptor (Pdfr)	
CG11711 gene product from transcript CG11711-RA (Mob2)	
punt (put)	
egghead (egh)	
G protein alpha q subunit (Galphaq)	
Spinophilin (Spn)	
Innexin 2 (Inx2)	
tiwaz (twz)	
Protein tyrosine phosphatase 52F (Ptp52F)	
FER ortholog (*H. sapiens*) (FER)	
Basigin (Bsg)	
radish (rad)	
Tachykinin-like receptor at 99D (TkR99D)	
short neuropeptide F receptor (sNPF-R)	
beta-Tubulin at 60D (betaTub60D)	
5-hydroxytryptamine (serotonin) receptor 7 (5-HT7)	
Gustatory receptor 98a (Gr98a)	
frizzled 2 (fz2)	
roundabout 2 (robo2)	
Cadherin-N (CadN)	
Pigment-dispersing factor (Pdf)	

Cadherin-N2 (CadN2)	
frazzled (fra)	
Notch (N)	
CG7725 gene product from transcript CG7725-RB (rogdi)	
sidestep (side)	
SoxNeuro (SoxN)	
brain tumor (brat)	
5-hydroxytryptamine (serotonin) receptor 1A (5-HT1A)	
off-track (otk)	
CG42684 gene product from transcript CG42684-RB (CG42684)	
abrupt (ab)	
Adenosine deaminase acting on RNA (Adar)	
Ejaculatory bulb protein II (EbpII)	
Gustatory receptor 93c (Gr93c)	
Rho guanine nucleotide exchange factor at 64C (RhoGEF64C)	
fruitless (fru)	
Defence	
CG12225 gene product from transcript CG12225-RA (Spt6)	Toll (Tl)
Mediator complex subunit 6 (MED6)	invected (inv)
shotgun (shg)	defense repressor 1 (dnr1)
CG11313 gene product from transcript CG11313-RC (CG11313)	hedgehog (hh)
puffyeye (puf)	bunched (bun)
CG8492 gene product from transcript CG8492-RD (CG8492)	mustard (mtd)
big bang (bbg)	Calpain-A (CalpA)
atypical protein kinase C (aPKC)	highwire (hiw)
kurtz (krz)	virus-induced RNA 1 (vir-1)
G protein-coupled receptor kinase 2 (Gprk2)	
bunched (bun)	
grapes (grp)	
CG13465 gene product from transcript CG13465-RA (CG13465)	
FMRFamide Receptor (FMRFaR)	
Neuropeptide-like precursor 2 (Nplp2)	
poor gastrulation (pog)	
18 wheeler (18w)	

Autophagy-related 7 (Atg7)	
CG12913 gene product from transcript CG12913-RB (CG12913)	
Imaginal disc growth factor 1 (Idgf1)	
thioredoxin-2 (Trx-2)	
Imaginal disc growth factor 3 (Idgf3)	
Ectoderm-expressed 4 (Ect4)	
Macroglobulin complement-related (Mcr)	
Mitochondrial trifunctional protein alpha subunit (Mtpalpha)	
eyes absent (eya)	
Activating transcription factor-2 (Atf-2)	
SH2 ankyrin repeat kinase (Shark)	
Epidermal growth factor receptor (Egfr)	
CG9715 gene product from transcript CG9715-RA (CG9715)	
eye transformer (et)	
Glutactin (Glt)	
Focal adhesion kinase (Fak)	
Autophagy-related 6 (Atg6)	
Limpet (Lmpt)	
Turandot M (TotM)	
G protein alpha q subunit (Galphaq)	
CG8201 gene product from transcript CG8201-RV (par-1)	
FER ortholog (*H. sapiens*) (FER)	
CG6890 gene product from transcript CG6890-RA (Tollo)	
CG9904 gene product from transcript CG9904-RA (Seipin)	
Matrix metalloproteinase 1 (Mmp1)	
Ephexin (Exn)	
Myosuppressin receptor 2 (MsR2)	
mustard (mtd)	
Notch (N)	
Hemolectin (Hml)	
WW domain containing oxidoreductase (Wwox)	
CG6509 gene product from transcript CG6509-RA (CG6509)	
Transglutaminase (Tg)	
beta amyloid protein precursor-like (Appl)	

Neuronal Processes	
Shaker (Sh)	Toll (Tl)
CG30296 gene product from transcript CG30296-RE (RIC-3)	hippo (hpo)
minibrain (mnb)	rutabaga (rut)
atypical protein kinase C (aPKC)	jelly belly (jeb)
Odorant-binding protein 22a (Obp22a)	Chemosensory protein B 42b (CheB42b)
gooseberry (gsb)	Synaptojanin (Synj)
Sarco/endoplasmic reticulum Ca(2+)-ATPase (SERCA)	gryzun (gry)
dunce (dnc)	mustard (mtd)
Chemosensory protein A 98a (CheB98a)	CG34362 gene product from transcript CG34362-RI (CG34362)
defective proboscis extension response 9 (dpr9)	Odorant receptor 83c (Or83c)
Calmodulin (Cam)	bruchpilot (brp)
Sec15 ortholog (*S. cerevisiae*) (Sec15)	Gliotactin (Gli)
Octopamine beta2 receptor (Octbeta2R)	Odorant receptor 45b (Or45b)
G protein beta-subunit 76C (Gbeta76C)	Abelson interacting protein (Abi)
CG18408 gene product from transcript CG18408-RI (CAP)	Odorant receptor 35a (Or35a)
scribbled (scrib)	engrailed (en)
Sec6 ortholog (*S. cerevisiae*) (Sec6)	nicotinic Acetylcholine Receptor beta1 (nAChRbeta1)
Fic domain-containing protein (Fic)	CG33197 gene product from transcript CG33197-RP (mbl)
Rab3 GTPase activating protein (Rab3-GAP)	highwire (hiw)
Neuropilin and tolloid-like (Neto)	CG6129 gene product from transcript CG6129-RE (Rootletin)
Na channel protein 60E (NaCP60E)	
Transient receptor potential cation channel gamma (Trpgamma)	
Dpr-interacting protein eta (DIP-eta)	
shaggy (sgg)	
Dystrophin (Dys)	
pou domain motif 3 (pdm3)	
Epidermal growth factor receptor (Egfr)	
Rhodopsin 4 (Rh4)	
Focal adhesion kinase (Fak)	
seven in absentia (sina)	
spaghetti (spag)	

bruchpilot (brp)	
Odorant receptor 59a (Or59a)	
Odorant receptor 45b (Or45b)	
Spinophilin (Spn)	
Phosphatidylinositol 4-kinase III alpha (PI4KIIIalpha)	
Sialyltransferase (ST6Gal)	
Ephexin (Exn)	
CG42261 gene product from transcript CG42261-RB (CG42261)	
Odorant receptor 65b (Or65b)	
blistered (bs)	
Dynein heavy chain at 36C (Dhc36C)	
frizzled 2 (fz2)	
Odorant receptor 65c (Or65c)	
Ecdysone receptor (EcR)	
nicotinic Acetylcholine Receptor alpha6 (nAChRalpha6)	
muscarinic Acetylcholine Receptor, A-type (mAChR-A)	
CG7725 gene product from transcript CG7725-RB (rogdi)	
Notch (N)	
CG6490 gene product from transcript CG6490-RD (plum)	
Odorant receptor 67a (Or67a)	
5-hydroxytryptamine (serotonin) receptor 1A (5-HT1A)	
Glutamate oxaloacetate transaminase 2 (Got2)	
CG43155 gene product from transcript CG43155-RC (CG43155)	
Gustatory receptor 97a (Gr97a)	
Ca[2+]-channel protein alpha[[1]] subunit T (Ca-alpha1T)	
beta amyloid protein precursor-like (Appl)	
milkah (mil)	
Furin 1 (Fur1)	
beethoven (btv)	
Succinic semialdehyde dehydrogenase (Ssadh)	
Arrestin 1 (Arr1)	

CG10671 gene product from transcript CG10671-RA (CG10671)	
Odorant receptor 2a (Or2a)	
Extended synaptotagmin-like protein 2 ortholog (*H. sapiens*) (Esyt2)	
neither inactivation nor afterpotential C (ninaC)	
defective proboscis extension response 8 (dpr8)	
CG34387 gene product from transcript CG34387-RF (futsch)	
Ionotropic receptor 64a (Ir64a)	
Fasciclin 3 (Fas3)	
Excitatory amino acid transporter 1 (Eaat1)	
Ankyrin 2 (Ank2)	
cardinal (cd)	
Ca2+-channel-protein-beta-subunit (Ca-beta)	
Calcineurin B (CanB)	
CG34362 gene product from transcript CG34362-RI (CG34362)	
Octopamine beta1 receptor (Octbeta1R)	
Ataxin-2 binding protein 1 (A2bp1)	
Ionotropic receptor 92a (Ir92a)	
Ectoderm-expressed 4 (Ect4)	
sugar-free frosting (sff)	
Neuroligin 4 (Nlg4)	
defective proboscis extension response 6 (dpr6)	
bazooka (baz)	
Retinal Homeobox (Rx)	
Tenascin major (Ten-m)	
pumilio (pum)	
Gustatory receptor 93b (Gr93b)	
Dopamine/Ecdysteroid receptor (DopEcR)	
Huntingtin-interacting protein 14 (Hip14)	
CG18405 gene product from transcript CG18405-RE (Sema-1a)	
Glutactin (Glt)	
CG4329 gene product from transcript CG4329-RA (CG4329)	

CG32381 gene product from transcript CG32381-RC (unc-13-4A)	
Dpr-interacting protein epsilon (DIP-epsilon)	
Nitric oxide synthase (Nos)	
CG11711 gene product from transcript CG11711-RA (Mob2)	
G protein alpha q subunit (Galphaq)	
CG8201 gene product from transcript CG8201-RV (par-1)	
no mechanoreceptor potential C (nompC)	
CG5675 gene product from transcript CG5675-RF (X11L)	
no extended memory (nemy)	
radish (rad)	
Tachykinin-like receptor at 99D (TkR99D)	
Gustatory receptor 98a (Gr98a)	
Stasimon (stas)	
mustard (mtd)	
Neprilysin 3 (Nep3)	
Arrestin 2 (Arr2)	
CG34356 gene product from transcript CG34356-RF (CG34356)	
NMDA receptor 2 (Nmdar2)	
brain tumor (brat)	
CG42594 gene product from transcript CG42594-RD (CG42594)	
defective proboscis extension response 5 (dpr5)	
Adenosine deaminase acting on RNA (Adar)	
Gustatory receptor 93c (Gr93c)	
Dopamine N acetyltransferase (Dat)	
CG6492 gene product from transcript CG6492-RB (Ucp4A)	

In summary, I found that the *late* stocks take more divergent trajectories to achieve evening eclosion than the *early* chronotypes take, to achieve morning eclosion. Further, the high degree of exclusivity between *early* and *late* chronotypes in the differentiated loci seem to suggest that the targets of morning and evening selection pressure were different. Moreover, *early* chronotypes

are associated with polymorphisms in loci implicated in eye development and physiology, responses to light and temperature stimuli, and several genes regulating circadian behaviour; whereas *late* chronotypes are associated with polymorphisms in loci implicated in pupal formation, pupal photoreceptor maturation and ecdysone biosynthesis. Importantly, although several behaviours are strongly affected in the *late* chronotypes, relative to *control* stocks, our data offers a unique set to explore undiscovered roles of genes in regulating circadian and other behaviours correlated with divergent timing of eclosion. To do this, current efforts are directed towards building gene interaction networks to identify enriched pathways and novel regulators of such behaviours. Further, although in this thesis I only report results from analyses of differentiated SNPs between *early* and *control* and *late* and *control* stocks, our sequencing experiment also provides information regarding insertions and deletions, and similar analyses of these are underway.

8.2. RhythmicAlly: Your R and Shiny based open-source ally for the analysis of biological rhythms

Parts of this chapter have been published in the following research article:

Abhilash L and Sheeba V (2019) RhythmicAlly: Your R and Shiny based open-source ally for the analysis of biological rhythms. Journal of Biological Rhythms, 34(5): 551–561.

Circadian clocks are thought to have evolved to equip organisms with two critical functions, namely measuring the passage of time and recognising local time. Together these two functions contribute to the organism's ability to capitalise on a temporal niche that may enhance its survival and reproduction (Nikhil and Sharma, 2017). As researchers, we are interested in asking how these functions differ within and across species, for a wide range of reasons. Commonly measured parameters to answer such questions, are period of the oscillation under constant conditions, day-to-day variability in period, robustness of rhythm, phase-relationship of the rhythm under different environmental conditions, day-to-day stability of these phase-relationships, and of course inter-individual variation in period and phases. While many of these quantifications require manual or semi-automated detection of phase, estimates of period and power can be largely derived through the use of time-series analyses (Refinetti et al., 2007).

Time-series analysis to estimate period and robustness of rhythm has been of considerable interest since the early days of research on circadian rhythms. Among the earliest used tools were Fourier analysis, ANOVA and the autocorrelation function (Mercer, 1960; Refinetti et al., 2007). Over the years, there has been much effort in modifying and adapting different tools to suit our needs which gave rise to the Enright or χ^2 periodogram (Enright, 1965; Sokolov and Bushell, 1978), COSINOR (Halberg et al., 1967), Lomb-Scargle (Lomb, 1976), Maximum Entropy Spectral Analysis (reviewed in Dowse, 2013) and more recently wavelet based analysis for estimating

periodicity and predicting phases of behaviour (Leise, 2013; Leise et al., 2013). These are only a few of the commonly used time-series methods. For a history and more complete review of all methods please see Refinetti (2007), Dowse (2009), Diez-Noguera (2013) and Leise (2015). Although Leise et. al. (2013) propose the use of wavelet-based methods to predict phases, many studies still estimate phases of behaviour either subjectively or by using arbitrary thresholds.

Given the considerable investment in developing time-series analysis and phase prediction tools, we feel that there has not been a commensurate increase in software that helps researchers visualise and analyse their time-series data sets using these tools, in terms of cost, interactivity, and ease and efficiency of use. Although there are programs such as ClockLab (Actimetrics, Wilmette, IL, USA), the Chronobiology Kit (Stanford Software Systems), ActogramJ (Schmid et al., 2011) and Chronomics analysis toolkit (Gierke and Cornelissen, 2015) that are available for use, they have some combination of the aforementioned limitations. More recently, a free program was published for analysing *Drosophila* activity and sleep called ShinyR-DAM (Cichewicz and Hirsh, 2018). However, this program will be useful only for researchers working with *Drosophila*, and only for those that exclusively acquire data from the DAM (*Drosophila* Activity Monitor) system. Additionally, although very useful, this program allows only limited interactivity with the plots that are generated. Therefore, to have a general program that can analyse and visualise a wide variety of time-series data using highly interactive graphics and a comfortable Graphical User Interface (GUI), we have developed RhythmicAlly, which is written on the R platform (R Core Team, 2018) in collaboration with Shiny (Chang et al., 2018) and Shiny Dashboard (Chang and Rebeiro, 2018).

R is a free programming language meant to facilitate statistical analysis/computation and data visualisation. *R* is very useful because it can compile and run on a wide variety of operating systems such as Windows, UNIX and MacOS. The program is available for use under the GNU General Public License v2. Although, *R* has its own command line interface, there is RStudio which is a powerful GUI for *R*. Shiny and Shiny Dashboard are packages written to enable the creation of powerful and interactive applications by the use of "'reactive' binding" between user defined inputs and pre-coded outputs. Other packages that have been used to write RhythmicAlly and will not be cited in the rest of the text are "zoo" (Zeileis and Grothendieck, 2005) and "pracma" (Borchers, 2018). The "rollapply" and "Reshape" functions from packages "zoo" and "pracma" have been used to rearrange data to facilitate the plotting of actograms and averaging of data for each individual over cycles, respectively. RhythmicAlly has two components, and a brief description of their functionality follows. For information on initialising the application and other details see supplementary methods at the end of this section.

8.2.1. Installing *R*, RStudio and RhythmicAlly

The first step to use RhythmicAlly is to install *R* (https://www.r-project.org/) and RStudio (https://www.rstudio.com/). A more detailed explanation of *R* and RStudio installation can be found in the supplementary methods. Once installed, RhythmicAlly (https://github.com/abhilashlakshman/RhythmicAlly) can be initialised. The downloaded ZIP file must be extracted and inside the "RhythmicAlly-master" folder an "initialisation.R" file can be found. This must be opened and run in RStudio. Once initialisation is complete the following message will be prompted in the RStudio console, "Initialisation complete! RhythmicAlly is now ready for use". After this, every time RhythmicAlly needs to be used, RStudio must be opened and the following must be typed into the console:

shiny::runApp("path/location/of/the/For_DAM/or/Others/application/inside/the/RhythmicAlly-master/folder", launch.browser = TRUE). This should start RhythmicAlly and the home screen should look like the image shown in Figure 8.2.1.

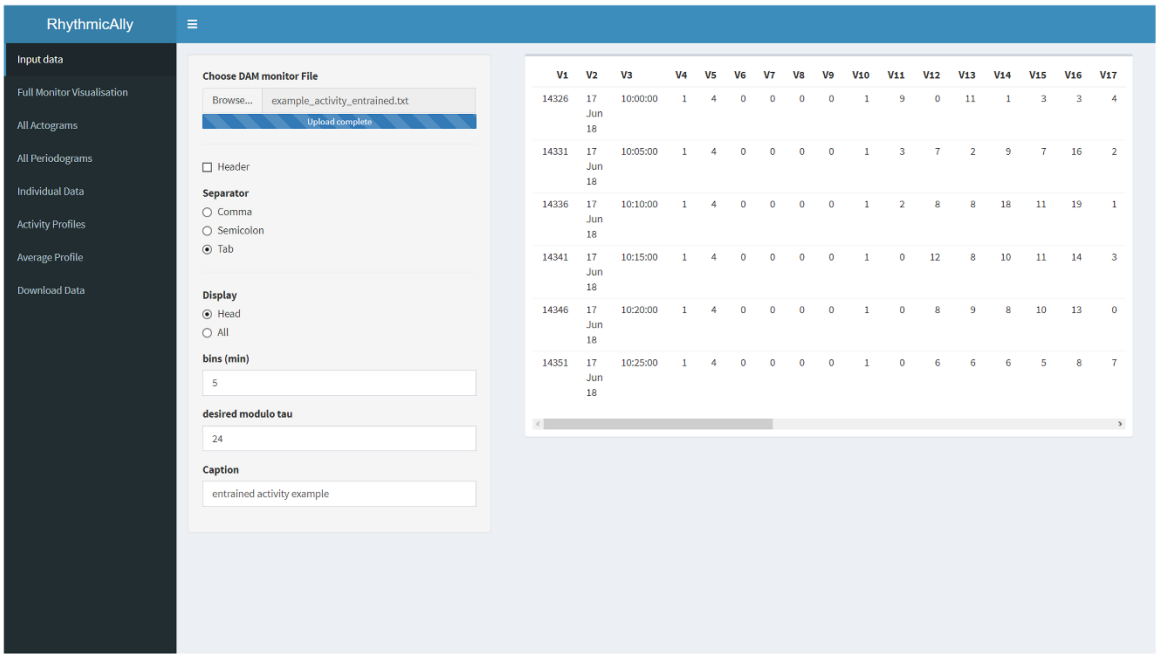

Figure 8.2.1: Screenshot of the home screen of the RhythmicAlly/For_DAM/ application. On the left side is displayed all the functionalities that the application offers. Once the input file is browsed and loaded, users can verify the data in the preview of the data set on the right side of the home screen. If the All option is selected under the Display input choice, the entire data set will be displayed on the right side for the user's perusal. The bins and modulo-τ must be entered carefully as they will be used for further analysis in the other tabs. The caption is important as all downloaded files will be labelled with the name users provide in this field.

8.2.2. RhythmicAlly/For_DAM/

The first component of RhythmicAlly is coded to analyse locomotor activity time-series data collected from *Drosophila melanogaster* using the DAM system made by TriKinetics (Waltham, MA, USA). The first page is the input page and users can browse and load their scanned DAM monitor files. In the same page, input regarding the bins in which the data were saved, modulo-τ and caption need to be entered (Figure 8.2.1). All subsequent tabs analyse data using the bins and

modulo-τ specified here and the caption provided by the user must have a unique identity because all analysed files for download will use this name to save files on the user's local disk.

8.2.2.1. Full Monitor Visualisation

This is a useful feature enabling visualisation of all 32 channels in one window that can reveal inter-individual variation in time-series across all the cycles of data (Figure 8.2.2). Along the *x*-axis, time-series is plotted for each individual as a heat-map and along the *y*-axis are individuals. There is a reactive input variable in this page that allows the user to modify the maximum colour intensity so as to set a threshold on the maximum activity in the heat-map thereby allowing easy visualisation. This plot allows one to see how well rhythms of all individuals are aligned with each other and with reference to local time. Additionally, users can easily visualise changes in such alignment across cycles. For instance, it is clear that inter-individual variation in phase of onset of activity is much higher than phase of offset of activity (Figure 8.2.2 – black arrows). This figure (and all other plots in this application) are made using "plotly" for R (Sievert, 2018) and therefore are highly interactive. Users can zoom into a few cycles of interest and look at just a few individuals that they want to in more detail. The figure can be downloaded as a '.png' file by clicking on the camera button on the top right corner of the figure. The last row of time-series in this heat-map is the average time-series of all the individuals.

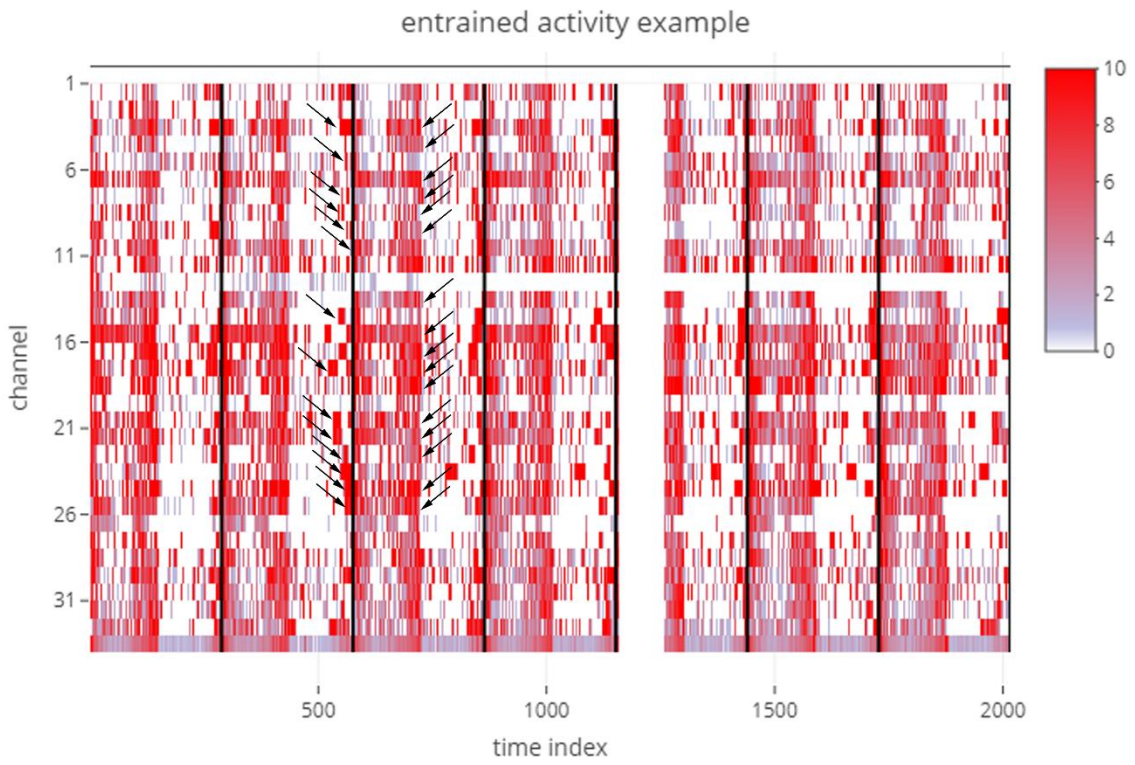

Figure 8.2.2: Figure downloaded as is from the *Full Monitor Visualisation* tab of an analysis session where the example data set labelled "example_activity_entrained.txt2" in the RhythmicAlly-master/For_DAM/ folder was used as input. This is an example data set of the locomotor activity of *D. melanogaster* recorded using the DAM system. Time-index is plotted along the *x*-axis i.e., if the input data are collected in 5-min bins and the first time-point in the data set is 10 AM, then a time-index of 100 would imply 500-mins after 10 AM which is ~6:20 PM. Each individual is arranged in sequence along the *y*-axis, and the colour indicates the amount of activity displayed by each individual at a given time during the experiment. Each black bar indicates the end of one cycle as defined by the modulo-τ input given by the user. Note here that the inter-individual variability in phase of onset of activity is much higher than that of phase of offset of activity (arrow heads). These are features that are not easy to see and interpret in the absence of visualisations of this kind. The gap in this example heat-map just after the end of the fourth cycle indicates a technical glitch in recording for the entire monitor.

8.2.2.2. All Actograms

This tab generates actograms in the form of a heat-map for each individual and displays it together, so users can visually compare activity patterns across all individuals that were recorded in the same monitor (Figure 8.2.3a). The inputs in this tab include one which can modify the number of plots

in the actogram and the maximum activity threshold in the actograms (similar to the input in the *Full Monitor Visualisation* tab). The last actogram is that of the averaged time-series across all individuals (Figure 8.2.3a – marked as "Batch"). I feel that the visualisation in this tab allows users to easily weed out individuals that are arrhythmic or that die in the middle of the experiment.

8.2.2.3. All Periodograms

This tab analyses time-series for all individuals using one of the three time-series analysis methods that are currently employed by the program, i.e., Enright or χ^2 periodogram, autocorrelation and Lomb-Scargle periodogram (Figure 8.2.3b). Codes to run these periodogram analyses are already published in the form of a very convenient *R*-package called "zeitgebr" (Geissmann and Garcia, 2018), and have been used by me in this application. Time resolution for the χ^2 periodogram analyses has been programmed to be the same as the binning resolution. Users can modify the period range and significance values according to their need while performing the analysis. Power versus period plots for all the individuals are simultaneously displayed with the help of an interactive chart. Moreover, when users move their cursor along these plots, period and power of the corresponding nearest point are displayed and stored in a table at the bottom of the tab on clicking.

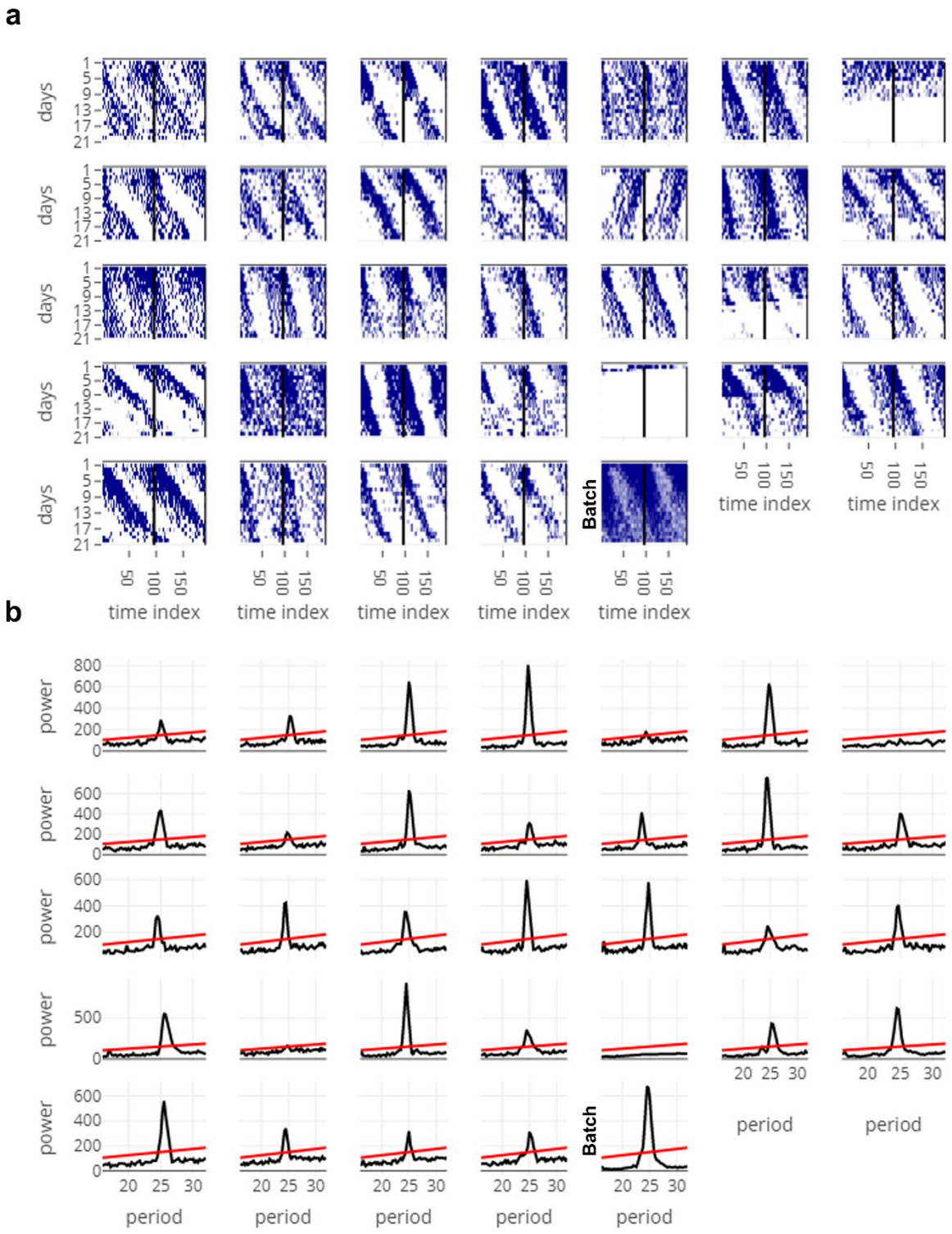

Figure 8.2.3: Figures from the *All Actograms* (a) and *All Periodograms* (b) tabs, downloaded as is. Data used here are obtained from free-running activity behaviour of *D. melanogaster* ("example_activity_freerunning.txt" in the RhythmicAlly-master/For_DAM/ folder). In (a), time-

index is plotted along the *x*-axis and days along the *y*-axis, and the actograms are double plotted. It is amply clear from a glance of all the actograms that most individuals show longer than 24-h free-running periodicities. Additionally, it is clear that individual 5 is arrhythmic and individuals 7 and 26 died soon after recording started. Panel (b) shows periodograms of all individuals whose actograms are displayed in panel (a). Period being tested is plotted along the *x*-axis and power along the *y*-axis. The red line is the significance line calculated based on the alpha input given by the user in the *All Periodograms* tab. In most other applications/software the period and power for each individual must be noted down separately thereby making it cumbersome. In RhythmicAlly users can move the cursor along the peak of the periodogram and can click on the peak, wherein the period and power at that point of click are stored in table below the plots in the *All Periodograms* tab. These data are then available for download as a ".csv" file in the *Download Data* tab, thereby making our application very efficient and fast.

8.2.2.4. Individual Data

This tab has a user-interface similar to that of ClockLab (Actimetrics, Wilmette, IL, USA). For each individual, an actogram is plotted and the periodogram for that individual is displayed (Figure 8.2.4). The input values for plotting the actograms are the individual id (referred to as channel number in the DAM system), the number of plots in the actogram, the threshold for maximum activity to be plotted, and the starting time of input data set (in decimal values, not in time format). The input values for the periodogram on the right side of this tab are taken from whatever input values were provided in the *All Periodograms* tab. To analyse day-to-day variability in period and/or phases, it is important to first identify and mark the phases of interest. Although there are recent non-subjective ways to identify phases of onset and offset of activity (Leise et al., 2013; Schlichting et al., 2016), researchers continue to prefer marking phases subjectively. In *Drosophila* activity time-series, this is partly due to noisy data, and smaller length of data sets compared to those that have been used in the examples shown in Leise et al. (2013). To the best of our knowledge, no freely available application allows subjective marking of phases. RhythmicAlly allows users to subjectively mark phases in the actogram (on click), which can be stored in the table within this tab (Figure 8.2.5). This, I am certain, will be a very useful feature

for many researchers who are unable to afford expensive software but need to manually mark phases of behaviour. In this tab, the actogram and periodogram will get updated every time the channel number is changed, but the table remains unaltered. So, phases of all individuals can be stored in the same table and downloaded, thereby making subsequent analyses of interest on a spreadsheet program like MS Excel easier for users.

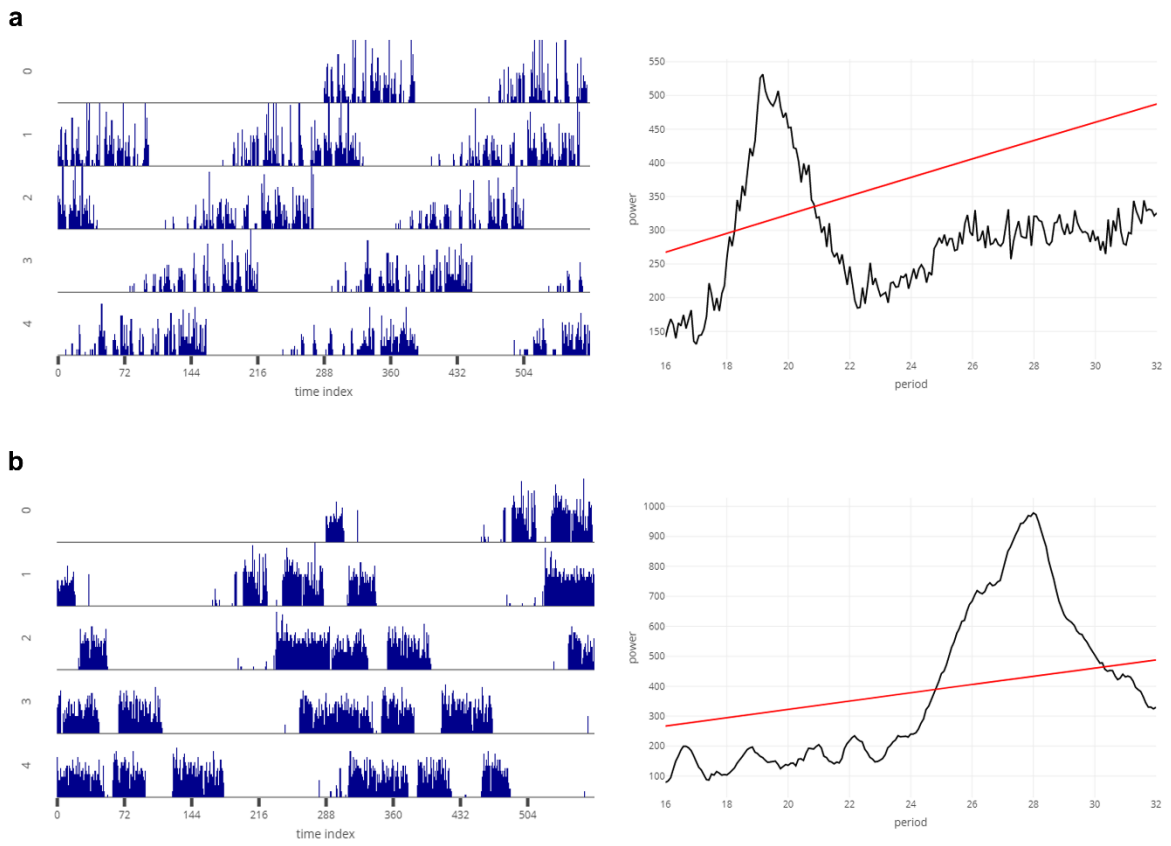

Figure 8.2.4: Representative actogram (left) and periodogram (right) for a fly (*D. melanogaster*) with shorter than 24-h (a) and longer than 24-h (b) free-running period, downloaded from the *Individual Data* tab as is. The *x*-axis and *y*-axis of the actograms and periodograms are the same as those described in Figure 8.2.3.

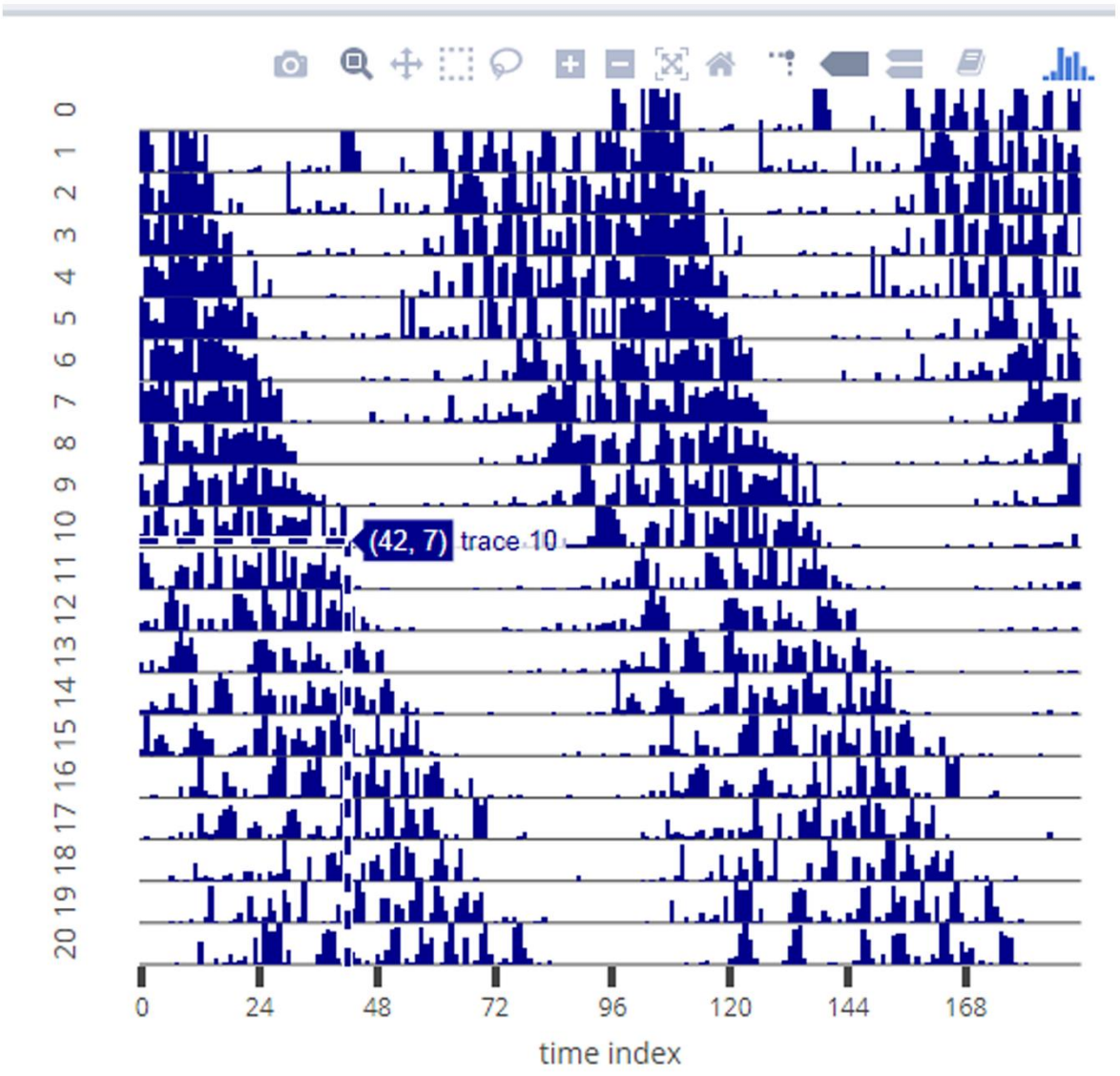

Figure 8.2.5: Example of the subjective phase-marking feature of RhythmicAlly. The representative actogram is a screenshot from the *Individual Data* tab. When the Toggle Spike Lines option is turned on, then as the user moves the cursor around over the actogram, there is a line showing the *x*- and *y*-coordinates at the point of the cursor. Users can move their cursor to the end of activity on each day (in this example, the cursor is pointed at the end of activity on day 10) and click. On this click, the subjectively estimated phase-of-offset of activity gets stored in a table in the lower part of the *Individual Data* tab. This can be done for each day and all individuals and can be together downloaded as a ".csv" file from the *Download Data* tab. Similarly, users can mark phases of onset, peak etc.

8.2.2.5. Activity Profiles

This tab shows the profiles for each individual's raw values averaged over all the cycles. One cycle's length is defined by the modulo-τ input from the first tab; therefore, the program can be used for visualising average profiles under DD and/or *T*-cycles with periodicities very different from 24-h. The data used for making this plot are displayed in a table at the bottom of the plots.

8.2.2.6. Average Profile

This tab displays the profile of activity averaged over all individuals. I think that this and the previous tab are useful for users, because they provides them with the opportunity to visualise all individuals simultaneously and look for subtle changes in the waveform of their behaviour such as inter-individual variation in night-time activity, anticipation, mid-day activity, phases of peaks etc.

8.2.2.7. Download Data

This tab has a drop-down menu that allows users to choose the data set of interest that they want to download. They can download the average activity profiles for each individual, or the period and power values that were stored on click, or the phases that were marked on click.

8.2.3. RhythmicAlly/Others/

In addition to data collected using the DAM system, researchers may have collected time-series data for certain other behaviours, either from flies or other model systems, e.g., locomotor activity, oviposition, eclosion and feeding time-series from any variety of animals, body temperature or blood pressure time-series from mammals, etc. I think that similar data visualisation tools may be of use to all such researchers. So, I extended the RhythmicAlly app to cater to such data too. Here I only describe the additional things that this application can do over and above what it does for

data acquired through the DAM system. An important feature to note here is that in the *Full Monitor Visualisation*, *All Actograms* and *Individual Data* tabs I have provided an additional input option which allows users to choose the minimum value on the *y*/*z*-axis (thereby allowing users to scale their axes appropriately). This is important because, for instance, in case of data such as body temperature, raster-plots that start plotting on the *y*-axis from 0 are not helpful for visualising rhythms that have an amplitude of ~3 °C or so around a mean temperature of ~37 °C.

8.2.3.1. Prop Ind Profiles (Proportion Individual Profiles)

Often researchers may be interested in profiles that are averaged over cycles for each individual sampling unit (for e.g. a vial or an individual), but the use of raw values for such purposes may be inappropriate. For instance, in case of a damped oscillation, averaging raw values over all cycles gives rise to a misleading profile. In such cases, it is worthwhile to compute values as a fraction of the total value for each cycle and then average these values over cycles. This is what is done in the *Prop Ind Profiles* tab. The equivalent of Activity Profiles tab in the RhythmicAlly/Others/ application is under the Raw Ind Profiles tab and representative figures from this tab are shown in Figure 8.2.6, left.

8.2.3.2. Rose plots

Circular histogram representation of data is displayed here (Figures 8.2.6a, middle and 8.2.6b, middle). Users can visualise rose plots for each individual and also for the average across all individuals. Often this is useful to observe distribution of data around the clock, when linear profiles are difficult to read due to high noise in behaviours, such as in the case of oviposition rhythms in *Drosophila*.

8.2.3.3. CoM

Phases are circular random variables and must be treated as such wherever possible (Batschelet, 1981). This tab computes the mean angle of the oscillation (Centre of Mass; CoM; represented as θ; a non-subjective phase marker) for each individual and the consolidation of the rhythm (r), and represents it on a polar plot (Figures 8.2.6a, right and 8.2.6b, right).

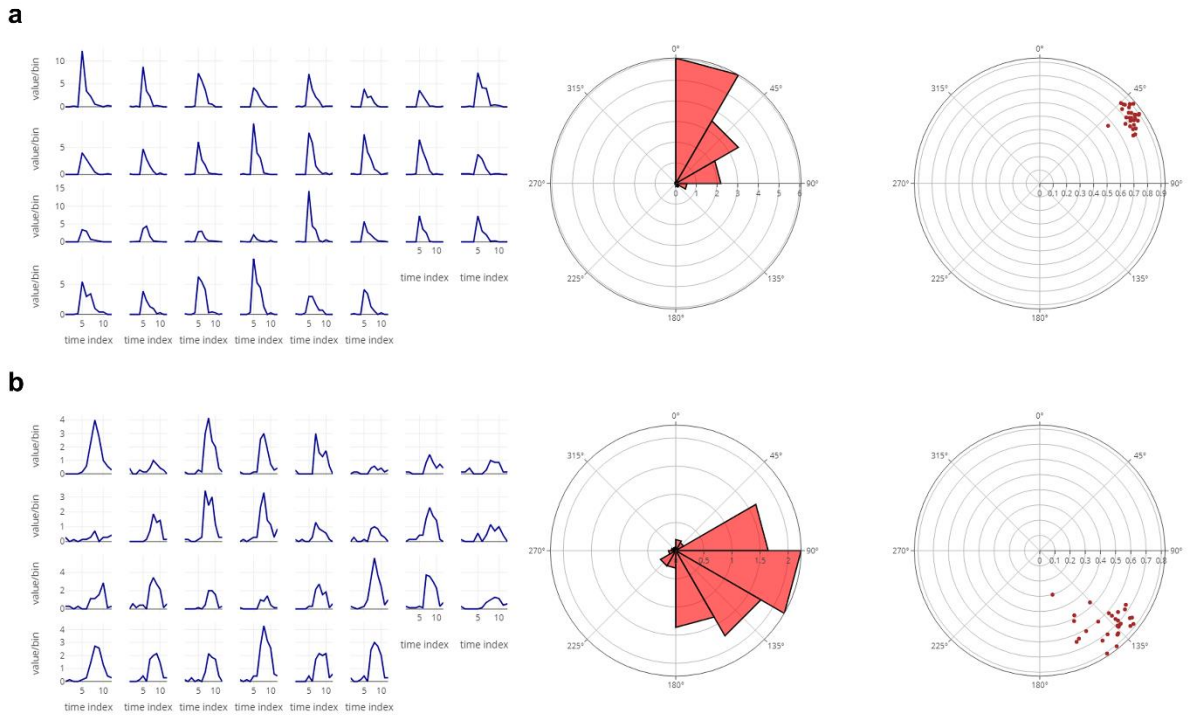

Figure 8.2.6: (a) The eclosion profiles of 30 independent vials averaged over 6 cycles of data for a *D. melanogaster* strain having advanced phase of eclosion (left). Also shown is the average rose plot of the eclosion profile averaged over all 30 vials (middle). The 0° on the rose plot refers to the Zeitgeber Time 00. The radial distance of each triangle on the rose plot indicates the total number of flies eclosing in the defined bin. The angular width of each triangle is the bin size. As is clear, peak of eclosion occurs just after lights ON in this case. On the right are displayed the CoM values for all vials. Each dot represents a single vial. The radial distance of each dot reflects the gate-width or consolidation of the eclosion rhythm and the angle it makes from 0° (ZT00) is reflective of the mean phase of the oscillation. (b) The eclosion profiles of 30 independent vials averaged over 6 cycles of data for a *D. melanogaster* strain having delayed phase of eclosion (left). Also shown is the average rose plot of the eclosion profile averaged over all 30 vials (middle). As is clear, in this case, peak of eclosion occurs 6-8-h after lights ON. On the right are displayed the

CoM values for all vials. Raw data for all the average profiles are displayed in a table below the plots in RhythmicAlly and are downloadable in the *Download Data* tab. The interactivity of the plots will allow users to gather much information regarding the shape of the waveform and phases in average profiles by just moving the cursor along the plots.

8.2.3.4. Download Data

In this part of the application, two additional data sets can be downloaded: the profiles computed by averaging the proportion of values and the phases of CoM.

To illustrate the utility of this program in analysing other time-series data, we visualised and analysed some example time-series from rodents. I visualised the activity of ice rats (*Otomys sloggetti*) collected using infrared (IR) captors and running wheels (Figure 8.2.7a), and activity and body temperature of mole-rats (*Cryptomys hottentotus pretoriae*) using IR and a passive integrated transponder (PIT) tag, respectively (Figure 8.2.7b). Data for the mole-rats have been published (Haupt et al., 2017), but that of the ice-rats are not yet published. Finally, I also analysed circatidal rhythms in activity/rest behaviour of the mangrove cricket (*Aptorenemobius asahinai*; Figure 8.2.8). The cricket data has earlier been published (Satoh et al., 2008) and can be referred to for comparisons.

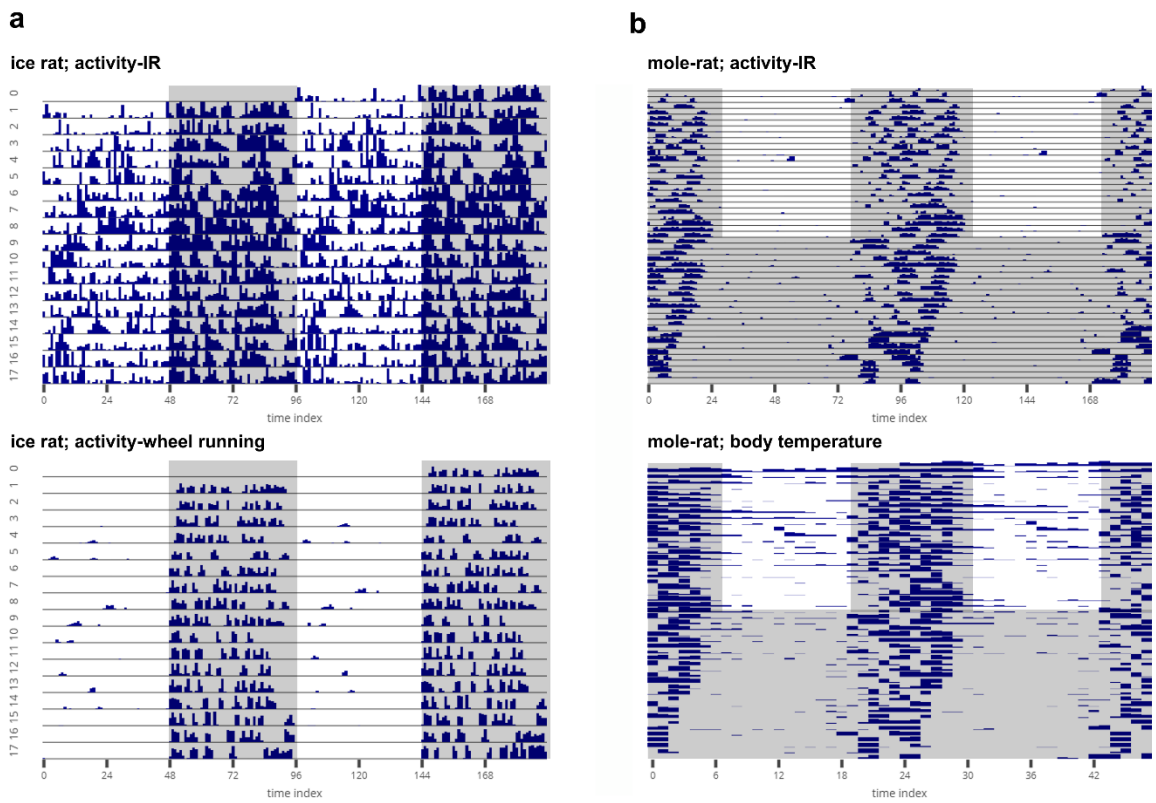

Figure 8.2.7: (a) Representative actograms of the locomotor activity of a single ice rat (*Otomys sloggetti*) as estimated using an infrared (IR) captor (top) and a running wheel (bottom). The rat was recorded under LD 12:12 at 25 °C. (b) Actogram of locomotor activity of a mole-rat measured using an IR captor (top), and raster-plot of body temperature of the same animal measured with a passive integrated transponder (PIT) tag (bottom). The mole-rat was recorded for 25 days under LD 12:12 at 30 °C and then under DD at 30 °C. The mole-rat data have been published elsewhere (Haupt et al., 2017). All the activity data sets are binned in 15-min intervals and the body temperature data are collected at 1-h intervals. All the grey shaded regions indicate scotophases. The data sets were provided by Maria Oosthuizen, University of Pretoria, South Africa.

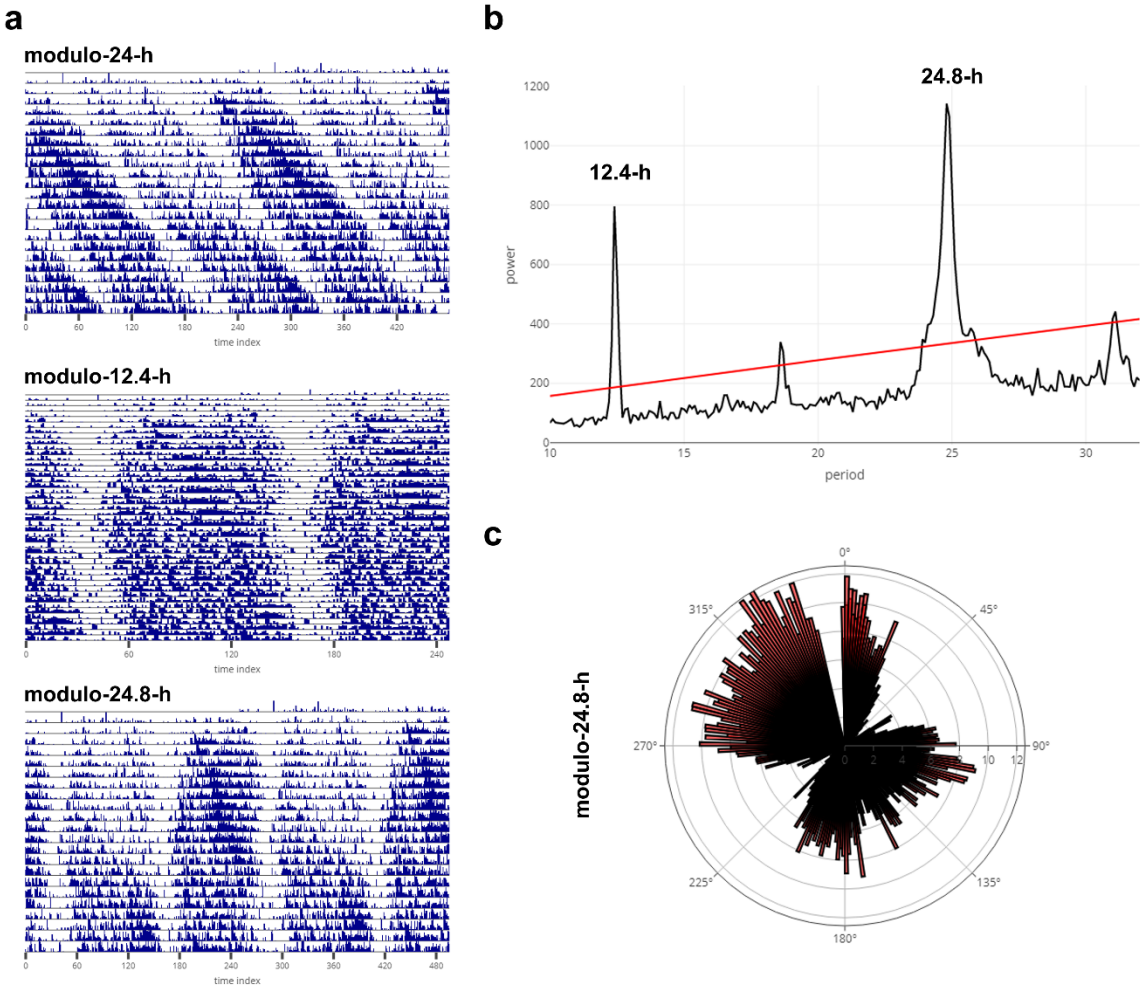

Figure 8.2.8: Representative actograms of a mangrove cricket (*Apteronemobius asahinai*; data shared by Aya Satoh, The Graduate University for Advanced Studies, Kanagawa, Japan) displaying circatidal rhythms downloaded from the *Individual Data* tab of RhythmicAlly. Activity of the cricket was recorded under constant darkness in 6-min intervals. The actogram is plotted as modulo-24-h (a-top) for the same animal displayed in Figure 1a in Satoh et al. (2008; see for comparison). Also shown are actograms for the same cricket under modulo-12.4-h (circatidal rhythm; a-middle) and under modulo-24.8-h, which shows two bouts of circatidal activity (a-bottom) within approximately a day (consistent with there being two bouts of low and high tides within a day). Panel (b) depicts the χ^2 periodogram for the same cricket (see Figure 1a in Satoh et al., 2008). The bimodality seen in the actogram (a-bottom) under modulo-24.8-h can also be visualised as a rose plot. The time series was averaged over all cycles with the length of one cycle being 24.8-h. This average is plotted as a rose plot in panel (c). 0° represents 12 AM local time and one can clearly see that there is a major bout of activity between 90° and 180° and another major bout between 270° to 360°.

All codes for running this application are uploaded on Github (https://github.com/abhilashlakshman/RhythmicAlly) under the General Public Licence version 3, along with a user manual and example data sets to familiarise users with the interface. I aim to keep the program up to date and hopefully improve the user's experience by modifying and adding new modules that will make the program more useful than what it is now. For instance, I am working on including newer methods of time-series analyses, and phase-shift estimates using objective phase-markers as has been used in Schlichting et al. (2016). Although the goal of RhythmicAlly was to cater to biological rhythms in the circadian range, changing parameters can also allow one to use the program to analyse ultradian or infradian rhythms (see Figure 8.2.8). Lastly, RhythmicAlly will appeal to researchers who are uncomfortable with coding due to the availability of a user-friendly GUI, and also to researchers who are familiar with coding and can very easily modify the codes to tailor the program specifically to their needs.

8.2.4. Supplementary Methods

8.2.4.1. *R*, RStudio and Initialising RhythmicAlly

RhythmicAlly is written on the *R* platform with the help of Shiny to make it interactive and user-friendly. The following is a step-by-step approach to initialise RhythmicAlly. It is important to have reasonably good internet connection for quick download and installation of all the programs required for RhythmicAlly to run.

1. Download and install *R* (at the time of the writing of this program the latest version of R was 3.5.2 or "Eggshell Igloo"). The latest version can be downloaded from this link: https://www.r-project.org/. It is important to note here that RhythmicAlly may not work as expected in older versions of R.

2. Download and install RStudio. RStudio is a graphical user interface (GUI) for the R platform and is easy to visualise and use. RStudio can be downloaded from here: https://www.rstudio.com/.
3. Download all the contents of the RhythmicAlly folder from Github (https://github.com/abhilashlakshman/RhythmicAlly.
4. Inside the folder there is an initialisation.R file, a user manual, and two subfolders.
5. One of the subfolders called "For_DAM" contains the application for running analyses when data is acquired using the DAM system; the other called "Others" contains the application for running analyses when data is acquired outside of the DAM system. Both these subfolders have a few example data sets in a tab delimited text file. Make sure that data is arranged in the same format as that of the data sets in the example files.
6. First, open the initialisation.R file in RStudio and run it. Select all the code (Ctrl+A) and then press Ctrl+Enter. This will install all the required packages for running RhythmicAlly. Once installation of all packages is complete there shall be a message on the console saying "Initialisation complete! RhythmicAlly is now ready for use".
7. The above steps need to be performed only the first time that this program is run.
8. Now open RStudio and type the following in the console and press the Enter key: "**shiny::runApp("*Location of the folder where RhythmicAlly is saved*", launch.browser = TRUE)**". While copying and pasting the command, do not copy the outer-most double quotes. The "launch.browser = TRUE" will make sure that the GUI opens in the system's default browser. It is preferable to use Google Chrome or Opera and to avoid Firefox and Edge. It is important to note here that the path must be in quotes and all subfolders must be separated with a forward slash and not a back slash.

8.2.4.2. Things to note

1. Please check the last updated date of RhythmicAlly. Ensure that the latest, most updated version of the program has been downloaded and installed before analyses.
2. The first time a tab is clicked, the program will first perform computations and then plot.
3. When this computation is happening, or when the data are getting updated from the input that has been provided, the plot region will grey out. Please wait for the new figure to be displayed.
4. Once the computation is complete, switching between tabs will immediately display respective plots without any delay. This is because the computations have already been done and stored. This, however, will not be the case if the input variable is updated.
5. In the RhythmicAlly/Others application, only a maximum of 32 individuals can be analysed at a time.

References

Abhilash L and Sharma VK (2016) On the relevance of using laboratory selection to study the adaptive value of circadian clocks. *Physiological Entomology, 41(4): 293–306.*

Abhilash L and Sharma VK (2017) Time Measurement in Living Systems: Human Understanding and Health Implications. In *Space, Time and the Limits of Human Understanding (Eds. Wuppuluri S and Ghirardi G): pp. 337–352. Springer, Cham.*

Abhilash L and Sharma VK (2020) Mechanisms of photic entrainment of activity/rest rhythms in populations of *Drosophila* selected for divergent timing of eclosion. *Chronobiology International 37(4): 469–484*.

Abhilash L and Sheeba V (2019) RhythmicAlly: Your R and Shiny–based open-source ally for the analysis of biological rhythms. *Journal of Biological Rhythms 34(5): 551–561*.

Abhilash L, Ghosh A and Sheeba V (2019) Selection for timing of eclosion results in co-evolution of temperature responsiveness in *Drosophila melanogaster*. *Journal of Biological Rhythms 34(6), 596–609.*

Abhilash L, Kalliyil A and Sheeba V (2020) Responses of activity rhythms to temperature cues evolve in *Drosophila* populations selected for divergent timing of eclosion. *Journal of Experimental Biology 223(11).*

Abhilash L, Ramakrishnan A, Priya S and Sheeba V (2020) Waveform plasticity under entrainment to 12-h *T*-cycles in *Drosophila melanogaster*: Behaviour, neuronal network and evolution. *Journal of Biological Rhythms 35(2): 145–157.*

Abraham U, Granada AE, Westermark PO, et al. (2010) Coupling governs entrainment range of circadian clocks. *Molecular Systems Biology 6(1): 438*.

Aguiar GF, da Silva HP and Marques N (1991) Patterns of daily allocation of sleep periods: a case study in an Amazonian riverine community. *Chronobiologia 18(1): 9–19*.

Akten B, Jauch E, Genova GK, et al. (2003) A role for CK2 in the *Drosophila* circadian oscillator. *Nature Neuroscience 6(3): 251–257.*

An H, Zhu Z, Zhou C, et al. (2014) Chronotype and a PERIOD3 variable number tandem repeat polymorphism in Han Chinese pilots. *International Journal of Clinical and Experimental Medicine 7(10): 3770–3776.*

Andrews S (2010) FastQC: A quality control tool for high throughput sequence data. *Babraham Bioinformatics*.

Archer SN, Robilliard DL, Skene DJ, et al. (2003) A length polymorphism in the circadian clock gene Per3 is linked to delayed sleep phase syndrome and extreme diurnal preference. *Sleep 26(4): 413–415*.

Aschoff J (1960) Exogenous and endogenous components in circadian rhythms. In *Cold Spring Harbor Symposia on Quantitative Biology 25: 11–28.*

Aschoff J (1979) Circadian rhythms: influences of internal and external factors on the period measured in constant conditions. *Zeitschrift fur Tierpsychologie 49(3): 225–249.*

Aschoff J and Pohl H (1978) Phase relations between a circadian rhythm and its zeitgeber within the range of entrainment. *Die Naturwissenschaften 65(2): 80–84*.

Aschoff J and Wever R (1962) Über Phasenbeziehungen zwischen biologischer Tagesperiodik und Zeitgeberperiodik. *Zeitschrift für Vergleichende Physiologie 46(2): 115–128.*

Aschoff J and Wever R (1966) Circadian period and phase-angle difference in chaffinches (*Fringilla coelebs L.*). *Comparative Biochemistry and Physiology 18(2): 397–404.*

Aschoff J, Fatranská M, Giedke H, et al. (1971) Human circadian rhythms in continuous darkness: entrainment by social cues. *Science 171(3967): 213–215*.

Ashburner M, Golic KG and Hawley RS (2005) *Drosophila*: *A Laboratory Handbook*. Cold Spring Harbor Laboratory Press.

Balzer I and Hardeland R (1988) Influence of temperature on biological rhythms. *International Journal of Biometeorology 32(4): 231–241*.

Barclay NL, Eley TC, Mill J, et al. (2011) Sleep quality and diurnal preference in a sample of young adults: Associations with 5HTTLPR, PER3, and CLOCK 3111. *American Journal of Medical Genetics, Part B: Neuropsychiatric Genetics 156(6): 681–690.*

Batschelet E (1981) *Circular Statistics in Biology*. Academic Press.

Beersma DGM, Comas M, Hut RA, et al. (2009) The progression of circadian phase during light exposure in animals and humans. *Journal of Biological Rhythms 24(2): 153–160.*

Beersma DGM, Daan S and Hut RA (1999) Accuracy of circadian entrainment under fluctuating light conditions: contributions of phase and period responses. *Journal of Biological Rhythms 14(4): 320–329.*

Bell-Pedersen D, Cassone VM, Earnest DJ, et al. (2005) Circadian rhythms from multiple oscillators: Lessons from diverse organisms. *Nature Reviews Genetics 6(7): 544–556.*

Berens P (2009) CircStat: A MATLAB Toolbox for Circular Statistics. *Journal of Statistical Software 31(10): 1–21*.

Bonduriansky R and Day T (2009) Nongenetic inheritance and its evolutionary implications. *Annual Review of Ecology, Evolution, and Systematics 40(1): 103–125.*

Borchers HW (2018) Pracma: Practical Numerical Math Functions. R package version 2.2.2. https://CRAN.R-project.org/package=pracma.

Bordyugov G, Abraham U, Granada AE, et al. (2015) Tuning the phase of circadian entrainment. *Journal of The Royal Society Interface 12(108): 20150282.*

Brown SA, Kunz D, Dumas A, et al. (2008) Molecular insights into human daily behavior. *Proceedings of the National Academy of Sciences, USA 105(5): 1602–1607.*

Bullock B (2019) An interdisciplinary perspective on the association between chronotype and well-being. *The Yale Journal of Biology and Medicine 92(2): 359–364.*

Bulthuis N, Spontak KR, Kleeman B, et al. (2019) Neuronal activity in non-LNv clock cells is required to produce free-running rest:activity rhythms in *Drosophila*. *Journal of Biological Rhythms 34(3): 249–271.*

Burke MK, Dunham JP, Shahrestani P, et al. (2010) Genome-wide analysis of a long-term evolution experiment with *Drosophila*. *Nature 467(7315): 587–590.*

Burke MK, King EG, Shahrestani P, et al. (2014) Genome-wide association study of extreme longevity in *Drosophila melanogaster*. *Genome Biology and Evolution 6(1): 1–11.*

Carpen JD, Archer SN, Skene DJ, et al. (2005) A single-nucleotide polymorphism in the 5′-untranslated region of the hPER2 gene is associated with diurnal preference. *Journal of Sleep Research 14(3): 293–297.*

Carpen JD, Von Schantz M, Smits M, et al. (2006) A silent polymorphism in the PER1 gene associates with extreme diurnal preference in humans. *Journal of Human Genetics 51(12): 1122–1125.*

Cassidy JJ, Jha AR, Posadas DM, et al. (2013) MiR-9a minimizes the phenotypic impact of genomic diversity by buffering a transcription factor. *Cell 155(7): 1556–1567.*

Chandrashekaran MK (2005) *Time in the Living World.* Universities Press.

Chang W and Ribeiro BB (2018) shinydashboard: Create Dashboards with 'Shiny'. R package version 0.7.0. https://CRAN.R-project.org/package=shinydashboard.

Chang W, Cheng J, Allaire JJ, Xie Y and McPherson J (2018) shiny: Web Application Framework for R. R package version 1.1.0. https://CRAN.R-project.org/package=shiny.

Cheng H-YM, Papp JW, Varlamova O, et al. (2007) microRNA modulation of circadian-clock period and entrainment. *Neuron 54(5): 813–829.*

Chou YH and Chien CT (2002) Scabrous controls ommatidial rotation in the *Drosophila* compound eye. *Developmental Cell 3(6): 839–850.*

Cichewicz K and Hirsh J (2018) ShinyR-DAM: a program analyzing *Drosophila* activity, sleep and circadian rhythms. *Communications Biology 1(1): 1-5.*

Cingolani P, Platts A, Wang LL, et al. (2012) A program for annotating and predicting the effects of single nucleotide polymorphisms, SnpEff: SNPs in the genome of *Drosophila melanogaster* strain w1118; iso-2; iso-3. *Fly 6(2): 80–92.*

Cirelli C, Bushey D, Hill S, et al. (2005) Reduced sleep in *Drosophila* shaker mutants. *Nature 434(7037): 1087–1092.*

Clayton DL and Paietta J V. (1972) Selection for circadian eclosion time in *Drosophila melanogaster*. *Science 178(4064): 994–995.*

Comas M, Beersma DGM, Spoelstra K, et al. (2006) Phase and period responses of the circadian system of mice (*Mus musculus*) to light stimuli of different duration. *Journal of Biological Rhythms 21(5): 362–372.*

Comas M, Beersma DGM, Spoelstra K, et al. (2007) Circadian response reduction in light and response restoration in darkness: a "skeleton" light pulse PRC study in mice (*Mus musculus*). *Journal of Biological Rhythms 22(5): 432–444.*

Cornelissen G (2014) Cosinor-based rhythmometry. *Theoretical Biology and Medical Modelling 11(1): 16.*

Cutler DJ and Jensen JD (2010) To pool, or not to pool? *Genetics 186(1): 41–43.*

Daan S (1977) Tonic and phasic effects of light in the entrainment of circadian rhythms. *Annals of the New York Academy of Sciences 290(1): 51–59.*

Daan S (1981) Adaptive daily strategies in behavior. In *Biological Rhythms: 275–298. Springer, Boston, MA.*

Daan S, Colin Pittendrigh, and Jürgen Aschoff (2000) The natural entrainment of circadian systems. *Journal of Biological Rhythms 15(3): 195–207.*

Daan S (2010) A History of Chronobiological Concepts. In *The Circadian Clock: 1–35. Springer, New York, NY.*

Daan S and Aschoff J (2001) The entrainment of circadian systems. In *Circadian Clocks: 7–43. Springer, Boston, MA.*

Daan S and Pittendrigh CS (1976) A functional analysis of circadian pacemakers in nocturnal rodents III. Heavy water and constant light: Homeostasis of frequency? *Journal of Comparative Physiology A 106(3): 267–290.*

Daan S, Spoelstra K, Albrecht U, et al. (2011) Lab mice in the field: Unorthodox daily activity and effects of a dysfunctional circadian clock allele. *Journal of Biological Rhythms 26(2): 118–129.*

Darwin C and Darwin F (1881) *The Power of Movement in Plants.* Appleton.

Das A and Sheeba V (2017) Temperature input for rhythmic behaviours in flies: The role of remperature-sensitive ion channels. In *Biological Timekeeping: Clocks, Rhythms and Behaviour: 405–424. Springer, New Delhi.*

De J, Varma V, Saha S, et al. (2013) Significance of activity peaks in fruit flies, *Drosophila melanogaster*, under seminatural conditions. *Proceedings of the National Academy of Sciences, USA 110(22): 8984–8989.*

DeCoursey PJ (1960a) Daily light sensitivity rhythm in a rodent. *Science 131(3392): 33–35.*

DeCoursey PJ (1960b) Phase control of activity in a rodent. *Cold Spring Harbor symposia on Quantitative Biology 25: 49–55.*

DeCoursey PJ, Krulas JR, Mele G, et al. (1997) Circadian performance of suprachiasmatic nuclei (SCN)-lesioned antelope ground squirrels in a desert enclosure. *Physiology & Behavior 62(5): 1099–1108.*

DeCoursey PJ, Walker JK and Smith SA (2000) A circadian pacemaker in free-living chipmunks: Essential for survival? *Journal of Comparative Physiology - A Sensory, Neural, and Behavioral Physiology 186(2): 169–180.*

Delventhal R, O'Connor RM, Pantalia MM, et al. (2019) Dissection of central clock function in *Drosophila* through cell-specific CRISPR-mediated clock gene disruption. *eLife 8.*

Díez-Noguera A (2013) Methods for serial analysis of long time series in the study of biological rhythms. *Journal of Circadian Rhythms 11(1): 7.*

Ditty JL, Williams SB and Golden SS (2003) A cyanobacterial circadian timing mechanism. *Annual Review of Genetics 37(1): 513–543.*

Dodd AN, Salathia N, Hall A, et al. (2005) Plant circadian clocks increase photosynthesis, growth, survival, and competitive advantage. *Science 309(5734): 630–633.*

Dominoni DM, Helm B, Lehmann M, et al. (2013) Clocks for the city: Circadian differences between forest and city songbirds. *Proceedings of the Royal Society B: Biological Sciences 280(1763): 20130593.*

Dowse HB (2009) Analyses for physiological and behavioral rhythmicity. *In Methods in Enzymology: 141–174. Academic Press.*

Dowse HB (2013) Maximum entropy spectral analysis for circadian rhythms: theory, history and practice. *Journal of Circadian Rhythms 11(1): 6.*

Drake CL, Belcher R, Howard R, et al. (2015) Length polymorphism in the Period 3 gene is associated with sleepiness and maladaptive circadian phase in night-shift workers. *Journal of Sleep Research 24(3): 254–261.*

Duffy JF and Czeisler CA (2002) Age-related change in the relationship between circadian period, circadian phase, and diurnal preference in humans. *Neuroscience Letters 318(3): 117–120.*

Duffy JF and Wright KP (2005) Entrainment of the human circadian system by light. *Journal of Biological Rhythms 20(4): 326–338.*

Duffy JF, Rimmer DW and Czeisler CA (2001) Association of intrinsic circadian period with morningness–eveningness, usual wake time, and circadian phase. *Behavioral Neuroscience 115(4): 895–899.*

Dunlap JC, Loros JJ and DeCoursey PJ (2004) *Chronobiology: Biological Timekeeping*. Sinauer Associates.

Ebisawa T, Uchiyama M, Kajimura N, et al. (2001) Association of structural polymorphisms in the human period3 gene with delayed sleep phase syndrome. *EMBO Reports 2(4): 342–346.*

Eck S, Helfrich-Förster C and Rieger D (2016) The timed depolarization of morning and evening oscillators phase shifts the circadian clock of *Drosophila*. *Journal of Biological Rhythms 31(5): 428–442*.

Emery IF, Noveral JM, Jamison CF, et al. (1997) Rhythms of *Drosophila* period gene expression in culture. *Proceedings of the National Academy of Sciences, USA 94(8): 4092–4096.*

Enright JT (1965) The search for rhythmicity in biological time-series. *Journal of Theoretical Biology 8: 426–468.*

Evantal N, Anduaga AM, Bartok O, et al. (2018) Thermosensitive alternative splicing senses and mediates temperature adaptation in *Drosophila*. *bioRxiv: 503409.*

Fetting JL, Spencer SA and Wolff T (2009) The cell adhesion molecules Echinoid and Friend of Echinoid coordinate cell adhesion and cell signaling to regulate the fidelity of ommatidial rotation in the *Drosophila* eye. *Development 136(19): 3323–3333.*

Fleury F, Allemand R, Vavre F, et al. (2000) Adaptive significance of a circadian clock: temporal segregation of activities reduces intrinsic competitive inferiority in *Drosophila* parasitoids. *Proceedings Biological Sciences 267(1447): 1005–1010.*

Foley L, Ling J, Joshi R, et al. (2018) PSI controls tim splicing and circadian period in *Drosophila*. *bioRxiv: 504282.*

Frías-Lasserre D, S AL and Villagra CA (2019) Differences in larval emergence chronotypes for sympatric *Rhagoletis brncici frías* and *Rhagoletis conversa* (*Bréthes*) (*Diptera, Tephritidae*). *Revista Brasileira de Entomologia 63(3): 195–198.*

Futschik A and Schlötterer C (2010) The next generation of molecular markers from massively parallel sequencing of pooled DNA samples. *Genetics 186(1): 207–218.*

Futuyma DJ and Bennett AF (2009) The importance of experimental studies in evolutionary biology. In *Experimental Evolution: Concepts, Methods, and Applications of Selection Experiments. University of California Press:15–30.*

García-Allegue R, Lax P, Madariaga AM, et al. (1999) Locomotor and feeding activity rhythms in a light-entrained diurnal rodent, *Octodon* degus. *American Journal of Physiology-Regulatory, Integrative and Comparative Physiology 277(2): 523–531.*

Garland T and Rose MR (2009) *Experimental evolution: Concepts, methods, and applications of selection experiments.* University of California Press.

Garud NR, Messer PW, Buzbas EO, et al. (2015) Recent selective sweeps in North American *Drosophila melanogaster* show signatures of soft sweeps. *PLoS Genetics, 11(2).*

Geissmann Q and Garcia L (2018) zeitgebr: Analysis of circadian behaviours. R package version 0.3.3. https://CRAN.R-project.org/package=zeitgebr.

Gentile C, Sehadova H, Simoni A, et al. (2013) Cryptochrome antagonizes synchronization of *Drosophila*'s circadian clock to temperature cycles. *Current Biology 23(3): 185–195.*

Ghezzi A, Liebeskind BJ, Thompson A, et al. (2014) Ancient association between cation leak channels and Mid1 proteins is conserved in fungi and animals. *Frontiers in Molecular Neuroscience 7(15).*

Gorman MR and Elliott JA (2003) Entrainment of 2 subjective nights by daily light:dark:light:dark cycles in 3 rodent species. *Journal of Biological Rhythms 18(6): 502–512.*

Gorman MR and Elliott JA (2004) Dim nocturnal illumination alters coupling of circadian pacemakers in Siberian hamsters, *Phodopus sungorus*. *Journal of Comparative Physiology A 190(8): 631–639.*

Gorman MR, Harrison EM and Evans JA (2017) Circadian waveform and its significance for clock organization and plasticity. In *Biological Timekeeping: Clocks, Rhythms and Behaviour. New Delhi: Springer India: 59–79.*

Gottlieb DJ, O'Connor GT and Wilk JB (2007) Genome-wide association of sleep and circadian phenotypes. *BMC Medical Genetics 8(S1): S9.*

Granada AE, Bordyugov G, Kramer A, et al. (2013) Human chronotypes from a theoretical perspective. *PLoS One 8(3).*

Grima B, Chélot E, Xia R, et al. (2004) Morning and evening peaks of activity rely on different clock neurons of the *Drosophila* brain. *Nature 431(7010): 869–873.*

Halberg F, Tong YL and Johnson EA (1967) Circadian system phase, an aspect of temporal morphology: procedures and illustrative examples. In *The Cellular Aspects of Biorhythms: 20–48. Springer, Berlin.*

Hall JC (2003) Genetics and molecular biology of rhythms in *Drosophila* and other insects. *Advances in Genetics (48)*.

Hamblen-Coyle MJ, Wheeler DA, Rutila JE, et al. (1992) Behavior of period-altered circadian rhythm mutants of *Drosophila* in light:dark cycles (Diptera: *Drosophilidae*). *Journal of Insect Behavior 5(4): 417–446.*

Hamner KC, Finn JC, Sirohi GS, et al. (1962) The biological clock at the south pole. *Nature 195(4840): 476–480.*

Hardin PE (2011) *Molecular genetic analysis of circadian timekeeping in Drosophila. In: Advances in Genetics. Academic Press Inc.: 141–173.*

Harker JE (1956) Factors controlling the diurnal rhythm of activity of *Periplaneta americana l. Journal of Experimental Biology 33(1).*

Harrison EM, Walbeek TJ, Sun J, et al. (2016) Extraordinary behavioral entrainment following circadian rhythm bifurcation in mice. *Scientific Reports 6(1): 38479.*

Hartl DL and Clark AG (1997) *Principles of Population Genetics.* Sinauer Associates.

Hastings JW and Sweeney BM (1958) A persistent diurnal rhythm of luminescence in *Gonyaulax polyedra*. *The Biological Bulletin 115(3): 440–458.*

Haupt M, Bennett NC and Oosthuizen MK (2017) Locomotor activity and body temperature patterns over a temperature gradient in the Highveld mole-rat (*Cryptomys hottentotus pretoriae*). *PLoS One 12: e0169644.*

Hazlerigg DG, Ebling FJP and Johnston JD (2005) Photoperiod differentially regulates gene expression rhythms in the rostral and caudal SCN. *Current Biology 15(12): 449-450.*

Head LM, Tang X, Hayley SE, et al. (2015) The Influence of Light on Temperature Preference in *Drosophila*. *Current Biology 25(8): 1063–1068.*

Helfrich-Förster C (2009) Does the morning and evening oscillator model fit better for flies or mice? *Journal of Biological Rhythms 24(4): 259–270.*

Helfrich-Förster C (2017) The *Drosophila* clock system. In *Biological Timekeeping: Clocks, Rhythms and Behaviour. New Delhi: Springer India: 133–176.*

Helm B and Visser ME (2010) Heritable circadian period length in a wild bird population. *Proceedings of the Royal Society B: Biological Sciences 277(1698): 3335–3342.*

Horn M, Mitesser O, Hovestadt T, et al. (2019) The circadian clock improves fitness in the fruit fly, *Drosophila melanogaster*. *Frontiers in Physiology 10: 1374.*

Hu Y, Shmygelska A, Tran D, et al. (2016) GWAS of 89,283 individuals identifies genetic variants associated with self-reporting of being a morning person. *Nature Communications 7(1): 1-9.*

Hur Y-M, Jr TJB and Lykken DT (1998) Genetic and environmental influence on morningness–eveningness fn2. *Personality and Individual Differences 25(5): 917–925.*

Imafuku M and Haramura T (2011) Activity rhythm of *Drosophila* kept in complete darkness for 1300 generations. *Zoological Science 28(3): 195–198.*

Ito C and Tomioka K (2016) Heterogeneity of the peripheral circadian systems in *Drosophila melanogaster*: A review. *Frontiers in Physiology 7(8).*

Iwase T, Kajimura N, Uchiyama M, et al. (2002) Mutation screening of the human Clock gene in circadian rhythm sleep disorders. *Psychiatry Research 109(2): 121–128.*

Jagota A, De La Iglesia HO and Schwartz WJ (2000) Morning and evening circadian oscillations in the suprachiasmatic nucleus in vitro. *Nature Neuroscience 3(4): 372–376.*

Johard HAD, Yoishii T, Dircksen H, et al. (2009) Peptidergic clock neurons in *Drosophila*: Ion transport peptide and short neuropeptide F in subsets of dorsal and ventral lateral neurons. *The Journal of Comparative Neurology 516(1): 59–73.*

Johnson CH, Elliott JA and Foster R (2003) Entrainment of circadian programs. *Chronobiology International 20(5): 741–74.*

Johnsson A, Karlsson HG and Engelmann W (1973) Phase shift effects in the *Kalanchoe* petal rhythm due to two or more light pulses. A theoretical and experimental study. *Physiologia Plantarum 28(1): 134–142.*

Jones SE, Lane JM, Wood AR, et al. (2019) Genome-wide association analyses of chronotype in 697,828 individuals provides insights into circadian rhythms. *Nature Communications 10(1).*

Jones SE, Tyrrell J, Wood AR, et al. (2016) Genome-wide association analyses in 128,266 individuals identifies new morningness and sleep duration loci. *PLoS Genetics 12(8).*

Kalmbach DA, Schneider LD, Cheung J, et al. (2017) Genetic basis of chronotype in humans: Insights from three landmark GWAS. *Sleep 40(2).*

Kalmus H (1940) Diurnal rhythms in the *axolotl* larva and in *Drosophila*. *Nature 3663 (1940): 72–73.*

Kant I (1781) *Critique of Pure Reason*. New York, NY: Macmillan.

Karasov T, Messer PW and Petrov DA (2010) Evidence that adaptation in *Drosophila* is not limited by mutation at single sites. *PLoS genetics 6(6).*

Katzenberg D, Young T, Finn L, et al. (1998) A CLOCK polymorphism associated with human diurnal preference. *Sleep 21(6).*

Kawecki TJ, Lenski RE, Ebert D, et al. (2012) Experimental evolution. *Trends in Ecology & Evolution 27(10): 547–560.*

Kempinger L, Dittmann R, Rieger D, et al. (2009) The nocturnal activity of fruit flies exposed to artificial moonlight is partly caused by direct light effects on the activity level that bypass the endogenous clock. *Chronobiology International 26(2): 151–166.*

Kerkhof GA and Van Dongen HP (1996) Morning-type and evening-type individuals differ in the phase position of their endogenous circadian oscillator. *Neuroscience Letters 218(3): 153–156.*

Kippert F (1987) Endocytobiotic coordination, intracellular calcium signaling, and the origin of endogenous rhythms. *Annals of the New York Academy of Sciences 503(1): 476–495.*

Kivelä L, Papadopoulos MR and Antypa N (2018) Chronotype and psychiatric disorders. *Current Sleep Medicine Reports 4(2): 94–103.*

Klei L, Reitz P, Miller M, et al. (2005) Heritability of morningness-eveningness and self-report sleep measures in a family-based sample of 521 hutterites. *Chronobiology International 22(6): 1041–1054.*

Koboldt DC, Chen K, Wylie T, et al. (2009) VarScan: Variant detection in massively parallel sequencing of individual and pooled samples. *Bioinformatics 25(17): 2283–2285.*

Konopka RJ (1972) Circadian clock mutants of *Drosophila melanogaster*. *Doctoral dissertation, California Institute of Technology.*

Konopka RJ and Benzer S (1971) Clock mutants of *Drosophila melanogaster*. *Proceedings of the National Academy of Sciences, USA 68(9): 2112–2116.*

Koren D, Dumin M and Gozal D (2016) Role of sleep quality in the metabolic syndrome. *Diabetes, metabolic syndrome and obesity: targets and therapy 9, 281.*

Koskenvuo M, Hublin C, Partinen M, et al. (2007) Heritability of diurnal type: A nationwide study of 8753 adult twin pairs. *Journal of Sleep Research 16(2): 156–162.*

Kramer G (1952) Experiments on bird orientation. *Ibis 94(2): 265–285.*

Kula E, Levitan ES, Pyza E, et al. (2006) PDF Cycling in the dorsal protocerebrum of the *Drosophila* brain is not necessary for circadian clock function. *Journal of Biological Rhythms 21(2): 104–117.*

Kumar S, Kumar D, Paranjpe DA, et al. (2007) Selection on the timing of adult emergence results in altered circadian clocks in fruit flies *Drosophila melanogaster*. *The Journal of Experimental Biology 210(5): 906–918.*

Kumar V (ed.) (2017) *Biological timekeeping: Clocks, Rhythms and Behaviour*. Springer India.

Kunorozva L, Stephenson KJ, Rae DE, et al. (2012) Chronotype and PERIOD3 variable number tandem repeat polymorphism in individual sports athletes. *Chronobiology International 29(8): 1004–1010.*

Kureck A (1979) Two circadian eclosion times in *Chironomus thummi* (Diptera), alternately selected with different temperatures. *Oecologia 40(3): 311–323.*

Lakin-Thomas PL, Brody S and Coté GG (1991) Amplitude model for the effects of mutations and temperature on period and phase resetting of the *Neurospora* circadian oscillator. *Journal of Biological Rhythms 6(4): 281–297.*

Lane JM, Vlasac I, Anderson SG, et al. (2016) Genome-wide association analysis identifies novel loci for chronotype in 100,420 individuals from the UK Biobank. *Nature Communications 7(1): 1-10.*

Langmead B, Salzberg SL and Langmead (2013) Bowtie2. *Nature Methods 9: 357-359.*

Lear BC, Merrill CE, Lin JM, et al. (2005) A G Protein-coupled receptor, groom-of-PDF, is required for PDF neuron action in circadian behavior. *Neuron 48(2): 221–227.*

Lee Gierke C and Cornelissen G (2016) Chronomics analysis toolkit (CATkit). *Biological Rhythm Research 47(2): 163–181*.

Lehmann M, Spoelstra K, Visser ME, et al. (2012) Effects of temperature on circadian clock and chronotype: An experimental study on a passerine bird. *Chronobiology International 29(8): 1162–1171*.

Leise TL (2013) Wavelet analysis of circadian and ultradian behavioral rhythms. *Journal of Circadian Rhythms 11: 5.*

Leise TL (2015) Wavelet-based analysis of circadian behavioral rhythms. In *Methods in enzymology: 95–119. Academic Press.*

Leise TL, Indic P, Paul MJ and Schwartz WJ (2013). Wavelet meets actogram. *Journal of Biological Rhythms 28(1): 62-68.*

Levandowsky M (1981) Endosymbionts, biogenic amines, and a heterodyne hypothesis for circadian rhythms. *Annals of the New York Academy of Sciences 361(1): 369–375.*

Li H and Durbin R (2010) Fast and accurate long-read alignment with Burrows-Wheeler transform. *Bioinformatics 26(5): 589–595.*

Li H, Handsaker B, Wysoker A, et al. (2009) The Sequence Alignment/Map format and SAMtools. *Bioinformatics 25(16): 2078-2079.*

Lin Y, Stormo GD and Taghert PH (2004) The neuropeptide pigment-dispersing factor coordinates pacemaker interactions in the *Drosophila* circadian system. *Journal of Neuroscience 24(36): 7951–7957.*

Liu S, Lamaze A, Liu Q, et al. (2014) WIDE AWAKE mediates the circadian timing of sleep onset. *Neuron 82(1): 151–166.*

Liu Y, Merrow M, Loros JJ, et al. (1998) How temperature changes reset a circadian oscillator. *Science 281(5378): 825–829.*

Lomb N (1976) Least-squares frequency analysis of unequally spaced data. *Astrophys Space Sci 39: 447–462.*

Lund U and Agostinelli C (2018) CircStats: Circular Statistics, from Topics in Circular Statistics (2001).

MacKay TFC, Richards S, Stone EA, et al. (2012) The *Drosophila melanogaster* genetic reference panel. *Nature 482(7384): 173–178.*

Majercak J, Sidote D, Hardin PE, et al. (1999) How a circadian clock adapts to seasonal decreases in temperature and day length. *Neuron 24(1): 219–230.*

Manfredini R, Fabbian F, Cappadona R, et al. (2018) Daylight saving time, circadian rhythms, and cardiovascular health. *Internal and Emergency Medicine 13(5): 641–646.*

Mardia K V. (1976) Linear-circular correlation coefficients and rhythmometry. *Biometrika 63(2): 403.*

Martin M (2011) Cutadapt removes adapter sequences from high-throughput sequencing reads. *EMBnet.journal 17(1).*

Martinek S, Inonog S, Manoukian AS, et al. (2001) A role for the segment polarity gene shaggy/GSK-3 in the *Drosophila* circadian clock. *Cell 105(6): 769–779.*

McNabb SL, Truman JW and Zitnan D (2008) Light and peptidergic eclosion hormone neurons stimulate a rapid eclosion response that masks circadian emergence in *Drosophila*. *The Journal of Experimental Biology 211(14): 2263–2274.*

McTaggart JE (1908) The Unreality of Time and Mind. Oxford University Press Association.

Means JC, Venkatesan A, Gerdes B, et al. (2015) *Drosophila* Spaghetti and Doubletime link the circadian clock and light to caspases, apoptosis and tauopathy. *PLOS Genetics 11(5): e1005171.*

Menegazzi P, Dalla Benetta E, Beauchamp M, et al. (2017) Adaptation of circadian neuronal network to photoperiod in high-latitude European *Drosophilids*. *Current Biology 27(6): 833–839.*

Menegazzi P, Yoshii T and Helfrich-Förster C (2012) Laboratory versus nature: The two sides of the *Drosophila* circadian clock. *Journal of Biological Rhythms 27(6): 433–442.*

Mercer DM (1960) Analytical methods for the study of periodic phenomena obscured by random fluctuations. In *Cold Spring Harbor Symposia on Quantitative Biology: 73–86.*

Mezan S, Daniel Feuz J, Deplancke B, et al. (2016) PDF signaling is an integral part of the *Drosophila* circadian molecular oscillator. *Cell Reports 17: 708–719.*

Mishima K, Tozawa T, Satoh K, et al. (2005) The 3111T/C polymorphism of hClock is associated with evening preference and delayed sleep timing in a Japanese population sample. *American Journal of Medical Genetics - Neuropsychiatric Genetics 133 B(1): 101–104.*

Mitsui A, Kumazawa S, Takahashi A, et al. (1986) Strategy by which nitrogen-fixing unicellular cyanobacteria grow photoautotrophically. *Nature 323(6090): 720–722.*

Montelli S, Mazzotta G, Vanin S, et al. (2015) period and timeless mRNA splicing profiles under natural conditions in *Drosophila melanogaster*. *Journal of Biological Rhythms 30(3): 217–227.*

Moore-Ede MC, Sulzman FM and Fuller CA (1982) *The Clocks That Time Us: Physiology of the Circadian Timing System*. Harvard University Press.

Morioka E, Matsumoto A and Ikeda M (2012) Neuronal influence on peripheral circadian oscillators in pupal *Drosophila* prothoracic glands. *Nature Communications 3(1): 1–11.*

Mullins C, Hartnell LM and Bonifacino JS (2000) Distinct requirements for the AP-3 adaptor complex in pigment granule and synaptic vesicle biogenesis in *Drosophila melanogaster*. *Molecular and General Genetics 263(6): 1003–1014.*

Murad A, Emery-Le M and Emery P (2007) A subset of dorsal neurons modulates circadian behavior and light responses in *Drosophila*. *Neuron 53(5): 689–701.*

Myers EM, Yu J and Sehgal A (2003) Circadian control of eclosion: Interaction between a central and peripheral clock in *Drosophila melanogaster*. *Current Biology 13(6): 526–533.*

Naito E, Watanabe T, Tei H, et al. (2008) Reorganization of the suprachiasmatic nucleus coding for day length. *Journal of Biological Rhythms 23(2): 140–149.*

Newby LM and Jackson FR (1991) *Drosophila* ebony mutants have altered circadian activity rhythms but normal eclosion rhythms. *Journal of Neurogenetics 7(2–3): 85–101.*

Nielsen R, Hellmann I, Hubisz M, et al. (2007) Recent and ongoing selection in the human genome. *Nature Reviews Genetics 8(11): 857.*

Nikhil K, Abhilash L and Sharma VK (2016) Molecular correlates of circadian clocks in fruit fly *Drosophila melanogaster* populations exhibiting early and late emergence chronotypes. *Journal of Biological Rhythms 31(2): 125–141.*

Nikhil K, Goirik G, Ratna K, et al. (2014) Role of temperature in mediating morning and evening emergence chronotypes in fruit flies *Drosophila melanogaster*. *Journal of Biological Rhythms 29(6): 427–441.*

Nikhil K, Vaze KM, Ratna K, et al. (2016) Circadian clock properties of fruit flies *Drosophila melanogaster* exhibiting early and late emergence chronotypes. *Chronobiology International 33(1): 22–38.*

Nikhil KL and Sharma VK (2017) On the origin and implications of circadian timekeeping: An evolutionary perspective. In *Biological Timekeeping: Clocks, Rhythms and Behaviour.* Springer (India) Private Ltd.*: 81–129.*

Nitabach MN, Wu Y, Sheeba V, et al. (2006) Electrical hyperexcitation of lateral ventral pacemaker neurons desynchronizes downstream circadian oscillators in the fly circadian circuit and induces multiple behavioral periods. *Journal of Neuroscience 26(2): 479–489.*

O'Donnell AJ, Schneider P, McWatters HG, et al. (2011) Fitness costs of disrupting circadian rhythms in malaria parasites. *Proceedings of the Royal Society B: Biological Sciences 278(1717): 2429–2436.*

Ocampo-Garcés A, Mena W, Hernández F, et al. (2006) Circadian chronotypes among wild-captured west Andean octodontids. *Biological Research 39(2): 209–20.*

Oda GA and Friesen WO (2011) Modeling two-oscillator circadian systems entrained by two environmental cycles. *PLoS ONE 6(8).*

Orozco-Terwengel P, Kapun M, Nolte V, et al. (2012) Adaptation of *Drosophila* to a novel laboratory environment reveals temporally heterogeneous trajectories of selected alleles. *Molecular Ecology 21(20): 4931–4941.*

Osland TM, Bjorvatn B, Steen VM, et al. (2011) Association study of a variable-number tandem repeat polymorphism in the clock gene period3 and chronotype in norwegian university students. *Chronobiology International 28(9): 764–770.*

Ouyang Y, Andersson CR, Kondo T, et al. (1998) Resonating circadian clocks enhance fitness in cyanobacteria. *Proceedings of the National Academy of Sciences, USA 95(15): 8660–8664.*

Parsons MJ, Lester KJ, Barclay NL, et al. (2014) Polymorphisms in the circadian expressed genes PER3 and ARNTL2 are associated with diurnal preference and GNβ3 with sleep measures. *Journal of Sleep Research 23(5): 595–604.*

Pedrazzoli M, Louzada FM, Pereira DS, et al. (2007) Clock polymorphisms and circadian rhythms phenotypes in a sample of the Brazilian population. *Chronobiology International 24(1): 1–8.*

Pegoraro M, Picot E, Hansen CN, et al. (2015) Gene expression associated with early and late chronotypes in *Drosophila melanogaster*. *Frontiers in Neurology 6: 100.*

Perea CS, Niño CL, López-León S, et al. (2014) Study of a functional polymorphism in the PER3 gene and diurnal preference in a Colombian Sample. *The Open Neurology Journal 8: 7–10.*

Pereira DS, Tufik S, Louzada FM, et al. (2005) Association of the length polymorphism in the human Per3 gene with the delayed sleep-phase syndrome: Does latitude have an influence upon it? *Sleep 28(1): 29–32.*

Phillips MA, Long AD, Greenspan ZS, et al. (2016) Genome-wide analysis of long-term evolutionary domestication in *Drosophila melanogaster*. *Scientific Reports 6(1): 1–12.*

Pírez N, Christmann BL and Griffith LC (2013) Daily rhythms in locomotor circuits in *Drosophila* involve PDF. *Journal of Neurophysiology 110(3): 700–708.*

Pittendrigh CS (1954) On temperature independence in the clock system controlling emergence time in *Drosophila*. *Proceedings of the National Academy of Sciences, USA 40(10): 1018–1029.*

Pittendrigh CS (1960) Circadian rhythms and the circadian organization of living systems. In Cold Spring Harbor Symposia on Quantitative Biology 25: *159–184.*

Pittendrigh CS (1965) Biological clocks: The functions, ancient and modern, of circadian oscillations. *Science and the Sixties 96–111.*

Pittendrigh CS (1967) Circadian systems. I. The driving oscillation and its assay in *Drosophila pseudoobscura*. *Proceedings of the National Academy of Sciences, USA 58(4): 1762–1767.*

Pittendrigh CS (1974) Circadian oscillations in cells and the circadian organisation of multicellular systems. In *The Neurosciences: Third Study Program*. Cambridge: 432–458.

Pittendrigh CS (1981) Circadian Systems: Entrainment. In *Biological Rhythms*. Boston, MA: 95–124.

Pittendrigh CS and Bruce V (1959) Daily rhythms as coupled oscillator systems and their relation to thermoperiodism and photoperiodism. In *Photoperiodism and related phenomena in plants and animals*. American Association for the Advancement of Science, Washington DC: 475–505.

Pittendrigh CS and Daan S (1976a) A functional analysis of circadian pacemakers in nocturnal rodents IV. Entrainment: Pacemaker as clock. *Journal of Comparative Physiology A 106(3): 291–331.*

Pittendrigh CS and Daan S (1976b) A functional analysis of circadian pacemakers in nocturnal rodents V. Pacemaker structure: A clock for all seasons. *Journal of Comparative Physiology A 106(3): 333–355.*

Pittendrigh CS and Minis DH (1971) The photoperiodic time measurement in *Pectinophora gossypiella* and its relation to the circadian system in that species. In *Biochronometry. Washington District of Columbia: 212–250.*

Pittendrigh CS and Skopik SD (1970) Circadian systems. V. The driving oscillation and the temporal sequence of development. *Proceedings of the National Academy of Sciences, USA 65(3): 500–507.*

Pittendrigh CS and Takamura T (1987) Temperature dependence and evolutionary adjustment of critical night length in insect photoperiodism. *Proceedings of the National Academy of Sciences, USA 84(20): 7169–7173.*

Pittendrigh CS, Bruce V and Kaus P (1958) On the significance of transients in daily rhythms. *Proceedings of the National Academy of Sciences, USA 44(9): 965–973.*

Porter JA and Montell C (1993) Distinct roles of the *Drosophila* ninaC kinase and myosin domains revealed by systematic mutagenesis. *Journal of Cell Biology 122(3): 601–612.*

Potdar S and Vasu S (2012) Large ventral lateral neurons determine the phase of evening activity peak across photoperiods in *Drosophila melanogaster*. *Journal of Biological Rhythms 27(4): 267–279.*

Prakash P, Nambiar A and Sheeba V (2017) Oscillating PDF in termini of circadian pacemaker neurons and synchronous molecular clocks in downstream neurons are not sufficient for sustenance of activity rhythms in constant darkness. *PLoS ONE 12(5): e0175073.*

Qiu J and Hardin PE (1996) Developmental state and the circadian clock interact to influence the timing of eclosion in *Drosophila melanogaster*. *Journal of Biological Rhythms 11(1): 75–86.*

R Core Team (2018) R: A language and environment for statistical computing. R Foundation for Statistical Computing, Vienna, Austria. URL https://www.R-project.org/.

Reed LK, Lee K, Zhang Z, et al. (2014) Systems genomics of metabolic phenotypes in wild-type *Drosophila melanogaster*. *Genetics 197(2): 781-793.*

Refinetti R, Cornélissen G and Halberg F (2007) Procedures for numerical analysis of circadian rhythms. *Biological Rhythm Research 38: 275–325.*

Refinetti R, Wassmer T, Basu P, et al. (2016) Variability of behavioral chronotypes of 16 mammalian species under controlled conditions. *Physiology and Behavior 161: 53–59.*

Reimand J, Kull M, Peterson H, et al. (2007) G:Profiler-a web-based toolset for functional profiling of gene lists from large-scale experiments. *Nucleic Acids Research 35(suppl_2): W193-W200.*

Rémi J, Merrow M and Roenneberg T (2010) A circadian surface of entrainment: Varying T, τ, and photoperiod in *Neurospora crassa*. *Journal of Biological Rhythms 25(5): 318–328.*

Remolina S, Chang P and Leips J (2012) Genomic basis of aging and life history evolution in *Drosophila melanogaster*. *Evolution: International Journal of Organic Evolution 66(11): 3390–3403.*

Renn SCP, Park JH, Rosbash M, et al. (1999) A pdf neuropeptide gene mutation and ablation of PDF neurons each cause severe abnormalities of behavioral circadian rhythms in *Drosophila. Cell 99(7): 791–802.*

Rensing L and Ruoff P (2002) Temperature effect on entrainment, phase shifting, and amplitude of circadian clocks and its molecular bases. *Chronobiology International 19(5): 807–864.*

Robilliard DL, Archer SN, Arendt J, et al. (2002) The 3111 Clock gene polymorphism is not associated with sleep and circadian rhythmicity in phenotypically characterized human subjects. *Journal of Sleep Research 11(4): 305–312.*

Roenneberg T and Merrow M (2016) The circadian clock and human health. *Current Biology 26(10): 432–443.*

Roenneberg T, Allebrandt KV, Merrow M, et al. (2012) Social jetlag and obesity. *Current Biology 22(10): 939–943.*

Roenneberg T, Daan S and Merrow M (2003) The art of entrainment. *Journal of Biological Rhythms 18(3): 183–194.*

Roenneberg T, Dragovic Z and Merrow M (2005) Demasking biological oscillators: properties and principles of entrainment exemplified by the Neurospora circadian clock. *Proceedings of the National Academy of Sciences, 102(21): 7742–7747.*

Roenneberg T, Hut R, Daan S, et al. (2010) Entrainment concepts revisited. *Journal of Biological Rhythms 25(5): 329–339.*

Roenneberg T, Rémi J and Merrow M (2010) Modeling a circadian surface. *Journal of Biological Rhythms 25(5): 340–349.*

Roenneberg T, Pilz LK, Zerbini G, et al. (2019) Chronotype and social jetlag: A (self-) critical review. *Biology 8(3): 54.*

Roenneberg T, Tan Y, Dragovic Z, et al. (2005) Chronoecology from fungi to humans. In *Biological Rhythms (eds. Honma K et al.) pp. 73*. Hokkaido University Press, Sapporo, Japan.

Ruoff P, Vinsjevik M, Monnerjahn C, et al. (1999) The Goodwin oscillator: On the importance of degradation reactions in the circadian clock. *Journal of Biological Rhythms 14(6): 469–479.*

Satoh A, Yoshioka E and Numata H (2008) Circatidal activity rhythm in the mangrove cricket *Apteronemobius asahinai. Biology Letters 4: 233–236.*

Saunders DS (2002) *Insect Clocks.* Elsevier.

Schlichting M, Menegazzi P, Lelito KR, Yao Z, Buhl E, Dalla Benetta E, Bahle A, Denike J, Hodge JJ, Helfrich-Förster C and Shafer OT (2016) A neural network underlying circadian entrainment and photoperiodic adjustment of sleep and activity in *Drosophila*. *Journal of Neuroscience 36: 9084–9096*.

Schlichting M, Weidner P, Diaz M, et al. (2019) Light-mediated circuit switching in the *Drosophila* neuronal clock network. *bioRxiv: 515478.*

Schlichting Matthias, Díaz MM, Xin J, et al. (2019) Neuron-specific knockouts indicate the importance of network communication to *Drosophila* rhythmicity. *eLife 8.*

Schmid B, Helfrich-Förster C and Yoshii T (2011) A new ImageJ plug-in "ActogramJ" for chronobiological analyses. *Journal of Biological Rhythms 26(5): 464–467.*

Schwartz MD and Smale L (2005) Individual differences in rhythms of behavioral sleep and its neural substrates in nile grass rats. *Journal of Biological Rhythms 20(6): 526–537.*

Selcho M, Millán C, Palacios-Muñoz A, et al. (2017) Central and peripheral clocks are coupled by a neuropeptide pathway in *Drosophila*. *Nature Communications 8: 15563.*

Shafer OT, Levine JD, Truman JW, et al. (2004) Flies by night: Effects of changing day length on *Drosophila*'s circadian clock. *Current Biology 14(5): 424–432.*

Shakhmantsir I, Nayak S, Grant GR, et al. (2018) Spliceosome factors target timeless (tim) mRNA to control clock protein accumulation and circadian behavior in *Drosophila*. *Elife 7: e39821.*

Sharma VK, Chandrashekaran MK and Singaravel M (1998) Relationship between period and phase angle differences in *Mus booduga* under abrupt versus gradual light-dark transitions. *Naturwissenschaften 85(4): 183–186.*

Sheeba V, Chandrashekaran MK, Joshi A, et al. (2002) Locomotor activity rhythm in *Drosophila melanogaster* after 600 generations in an aperiodic environment. *Naturwissenschaften 89(11): 512–514.*

Sheeba V, Nihal M, Mathew SJ, et al. (2001) Does the difference in the timing of eclosion of the fruit fly *Drosophila melanogaster* reflect differences in the circadian organization? *Chronobiology International 18(4): 601–612.*

Sheeba V, Sharma VK, Chandrashekaran MK, et al. (1999) Persistence of eclosion rhythm in *Drosophila melanogaster* after 600 generations in an aperiodic environment. *Naturwissenschaften 86(9): 448–449.*

Sheeba V., Chandrashekaran MK, Joshi A, et al. (2001) Persistence of oviposition rhythm in individuals of *Drosophila melanogaster* reared in an aperiodic environment for several hundred generations. *Journal of Experimental Zoology 290(5): 541–549.*

Shindey R, Varma V, Nikhil KL, et al. (2016) Evolution of robust circadian clocks in *Drosophila melanogaster* populations reared in constant dark for over 330 generations. *The Science of Nature, 103(9–10): 74.*

Sievert C (2018) plotly for R. https://plotly-book.cpsievert.me.

Skene DJ and Arendt J (2006) Human circadian rhythms: Physiological and therapeutic relevance of light and melatonin. *Annals of Clinical Biochemistry 43(5): 344–353.*

Sokolove PG and Bushell WN (1978) The chi square periodogram: its utility for analysis of circadian rhythms. *J Theor Biol 72: 131–160.*

Srivastava M, Varma V, Abhilash L, et al. (2019) Circadian clock properties and their relationships as a function of free-running period in *Drosophila melanogaster*. *Journal of Biological Rhythms 34(3): 231–248.*

Stoleru D, Nawathean P, Fernández M de la P, et al. (2007) The *Drosophila* circadian network is a seasonal timer. *Cell 129(1): 207–219.*

Stoleru D, Peng Y, Agosto J, et al. (2004) Coupled oscillators control morning and evening locomotor behaviour of *Drosophila*. *Nature 431(7010): 862.*

Stuber EF, Dingemanse NJ, Kempenaers B, et al. (2015) Sources of intraspecific variation in sleep behaviour of wild great tits. *Animal Behaviour 106: 201–221.*

Sulzman FM, Ellman D, Fuller CA, et al. (1984) *Neurospora* circadian rhythms in space: a reexamination of the endogenous-exogenous question. *Science 225: 232–234.*

Swade RH (1969) Circadian rhythms in fluctuating light cycles: Toward a new model of entrainment. *Journal of Theoretical Biology 24(2): 227–239.*

Taylor SR, Webb AB, Smith KS, et al. (2010) Velocity response curves support the role of continuous entrainment in circadian clocks. *Journal of Biological Rhythms 25(2): 138–149.*

Tearle R (1991) Tissue specific effects of ommochrome pathway mutations in *Drosophila melanogaster*. *Genetical Research 57(3): 257–266.*

Tobler R, Franssen SU, Kofler R, et al. (2014) Massive habitat-specific genomic response in *D. melanogaster* populations during experimental evolution in hot and cold environments. *Molecular Biology and Evolution 31(2): 364–375.*

Turner TL and Miller PM (2012) Investigating natural variation in *Drosophila* courtship song by the evolve and resequence approach. *Genetics 191(2): 633-642.*

Turner TL, Stewart AD, Fields AT, et al. (2011) Population-based resequencing of experimentally evolved populations reveals the genetic basis of body size variation in *Drosophila melanogaster*. *PLoS Genetics 7(3).*

Vanin S, Bhutani S, Montelli S, et al. (2012) Unexpected features of *Drosophila* circadian behavioural rhythms under natural conditions. *Nature 484(7394): 371–375.*

Varma V, Mukherjee N, Kannan NN, et al. (2013) Strong (type 0) phase resetting of activity-rest rhythm in fruit flies, *Drosophila Melanogaster*, at Low Temperature. *Journal of Biological Rhythms 28(6): 380–389.*

Vaze K.M., Nikhil KL, Abhilash L, et al. (2012) Early-and late-emerging *Drosophila melanogaster* fruit flies differ in their sensitivity to light during morning and evening. *Chronobiology International 29(6): 674–682.*

Vaze KM and Sharma VK (2013) On the adaptive significance of circadian clocks for their owners. *Chronobiology International 30(4): 413–433.*

Vaze Koustubh M., Kannan NN, Abhilash L, et al. (2012) Chronotype differences in *Drosophila* are enhanced by semi-natural conditions. *Naturwissenschaften 99(11): 967–971.*

Vaze Koustubh M., KL N, Abhilash L, et al. (2012) Early- and late-emerging *Drosophila melanogaster* fruit flies differ in their sensitivity to light during morning and evening. *Chronobiology International 29(6): 674–682.*

Veleri S, Brandes C, Helfrich-Förster C, et al. (2003) A self-sustaining, light-entrainable circadian oscillator in the *Drosophila* brain. *Current Biology 13(20): 1758–1767.*

Viola AU, Archer SN, James LMM, et al. (2007) PER3 polymorphism predicts sleep structure and waking performance. *Current Biology 17(7): 613–618.*

Vitaterna MH, Ko CH, Chang A-M, et al. (2006) The mouse Clock mutation reduces circadian pacemaker amplitude and enhances efficacy of resetting stimuli and phase-response curve amplitude. *Proceedings of the National Academy of Sciences, USA 103(24): 9327–9332.*

Vivanco P, Rol MÁ and Madrid JA (2009) Two steady-entrainment phases and graded masking effects by light generate different circadian chronotypes in *Octodon* degus. *Chronobiology International 26(2): 219–241.*

Vivanco P, Rol MA and Madrid JA (2010) Pacemaker phase control versus masking by light: Setting the circadian chronotype in dual *Octodon* degus. *Chronobiology International 27(7): 1365–1379.*

Voets T and Nilius B (2003) TRPs make sense. *The Journal of Membrane Biology 192(1): 1–8.*

Voight BF, Kudaravalli S, Wen X, et al. (2006) A map of recent positive selection in the human genome. *PLoS Biology 4(3).*

Von Schantz M, Taporoski TP, Horimoto ARVR, et al. (2015) Distribution and heritability of diurnal preference (chronotype) in a rural Brazilian family-based cohort, the Baependi study. *Scientific Reports 5*.

Watanabe T, Naito E, Nakao N, et al. (2007) Bimodal clock gene expression in mouse suprachiasmatic nucleus and peripheral tissues under a 7-hour light and 5-hour dark schedule. *Journal of Biological Rhythms 22(1): 58–68.*

Winfree AT (1973) Resetting the amplitude of *Drosophila*'s circadian chronometer. *Journal of Comparative Physiology 85(2): 105–140.*

Wright KP, Gronfier C, Duffy JF, et al. (2005) Intrinsic period and light intensity determine the phase relationship between melatonin and sleep in humans. *Journal of Biological Rhythms 20(2): 168–177.*

Wu S, Refinetti R, Kok LT, et al. (2014) Photoperiod and temperature effects on the adult eclosion and mating rhythms in *Pseudopidorus fasciata* (Lepidoptera: *Zygaenidae*). *Environmental Entomology 43(6): 1650–1655.*

Xu XZS, Chien F, Butler A, et al. (2000) TRPγ, a *Drosophila* TRP-related subunit, forms a regulated cation channel with TRPL. *Neuron 26(3): 647–657.*

Yadlapalli S, Jiang C, Bahle A, et al. (2018) Circadian clock neurons constantly monitor environmental temperature to set sleep timing. *Nature 555(7694): 98–102.*

Yan L, Silver R and Gorman M (2010) Reorganization of suprachiasmatic nucleus networks under 24-h LDLD conditions. *Journal of Biological Rhythms 25(1): 19–27.*

Yoshii T, Vanin S, Costa R, et al. (2009) Synergic entrainment of *Drosophila*'s circadian clock by light and temperature. *Journal of Biological Rhythms 24(6): 452–464.*

Yuan Q, Joiner WJ and Sehgal A (2006) A sleep-promoting role for the *Drosophila* serotonin receptor 1A. *Current Biology 16(11): 1051–1062.*

Zar JH (1999) *Biostatistical Analysis.* Prentice Hall.

Zeileis A and Grothendieck G (2005) zoo: S3 Infrastructure for regular and irregular time series. *Journal of Statistical Software 14: 1–27.*

Zhang L, Chung BY, Lear BC, et al. (2010) A subset of circadian neurons coordinates light and PDF signaling to produce robust daily behavior in *Drosophila*. *Current Biology 20(7): 591.*

Zhang Y, Lamba P, Guo P, et al. (2016) miR-124 regulates the phase of *Drosophila* circadian locomotor behavior. *The Journal of Neuroscience 36(6): 2007–2013.*

Zhang Y, Liu Y, Bilodeau-Wentworth D, et al. (2010) Light and temperature control the contribution of specific DN1 neurons to *Drosophila* circadian behavior. *Current Biology 20(7): 600–605.*

Zhou D, Udpa N, Gersten M, et al. (2011) Experimental selection of hypoxia-tolerant *Drosophila melanogaster*. *Proceedings of the National Academy of Sciences, USA 108(6): 2349-2354.*